

Eight new species of *Otacilia* (Araneae: Phrurolithidae) from southern China

Ke-ke Liu¹, Yuan-hao Ying¹, Yu-xin Xiao¹, Jing Yan¹, Yong-hong Xiao¹

¹ College of Life Science, Jinggangshan University, Ji'an 343009, Jiangxi, China

Corresponding author: Yong-hong Xiao (yonghongxiao01@126.com)

Academic editor: C. Haddad | Received 8 July 2020 | Accepted 15 September 2020 | Published 27 October 2020

<http://zoobank.org/9FCC47DB-C8AA-4B3F-89A2-3FD3B69A02A9>

Citation: Liu K-K, Ying Y-H, Xiao Y-X, Yan J, Xiao Y-H (2020) Eight new species of *Otacilia* (Araneae: Phrurolithidae) from southern China. ZooKeys 979: 1–33. <https://doi.org/10.3897/zookeys.979.56273>

Abstract

Eight new *Otacilia* species were collected from Ji'an City, Jiangxi Province, China during a survey of the phrurolithid fauna of the region: *Otacilia bizhouica* Liu, **sp. nov.** (♂♀), *O. gougunao* Liu, **sp. nov.** (♂), *O. nanhuashanica* Liu, **sp. nov.** (♂♀), *O. subfabiformis* Liu, **sp. nov.** (♂♀), *O. wugongshanica* Liu, **sp. nov.** (♂♀), *Otacilia yusishanica* Liu, **sp. nov.** (♂♀), *O. zaoshiica* Liu, **sp. nov.** (♂♀) and *O. ziyaoshanica* Liu, **sp. nov.** (♀). All species are described and illustrated with photographs and SEM micrographs, and their distribution is also mapped.

Keywords

Jiangxi Province, sac spider, Taxonomy

Introduction

During the past five years, the total number of phrurolithid species recorded from China has almost doubled, with most of the newly discovered species being endemic to the country (WSC 2015–2019). All of them (47 species) were discovered in southern China and most belong to the genus *Otacilia* Thorell, 1897 (WSC 2020). However, there are still many poorly known *Otacilia* species from southern China with unusual morphological characteristics.

Otacilia is the most diverse of the 15 phrurolithid genera (WSC 2020). In recent major reviews of the genus, 27 species *Phrurolithus* C.L. Koch, 1839 were transferred to *Otacilia* (Zamani & Marusik, 2020) and one new genus, *Aboculus* Liu, 2020, was erected (Liu et al. 2020). Recently, seven new species and one new combination were recorded from Jinggang Mountain National Nature Reserve in Jiangxi Province, which is the first report on phrurolithid spiders from this province (Liu et al. 2020). Their distribution also implies that *Otacilia* species may be abundant in this province.

When we focused on sac spiders in the Jiangxi Province of southern China, many unknown *Otacilia* species with unusual characters were found. Therefore, eight new *Otacilia* species were identified and are described here.

Materials and methods

Specimens were examined using a Zeiss Stereo Discovery V12 stereomicroscope with a Zoom Microscope System. Both male palps and female copulatory organs were dissected and examined in 75% ethanol, using a Zeiss Axio Scope A1 compound microscope with a KUY NICE CCD. The epigynes were cleared with pancreatin solution. Specimens, including dissected male palps and epigynes, were stored in 80% ethanol after examination. All the specimens are deposited in Animal Specimen Museum, College of Life Science, Jinggangshan University (ASM-JGSU).

The measurements were taken with ImageView CM2000 software and are given in millimetres. The body length of all specimens excludes the chelicerae and spinnerets. Terminology of the male and female genitalia follows Jäger and Wunderlich (2012), Ramírez (2014), Jäger and Dimitrov (2019), Liu et al. (2019) and Zamani and Marusik (2020). Promarginal and retromarginal teeth on the chelicerae are given as the first, second, third, etc., and measured from the base of the fang to the distal groove.

Leg measurements are given as total length (femur, patella, tibia, metatarsus, tarsus). Leg spines are documented by dividing each leg segment into two aspects: prolateral (p) and retrolateral (r) and indicating the ventral (v) spines as single (1) or paired (2), e.g., femur I pv1111; tibia I v2222. Dorsal spines on femora are recorded separately.

The abbreviations used in the text are as follows:

Eyes

ALE = anterior lateral eye

AME = anterior median eye

MOA = median ocular area

PLE = posterior lateral eye

PME = posterior median eye

Male palp

DTA = dorsal tibial apophysis

dTA = distal tegular apophysis

E = embolus

FA = femoral apophysis
Gr = groove
RTA = retrolateral tibial apophysis
rTA = retrolateral tegular apophysis
SD = sperm duct
VTA = ventral tibial apophysis

Epigyne

B = bursa
CD = copulatory duct
CO = copulatory opening
CT = connecting tube
FD = fertilization duct
GA = glandular appendage
MS = median septum
Spe = spermathecae

Taxonomy

Family Phrurolithidae Banks, 1892

Genus *Otacilia* Thorell, 1897

Otacilia bizhouica Liu, sp. nov.

<http://zoobank.org/3B75F002-AA06-4D64-A017-56DEA6E52213>

Figures 1–3, 22

Type material. *Holotype*: ♂, China, Jiangxi Province, Ji'an City, Suichuan county, Bizhou Town, Baishuixian Village, Dakeng Group, 26°19'55.98"N, 114°44'08.72"E, 362 m, 4 October 2019, leg. Ke-ke Liu et al. *Paratypes*: 2 ♀, with the same data as holotype.

Etymology. The specific name derived from the type locality, Bizhou Town; adjective.

Diagnosis. The male of the new species is similar to *Otacilia liupan* Hu & Zhang, 2011 in having a short retrolateral tibial apophysis bending inwards to the base of the cymbium and the sub-circular sperm duct (see Hu and Zhang 2011: 60, figs 2–5), but can be separated from it by the thick retrolateral tegular apophysis (Figs 1D, E, 2A, B) (vs. thin) and a stubby pipe-shaped retrolateral tibial apophysis in dorsal view (Figs 1E, F, 2C) (vs. finger-like). The females resemble those of *O. ovoidea* Liu, 2020 in having sclerotized epigynal ridges (Fig. 3C, D), but can be separated from it by the rectangular median septum (vs. funnel-shaped) and the U-shaped spermathecae (vs. globular) (see Liu et al. 2020: 22, fig. 14C, D).

Description. Male (Holotype). Habitus as in Fig. 1A, B. Total length 3.56, carapace 1.56 long, 1.33 wide. Eye sizes and interdistances: AME 0.09, ALE 0.10, PME 0.08, PLE 0.09; ALE–AME 0.01, AME–AME 0.05, PLE–PME 0.06, PME–PME 0.12,



Figure 1. *Otacilia bizhouica* sp. nov., male holotype. **A** habitus, dorsal view **B** same, ventral view **C** palp, prolateral view **D** same, ventral view **E** same, retrolateral view **F** same, dorsal view. Scale bars: 0.5 mm (**A**, **B**), 0.1 mm (**C–F**). Abbreviations: dTA – distal tegular apophysis, E – embolus, FA – femoral apophysis, RTA – retrolateral tibial apophysis, rTA – retrolateral tegular apophysis, SD – sperm duct.

ALE–ALE 0.24, PLE–PLE 0.38, ALE–PLE 0.07, AME–PME 0.10, AME–PLE 0.16. MOA 0.25 long, frontal width 0.21, posterior width 0.26. Chelicerae (Fig. 1A, B) with three promarginal (proximal largest, distal smallest) and six retromarginal teeth (distal largest, 5th smallest). Sternum (Fig. 1B), posterior end triangular, relatively blunt. Pedi-

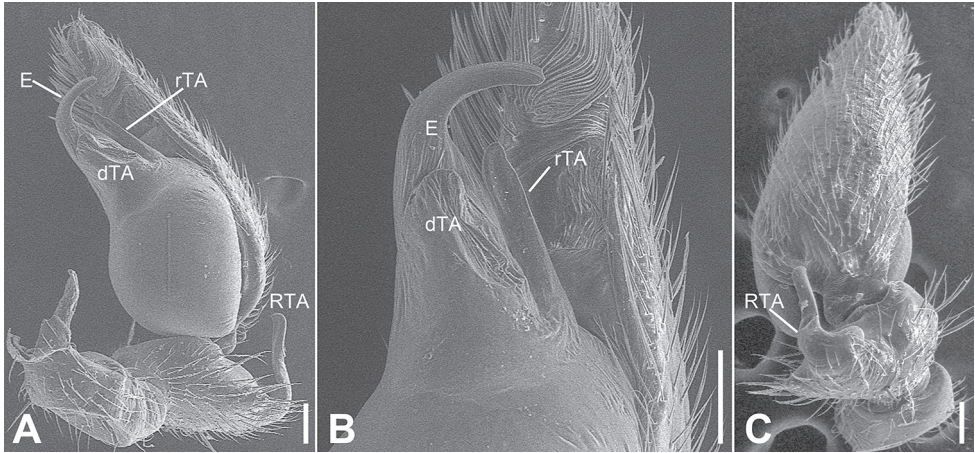


Figure 2. SEM micrographs of *Otacilia bizhouica* sp. nov., palp of male holotype. **A** ventro-retrolateral view **B** same, detail of embolus, distal tegular apophysis and retrolateral tegular apophysis **C** dorsal view, detail of retrolateral tibia apophysis. Scale bars: 0.1 mm. Abbreviations: dTA – distal tegular apophysis, E – embolus, RTA – retrolateral tibial apophysis, rTA – retrolateral tegular apophysis.

cel 0.2 long. Abdomen (Fig. 1A, B) 1.80 long, 1.06 wide. Leg measurements: I 6.46 (1.75, 0.58, 2.03, 1.53, 0.57); II 5.28 (1.32, 0.56, 1.55, 1.21, 0.64); III 4.39 (1.08, 0.42, 1.09, 1.16, 0.64); IV 7.31 (1.94, 0.61, 1.75, 2.01, 1.00). Leg spination (Fig. 1A, B): femur I with two dorsal spines; femora II–IV with one dorsal spine each; femora I pv1111, II pv111; tibiae I v22222222, II v2222222; metatarsi I v2222, II v222.

Colouration (Fig. 1A, B). Carapace yellow-brown, with radial, irregular dark yellow-brown mottled markings on surface. Chelicerae yellow-brown. Endites yellow, mottled. Sternum yellow, lateral margins with dark mottled markings. Legs yellow. Abdomen yellow-brown, with pair of large triangular yellowish spots on posterior dorsal scutum, three light chevron-shaped stripes on sub-medial part, and yellowish arch-shaped stripe posteriorly; weak dorsal scutum in anterior half; venter with H-shaped and pair of sloping markings posteriorly.

Palp (Figs 1C–F, 2). Femoral apophysis well-developed, as wide as half of femoral length. Patella unmodified. Tibia with large retrolateral apophysis, as long as tibial length, apex blunt, bending inwards to base of cymbium, with a broad base and a basal apophysis, directed dorsally in dorsal view. Cymbium width less than half of its length. Bulb broad oval, with sub-circular sperm duct, apophyses absent. Embolus hook-shaped, thick, with broad triangular base. Retrolateral tegular apophysis straight, thick, submedial part covered by distal tegular apophysis. Distal tegular apophysis oval, arising from base of embolus and retrolateral sperm duct.

Female (paratype). Habitus as in Fig. 3A, B. Lighter than male. Total length 4.04, carapace 1.68 long, 1.45 wide. Eye sizes and interdistances: AME 0.08, ALE 0.09, PME 0.09, PLE 0.08, AME–AME 0.05, AME–ALE 0.02, PME–PME 0.13, PME–PLE 0.06, AME–PME 0.05, AME–PLE 0.17, ALE–ALE 0.23, PLE–PLE 0.37, ALE–

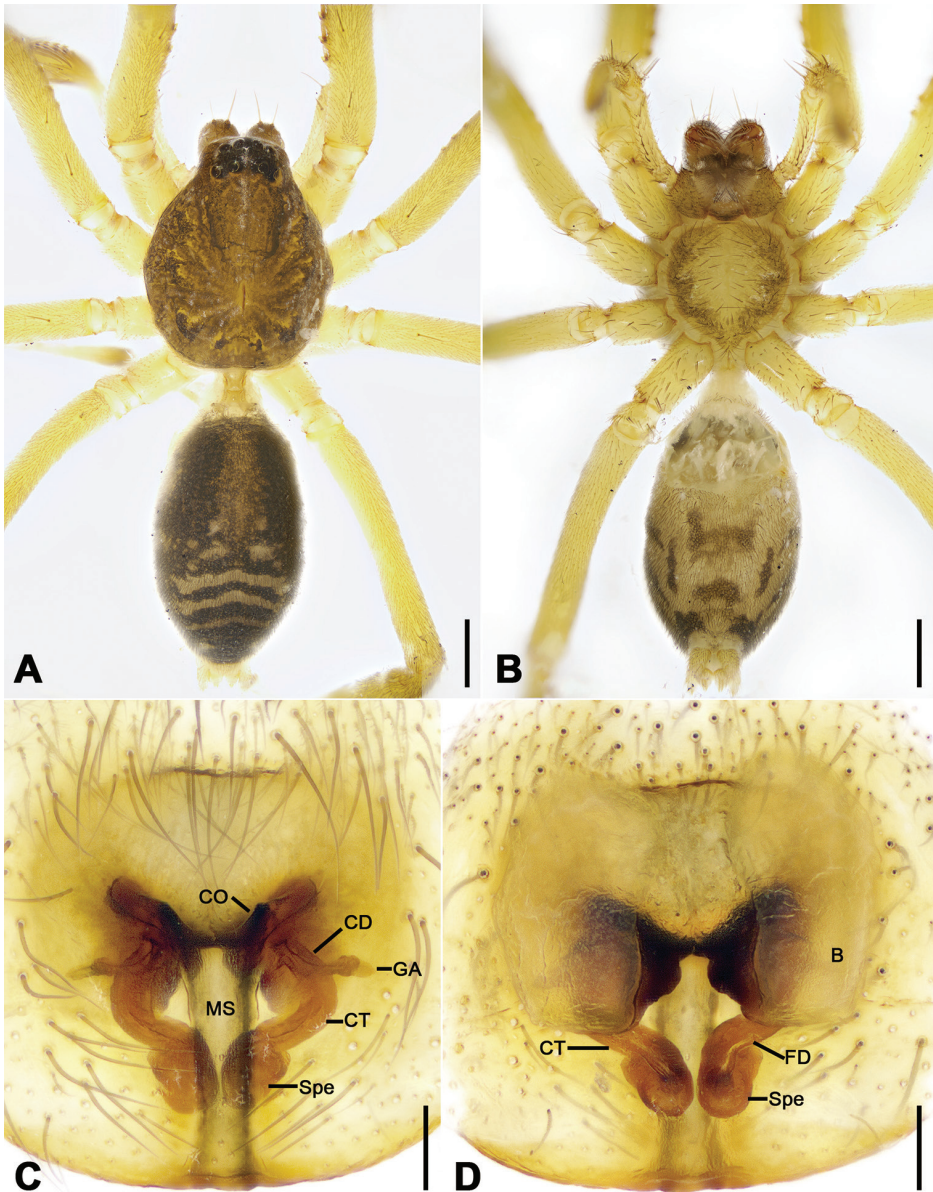


Figure 3. *Otacilia bizhouica* sp. nov., female paratype. **A** habitus, dorsal view **B** same, ventral view **C** epigyne, ventral view **D** epigyne, dorsal view. Scale bars: 0.5 mm (**A**, **B**), 0.1 mm (**C**, **D**). Abbreviations: B – bursa, CD – copulatory duct, CO – copulatory opening, CT – connecting tube, FD – fertilization ducts, GA – glandular appendage, MS – median septum, Spe – spermathecae.

PLE 0.1. MOA 0.25 long, frontal width 0.20, posterior width 0.27. Chelicerae (Fig. 3A, B) with three promarginal (proximal largest, distal smallest) and five retromarginal teeth (distal largest, fourth smallest). Pedicel 0.3 long. Abdomen (Fig. 3A) 2.05 long, 1.2 wide. Leg (Fig. 3A, B) measurements: I 6.35 (1.53, 0.48, 2.25, 1.41, 0.68); II 5.83

(1.52, 0.63, 1.68, 1.30, 0.70); III 4.66 (1.21, 0.51, 1.06, 1.18, 0.70); IV 7.32 (1.97, 0.57, 1.72, 2.11, 0.95). Leg spination (Fig. 3A, B): tibiae I v22222222, II v2222222.

Epigyne (Fig. 3C, D). Epigynal plate funnel-shaped, posterior with elongate rectangular median septum. Copulatory ducts, glandular appendages, connecting tubes and spermathecae distinctly visible through integument in intact epigyne. Anterior fovea separated by weakly sclerotized transverse margin, medially with V-shaped sclerotized plug, covering copulatory openings. Copulatory ducts broad, short, posteriorly with pair of kidney-shaped transparent bursae medially. Glandular appendages relatively long, located on anterior of copulatory ducts, extending postero-laterally. Connecting tubes short, broad, as long as copulatory ducts, located between glandular appendages and spermathecae, posteriorly close to each other. Spermathecae U-shaped, anterior part slightly separated, posterior part touching. Fertilization duct short, located sub-medially on spermathecae, directed anterolaterally.

Distribution. Known only from the type locality in Jiangxi Province, China (Fig. 22).

***Otacilia gougnao* Liu, sp. nov.**

<http://zoobank.org/20022BC6-E020-4F2E-B8D0-8CF2C88B81A1>

Figures 4, 5, 22

Type material. Holotype: ♂, China, Jiangxi Province, Ji'an City, Suichuan county, Nanjiang Town, Xiajiaoling Village, 26°00'39.41"N, 114°01'03.91"E, 979 m, 5 October 2019, leg. Ke-ke Liu et al. **Paratypes:** 3 ♂, with same data as holotype.

Etymology. The specific name refers to a famous tea from the type locality, Gougnao, which is planted on the mountainsides of Suichuan County; noun in apposition.

Diagnosis. The males of the new species resemble those of *O. bizhouica* sp. nov. in having an ovoid membranous distal regular apophysis and hook-shaped embolus (Fig. 1C–F), but can be distinguished from it by the sternum with a sharpened end (Fig. 4B) (vs. relatively blunt), the retrolateral tibial apophysis with a submedial apophysis prolaterally (Figs 4E, F, 5C) (vs. with a basal apophysis prolaterally) and the retrolateral regular apophysis with a slightly curved apex (Figs 4D, E, 5) (vs. straight apex).

Description. Male (holotype). Habitus as in Fig. 4A, B. Total length 3.49, carapace 1.87 long, 1.44 wide. Eye sizes and interdistances: AME 0.09, ALE 0.09, PME 0.08, PLE 0.09, AME–AME 0.05, AME–ALE 0.03, PME–PME 0.14, PME–PLE 0.07, AME–PME 0.1, AME–PLE 0.18, ALE–ALE 0.26, PLE–PLE 0.41, ALE–PLE 0.13. MOA 0.25 long, frontal width 0.22, posterior width 0.29. Chelicerae (Fig. 4B) with three promarginal (proximal largest, distal smallest) and six retromarginal teeth (distal largest, proximal smallest, others equal in size). Sternum posteriorly pointed. Pedicel 0.10 long. Abdomen (Fig. 4A, B), 1.67 long, 1.00 wide. Leg measurements (Fig. 4A, B): I 6.46 (1.66, 0.57, 2.12, 1.42, 0.69); II 5.07 (1.21, 0.54, 1.59, 1.05, 0.68); III 4.81 (1.25, 0.50, 1.03, 1.29, 0.74); IV 7.74 (2.41, 0.62, 1.71, 2.21, 0.79). Leg spination (Fig. 4A, B): femur I with two dorsal spines, femora II–IV with one dorsal spine each; femora I pv1111, pv111 (right), II pv111; tibiae I v2222222, II v2222222; metatarsi I v2222, II v2222.

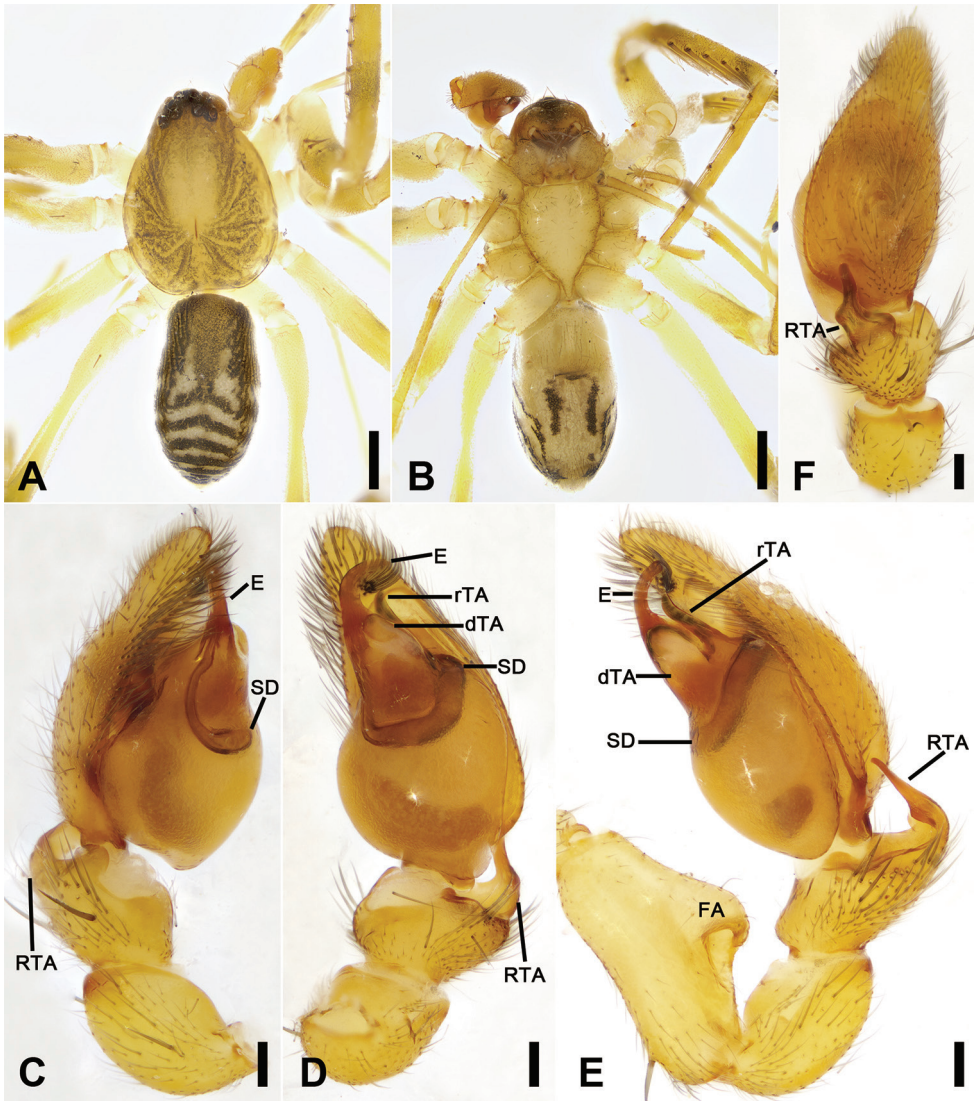


Figure 4. *Otacilia gougunao* sp. nov., male holotype. **A** habitus, dorsal view **B** same, ventral view **C** palp, prolateral view **D** same, ventral view **E** same, retrolateral view **F** same, dorsal view, slightly retrolateral. Scale bars: 0.5 mm (**A, B**), 0.1 mm (**C–F**). Abbreviations: dTA – distal tegular apophysis, E – embolus, rTA – retrolateral tegular apophysis, RTA – retrolateral tibial apophysis, SD – sperm duct.

Colouration (Fig. 4A, B). Carapace yellow, with radial, irregular dark stripes submarginally and arc-shaped dark stripes around margin. Chelicerae yellow-brown. Endites and labium yellow, mottled. Legs yellow. Abdomen dark brown, with pair of racket-shaped yellowish spots at posterior of dorsal scutum, three light chevron-shaped stripes on sub-medial part, and two yellowish arc-shaped stripes posteriorly; weak dorsal scutum in anterior half; venter with N-shaped marking and pair sloping markings posteriorly.

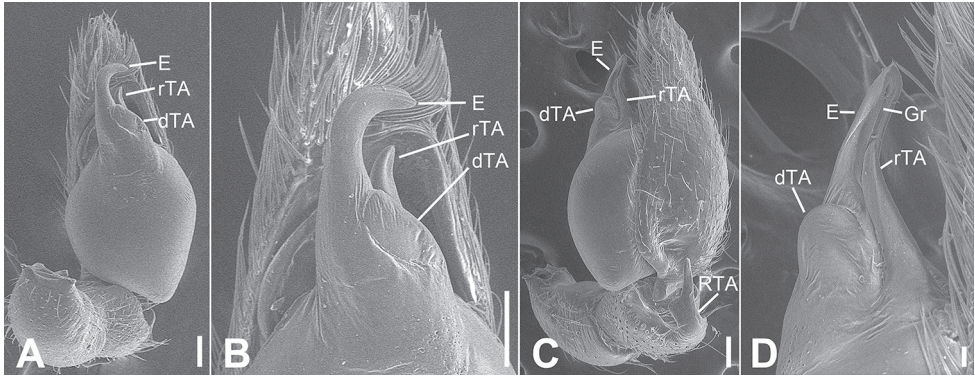


Figure 5. SEM micrographs of *Otacilia gougunao* sp. nov., palp of male holotype. **A** ventral view **B** same, detail of embolus, distal tegular apophysis and retrolateral tegular apophysis **C** same, retro-dorsolateral view **D** same, detail of embolus, embolic groove, distal tegular apophysis and retrolateral tegular apophysis. Scale bars: 0.1 mm (**A–C**), 20 μ m (**D**). Abbreviations: dTA – distal tegular apophysis, E – embolus, Gr – groove, RTA – retrolateral tibial apophysis, rTA – retrolateral tegular apophysis.

Palp (Figs 4C–F, 5). Femoral apophysis well-developed, width more than half of femoral length. Patella unmodified. Tibia with large retrolateral apophysis, less than tibial length, apex blunt, bending inwards to base of cymbium, with submedian apophysis prolaterally and basal apophysis retrolaterally. Cymbium width less than half of its length. Bulb broad oval, with U-shaped sperm duct, apophyses absent. Embolus hook-like, thick, with broad triangular base and narrowed groove, apart from retrolateral tegular apophysis and distal tegular apophysis. Retrolateral tegular apophysis clavate, thick, with slightly curved apex, directed anterolaterally, more than basal 2/3 covered by distal tegular apophysis in ventral view. Distal tegular apophysis oval, arising from base of embolus and retrolateral sperm duct.

Female. Unknown.

Distribution. Known only from the type locality in Jiangxi Province, China (Fig. 22).

***Otacilia nanhuashanica* Liu, sp. nov.**

<http://zoobank.org/34A24780-C0E2-4C27-BA43-5F89EF751B67>

Figures 6–8, 22

Type material. Holotype: ♂, China, Jiangxi Province, Ji'an City, Yongxin County, Nanhua Mt., 26°50'22.02"N, 114°15'47.05"E, 1130 m, 3 October 2019, leg. Ke-ke Liu et al. **Paratypes:** 1 ♂, 2 ♀, with same data as holotype; 1 ♂ (right palp broken in collection), Zhongcun, 26°49'37.77"N, 114°13'14.55"E, 3 October 2019, leg. Ke-ke Liu et al.

Etymology. The specific name is derived from the type locality, Nanhushan; adjective.

Diagnosis. The males of the new species are similar to *Otacilia hengshan* (Song, 1990) in having a hook-shaped embolus, semi-circular sperm duct and a clavate retrolateral tegular apophysis (see Hu and Zhang 2011: 62, fig. 9–11), but can be separated

from it by the embolus with a trapezoid base (Figs 6D, 7A, B) (vs. parallel-sided) and the thin clavate retrolateral tegular apophysis (Figs 6D, E, 7A, B) (vs. thick). The females resemble *O. hengshan* in having narrow and convergent connecting tubes (see Hu and Zhang 2011: 62, fig. 13, 15), but can be separated from it by the epigyne with a broad sub-trapezoid median septum (Fig. 8C) (vs. slender).

Description. Male (holotype). Habitus as in Fig. 6A, B. Total length 3.63, carapace 1.79 long, 1.51 wide. Eye sizes and interdistances: AME 0.11, ALE 0.09, PME 0.08, PLE 0.1, AME–AME 0.06, AME–ALE 0.02, PME–PME 0.13, PME–PLE

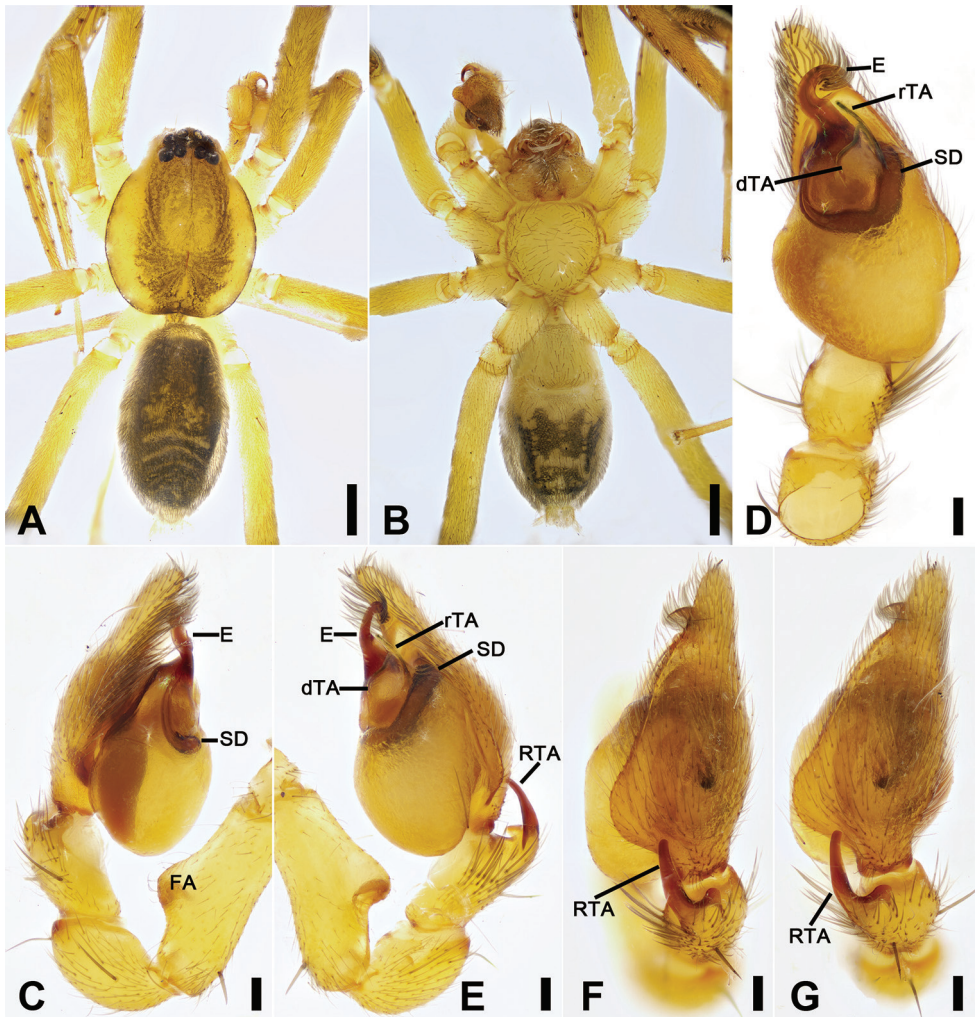


Figure 6. *Otacilia nanhuashanica* sp. nov., male holotype. **A** habitus, dorsal view **B** same, ventral view **C** palp, prolateral view **D** same, ventral view **E** same, retrolateral view **F** same, retro-dorsal view **G** same, dorsal view. Scale bars: 0.5 mm (**A**, **B**), 0.1 mm (**C**–**G**). Abbreviations: dTA – distal tegular apophysis, E – embolus, FA – femoral a pophysis, rTA – retrolateral tegular apophysis, RTA – retrolateral tibial apophysis, SD – sperm duct.

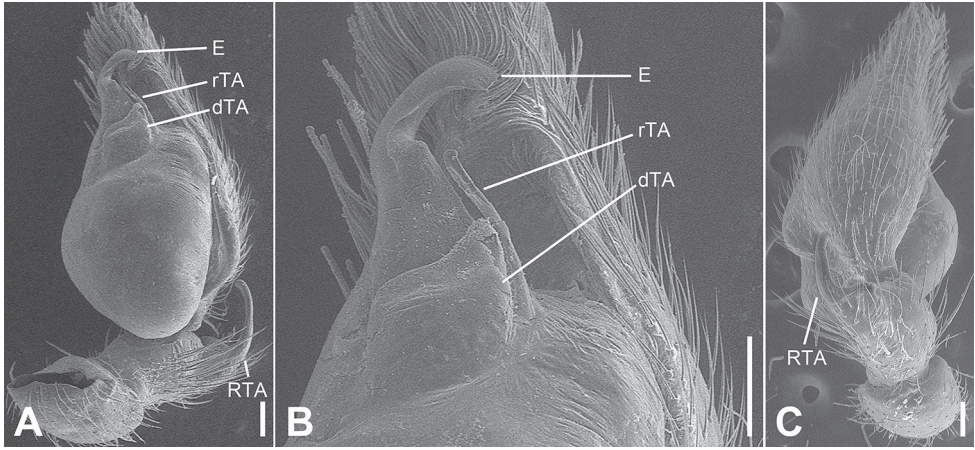


Figure 7. SEM micrographs of *Otacilia nanhuashanica* sp. nov., palp of male holotype. **A** ventro-retrolateral view **B** same, detail of embolus, distal tegular apophysis and retrolateral tegular apophysis **C** same, dorsal view. Scale bars: 0.1 mm (**A–C**). Abbreviations: dTA – distal tegular apophysis, E – embolus, RTA – retrolateral tibial apophysis, rTA – retrolateral tegular apophysis.

0.08, AME–PME 0.12, AME–PLE 0.18, ALE–ALE 0.31, PLE–PLE 0.44, ALE–PLE 0.1. MOA 0.30 long, frontal width 0.27, posterior width 0.30. Chelicerae (Fig. 6A, B) with three promarginal (middle largest, distal smallest) and five retromarginal teeth (distal largest, fourth smallest, first to third equal in size). Sternum (Fig. 6B) with small triangular, blunt end. Abdomen (Fig. 6A, B) 1.90 long, 1.08 wide. Leg measurements (Fig. 6A, B): I 7.31 (1.76, 0.67, 2.21, 1.75, 0.92); II 6.03 (1.54, 0.59, 1.71, 1.35, 0.84); III 4.75 (1.07, 0.57, 1.19, 1.20, 0.72); IV 7.78 (2.14, 0.62, 1.85, 2.14, 1.03). Leg spination (Fig. 6A, B): femur I with two dorsal spines, femora II–IV with one dorsal spine each; femora I pv1111, II pv11, pv111 (right); tibiae I v22222222, II v22222222; metatarsi I v2222, II pv2222.

Colouration (Fig. 6A, B). Carapace yellow-brown, medially with radial, irregular dark brown mottled markings on surface and arc-shaped dark stripes around margin. Fovea distinct, black. Chelicerae yellow-brown. Endites and labium yellow, with abundant setae on surface. Legs yellow. Abdomen dark brown, with pair of large irregular spots on posterior of dorsal scutum, three light chevron-shaped stripes on sub-medial part, and yellowish arc-shaped stripe posteriorly; weak dorsal scutum in anterior half; venter with two pairs of W-shaped markings posteriorly.

Palp (Figs 6C–F, 7). Femoral apophysis well-developed, width longer than half of its length. Patella unmodified. Retrolateral tibial apophysis less than tibial length, bending inward to base of cymbium, with clear apophysis located retrolaterally at base and blunt apex in dorsal view. Sperm duct C-shaped, strongly sclerotized, around base of retrolateral tegular apophysis, distal tegular apophysis and embolus. Retrolateral tegular apophysis clavate, longer than distal tegular apophysis. Distal tegular apophysis ampulla-like, covering half of retrolateral tegular apophysis. Embolus with trapezoidal base and short hook-like tip.



Figure 8. *Otacilia nanhuashanica* sp. nov., female paratype. **A** habitus, dorsal view **B** same, ventral view **C** epigyne, ventral view **D** epigyne, dorsal view. Scale bars: 0.5 mm (**A, B**), 0.1 mm (**C, D**). Abbreviations: B – bursa, CD – copulatory duct, CO – copulatory opening, CT – connecting tube, FD – fertilization ducts, GA – glandular appendage, MS – median septum, Spe – spermathecae.

Female (paratype). Habitus as in Fig. 8A, B. Total length 3.91, carapace 1.84 long, 1.61 wide. Eye sizes and interdistances: AME 0.1, ALE 0.11, PME 0.09, PLE 0.09, AME–AME 0.06, AME–ALE 0.02, PME–PME 0.12, PME–PLE 0.06, AME–PME 0.10, AME–PLE 0.19, ALE–ALE 0.29, PLE–PLE 0.42, ALE–PLE 0.11. MOA 0.26 long, front width 0.23, posterior width 0.31. Chelicerae (Fig. 8A, B) with three promarginal (middle largest, distal smallest) and six retromarginal teeth (distal largest, proximal smallest, second to fourth equal in size, 5th and 6th with a same base). Abdomen (Fig. 14A, B) 2.03 long, 1.25 wide. Legs (Fig. 8A, B) measurements: I 7.77 (1.94, 0.72, 2.45, 1.84, 0.82); II 6.36 (1.63, 0.63, 1.78, 1.64, 0.68); III 5.31 (1.44, 0.60, 1.15, 1.32, 0.80); IV 8.26 (2.29, 0.69, 1.98, 2.22, 1.08). Leg spination (Fig. 8A, B): femora I–IV with one dorsal spine each; femora I p11111, p1111(right), II p111; tibiae I v22222222, II v22222222.

Epigyne (Fig. 8C, D). Epigynal plate mask-shaped, sub-medially with pair of oval copulatory openings, posteriorly with sub-trapezoidal median septum. Copulatory ducts, glandular appendages, connecting tubes and spermathecae distinctly visible through integument in intact epigyne. Copulatory ducts relatively broad, located between copulatory openings and glandular appendages, posteriorly with pair of large bean-shaped transparent bursae. Glandular appendages very short, partly covered by bursae, located on anterior of connecting tubes. Connecting tubes longer than copulatory ducts, converging postero-medially, located between glandular appendages and spermathecae. Spermathecae slightly expanded, separated by less width of septum, directed medially. Fertilization duct short, directed anteriorly.

Distribution. Known only from the type locality in Jiangxi Province, China (Fig. 22).

***Otacilia subfabiformis* Liu, sp. nov.**

<http://zoobank.org/1EA8C0FA-3A76-4C55-8149-BAB6E83B446F>

Figures 9–11, 22

Type material. Holotype: ♂, China, Jiangxi Province, Ji'an City, Anfu County, Taisihan Town, Wugong Mt., near the ticket office, 27°27'10.79"N, 114°11'8.24"E, 4 January 2020, leg. Ke-ke Liu et al. **Paratypes:** 1 ♂, 1 ♀, with same data as holotype.

Etymology. The specific name is derived from that of a similar species, *O. fabiformis* Liu et al. 2019; adjective.

Diagnosis. The males of the new species are similar to *Otacilia fabiformis* Liu, Xu, Xiao, Yin & Peng, 2019 in having a spine-like embolus, a C-shaped sperm duct and a swollen bulb (see Liu et al. 2019: 444, fig. 6C), but can be separated from it by the retrolateral tibial apophysis with a sharp apex (Figs 9E, F, 10D) (vs. with a blunt tip), the retrolateral tegular apophysis with a thin retrolateral part (Figs 9D, E, 10A, B, E) (vs. with broad retrolateral part). The female resembles *O. fabiformis* in having large and touching bursae (see Liu et al. 2019: 444, fig. 7C), but can be separated from it by the slightly curved and separated connecting tubes

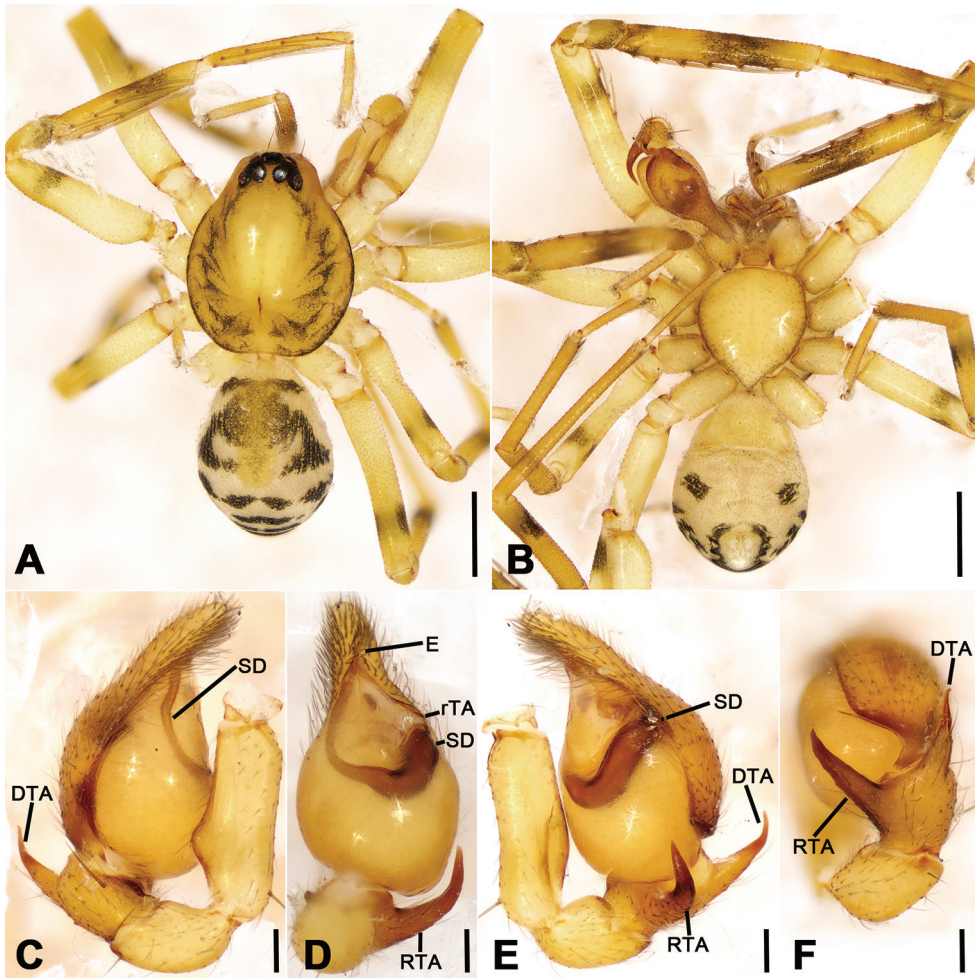


Figure 9. *Otacilia subfabiformis* sp. nov., male holotype. **A** habitus, dorsal view **B** same, ventral view **C** palp, prolateral view **D** same, ventral view **E** same, retrolateral view **F** same, dorsal view. Scale bars: 0.5 mm (**A**, **B**), 0.1 mm (**C**–**F**). Abbreviations: DTA– dorsal tibial apophysis, dTA – distal tegular apophysis, E – embolus, FA – femoral apophysis, RTA – retrolateral tibial apophysis, rTA – retrolateral tegular apophysis, SD – sperm duct.

medially located (Fig. 11D) (vs. the strongly curved and separated connecting tubes laterally located).

Description. Male (holotype). Habitus as in Fig. 9A, B. Total length 2.39, carapace 1.18 long, 1.01 wide. Eye sizes and interdistances: AME 0.05, ALE 0.08, PME 0.07, PLE 0.07, AME–AME 0.02, AME–ALE 0.02, PME–PME 0.06, PME–PLE 0.04, AME–PME 0.07, AME–PLE 0.12, ALE–ALE 0.14, PLE–PLE 0.29, ALE–PLE 0.05. MOA 0.19 long, frontal width 0.12, posterior width 0.21. Chelicerae (Fig. 9A, B) with three promarginal (proximal largest, distal smallest) and two retromarginal teeth (distal larger). Sternum (Fig. 9B) with small triangular, blunt end. Pedicel 0.13

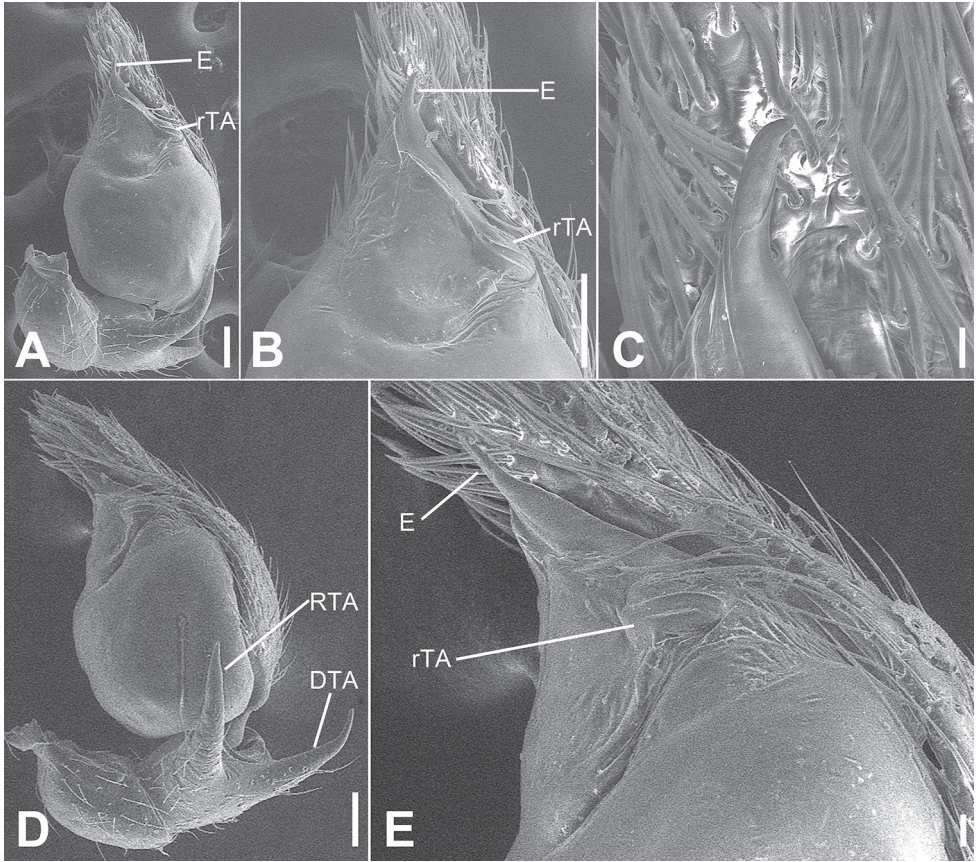


Figure 10. SEM micrographs of *Otacilia subfabiformis* sp. nov., palp of male holotype. **A** ventral view **B** same, detail of embolus and retrolateral tegular apophysis **C** same, detail of embolus **D** retrolateral view **E** same, detail of embolus and retrolateral tegular apophysis. Scale bars: 0.1 mm (**A, B, D**), 10 μ m (**C**), 20 μ m (**E**). Abbreviations: DTA – dorsal tibial apophysis, E – embolus, FA – femoral apophysis, RTA – retrolateral tibial apophysis, rTA – retrolateral tegular apophysis.

long. Abdomen (Fig. 9A, B) 1.24 long, 0.84 wide. Leg measurements: I 4.36 (1.17, 0.40, 1.25, 1.09, 0.45); II 3.62 (0.91, 0.37, 0.96, 0.85, 0.36); III 3.45 (0.75, 0.26, 0.74, 0.83, 0.42); IV 3.79 (1.18, 0.36, 0.96, 1.29, 0.68). Leg spination (Fig. 9A, B): femora I–IV without dorsal spine each; femora I p111 II p11; tibiae I v222222, II v222222; metatarsi I v2222, II v222.

Colouration (Fig. 9A, B). Carapace yellow, with radial, irregular dark stripes mediolaterally and arc-shaped dark stripes around margin. Fovea distinct, black. Chelicerae, endites and labium yellow. Sternum yellow, margins with dark brown mottled spots. Legs yellow, femora I–IV each with black annulation; patellae I with black annulation; tibiae I with blackish-brown stripes, II–IV with blackish-brown annulations; metatarsi I–IV with blackish-brown annulations. Abdomen yellowish white, anteriorly with blackish-brown stripe, with round blackish-brown spots located in median dorsal scu-

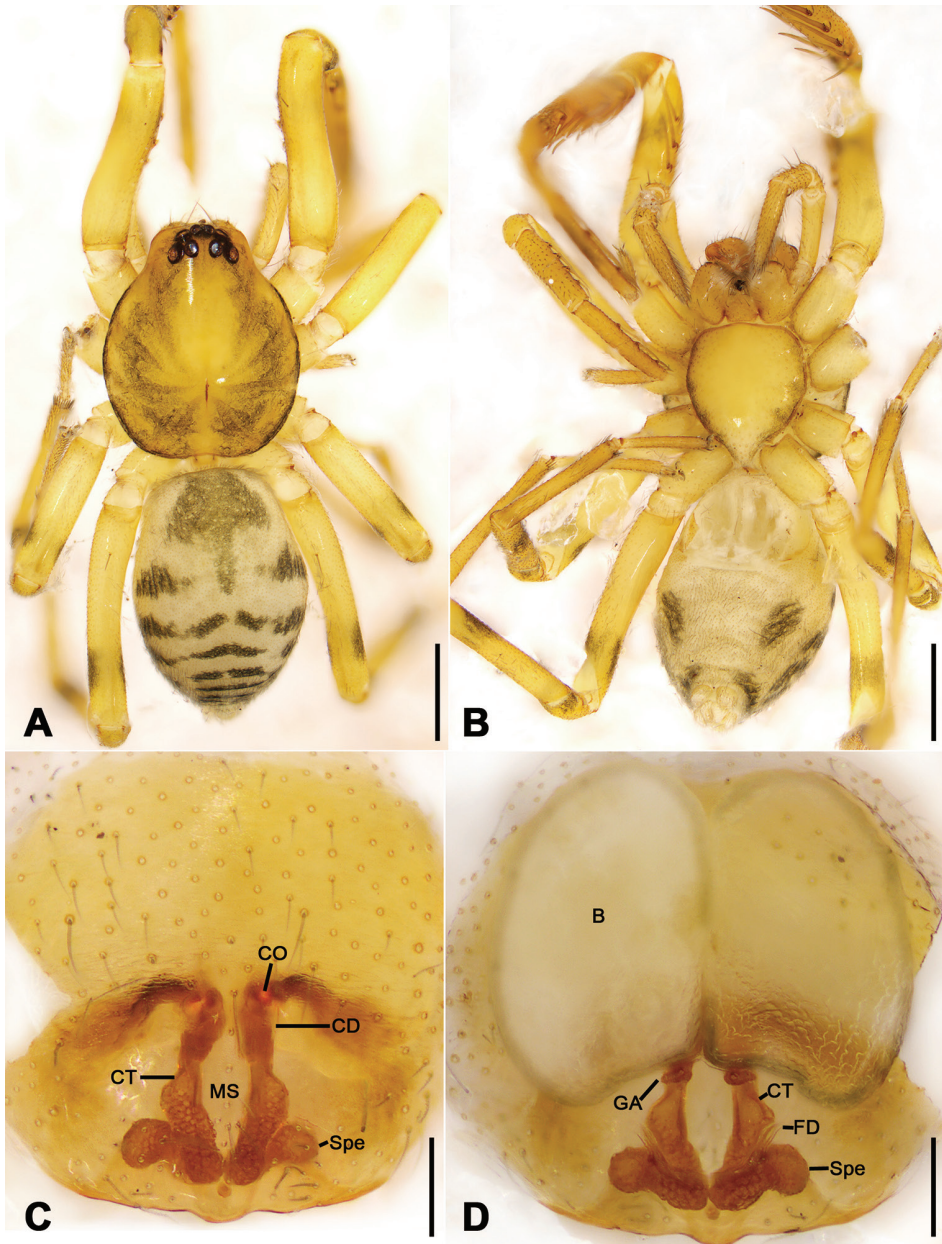


Figure 11. *Otacilia subfabiformis* sp. nov., female paratype. **A** habitus, dorsal view **B** same, ventral view **C** epigyne, ventral view **D** epigyne, dorsal view. Scale bars: 0.5 mm (**A**, **B**), 0.1 mm (**C**, **D**). Abbreviations: B – bursa, CD – copulatory duct, CO – copulatory opening, CT – connecting tube, FD – fertilization ducts, GA – glandular appendage, MS – median septum, Spe – spermathecae.

tum and pair of L-shaped blackish-brown stripes located at posterior of dorsal scutum, pair of oval blackish-brown spots on sub-median part, three blackish-brown stripes on posterior part; venter with pair of blackish-brown spots posterolaterally.

Palp (Figs 9C–F, 10). Femoral apophysis weakly sclerotized, width less than half of its length. Patella unmodified. Retrolateral tibial apophysis large, bending to posterior bulb, longer than tibia, with sharp apex. Dorsal tibial apophysis large, longer than tibia, with fine tip in retrolateral view. Sperm duct C-shaped, strongly sclerotized, around base of retrolateral tegular apophysis and embolus. Retrolateral tegular apophysis large, protruding retrolaterally, with narrow retrolateral part. Embolus short, spine-like.

Female (paratype). Habitus as in Fig. 11A, B. Total length 2.54, carapace 1.17 long, 1.02 wide. Eye sizes and interdistances: AME 0.06, ALE 0.07, PME 0.07, PLE 0.07, AME–AME 0.01, AME–ALE 0.01, PME–PME 0.06, PME–PLE 0.03, AME–PME 0.06, AME–PLE 0.11, ALE–ALE 0.28, PLE–PLE 0.37, ALE–PLE 0.05. MOA 0.18 long, frontal width 0.12, posterior width 0.20. Chelicerae (Fig. 11A, B) with three promarginal (proximal largest, distal smallest) and two retromarginal teeth (distal larger, with same base). Sternum (Fig. 11B) gradually pointed. Pedicel 0.10 long. Abdomen (Fig. 11A, B) 1.29 long, 0.92 wide. Leg measurements: I 4.07 (1.06, 0.42, 1.16, 1.02, 0.41); II 3.62 (0.80, 0.30, 1.06, 1.02, 0.44); III 2.98 (0.79, 0.34, 0.63, 0.75, 0.47); IV 4.21 (1.14, 0.36, 0.89, 1.21, 0.61). Leg spination (Fig. 11A, B): femur I with two dorsal spines, femora II, III, and IV with one dorsal spine each; femur I p111; tibiae I v2222222, II v222222; metatarsi I v2222, II v2222.

Colouration (Fig. 11A, B). Lighter than males. Abdomen, anteriorly with mushroom-like dark brown spot.

Epigyne (Fig. 11C, D). Epigynal plate tree-like, antero-medially with pair of concave copulatory openings, with sub-columnar median septum. Copulatory ducts, connecting tubes and spermathecae distinctly visible through integument in intact epigyne. Copulatory ducts relatively narrow, located between copulatory openings and glandular appendages, posteriorly with pair of large, bean-shaped, transparent bursae. Glandular appendages short, near base of bursae, located on anterior of connecting tubes. Connecting tubes slightly longer than copulatory ducts, located between glandular appendages and spermathecae, median part slightly expanded. Spermathecae globular peanut-shaped, touching. Fertilization duct long, anteriorly directed.

Distribution. Known only from the type locality in Jiangxi Province, China (Fig. 22).

***Otacilia wugongshanica* Liu, sp. nov.**

<http://zoobank.org/5E87C18C-ADCF-4CB8-890F-2EF2EBD34B1C>

Figures 12–14, 22

Type material. Holotype: ♂, China, Jiangxi Province, Ji'an City, Anfu County, Taishan Town, Wugong Mt., near the ticket office, 27°27'10.79"N, 114°11'8.24"E, 4 January 2020, leg. Ke-ke Liu et al. **Paratypes:** 2 ♂, 4 ♀, with same data as holotype; 3 ♀, 27°28'25.57"N, 114°12'39.24"E, 633 m, other data as holotype; 3 ♀, 27°28'07.98"N, 114°12'09.55"E, 800 m, other data as holotype; 2 ♂, 1 ♀, Anfu County, Taishan Town, Wenshan Village, Yangshimu Scenic Spot, Grand Canyon, 27°31'43.36"N, 114°14'32.97"E, 552 m, 5 January 2020, leg. Ke-ke Liu et al.

Etymology. The specific name refers to the type locality, Wugongshan; adjective.

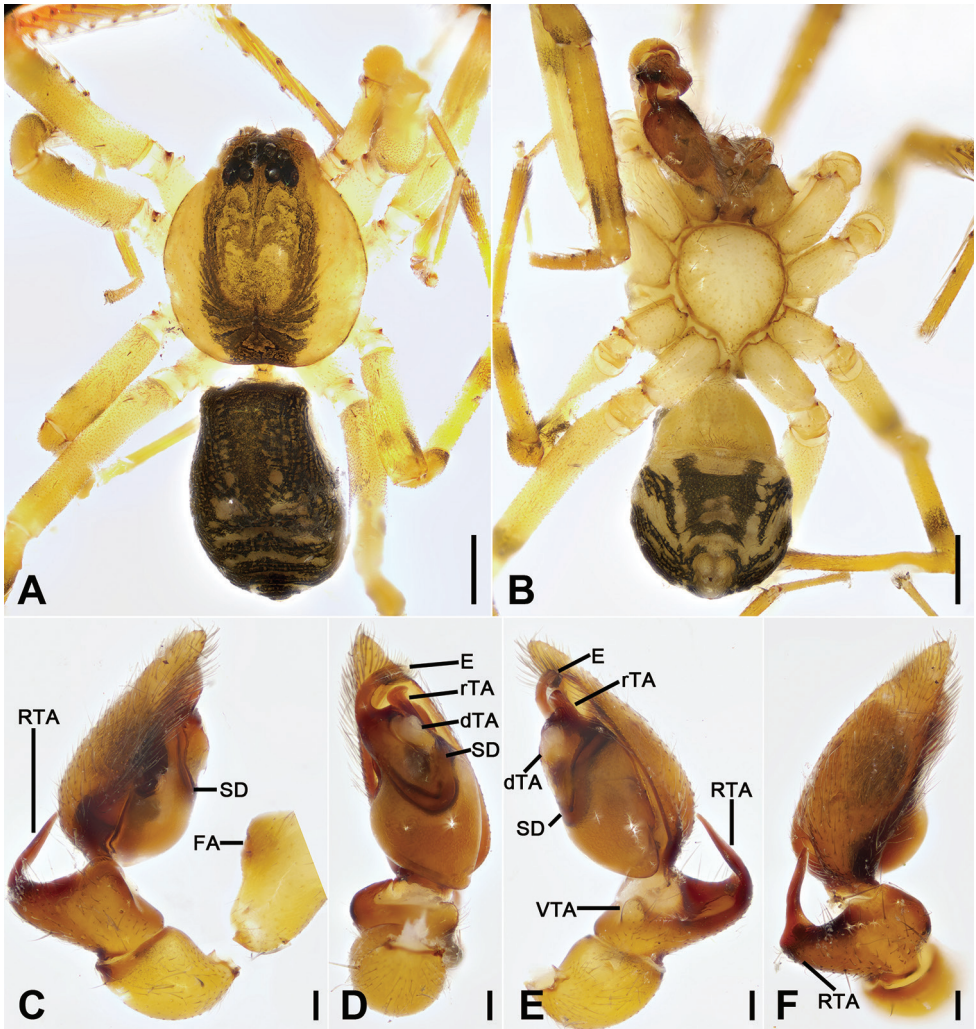


Figure 12. *Otacilia wugongshanica* sp. nov., male holotype. **A** habitus, dorsal view **B** same, ventral view **C** palp, prolateral view **D** same, ventral view **E** same, ventro-retrolateral view **F** same, dorsal view. Scale bars: 0.5 mm (**A**, **B**), 0.1 mm (**C**–**F**). Abbreviations: dTA – distal tegular apophysis, E – embolus, FA – femoral apophysis, RTA – retrolateral tibial apophysis, rTA – retrolateral tegular apophysis, SD – sperm duct, VTA – ventral tibial apophysis.

Diagnosis. The males of the new species are similar to *Otacilia dawuishan* Liu, Xu, Xiao, Yin & Peng, 2019 in having a strong hook-shaped embolus, thick retrolateral regular apophysis and a finger-like retrolateral tibial apophysis (see Liu et al. 2019: 441, fig. 3B–D), but can be separated from it by the distal tegular apophysis with an oval base (Figs 12D, 13A, B) (vs. with a round base and a mastoid-shaped retrolateral part), the V-shaped sperm duct (Figs 12D, E, 13A, B) (vs. C-shaped) and the retrolateral tibial apophysis with a sharply narrowed basal part (Fig. 12F) (vs. gradually

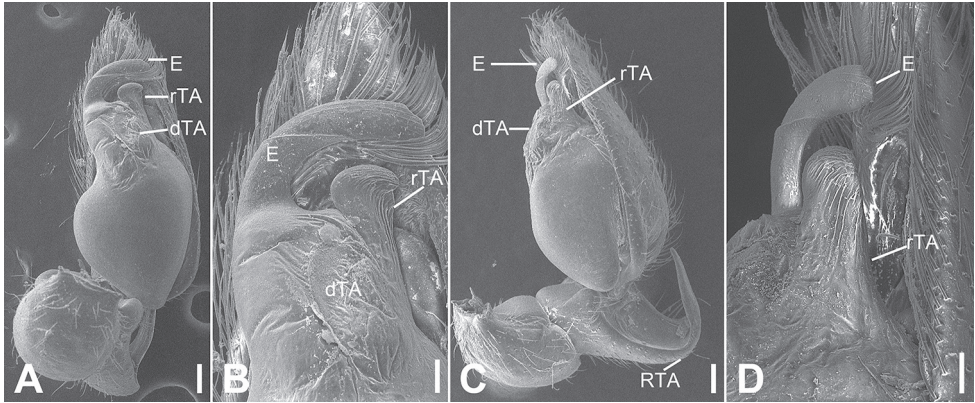


Figure 13. SEM micrographs of *Otacilia wugongshanica* sp. nov., palp of male holotype. **A** ventral view **B** same, detail of embolus, distal tegular apophysis and retrolateral tegular apophysis **C** vento-retrolateral view **D** same, detail of embolus and retrolateral tegular apophysis. Scale bars: 0.1 mm (**A, C**), 40 μ m (**B, D**). Abbreviations: dTA – distal tegular apophysis, E – embolus, RTA – retrolateral tibial apophysis, rTA – retrolateral tegular apophysis.

narrowed basal part). The females can be distinguished from *O. daweishan* (see Liu et al. 2019: 441, fig. 4B, C) by the narrowed median septum (Fig. 14C) (vs. broad, sub-triangular median septum) and the transverse epigynal sclerotized ridge (Fig. 14C) (vs. M-shaped).

Description. Male (holotype). Habitus as in Fig. 12A, B. Total length 3.52, carapace 1.74 long, 1.50 wide. Eye sizes and interdistances: AME 0.08, ALE 0.08, PME 0.07, PLE 0.09, AME–AME 0.05, AME–ALE 0.03, PME–PME 0.13, PME–PLE 0.07, AME–PME 0.10, AME–PLE 0.18, ALE–ALE 0.26, PLE–PLE 0.44, ALE–PLE 0.10. MOA 0.25 long, frontal width 0.21, posterior width 0.29. Cervical groove and fovea distinct. Chelicerae (Fig. 12A, B) with three promarginal (middle largest, distal smallest) and six retromarginal teeth (distal largest, third smallest). Sternum (Fig. 12B) with blunt posterior end. Abdomen (Fig. 12A, B) 1.73 long, 1.16 wide, weak dorsal scutum in anterior half. Leg measurements: I 7.31 (1.83, 0.60, 2.27, 1.80, 0.81); II 5.91 (1.55, 0.52, 1.64, 1.40, 0.80); III 5.00 (1.21, 0.50, 1.19, 1.28, 0.82); IV 7.72 (2.07, 0.60, 1.85, 2.25, 0.95). Leg spination (Fig. 12A, B): femur I with two dorsal spines, femora II–IV with one dorsal spine each; femora I pv1111, II pv11; tibiae I v22222222, II v2222222; metatarsi I v2222, II v222.

Colouration (Fig. 12A, B). Carapace yellow, with radial irregular dark stripes medially and arch-shaped dark stripes around margin. Chelicerae yellow-brown. Endites yellow. Labium yellow-brown. Sternum yellow. Legs yellow, with blackish-brown annulations on distal part of femora and tibiae. Abdomen dark brown, with pair of oval and pair of large irregular yellowish spots on posterior of dorsal scutum, three light chevron-shaped stripes in posterior part, and yellowish arch-shaped stripe in front of anal tubercle; venter with sub-trapezoid blackish-brown spot posteromedially and pair of sloping blackish-brown stripes posterolaterally.

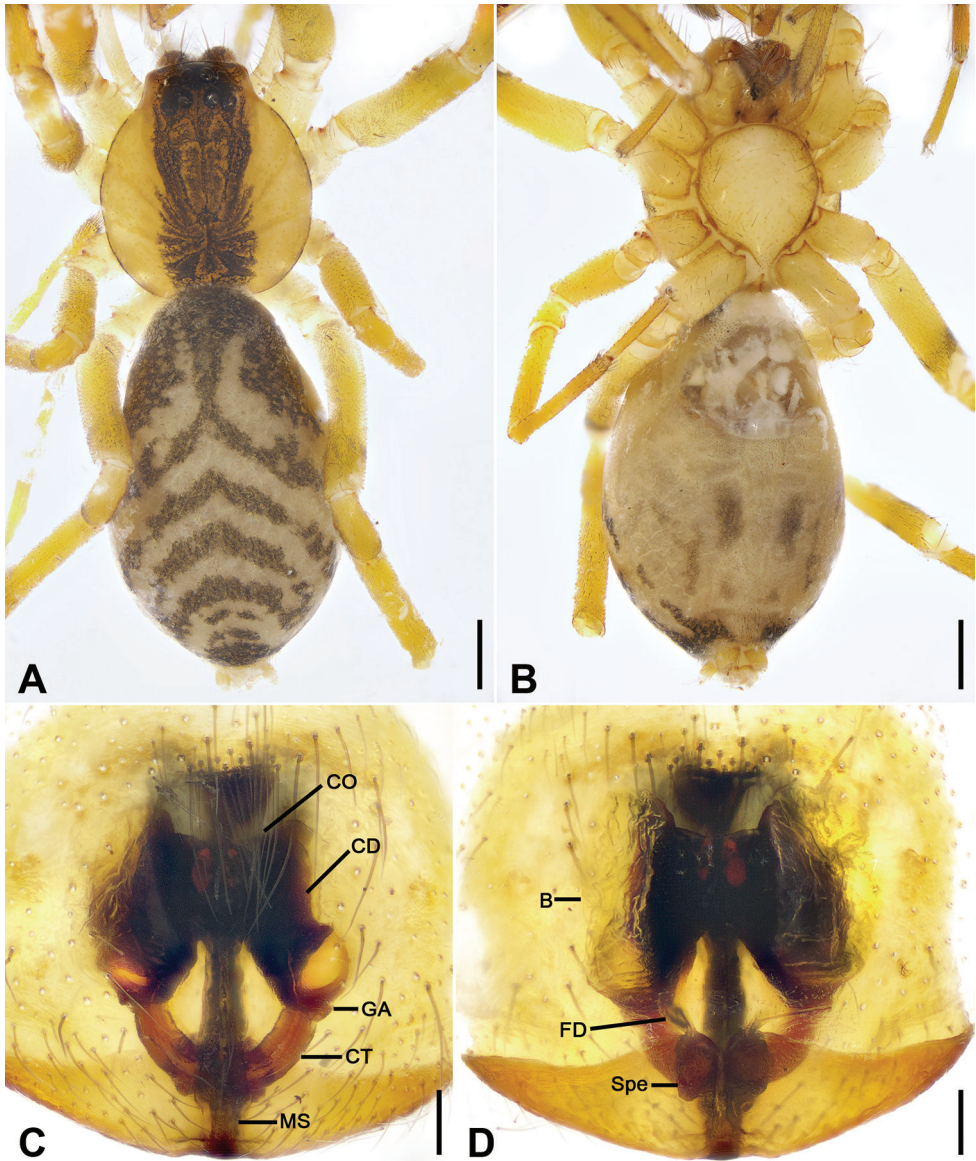


Figure 14. *Otacilia wugongshanica* sp. nov., female paratype. **A** habitus, dorsal view **B** same, ventral view **C** epigyne, ventral view **D** epigyne, dorsal view. Scale bars: 0.5 mm (**A, B**), 0.1 mm (**C, D**). Abbreviations: B – bursa, CD – copulatory duct, CO – copulatory opening, CT – connecting tube, FD – fertilization ducts, GA – glandular appendage, MS – median septum, Spe – spermathecae.

Palp (Figs 12C–F, 13). Femoral apophysis well-developed, width less than half of its length. Patella unmodified. Retrolateral tibial apophysis large, longer than tibia, finger-like, bending inwards towards the base of cymbium, with sharply narrowed basal part and slightly blunt tip. Ventral tibial apophysis small, blunt. Sperm duct V-

shaped, strongly sclerotized, around base of retrolateral tegular apophysis, distal tegular apophysis and embolus. Retrolateral tegular apophysis clavate, slightly shorter than embolus, apex slightly curved. Distal tegular apophysis triangular, with oval base, covering half of retrolateral tegular apophysis. Embolus thick, hook-shaped, with broad base and blunt tip.

Female (paratype). Habitus as in Fig. 14A, B. Darker than males (Fig. 14A, B). Total length 4.31, carapace 1.55 long, 1.53 wide. Eye sizes and interdistances: AME 0.09, ALE 0.1, PME 0.07, PLE 0.08, AME–AME 0.06, AME–ALE 0.03, PME–PME 0.14, PME–PLE 0.08, AME–PME 0.11, AME–PLE 0.19, ALE–ALE 0.28, PLE–PLE 0.42, ALE–PLE 0.12. MOA 0.25 long, frontal width 0.22, posterior width 0.29. Chelicerae (Fig. 14A, B) with three promarginal (middle largest, distal smallest) and seven retromarginal teeth (distal largest, 6th smallest). Abdomen (Fig. 14A, B) 2.58 long, 1.80 wide. Leg measurements (Fig. 14A, B): I 6.59 (1.70, 0.63, 2.07, 1.60, 0.59); II 5.86 (1.49, 0.62, 1.64, 1.35, 0.76); III 3.91 (1.03, 0.45, 0.87, 0.95, 0.61); IV 7.34 (1.86, 0.59, 1.82, 2.09, 0.98). Leg spination: femora I pv1111, II pv111; tibiae I v22222222, II v22222222.

Colouration (Fig. 14A, B). Abdomen dark brown, with pair of L-shaped yellowish stripes anteriorly and broad arc-shaped mottled stripes posteriorly.

Epigyne (Fig. 14C, D). Epigynal plate bow-shaped, anteriorly with transverse sclerotized ridge and strongly sclerotized fovea, anteromedially with pair of oval copulatory openings, posteromedially with narrowed median septum. Copulatory ducts, glandular appendages and connecting tubes distinctly visible through integument in intact epigyne. Copulatory ducts broad, slightly sloping, located between copulatory openings and glandular appendages, posteriorly with pair of large, bean-shaped transparent bursae. Glandular appendages short, partly covered by bursae, located on anterior of connecting tubes. Connecting tubes shorter than copulatory ducts, posterior part convergent. Spermathecae oval, touching. Fertilization ducts short, located apically on spermathecae, directed anterolaterally.

Distribution. Known only from the type locality in Jiangxi Province, China (Fig. 22).

***Otacilia yusishanica* Liu, sp. nov.**

<http://zoobank.org/0CD9F210-2A0D-4292-94F6-76F55F8EA7D2>

Figures 15–17, 22

Type material. Holotype: ♂, China, Jiangxi Province, Ji'an City, Xiajiang County, Yusi Mt., 27°33'05.52"N, 115°16'16.88"E, 202 m, 7 October 2019, leg. Ke-ke Liu et al. **Paratypes:** 5 ♂, 4 ♀, 4 juveniles, with same data as holotype.

Etymology. The specific name refers to the type locality, Yusishan; adjective.

Diagnosis. The males of the new species are similar to *Otacilia acutangula* Liu, 2020 in having a thick hook-shaped embolus, a C-shaped sperm duct and a finger-like retrolateral tibial apophysis (see Liu et al. 2020: 13, fig. 7C–F), but can be separated from it by the retrolateral tibial apophysis with a straight tip in retrolateral

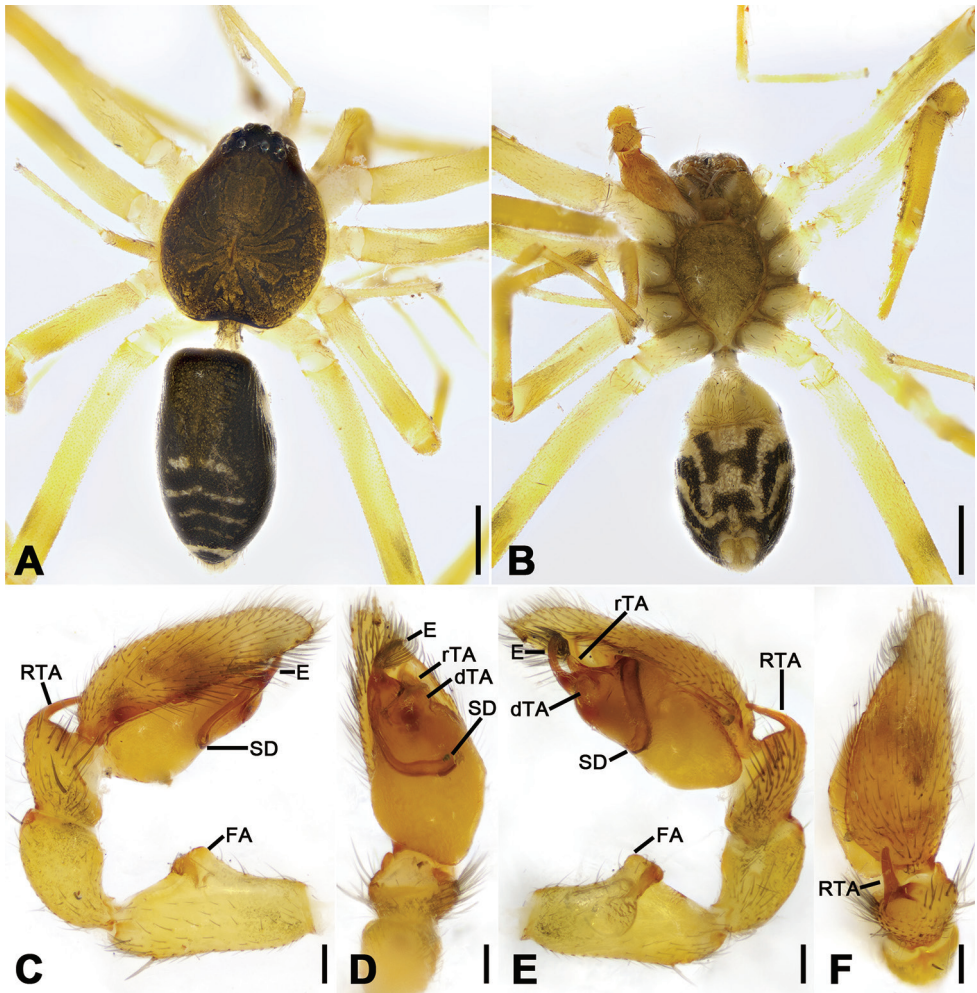


Figure 15. *Otacilia yusishanica* sp. nov., male holotype. **A** habitus, dorsal view **B** same, ventral view **C** palp, prolateral view **D** same, ventral view **E** same, ventro-retrolateral view **F** same, dorsal view. Scale bars: 0.5 mm (**A**, **B**), 0.1 mm (**C–F**). Abbreviations: dTA – distal tegular apophysis, E – embolus, FA – femoral apophysis, RTA – retrolateral tibial apophysis, rTA – retrolateral tegular apophysis, SD – sperm duct.

view (Figs 15D, E, 16A, B, D) (vs. with a slightly curved tip). The females resemble *O. acutangula* in having small bursae and thin connecting tubes (see Liu et al. 2020: 13, fig. 8C, D), but can be distinguished from it by the rectangular median septum (Fig. 17C) (vs. triangular) and the widely separated spermathecae (Fig. 17D) (vs. proximate spermatheca).

Description. Male (holotype). Habitus as in Fig. 15A, B. Total length 3.29, carapace 1.48 long, width 1.21 wide. Eye sizes and interdistances: AME 0.07, ALE 0.08, PME 0.06, PLE 0.07, AME–AME 0.05, AME–ALE 0.02, PME–PME 0.11, PME–PLE 0.06, AME–PME 0.09, AME–PLE 0.17, ALE–ALE 0.23, PLE–PLE 0.37,

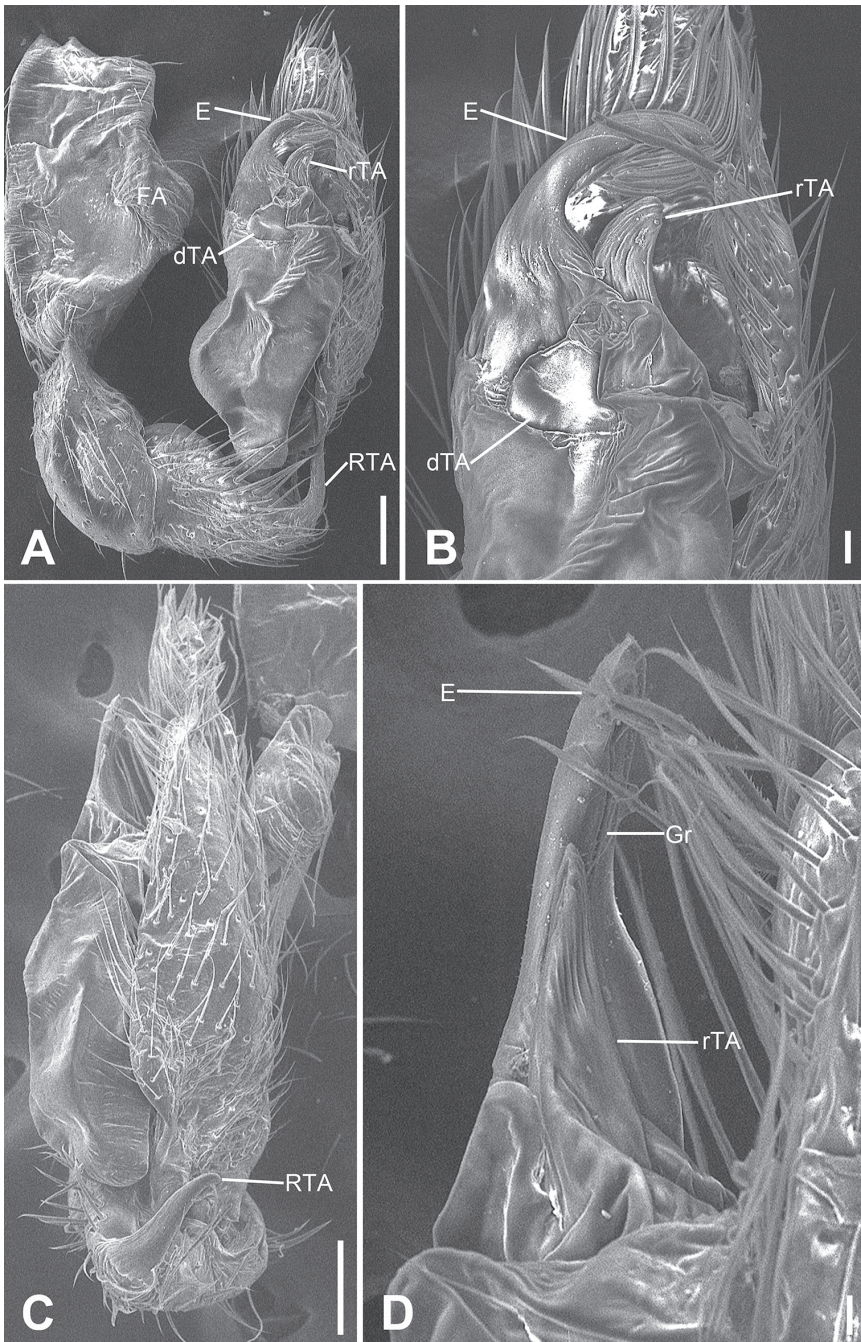


Figure 16. SEM micrographs of *Otacilia yusishanica* sp. nov., palp of male holotype. **A** ventral view **B** same, detail of embolus, distal tegular apophysis and retrolateral tegular apophysis **C** retro-dorsal view **D** same, detail of embolus, embolic groove and retrolateral tegular apophysis. Scale bars: 0.1 mm (**A, C**), 20 μ m (**B**), 10 μ m (**D**). Abbreviations: dTA – distal tegular apophysis, E – embolus, Gr – groove, RTA – retrolateral tibial apophysis, rTA – retrolateral tegular apophysis.

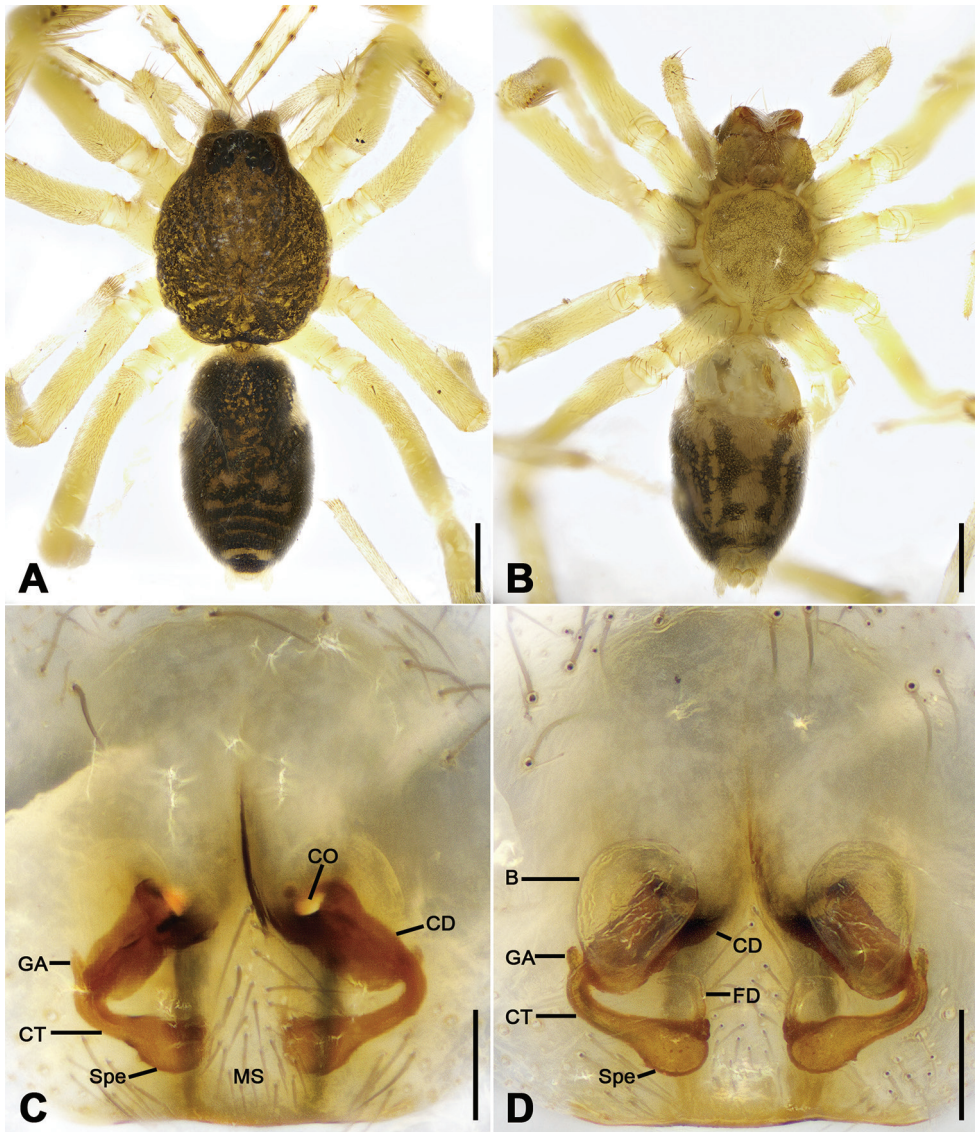


Figure 17. *Otacilia yusishanica* sp. nov., female paratype. **A** habitus, dorsal view **B** same, ventral view **C** epigyne, ventral view **D** epigyne, dorsal view. Scale bars: 0.5 mm (**A**, **B**), 0.1 mm (**C**, **D**). Abbreviations: B – bursa, CD – copulatory duct, CO – copulatory opening, CT – connecting tube, FD – fertilization ducts, GA – glandular appendage, MS – median septum, Spe – spermathecae.

ALE-PLE 0.10. MOA 0.24 long, frontal width 0.20, posterior width 0.25. Chelicerae (Fig. 15A, B) with three promarginal (proximal largest, distal smallest) and six retromarginal teeth (distal larger, others equal in size). Sternum (Fig. 15B) longer than wide. Pedicel 0.28 long. Abdomen (Fig. 15A, B) 1.58 long, 0.92 wide. Leg measurements: I 6.45 (1.65, 0.51, 1.94, 1.53, 0.82); II 5.13 (1.28, 0.53, 1.39, 1.18, 0.75); III

4.35 (1.12, 0.46, 0.94, 1.18, 0.65); IV 7.05 (1.92, 0.57, 1.67, 1.89, 1.00). Leg spination (Fig. 15A, B): femora I–IV with one dorsal spine each; femora I pv1111, II pv11; tibiae I v2222222, II v2222222; metatarsi I v2222, II v222.

Colouration (Fig. 15A, B). Carapace yellow-brown, with irregular, dark yellow, radial strips mediolaterally. Fovea distinct, black. Chelicerae, endites, labium, and sternum yellow-brown. Legs yellow, without dark annulations. Abdomen dark brown, with pair of pale stripes located at posterior of dorsal scutum, three light chevron-shaped stripes in posterior part and one yellowish arc-shaped stripe in front of anal tubercle; venter with H-shaped blackish-brown stripe posteromedially, pair of sloping blackish-brown stripes posterolaterally and N-shaped blackish-brown stripe posteriorly.

Palp (Figs 15C–E, 16). Femoral apophysis well-developed, width more than half of its length. Patella unmodified. Retrolateral tibial apophysis small, less than tibia length, bending inward toward base of cymbium, with straight tip in retrolateral view. Sperm duct C-shaped, strongly sclerotized, around base of subterminal apophysis and embolus. Distal regular apophysis, membranous, extruding retrolaterally, covering most of retrolateral regular apophysis. Embolus spine-like, thick, with broad base and blunt apex, embolic groove narrowed.

Female (paratype). Habitus as in Fig. 17A, B. Lighter than males. Total length 3.30, carapace 1.57 long, 1.35 wide. Eye sizes and interdistances: AME 0.07, ALE 0.06, PME 0.05, PLE 0.07, AME–AME 0.07, AME–ALE 0.04, PME–PME 0.10, AME–PME 0.10, AME–PLE 0.18, ALE–ALE 0.24, PLE–PLE 0.36, ALE–PLE 0.12. MOA 0.23 long, frontal width 0.19, posterior width 0.25. Chelicerae (Fig. 17A, B) with three promarginal (proximal largest, distal smallest) and five retro-marginal teeth (distal largest, second smallest, all teeth with a same base). Pedicel 0.10 long. Abdomen (Fig. 17A, B) 1.63 long, 1.00 wide. Leg measurements (Fig. 17A, B): I 6.87 (1.87, 0.61, 2.05, 1.61, 0.73); II 5.00 (1.27, 0.47, 1.41, 1.15, 0.70); III 4.49 (1.16, 0.51, 0.99, 1.06, 0.77); IV 7.09 (1.82, 0.61, 1.73, 2.00, 0.93). Leg spination (Fig. 17A, B): femora I pv1111, II pv11; tibiae I v22222222, II v22222222; metatarsi I v2222, II v2222.

Colouration (Fig. 17A, B). Darker than males. Abdomen, venter with two pairs of dark brown stripes posteriorly, median one touching.

Epigyne (Fig. 17C, D). Epigynal plate bow-like, anterior margin weakly sclerotized, arc-shaped, medially with pair of hole-shaped copulatory openings, posteriorly with rectangular median septum. Copulatory ducts, glandular appendages, connecting tubes and spermathecae distinctly visible through integument in intact epigyne. Copulatory ducts between copulatory openings and glandular appendages, sloping laterally, broad, short, posteriorly with pair of small, oval, transparent bursae. Glandular appendages short, located on anterior of connecting tubes, near base of bursae. Connecting tubes slightly shorter than copulatory ducts, slightly curved forwards. Spermathecae slightly expanded, elongated, separated by mark of median septum. Fertilization duct short, directed anterolaterally.

Distribution. Known only from the type locality in Jiangxi Province, China (Fig. 22).

***Otacilia zaoshiica* Liu, sp. nov.**

<http://zoobank.org/DA024E13-9A9F-412F-AFCB-93C9906AA61F>

Figures 18–20, 22

Type material. Holotype: ♂, China, Jiangxi Province, Ji'an City, Xingan County, Zaoshi Village, 27°46'15.63"N, 115°39'38.10"E, 589 m, 7 October 2019, leg. Ke-ke Liu et al. **Paratypes:** 4 ♂, 1 ♀, 4 juveniles, with same data as holotype.

Etymology. The specific name is derived from the type locality, Zaoshi village, which is one of the famous traditional villages; adjective.

Diagnosis. The males of the new species are similar to *O. yusishanica* sp. nov. described above in having a finger-like retrolateral tibial apophysis (Fig. 15C–F), but can be separated from it by the arc-shaped embolic base (Figs 18D, 19A, B) (vs. triangular)

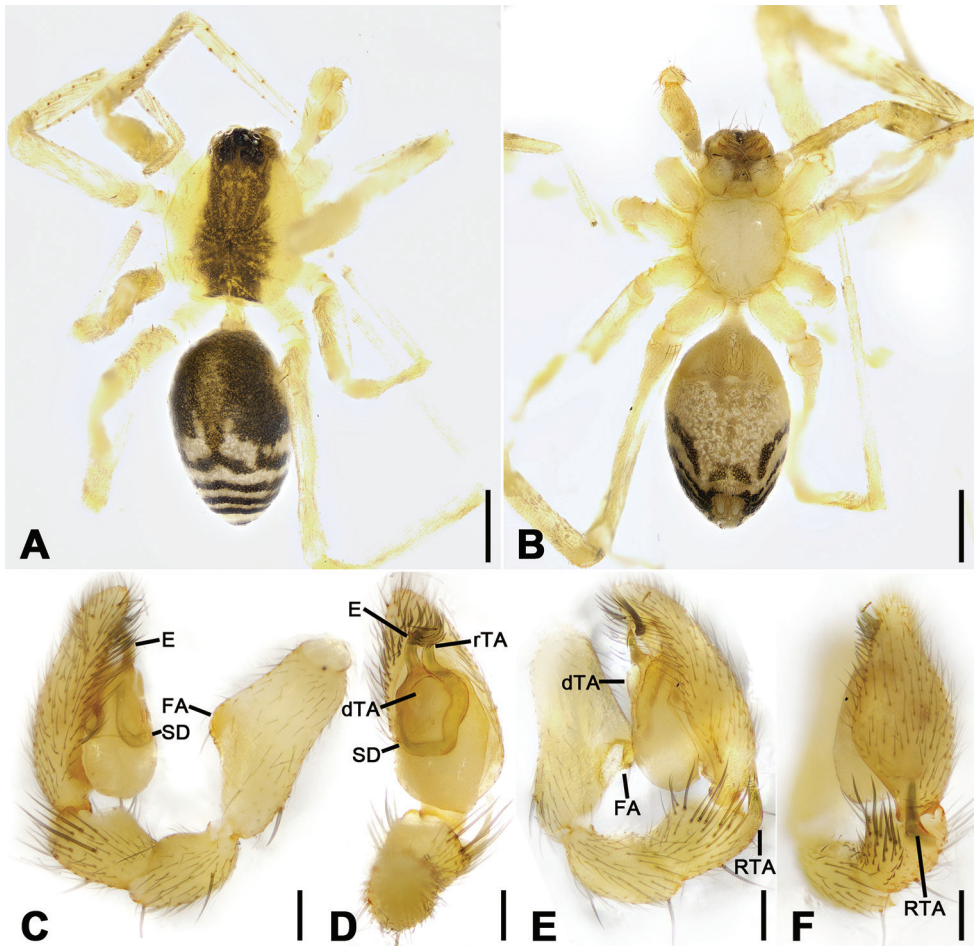


Figure 18. *Otacilia zaoshiica* sp. nov., male holotype. **A** habitus, dorsal view **B** same, ventral view **C** palp, prolateral view **D** same, ventral view **E** same, ventro-retrolateral view **F** same, dorsal view. Scale bars: 0.5 mm (**A, B**), 0.1 mm (**C–F**). Abbreviations: dTA – distal tegular apophysis, E – embolus, FA – femoral apophysis, RTA – retrolateral tibial apophysis, rTA – retrolateral tegular apophysis, SD – sperm duct.

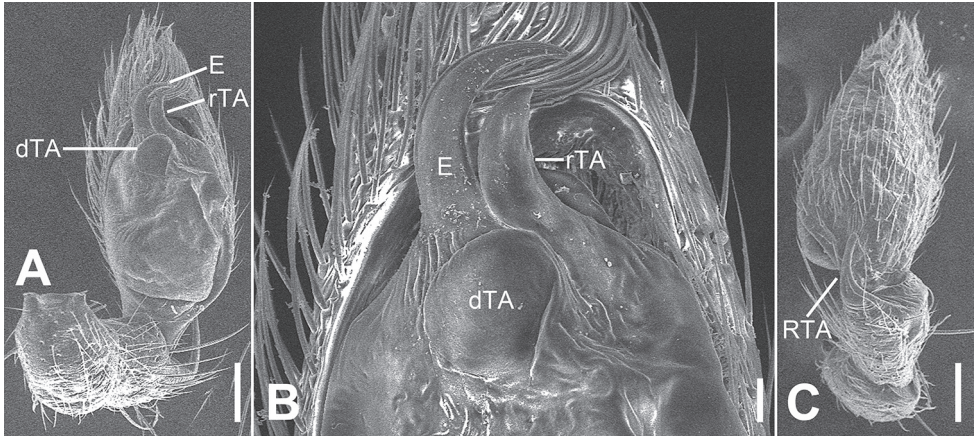


Figure 19. SEM micrographs of *Otacilia zaoshiica* sp. nov., palp of male holotype. **A** ventral view **B** same, detail of embolus, distal tegular apophysis and retrolateral tegular apophysis **C** dorsal view. Scale bars: 0.1 mm (**A, C**), 20 μ m (**B**). Abbreviations: dTA – distal tegular apophysis, E – embolus, RTA – retrolateral tibial apophysis, rTA – retrolateral tegular apophysis.

and the retrolateral tegular apophysis accompanied by the embolus (Figs 18D, 19A, B) (vs. separated). The females resemble *O. yusishanica* sp. nov. by having a broad median septum and the thin connecting tubes (Fig. 17C, D), but can be separated from it by the saddle-shaped copulatory openings (Fig. 20C) (vs. oval) and the spermatheca separated by approximately 1/3 of the median septum width (Fig. 20D) (vs. 2/3).

Description. Male (holotype). Habitus as in Fig. 18A, B. Total length 2.90, carapace 1.21 long, width 1.03 wide. Eye sizes and interdistances: AME 0.05, ALE 0.06, PME 0.05, PLE 0.06, AME–AME 0.07, AME–ALE 0.03, PME–PME 0.12, PME–PLE 0.05, AME–PME 0.10, AME–PLE 0.12, ALE–ALE 0.21, PLE–PLE 0.31, ALE–PLE 0.1. MOA 0.20 long, frontal width 0.15, posterior width 0.19. Chelicerae (Fig. 18A, B) with three promarginal (proximal largest, second smallest) and five retromarginal teeth (distal largest, second smallest). Sternum (Fig. 18B) longer than wide. Pedicel 0.21 long. Abdomen (Fig. 18A, B) 1.51 long, 0.86 wide. Leg measurements: I 4.92 (1.24, 0.41, 1.50, 1.06, 0.71); II 3.86 (1.08, 0.45, 1.04, 0.99, 0.30); III 3.11 (0.84, 0.31, 0.69, 0.83, 0.44); IV 5.75 (1.64, 0.43, 1.37, 1.59, 0.72). Leg spination (Fig. 18A, B): femora I–IV with one dorsal spine each; femora I pv1111, II pv11; tibiae I v2222222, II v2222222; metatarsi I v2222, II v2222.

Colouration (Fig. 18A, B). Carapace yellow, medially with broad dark brown mottled markings. Fovea distinct, black. Chelicerae, endites, labium and sternum yellow-brown. Legs yellow, without dark annulations. Abdomen dark brown, with pair of round and oval pale spots located at posterior of dorsal scutum and three light chevron-shaped stripes in posterior part, and one yellowish transversal stripe in front of anal tubercle.

Palp (Figs 18C–F, 19). Femoral apophysis well-developed, width more than half of its length. Patella unmodified. Retrolateral tibial apophysis large, longer than tibia, sword-like in ventral view, bending inward to base of cymbium, medial part widened and slightly curved, with strong spine-like tip. Sperm duct U-shaped, strongly scler-



Figure 20. *Otacilia zaoshiica* sp. nov., female paratype. **A** habitus, dorsal view **B** same, ventral view **C** epigyne, ventral view **D** epigyne, dorsal view. Scale bars: 0.5 mm (**A**, **B**), 0.1 mm (**C**, **D**). Abbreviations: B – bursa, CD – copulatory duct, CO – copulatory opening, CT – connecting tube, FD – fertilization ducts, GA – glandular appendage, MS – median septum, Spe – spermathecae.

rotized, around base of subterminal apophysis, distal tegular apophysis and embolus. Retrolateral tegular apophysis straight, broad, as long as embolus, anteriorly widened. Distal tegular apophysis membranous, fan-shaped, extending to median bulb. Embolus thick, hook-shaped, with broad base and blunt tip. Embolus relatively long, thick spine-like, with broad base and blunt apex.

Female (paratype). Habitus as in Fig. 20A, B. Lighter than males. Total length 3.07, carapace 1.36 long, 1.19 wide. Eye sizes and interdistances: AME 0.09, ALE

0.09, PME 0.08, PLE 0.08, AME–AME 0.04, AME–ALE 0.01, PME–PME 0.09, PME–PLE 0.06, AME–PME 0.06, AME–PLE 0.14, ALE–ALE 0.21, PLE–PLE 0.32, ALE–PLE 0.09. MOA 0.24 long, frontal width 0.20, posterior width 0.24. Chelicerae (Fig. 20A, B) with three promarginal (proximal largest, distal smallest) and six retromarginal teeth (distal largest, second smallest). Pedicel 0.17 long. Abdomen (Fig. 19A, B) 1.47 long, 0.97 wide. Leg measurements (Fig. 20A): I 5.63 (1.47, 0.51, 1.73, 1.25, 0.67); II 4.50 (1.20, 0.46, 1.25, 1.02, 0.57); III 3.84 (1.02, 0.43, 0.87, 0.93, 0.59); IV 6.14 (1.69, 0.55, 1.44, 1.71, 0.75). Leg spination (Fig. 20A, B): femora I pv1111, II pv111; tibiae I v22222222, II v2222222; metatarsi I v2222, II v222.

Epigyne (Fig. 20C, D). Epigynal plate mask-shaped, anterior margin slightly sclerotized, transverse, medially with pair of touching saddle-shaped copulatory openings, posteriorly with sub-trapezoidal median septum. Copulatory ducts, connecting tubes and spermathecae distinctly visible through integument in intact epigyne. Copulatory ducts between copulatory openings and glandular appendages, sloping laterally, proper broad, posteriorly with pair of large, oval, transparent bursae. Glandular appendages short, near the base of bursae. Connecting tubes slightly shorter than copulatory ducts, slightly curved backwards. Spermathecae slightly expanded, directed medially, separated by approximately 1/3 of median septum width. Fertilization ducts short, with semi-ovoid base, directed forward.

Distribution. Known only from the type locality in Jiangxi Province, China (Fig. 22).

***Otacilia ziyaoshanica* Liu, sp. nov.**

<http://zoobank.org/A2E72C0B-7B5C-4251-A47D-44451406E9C7>

Figures 21, 22

Type material. Holotype: ♀, China, Jiangxi Province, Ji'an City, Taihe County, Ziyao Mt., 26°42'49.38"N, 115°13'32.82"E, 198 m, 6 October 2019, leg. Ke-ke Liu et al.

Etymology. The specific name refers to the type locality, Ziyaoshan; adjective.

Diagnosis. The female of this species is similar to *Otacilia acutangula* Liu, 2020 and *O. macrospora* Fu, Zhang & Zhang, 2016 in having a M-shaped epigynal margin and concave anterior epigynal part (see Liu et al. 2020: 13, fig. 8C, D; Fu et al. 2016: 138, fig. 20, 21), but can be separated from them by the chelicerae with three retromarginal teeth (Fig. 21B) (vs. five in *O. acutangula* and *O. macrospora*) and the widely separated spermathecae (Fig. 21D) (vs. slightly separated in *O. acutangula* and *O. macrospora*).

Description. Female. Habitus as in Fig. 21A, B. Total length 3.45, carapace 1.60 long, 1.31 wide. Eye sizes and interdistances: AME 0.1, ALE 0.08, PME 0.06, PLE 0.08, AME–AME 0.05, AME–ALE 0.02, PME–PME 0.12, PME–PLE 0.06, AME–PME 0.08, AME–PLE 0.16, ALE–ALE 0.25, PLE–PLE 0.37, ALE–PLE 0.1. MOA 0.23 long, frontal width 0.23, posterior width 0.25. Chelicerae (Fig. 21A, B) with three promarginal (proximal largest, distal smallest) and three retromarginal teeth (distal largest, third smallest). Sternum (Fig. 21B), posteriorly proper blunt. Pedicel 0.14 long. Abdomen (Fig. 18A, B) 1.73 long, 1.20 wide. Leg measurements: I 6.20 (1.41, 0.57, 1.96, 1.50, 0.76); II 4.98 (1.07, 0.55, 1.51, 1.10, 0.75); III 4.39 (1.17, 0.39,

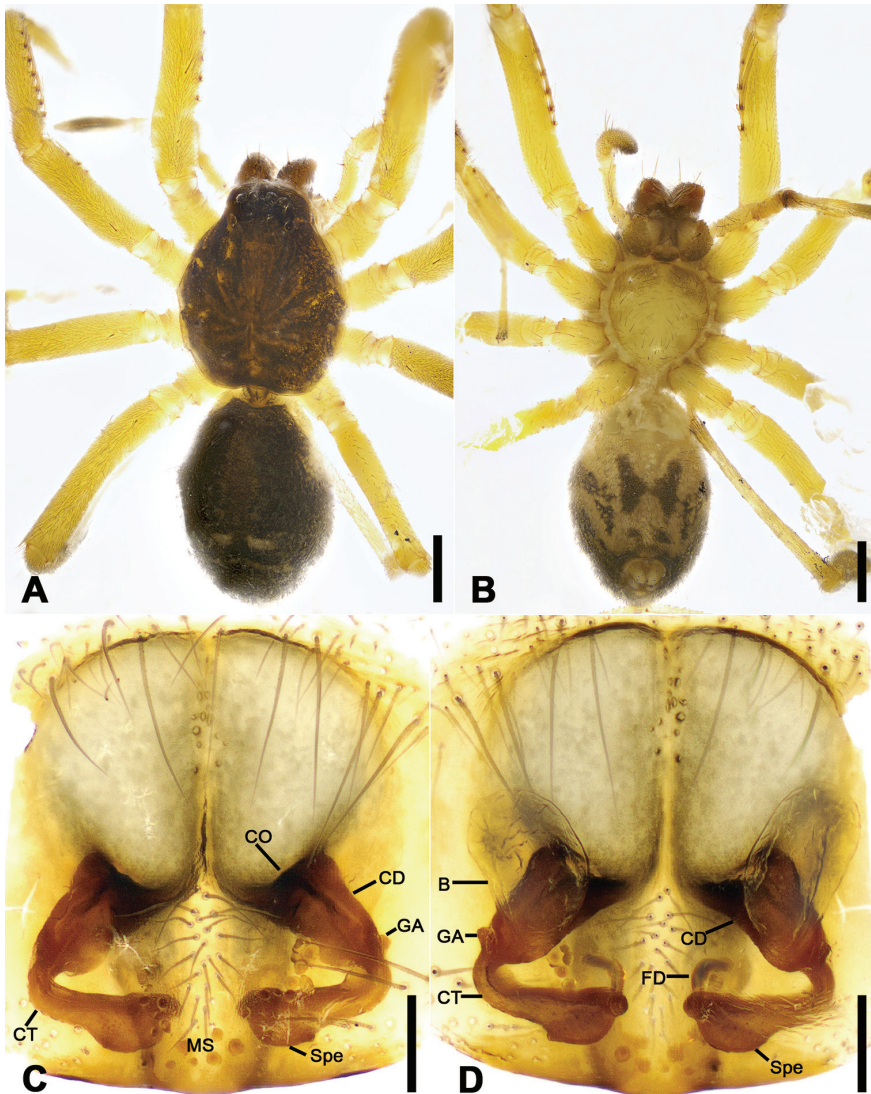


Figure 21. *Otacilia ziyaoshanica* sp. nov., female paratype. **A** habitus, dorsal view **B** same, ventral view **C** epigyne, ventral view **D** epigyne, dorsal view. Scale bars: 0.5 mm (**A**, **B**), 0.1 mm (**C**, **D**). Abbreviations: B – bursa, CD – copulatory duct, CO – copulatory opening, CT – connecting tube, FD – fertilization ducts, GA – glandular appendage, MS – median septum, Spe – spermathecae.

0.97, 1.17, 0.69); IV 6.63 (1.76, 0.59, 1.68, 1.64, 0.96). Leg spination (Fig. 18A, B): femora I–IV with 1 dorsal spine each; femora I p11111, p1111 (right), II p11; tibiae I v22222222, II v22222222; metatarsi I v2222, II v2222.

Colouration (Fig. 21A, B). Carapace yellow, with radial, irregular dark stripes mediolaterally. Sternum yellow, with yellow-brown margin. Legs yellow, without annula-

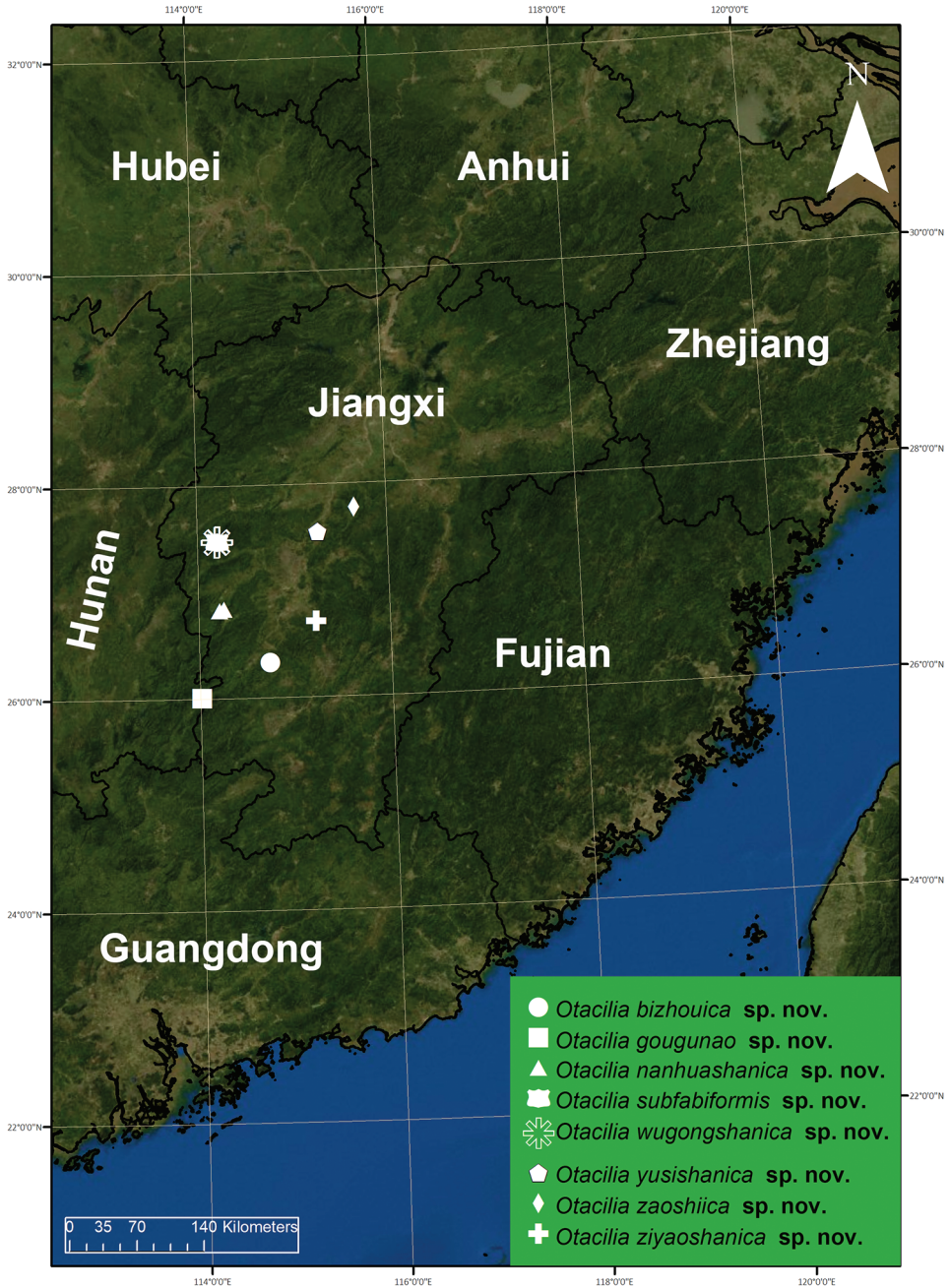


Figure 22. Records of *Otacilia bizhouica* sp. nov., *O. gougunao* sp. nov., *O. nanhuashanica* sp. nov., *O. subfabiformis* sp. nov., *O. wugongshanica* sp. nov., *O. yusishanica* sp. nov., *O. zaoshiica* sp. nov. and *O. ziyashanica*

tions on tibiae and distal part of femora, patellae and metatarsi. Abdomen brown, with abundant yellowish spots in dorsal view.

Epigyne (Fig. 21C, D). Epigynal plate mushroom like, anteriorly with M-shaped sclerotized margin, medially with pair of slit-like copulatory openings covered by epigynal plug, posteromedially with trapezoidal median septum. Copulatory ducts, glandular appendages, connecting tubes and spermathecae distinctly visible through integument in intact epigyne. Copulatory ducts short and broad, posteriorly with pair of large, oval, transparent bursae. Glandular appendages short, located on anterior of connecting tubes, near base of bursae. Connecting tubes longer than copulatory ducts, convergent. Spermathecae slightly expanded, separated by approximately 1/2 of median septum width. Fertilization ducts short, directed antero-laterally.

Male unknown.

Distribution. Known only from the type locality in Jiangxi Province, China (Fig. 22).

Discussion

At present, the genus *Otacilia* has an exclusively Asian distribution, with the highest number of species found in the subtropical and tropical areas of China. Up to now, 89 species of *Otacilia* are known from China, including the eight new species described above (WSC 2020). During the past six years, we focused on the sac spiders of South China, in areas such as the Guangxi Zhuang Autonomous Region, Guang Dong Province, Hunan Province and Jiangxi Province, and found that most *Otacilia* species live in mountainous regions and hills over 200 metres above sea level (Liu et al. 2019, 2020). Ji'an City is located at the middle section of the Luoxiao Mountains in South China, which is mainly surrounded by hilly topography. Many new *Otacilia* species have been found and recorded from different mountains in this area (Liu et al. 2019, 2020). It is interesting to note that these new species, including those newly described here, clearly appear on different mountains or different aspects of a single mountain. It is likely that the total number of known species of *Otacilia* will rapidly rise to 100 by the end of 2021, as our survey is focused on sac spiders. These results suggest that Jiangxi Province has a spectacular diversity of *Otacilia* and that it is necessary to continue surveying it in the future.

Acknowledgements

This paper benefited greatly from the helpful comments of Charles R. Haddad (subject editor) (Bloemfontein, Republic of South Africa), Dragomir Dimitrov (Sofia, Bulgaria) and Alireza Zamani (Turku, Finland). We thank Hui-pu Luo and Ze-yuan Meng (from Jinggangshan University) for their assistance during the field work. We also thank Nathalie Yonow for improving the English of the manuscript. This study was supported by the Natural Science Foundation of Jiangxi Province (20181BAB214008),

the Science and Technology Innovation Project for College Students, the Science and Technology Foundation of Jiangxi Provincial Department of Education (GJJ190543) and the Natural Science Foundation of China (31560592).

References

- Fu L, Zhang ZS, Zhang F (2016) Description of two new *Otacilia* species from Anhui, China (Araneae, Phrurolithidae). *Acta Zoologica Academiae Scientiarum Hungaricae* 62(2): 133–142. <https://doi.org/10.17109/azh.62.2.133.2016>
- Hu DS, Zhang F (2011) Description of a new *Otacilia* species from China, with transfer of two species from the genus *Phrurolithus* (Araneae: Corinnidae). *Zootaxa* 2993: 59–68. <https://doi.org/10.11646/zootaxa.2993.1.4>
- Jäger P, Dimitrov D (2019) *Otacilia fansipan* spec. nov., the second congener recorded from Vietnam (Arachnida: Araneae: Phrurolithidae). *Zootaxa* 4464(2): 233–240. <https://doi.org/10.11646/zootaxa.4664.2.5>
- Jäger P, Wunderlich J (2012) Seven new species of the spider genus *Otacilia* Thorell 1897 (Araneae: Corinnidae) from China, Laos and Thailand. *Beiträge zur Araneologie* 7: 251–271, 352–357.
- Liu KK, Xu X, Xiao YH, Yin HQ, Peng XJ (2019) Six new species of *Otacilia* from southern China (Araneae: Phrurolithidae). *Zootaxa* 4585(3): 438–458. <https://doi.org/10.11646/zootaxa.4585.3.2>
- Liu KK, Luo HP, Ying YH, Xiao YX, Xu X, Xiao YH (2020) A survey of Phrurolithidae spiders from Jinggang Mountain National Nature Reserve, Jiangxi Province, China. *ZooKeys* (in press). *ZooKeys* 947: 1–37. <https://doi.org/10.3897/zookeys.947.51175>
- World Spider Catalog. (2020) World Spider Catalog. Natural History Museum Bern. Version 21.0. Available from: <https://wsc.nmbe.ch/> (accessed 7 July 2020).
- Zamani A, Marusik YM (2020) A survey of Phrurolithidae (Arachnida: Araneae) in southern Caucasus, Iran and Central Asia. *Zootaxa* 4758(2): 311–329. <https://doi.org/10.11646/zootaxa.4758.2.6>

First record of the subfamily Epitraninae from Saudi Arabia (Hymenoptera, Chalcidoidea, Chalcididae), with the description of three new species

Neveen S. Gadallah¹, Ahmed M. Soliman^{2,3}, Hathal M. Al Dhafer²

1 Entomology Department, Faculty of Science, Cairo University, Giza, Egypt **2** Plant Protection Department, College of Food and Agriculture Sciences, King Saud University, P.O. BOX 2460, Riyadh 11451, Saudi Arabia **3** Zoology Department, Faculty of Science (Boys), Al-Azhar University, P.O. Box 11884, Nasr City, Cairo, Egypt

Corresponding author: Ahmed M. Soliman (amsoliman@ksu.edu.sa; ammsoliman@gmail.com)

Academic editor: K. van Achtenberg | Received 13 March 2020 | Accepted 23 September 2020 | Published 27 October 2020

<http://zoobank.org/2B5B9363-B75C-4392-A23A-78186989B7F3>

Citation: Gadallah NS, Soliman AM, Al Dhafer HM (2020) First record of the subfamily Epitraninae from Saudi Arabia (Hymenoptera, Chalcidoidea, Chalcididae), with the description of three new species. ZooKeys 979: 35–86. <https://doi.org/10.3897/zookeys.979.52059>

Abstract

The monotypic subfamily Epitraninae Burks, 1936 (Hymenoptera: Chalcidoidea, Chalcididae) is reported for the first time in Saudi Arabia. Seven *Epitranus* species are recorded in the Southwestern and Central regions of the Kingdom of Saudi Arabia, of which three species are new: *E. delvarei* Soliman & Gadallah, **sp. nov.** (female & male), *E. similis* Gadallah & Soliman, **sp. nov.** (male), and *E. subinops* Soliman & Gadallah, **sp. nov.** (female), are described and illustrated. Four new records, *E. clavatus* (Fabricius), *E. hamoni* complex, *E. inops* Steffan, and *E. torymoides* (Risbec), are also reported. An illustrated key to species is provided.

Keywords

Afrotropical, Arabian Peninsula, *Epitranus*, new records, new species

Introduction

Epitraninae Burks was first treated as tribe Chalcitellini by Ashmead (1904) with the type genus *Chalcitella* Westwood. This tribe was renamed Epitranini by Burks (1936) when the genus *Chalcitella* was treated as a junior synonym of *Epitranus* Walker. Habu (1960) raised Epitranini to the subfamily rank, Epitraninae, based on the fact that this group differs completely in its morphological characters from any other tribal taxa. The controversial taxonomic history of Epitraninae is well discussed by Bouček (1982). From the phylogenetic point of view, Epitraninae was treated as a tribe in the subfamily Dirhininae by Heraty et al. (2013) based on both morphological and molecular data. On the other hand, a recent phylogenetic study was carried out by Cruaud et al. (2020), treated it as a separate subfamily among the family Chalcididae, based on recent morphological and molecular data with novel computational approaches.

Members of Epitraninae are easily recognized by the following combination of characters: absence of cephalic horns; antennae inserted at lowermost part of face, very near to oral fossa on a protrusion or, most often, on a protruding lobe of frons “frontal lobe” (wrongly named clypeus by some authors), masking clypeus; frontal lobe with its free margin either rounded or denticulate, and may be divided by inter-antennal lamella; frons more or less flat; gena with strong posterior carina that extends into a flange; mesoscutellum simple, strongly convex and rounded at posterior margin; propodeum horizontal, its sculpturing clear and well-marked, areola often present medially; tegula flattened sometimes extends into a flange posteriorly to overlap base of hind wing; marginal vein of fore wing extremely long relative to the short stigmal vein and the reduced or absent postmarginal vein; metafemur with a comb of contiguous small teeth or spaced teeth following a large more or less triangular basal tooth; metatibia ending in a curved tibial spine, with a distinct tarsal scrobe, varying in length, that extends to reach a proximal sub-basal prominence; metasoma with a long narrow, striated petiole, several times as long as wide, or in some cases may be longer than half length of the gaster; gastral body rather small, compressed from side-to-side, and bulging ventrally, first gastral tergite occupying almost the total part of metasoma, thus mostly concealing the remaining tergites (Steffan 1957; Bouček 1982, 1988; Husain and Agarwal 1982; Narendran and van Achterberg 2016; Delvare 2017).

Sexual dimorphism is only slight (Bouček 1982). In the female, the metasoma is somewhat acuminate distally, with a pair of short dark ovipositor sheaths, the hypopygium ends at a short distance before the ovipositor sheaths (in male, the metasoma is shorter and blunt distally); in female the antenna shorter, more or less clavate, with apical flagellomeres shorter (in male, the antenna longer and filiform, with longer flagellomeres) (Bouček 1982).

All Epitraninae are now classified in a unique genus, *Epitranus* Walker (Bouček 1982, 1988; Narendran and van Achterberg 2016; Delvare 2017; Noyes 2019), which in turn comprises currently a total of 68 described species (Noyes 2019). The genus had been pulverized into several genera (see Bouček 1982, 1988), latter considered as synonyms by Burks (1936) and then Bouček (1982).

Little is known about the biology of Epitraninae. Hosts are known from only seven Oriental (Bouček 1982, 1988; Narendran 1989; Narendran and van Achterberg 2016; Noyes 2019), and a single Afrotropical species (Sauphanor et al. 1987). All of them parasitizing small lepidopteran moths of the families Crambidae, Pyralidae and Tineidae (Bouček 1982, 1988; Sauphanor et al. 1987; Narendran 1989; Narendran and van Achterberg 2016; Noyes 2019). This is in addition of two records, *E. chilkaensis* (Mani) reared from a nest of *Camponotus compressus* (Formicidae) (Narendran 1989) and *E. emissicius* Steffan that was found as living in subterranean nests of *Mastotermes* sp. (Mastotermitidae) (Rasplus 1993). Other few species are reported as having economic importance attacking lepidopteran pests infesting stored products (Sauphanor et al. 1987). Adults can be seen on foliage of trees and shrubs, and collected from fonds of woody plants, but usually not on grass (Bouček 1982, 1988). The relatively large ocelli in some species suggests their activity at dusk or even at night (Bouček 1982).

More than half number of *Epitranus* species are Oriental in distribution (54.65%) (Bouček 1982; Narendran and van Achterberg 2016), followed by the Afrotropical region (38%) (Schmitz 1946 under *Anacryptus*; Steffan 1957; Noyes 2019) and very little are Australasian (7.35%) (Girault 1913, 1914, 1915). Burks (1936) suggested their presence even in the Nearctic region, based on the proximity of Florida to St. Vincent and Cuba, where *Epitranus* species were found.

Concerning the fauna of the Arabian Peninsula, the only work dealing with this group, was that by Delvare (2017) in his revision of the whole family (Chalcididae) in the United Arab Emirates. He reported two *Epitranus* species, *E. hamoni* (Risbec) and *E. torymoides* (Risbec).

The present study is the first attempt to study the Epitraninae of the fauna of the Saudi Arabia. Four new records, *E. clavatus* (Fabricius), *E. hamoni* complex, *E. inops* Steffan, and *E. torymoides* (Risbec), as well as three new species are described and illustrated, *E. delvarei* sp. nov., *E. similis* sp. nov. and *E. subinops* sp. nov. A key to separate the species, as well as faunistic list are also provided.

Materials and methods

The present study is based on specimens collected from some mountains and wadis in Al-Baha, Asir and Jazan (southwestern regions of Saudi Arabia) and Riyadh (central region of Saudi Arabia) provinces (Fig. 31). Sampling was done by means of a sweeping net, vacuum machine (McCulloch GBV325 vacuum), and Malaise trap. Identifications of some species were done with the help of Gerard Delvare (Cirad, Montferrier-sur-Lez, France) during the visit of NG to Cirad, Montpellier. In addition, the authors used the keys and original descriptions of Schmitz (1946), Steffan (1957), and Bouček (1982). Morphological terms follow Bouček (1988). The terminology of body sculpture follows Harris (1979). Photographic images were taken using a Canon EOS 70D camera attached to a LEICA MZ-125 stereomicroscope. Individual source images were then stacked using HeliconFocus v6.22 (HeliconSoft Ltd) extended depth of field software.

Measurements were made with the help of an ocular micrometer. Further image processing was done using the software Adobe Photoshop CS5.1 (ver. 12.1x32) and Adobe Photoshop Lightroom 5.2 Final [ChingLiu]. The type specimens of the new species are deposited in King Saud University Museum of Arthropods (**KSMA**), Plant Protection Department, College of Food and Agriculture Sciences, King Saud University, Riyadh, Saudi Arabia. A representative of *E. torymoides* is kept in Efflatoun's Collection (EFC), Entomology Department, Faculty of Science, Cairo University, Giza, Egypt.

Abbreviations

AOL = Distance between median and lateral ocelli; **F1, F2, F3, F7** = first, second, third & seventh funicular segments; **Gt** = gastral tergite; **MPS** = multiparous plate sensilla; **MV** = marginal vein of fore wing; **OD** = lateral ocellus diameter; **OOL** = distance between lateral ocellus and inner eye margin; **POL** = distance between lateral ocelli; **SMV** = submarginal vein; **STV** = stigmal vein.

Systematic accounts

Epitranus Walker, 1834

For a complete list of synonyms, see Bouček (1982, 1988).

Key to species of the genus *Epitranus* in Saudi Arabia (mostly based on females)

- 1 *Both sexes*. Fore wing almost lacking venation, only base of SMV visible (Fig. 29C); flagellum between pedicel and clava with 7 flagellomeres, the two basal ones without MPS (Fig. 29B); frontal expansion not much developed, its ventral edge rounded and lacking indentations (Fig. 29A) ***Epitranus torymoides* (Risbec)**
- *Both sexes*. Fore wing with complete venation (e.g., see Fig. 3C); flagellum with 8 flagellomeres between pedicel and clava, only the transverse basal one (anellus) lacking MPS (e.g., Fig. 2D); frontal expansion absent (e.g., see Fig. 2B) or well developed and distinctly protruding (e.g., see Fig. 7B) **2**
- 2 *Both sexes*. Metafemur ventrally with at least 11 teeth following the large basal tooth, all teeth small, similar and contiguous (e.g., see Fig. 4A, B) **3**
- *Both sexes*. Metafemur ventrally with at most 9 teeth following the large basal one, the sub-basal teeth relatively larger than in alternate and more widely spaced (e.g., see Fig. 8D, E) **5**
- 3 Metatibia with oblique carina inside metatibial process (Fig. 13B); tarsal scrobe almost reaching sub-basal prominence (Fig. 13B); frons with supra antennal surface completely delimited by a step-like margin; mesoscutum with short setae and very small and sparse punctures on anterior third of middle lobe (Fig. 11E); bottom of punctures on mesonotum and metepimeron smooth (Figs 11E, 12B) ***Epitranus subinops* sp. nov.**

- Metatibial process without such carina (Figs 4B, 27C); tarsal scrobe shorter (Fig. 27C) or bottom of punctures granulate (densely reticulate) on mesonotum and metepimeron (Figs 2E, 3B); supra antennal surface at most delimited laterally, sometimes undifferentiated; mesoscutum with setae longer and punctures denser and coarser on the whole middle lobe (Figs 2E, 25B) **4**
- 4. Bottom of punctures granulate (densely reticulate) on mesoscutellum and metepimeron (Figs 2E, 3B); interspaces between punctures coriaceous (engraved network) on mesoscutum (Figs 2E, 3B); metatibia with tarsal scrobe almost reaching sub-basal prominence (Fig. 4B); mesoscutellum convex, its dorsal outline curved in lateral view (Figs 2E, 3B); no differentiated supra antennal surface ***Epitranus delvarei* sp. nov.**
- Bottom of punctures and interspaces smooth on mesonotum and metepimeron (Fig. 25A, B); tarsal scrobe of metatibia far from reaching sub-basal prominence (Fig. 27C); mesoscutellum flattened, its dorsal outline straight in lateral view (Fig. 25A, B); supra antennal surface delimited laterally by faint step-like margin ***Epitranus inops* Steffan**
- 5 *Both sexes.* Frontal expansion reduced to a transverse carina, hence clypeus visible in frontal view (Figs 18B, 22A); frons entirely densely and faintly reticulate and bearing very short, hardly discernible setae (Figs 18A, 22A); whole mesosoma, including shallow punctures and interspaces on mesonotum, bottom of areolae on propodeum, granulate (densely reticulate), thus appearing dull (Figs 18D, 20B, 21B, 24B), and metatibia with extremely weak sub-basal prominence (Fig. 19B); head and mesosoma partly testaceous (Figs 18A, D, 20B, 21A, B). *Female.* Interantennal projection expanded only as a small lamina. *Male.* Scape with deep and setose sub-basal excavation but lacking any dorsal row or patch of setae (Figs 22B, 24A)..... ***Epitranus hamoni* complex**
- *Both sexes.* Frontal expansion clearly expanded, overlapping clypeus (Figs 7B, 15B); upper frons and adorbital area alutaceous and with setiferous punctures (Figs 7A, 15A); interspaces or bottom of punctures on mesonotum smooth (Figs 7E, 14B), and metatibia with evident sub-basal prominence (Figs 8E, 16B); head and mesosoma with different pattern of color, partly reddish (Figs 7A, E, 14A, B). *Female.* Interantennal projection either expanded as a raised lamina (Fig. 15A) or completely absent (Fig. 7B). *Male.* Scape without such excavation but frequently with a row or brush setae dorsally (Fig. 6A) **6**
- 6 *Male.* Frontal expansion quite protruding with subantennal distance 3.7–4.5× as long as interantennal distance (Fig. 7B); expansion sub-trapezoidal in shape as its sides are straight and regularly converging ventrally (Fig. 7B); expansion otherwise bearing thick, lanceolate and whitish setae on either side of median carina, with deep submedian indentations on ventral edge (Fig. 7B); interantennal lamina absent (Fig. 7B); long, lanceolate and golden setae present on occiput (here sparsely) (Fig. 7C) and on pronotal collar (here as a double patch) (Fig. 7C); mesosoma with patches of long, lanceolate and silvery setae on pronotum above lateral panel, scapula, axilla, metepimeron, and on pre-spiracular areola of propodeum (Figs 7E, 8B) and with dense setation

masking integument beneath mesosoma and metacoxa (Fig. 6C); pronotal lateral carina extended dorsally on collar (Fig. 7E); propodeum with a Y-like raised carina mesally (Fig. 8A); metatibia with tarsal scrobe deep and smooth throughout, clearly reaching sub-basal prominence (Fig. 8E), metatibial process without oblique carina (Fig. 8E) *Epitranus similis* sp. nov.

- *Both sexes*. Frontal lobe less protruding than in alternate with subantennal distance ca. 1.7× as long as interantennal distance, without median longitudinal carina and lacking such setation, submedian indentations shallow and sides of expansion very slightly convex (Fig. 15B); interantennal lamina present (Fig. 15B); mesosoma without the setation as described above, the setae everywhere short and hair-like (Fig. 14A, B); pronotal carina restricted to sides (Fig. 14B); propodeum with median areola complete, somewhat tapering anteriorly (Fig. 15D); tarsal scrobe of metatibia not quite reaching sub-basal prominence and metatibial process with an oblique carina (Fig. 16C) *Epitranus clavatus* (Fabricius)

Description of the new species

Epitranus delvarei Soliman & Gadallah, sp. nov.

<http://zoobank.org/FC3FE0A6-CA05-4FBC-A6B1-85EF87E13E0C>

Figures 1–5

Type material. *Holotype* ♀: **Kingdom of Saudi Arabia**, Asir, Abha, Garf Raydah Natural Reserve [18°11'41"N, 42°23'45"E, Alt. 1865 m], sweeping net, 12.IV.2019, leg. Ahmed M. Soliman [KSMA]. *Paratypes*: 1 ♀, same data as for holotype [KSMA]; 2 ♂, **Kingdom of Saudi Arabia**, Al-Baha, Al Mikhwa, Shada Al-Ala Natural Reserve [19°50'34.95"N, 41°18'40.04"E, Alt. 1679 m], sweeping net, 7.IV.2019, leg. Ahmed M. Soliman [KSMA].

Diagnosis. Frontal lobe short, entire at free margin (Fig. 2B); frons finely reticulate (Fig. 2A); supra-antennal surface absent (Fig. 2A); OOL slightly longer than AOD, ca. 1.75× OD (Fig. 2C); scape ends just below median ocellus (Fig. 1C); F1 hardly longer than wide, as long as F2 (Fig. 2D); clava bi-segmented, sharply pointed apically (Fig. 2D); post-orbital carina joining genal carina at a level of ventral edge of eye (Fig. 3B); pronotal humeral angle sharp, clearly 90° (Fig. 2E); mesonotum densely punctured, bearing relatively long, golden lanceolate setae (Fig. 2E); bottom of punctures on mesonotum and metepimeron and of areola of propodeum granulate (densely reticulate) and dull (Figs 2E, 3B); propodeum with median areola complete, not much longer than adpetiolar areola, distinctly widened posteriorly (1.5× as long as wide) (Fig. 3A); metacoxa 2.5× as long as wide, widened basally (Fig. 1C); metafemur ventrally with 10–12 small teeth following the stout basal one (Fig. 4A, B); tarsal scrobe deep and smooth throughout, reaching sub-basal prominence (Fig. 4B); fore wing bare, only sparse white microtrichiae present on underside (Fig. 3C); STV evidently diverging from anterior margin of wing (Fig. 3C).

Description. *Female* (holotype, Figs 1–4). Body length: 3.8 mm; fore wing length: 2.3 mm.

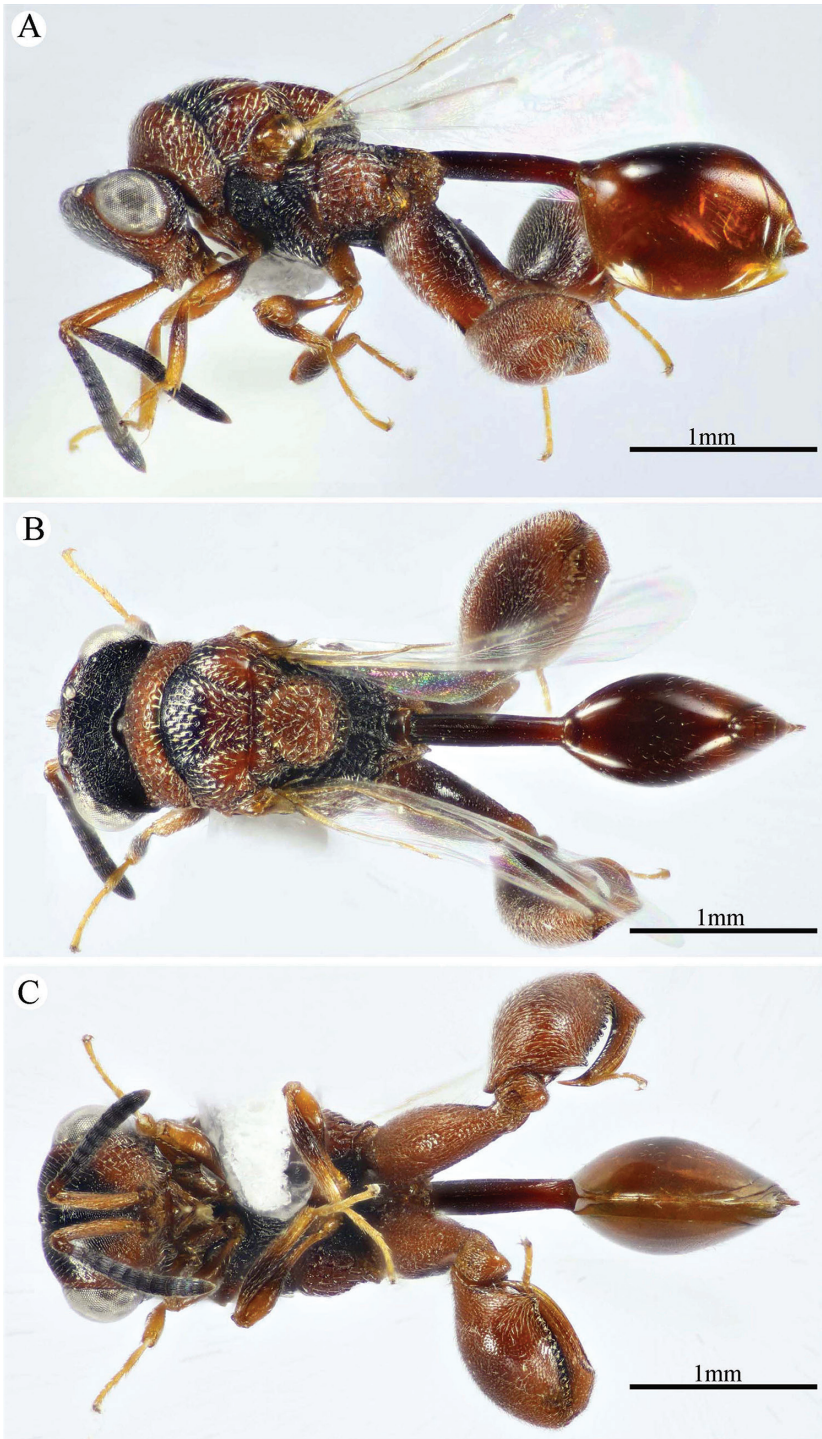


Figure 1. *Epitranus delvarei* Soliman & Gadallah, sp. nov. (holotype female). **A, B, C** habitus (lateral, dorsal and ventral views respectively).

Head (Fig. 2A–E). Slightly wider than mesoscutum in dorsal view (1.1×), distinctly transverse (1.5× as wide as high in frontal view), and ca. 2.8× as wide as its length in profile. Frontoververtex 1.6× as wide as eye height. Vertex almost smooth along OOD, finely densely punctate between lateral ocelli; AOL 0.85× OOL; OOL 1.75× OD; POL 2.14× OOL; discal surface not much expanded, squamosa reticulate, separated from orbit by 5–6 rows of piliferous points, and from median ocellus by three rows; orbital surface transversely alutaceous, laterally with fine upwardly directed long setae; preorbital carina extremely weak; malar area densely finely punctate; malar space 0.78× as long as eye height in lateral view; malar carina absent; suborbital carina distinct; gena coarsely foveolate, with inwardly directed fine setae; post-orbital carina lamellate, joining genal carina at a level of ventral edge of eye, strongly converging to the higher edge of the eye (nearly touching it); occipital area finely densely reticulate (with raised network), with some very superficial punctures in between; occipital carina, just above foramen magnum (or dorsally), relatively thick. Interantennal distance moderate (0.6× as wide as torulus diameter); a weak longitudinal carina could be seen between antennal toruli. Frontal lobe very short, not masking clypeus, with free margin entire.

Antenna (Fig. 2D). 13-segmented (clava bi-segmented), with sparse short setae; scape relatively long (1.28× as long as eye height), ends just below median ocellus; pedicel cylindrical, 1.65× as long as wide; anellus transverse (0.28× as long as wide); F1 1.1× as long as wide, as long as F2, slightly shorter than F7 (0.78×); clava sharply tapered apically, 2.5× as long as wide. Flagellomeres (except the first) bearing mostly a single row of MPS, two rows for preclaval.

Mesosoma (Figs 2E, 3A, B). 1.5× as long as mesoscutum width, with lanceolate setae. Pronotal collar 3.7× as wide as long, finely punctate, with fine sparse setae (setae adpressed and short), its sides slightly convex; lateral panel of pronotum rugose; humeral angle clearly 90°. Mesoscutum 2.7× as long as median length of pronotal collar, setiferous foveolate, the foveolae small anteriorly, with alutaceous interspaces, becoming larger with smooth interspaces posteriorly, widely spaced on scapula leaving smooth areas posteriorly. Notauli distinct, finely crenulate. Tegula broadly angulated posteriorly, smooth to finely alutaceous. Mesoscutellum hardly longer than wide (1.07×), densely setiferous foveolate, foveolae finely reticulate inside, with posterior margin broadly rounded. Axilla almost smooth. Propodeum with median areola distinctly widened posteriorly (1.5× as long as wide), weakly transversely carinate inside, extends to reach adpetiolar areola; prestigmatic areola with lanceolate, rather dense setae. Mesopleuron with adscrobal area coarsely foveolate, foveolae finely punctate inside; femoral depression finely transversely striated, ventral shelf of mesepisternum finely punctate, with adpressed setae. Metepimeron densely, closely foveolate throughout, with fine, adpressed lanceolate setae; metepisternum microreticulate, with two median carinae ending on a transverse posterior carina with two large teeth; adpetiolar area concave, with a large irregular projection posteriorly.

Wings (Fig. 3C). Fore wing 2.77× as long as wide, bare on upper and undersides; MV 0.68× as long as costal cell; STV slightly longer than wide, forming with anterior margin an angle of ca. 45°. Hind wing bare, with three hamuli.

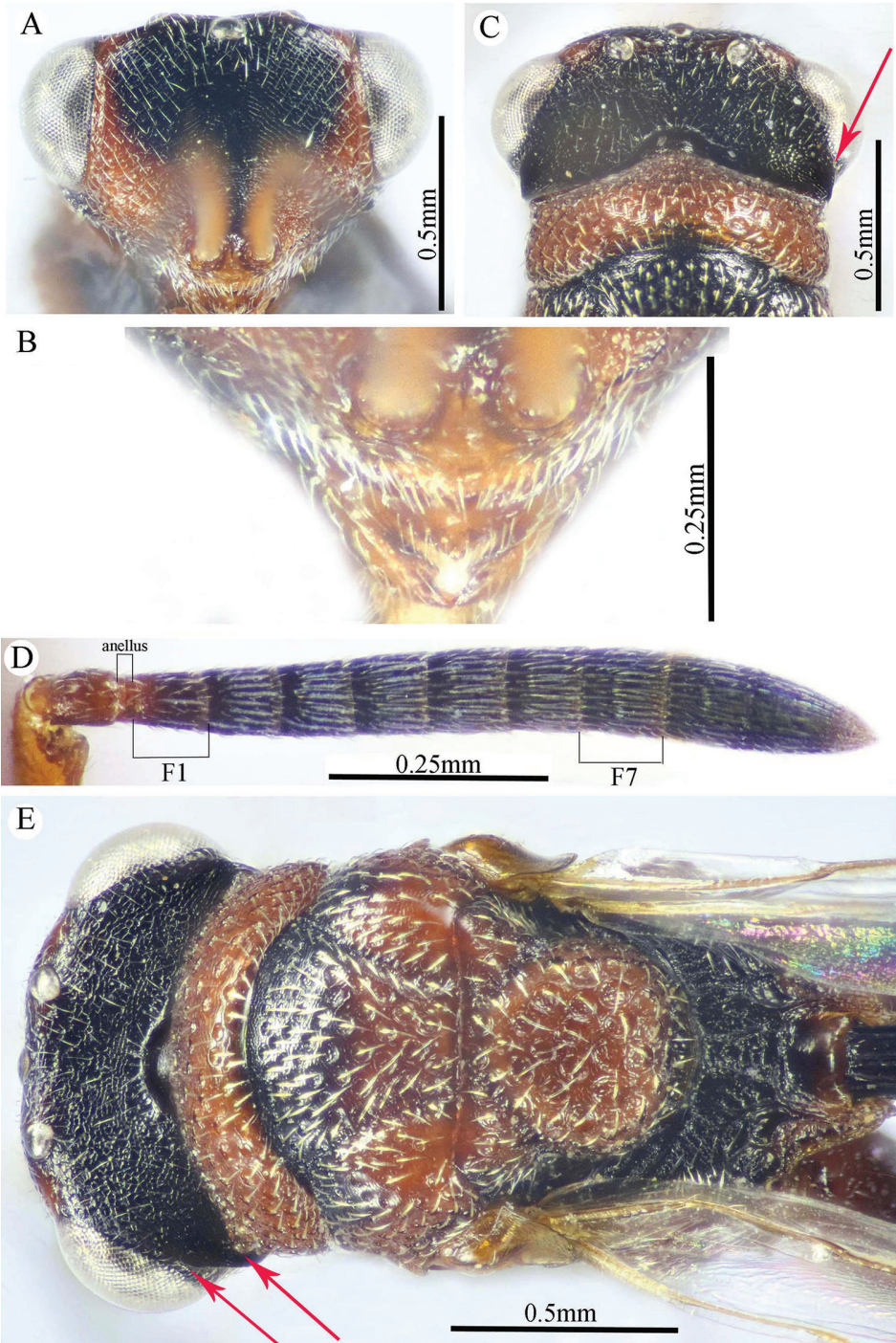


Figure 2. *Epitranus delwarei* Soliman & Gadallah, sp. nov. (holotype female) **A** head (frontal view) **B** lower part of face (frontal view) **C** head, pronotum & part of mesoscutum (dorsal view) **D** antennal pedicel and flagellum **E** head and mesosoma (dorsal view).

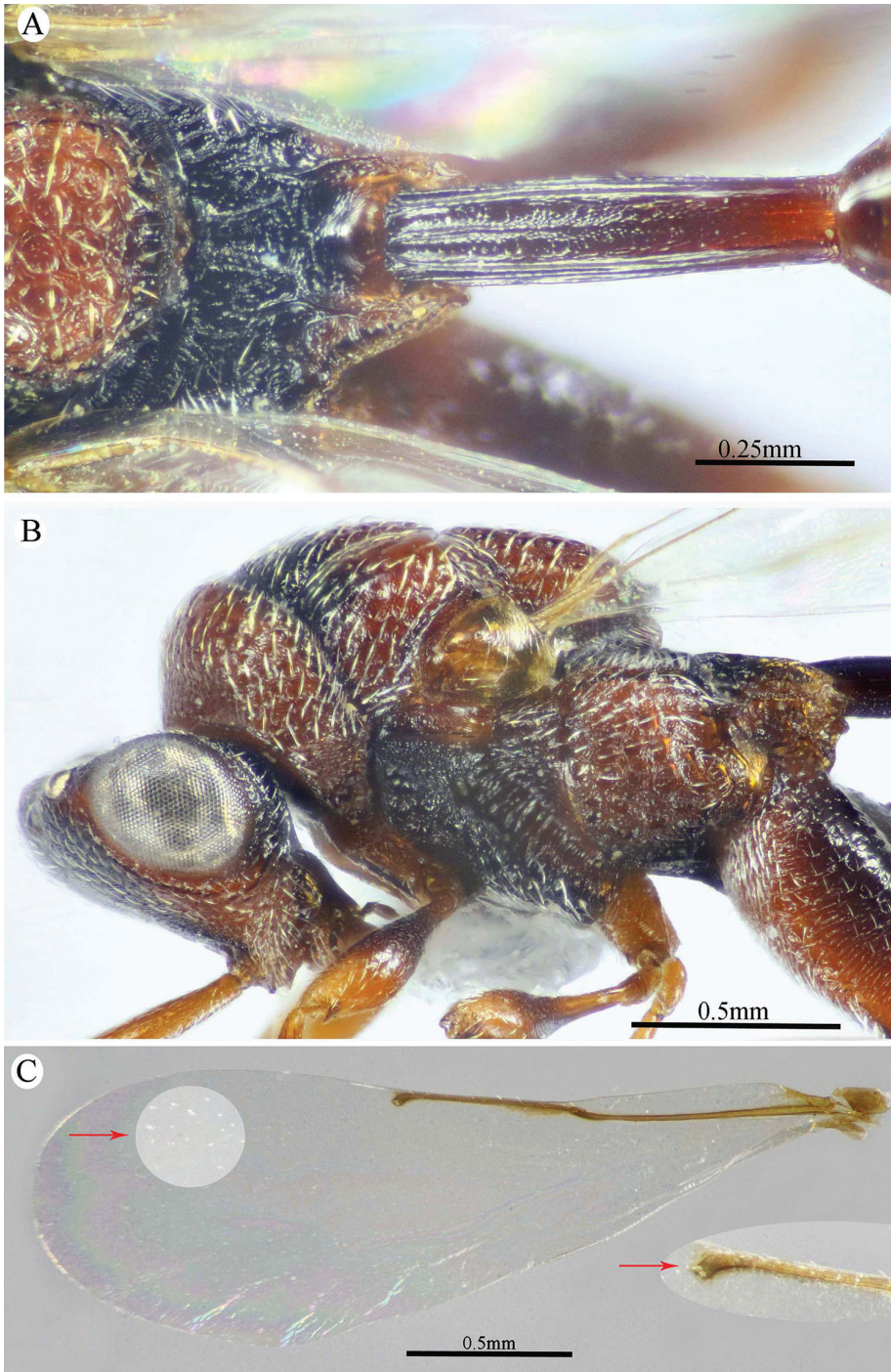


Figure 3. *Epitranus delvaei* Soliman & Gadallah, sp. nov. (holotype female) **A** part of mesoscutellum, metanotum, propodeum & gastral petiole (dorsal view) **B** head & mesosoma (lateral view) **C** fore wing (parts of wing membrane and MV and STV magnified).

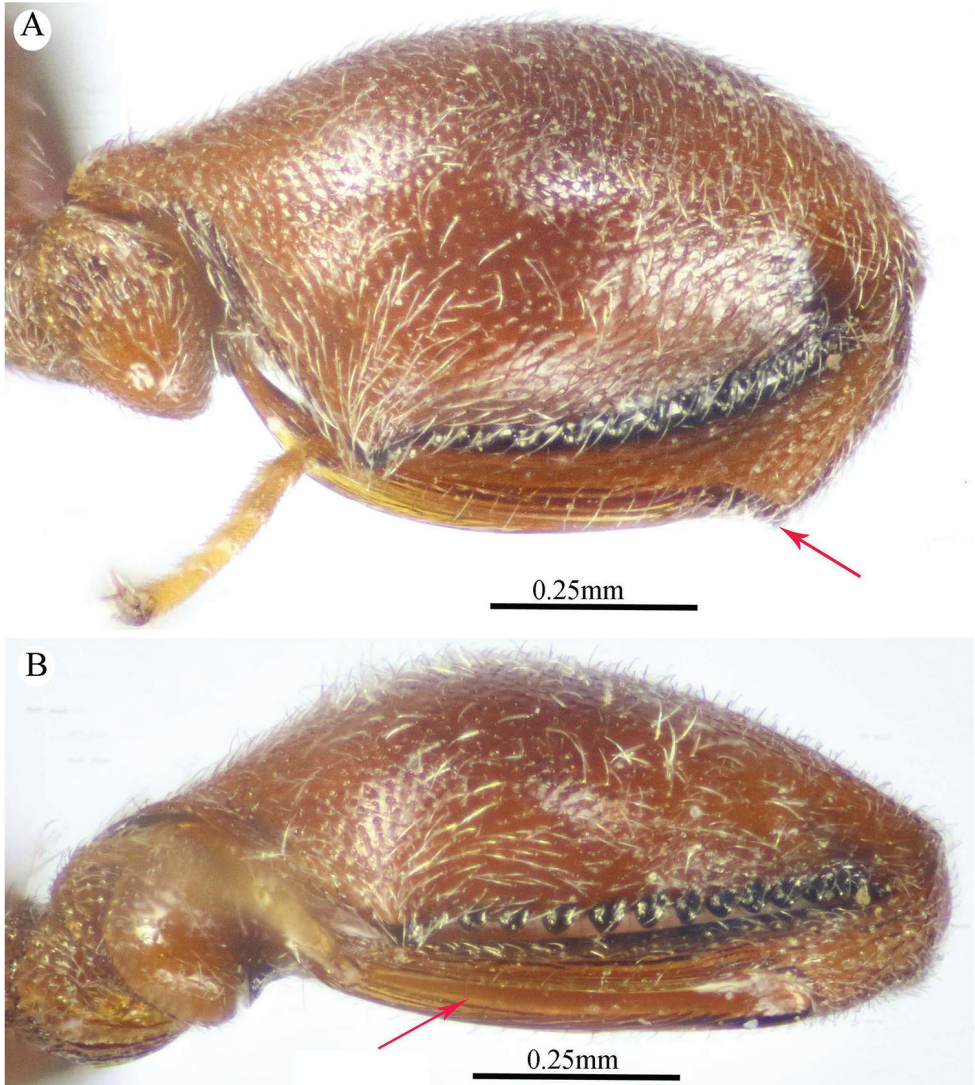


Figure 4. *Epitranus delvarei* Soliman & Gadallah, sp. nov. (holotype female) **A, B** hind leg, excluding coxa (outer and ventral views respectively).

Hind leg (Figs 1C, 4A, B). Metacoxa 2.5× as long as wide, widened basally, slightly shorter than metafemur (0.92×), finely transversely alutaceous on outer-dorsal face, rest densely punctured with short setae more densely distributed basoventrally. Metafemur 1.97× as long as wide, with dense setiferous punctures throughout, outer ventral margin with a stout tooth basally, followed by 12 smaller, similar teeth. Tarsal scrobe long, reaching sub-basal prominence; proximal fourth of metatibia finely punctate; edge of sub-basal prominence with four denticles concealed under white pubescence.

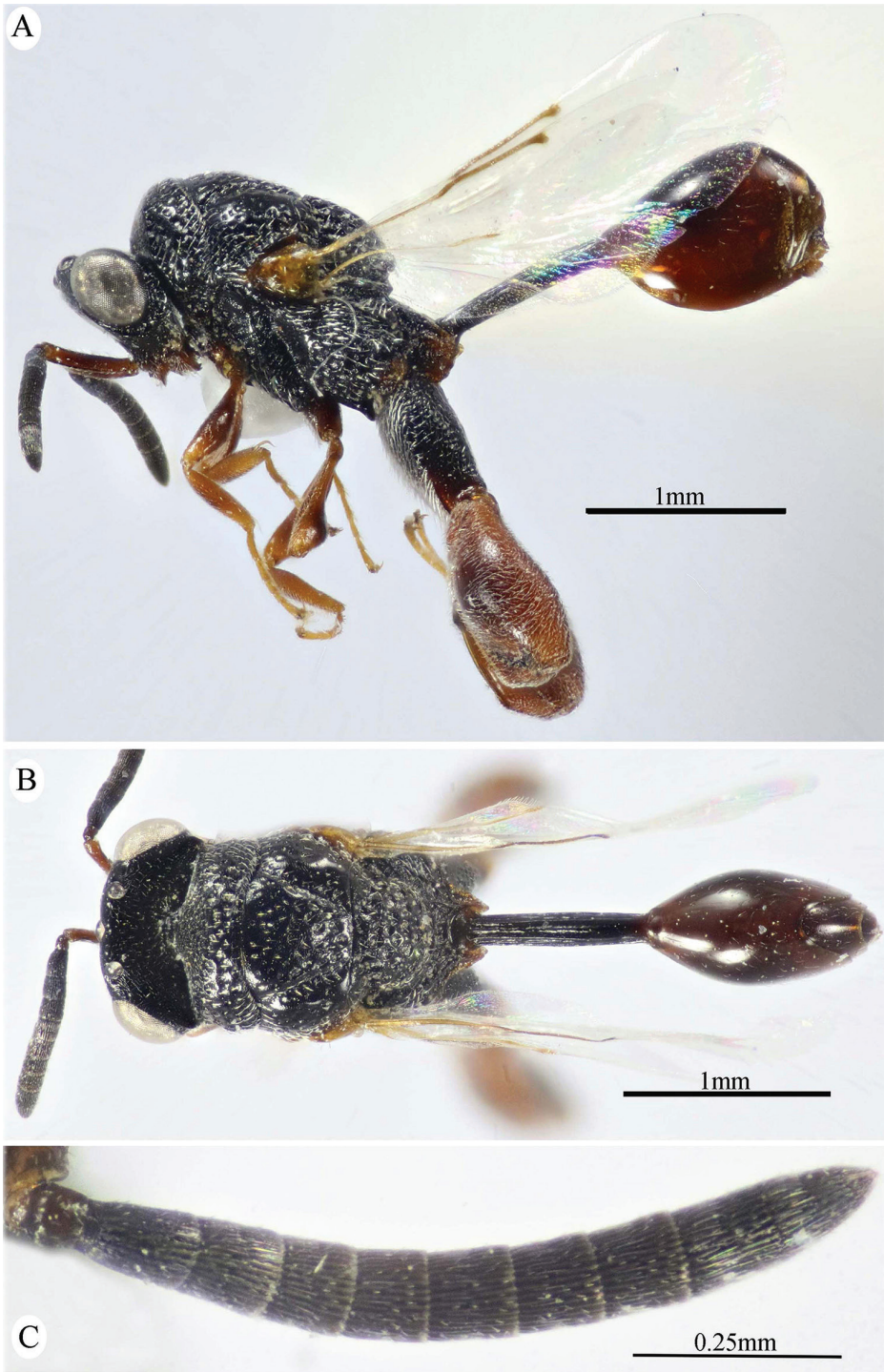


Figure 5. *Epitranus delvarei* Soliman & Gadallah, sp. nov. (paratype male) **A, B** habitus (lateral and dorsal views respectively) **C** antennal pedicel and flagellum.

Metasoma (Figs 1A–C, 3A). Petiole relatively short (4.5× as long as wide, 0.92× as long as dorsal length of Gt_1 , and 0.68× as long as gaster), with a weak incomplete median carina, extending along its basal half, two (sublateral and lateral) ridges extending along its whole length, area between sublateral ridges faintly coriaceous (smooth apically). Gaster subcircular in lateral view (1.45× as long as height), somewhat ovoid in dorsal view. Gt_1 long, occupying most of gaster (0.75× as long as the whole length of gaster in dorsal view), deeply concave posteriorly, mostly smooth (densely finely punctulate postero-laterally); remaining tergites short, densely finely punctulate, finely setose. Gt_2 slightly concave posteriorly. Ovipositor slightly extended to apex of gaster.

Color (Figs 1A–C, 3C). Head including antennal flagellomeres and clava are black, except a broad band around inner margin of eye, malar area, clypeus and antennal scape to anellus are reddish brown. Mesosoma including legs and metasoma reddish brown, except anterior third of mesoscutal middle lobe, antero-inner corner of scapula, posterior margin of mesoscutellum, dorsellum, most of propodeum and ovipositor are black; propodeum postero-laterally reddish brown; outer faces of fore and mid femora and tibiae, dorsal face of metacoxa, inner face of metafemur, basal two-thirds of petiole and Gt_1 dorsally with blackish tint. Tegula glassy yellowish red. Wings hyaline, with pale brown to yellowish veins.

Male (Paratype, Fig. 5A–C). Differs from the female in the following: AOL slightly longer than OOL (1.16×); OOL 1.2× as long as OD; POL 2.8× as long as OOL; interantennal distance 1.2× as long as antennal torulus diameter; F1 longer (1.4× as long as wide, 1.06 as long as F7); mesoscutum length 3.3× as long as pronotum median length; metacoxa shorter, ca. 1.18× as long as width; petiole longer (5.7× as long as wide), with medial carina extending along its whole length; head and mesosoma completely black (except clypeus and tegula); metacoxa and petiole mostly black.

Remarks. *Epitranus delwarei* differs from all species of the genus in having small teeth on the metafemur; the presence of dense reticulation in the bottom of punctures on mesoscutellum, metepimeron, as well as areola of propodeum; tarsal scrobe of metatibia reaching sub-basal prominence.

Hosts. Unknown.

Distribution. Saudi Arabia (Al-Baha and Asir regions).

Etymology. The new species is named *delwarei*, in honor of Gerard Delvare, for his kind efforts and help in the identification of several chalcid species.

***Epitranus similis* Gadallah & Soliman, sp. nov.**

<http://zoobank.org/A190D08C-92B7-4662-9660-B1C642740266>

Figures 6–9

Type material. *Holotype* ♂. **Kingdom of Saudi Arabia**, Asir, Abha, Garf Raydah Natural Reserve [18°11'35.74"N, 42°23'30.24"E, Alt. 1805 m], sweeping net, 5.IX.2015, leg. Ahmed M. Soliman [KSMA]; *Paratypes*: 2♂, **Kingdom of Saudi Arabia**, same data as for holotype [KSMA].

Diagnosis. Frontal lobe distinctly long, sub-trapezoidal in shape as its sides are straight and regularly converging ventrally, with a longitudinal median carina extending on its whole length, and free margin with three lobes (outer lobes notched subapically) (Fig. 7B); OOL 0.80–0.85× as long as OD, and ca. 0.5× as long as AOL (Fig. 7C); POL ca. 4.3× as long as OOL (Fig. 7C); F1 moderately long, ca. 1.7× as long as wide (Fig. 7D); pronotal collar laterally, scapula anterolaterally, propodeum on prestigmatic areola, mesepisternum, metepimeron dorsally and basoventral surface of metacoxa densely clothed with whitish setae masking integument beneath (Figs 6A, C, 8B); pronotal collum with dense, long golden setae on two submedian patches (Fig. 7C); propodeal median areola deep, with lateral ridges converging posteriorly to meet before the adpetiolar areola (Y-like raised carina) (Fig. 8A); metafemur toothed ventrally, with nine or ten spaced teeth following the stout sub-basal tooth (Fig. 8D, E); tarsal groove of metatibia fully occupying the completely delimited smooth and deep metatibial process, reaching the sub-basal prominence anteriorly (Fig. 8E); petiole very long, 7.12–7.65× as long as wide (Fig. 9A); gaster relatively short (1.25–1.40× as long as height in profile) (Fig. 6A).

Description. Male (holotype). Body length 5.5 mm. fore wing length 3.3 mm.

Head (Figs 7A–D, 8B). Triangular in frontal view, 1.25× as wide as high, wider than mesoscutum in dorsal view (1.2×), 2.6× as wide as its length in profile. Frontoververtex 1.5× as wide as eye height; AOL 2.0× OOL; OOL 0.85× OD; POL 4.3× OOL; supra antennal surface absent; frons transversely finely strigulate medially beneath antennal scape (at scrobe), laterally with sparse setiferous punctures, the setae lanceolate and long; preorbital carina absent; malar area mostly polished, with scattered superficial setiferous punctures; malar space ca. 0.6× as long eye height in profile; malar carina absent; gena broad, nearly smooth, with a row of setae directed inwards along post-orbital carina that is well-developed, lamellate and joining genal carina at a level of ventral edge of eye; post-orbital carina hardly converging to the higher edge of the eye (nearly parallel); suborbital carina weak. Occiput alutaceous, with sparse setiferous punctures (setae long and dispersed, pale yellow). Interantennal projection absent; interantennal distance ca. 0.5× as long as torulus diameter; frontal lobe quite long, with subantennal distance 4.0× as long as interantennal distance, ventral margin with two pairs of indentations delimiting three lobes, the outer ones are narrowly rounded; projection with a sharp longitudinal median carina extended throughout its length; surface of projection with long, lanceolate and whitish setae.

Antenna (Fig. 7D). Scape 1.35× as long as eye height, ending very closely to median ocellus, its ventral face strongly excavated, the excavation densely and finely pubescent; pedicel hardly longer than wide (1.15×); anellus transverse (0.4× as long as wide); F1 moderate, 1.7× as long as wide, 1.3× as long as F2 and F7 as well; clava 2.35× as long as wide.

Mesosoma (Figs 7C, E, 8A, B). 1.65× as long as mesoscutum width. Pronotal collar 2.45× as wide as long, mostly smooth on disc, with scattered punctures bearing fine setae; collar laterally and collum densely setiferous punctulate, the setae forming tufts that are inwardly oriented, white on the former and golden yellow on the latter;

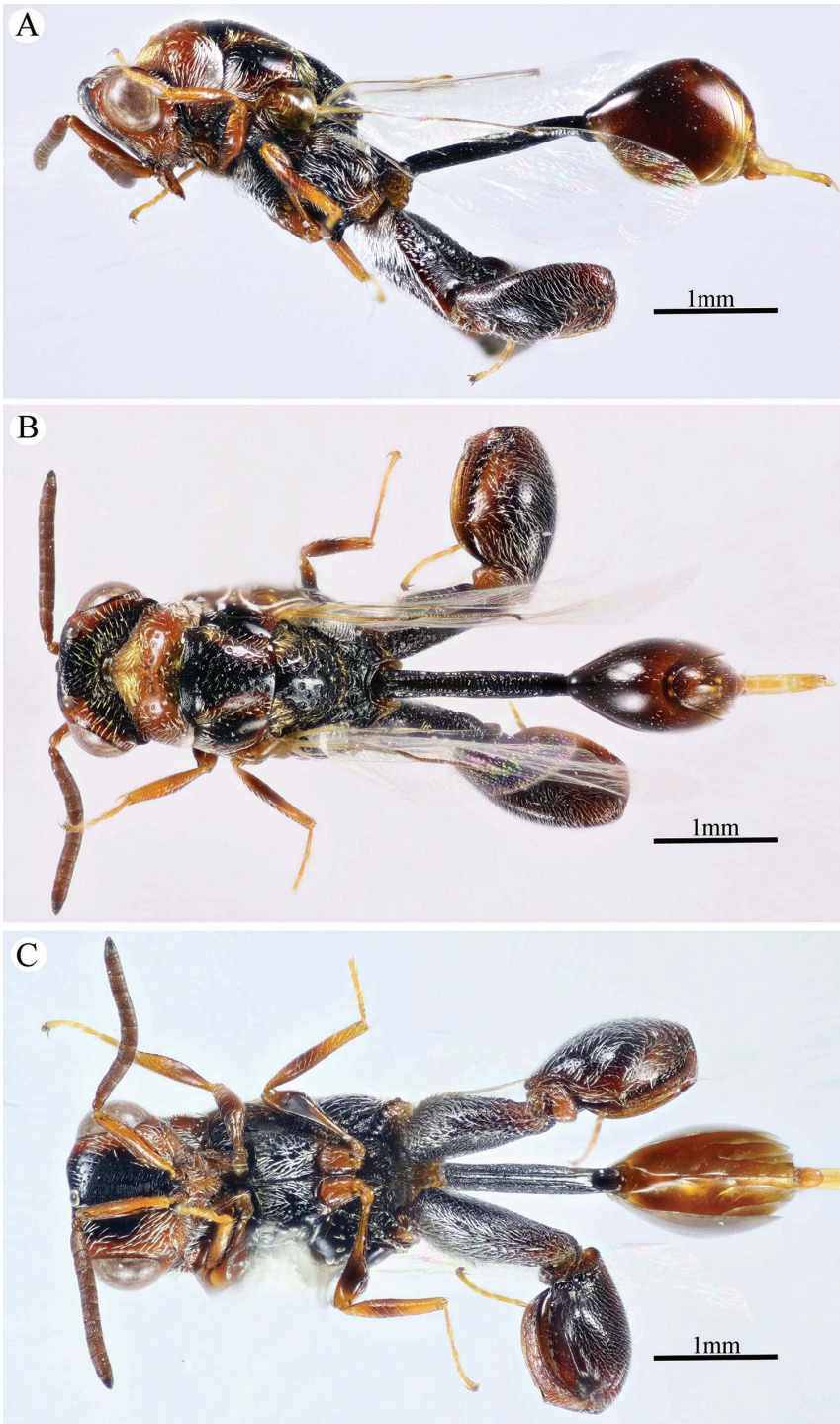


Figure 6. *Epitranus similis* Gadallah & Soliman, sp. nov. (holotype male) **A, B, C** habitus (lateral, dorsal, and ventral views respectively).

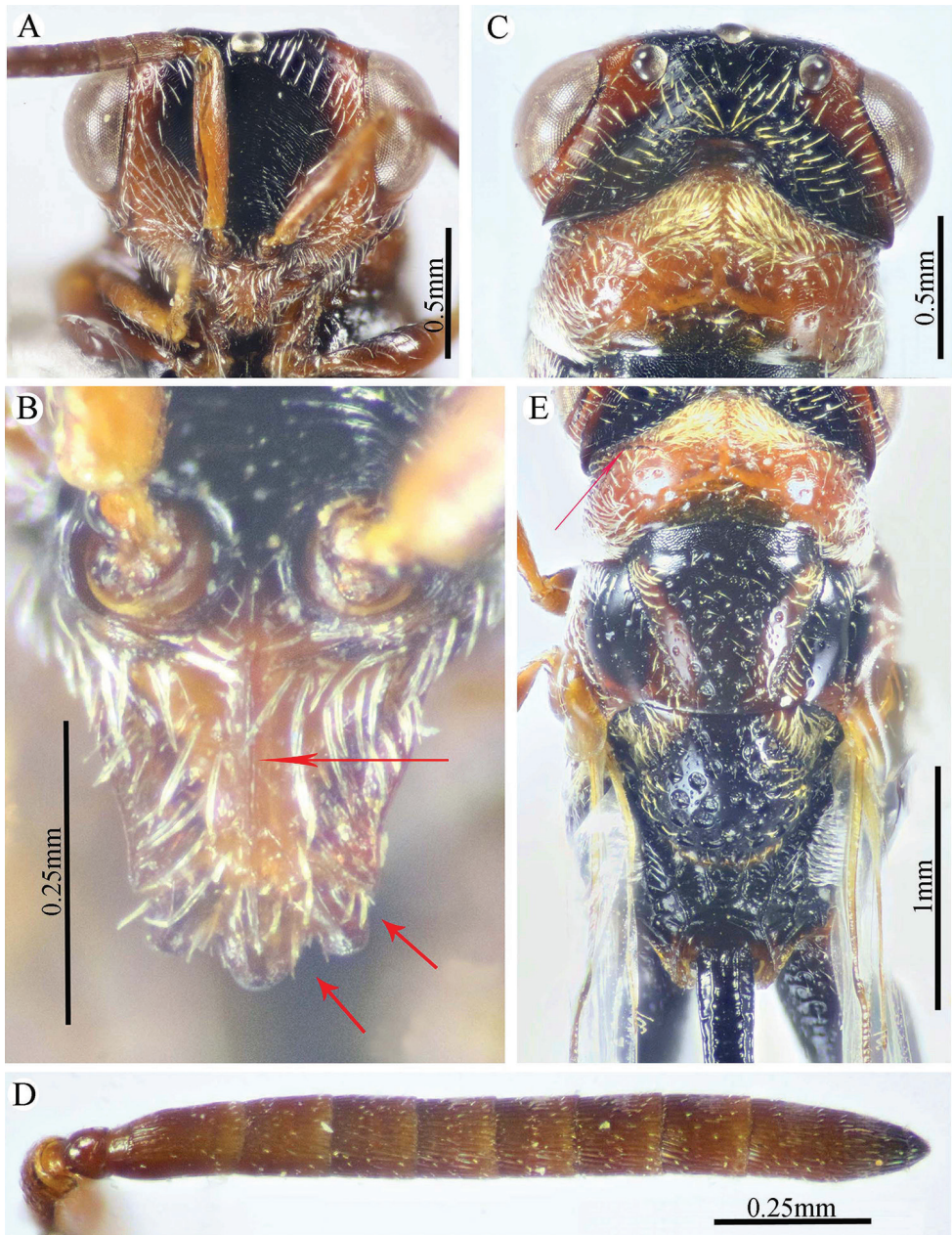


Figure 7. *Epitranus similis* Gadallah & Soliman, sp. nov. (holotype male) **A** head (frontal view) **B** lower part of face showing frontal lobe (frontal view) **C** head & pronotum (dorsal view) **D** antennal pedicel and flagellum **E** mesosoma and part of gastral petiole (dorsal view).

pronotal sides slightly convex; lateral carinae sharp and extending dorsally, not meeting medially; humeral angle rounded; pronotal lateral panel finely alutaceous, shiny. Mesoscutum 2.25× as long as median length of pronotum, middle lobe finely alutaceous

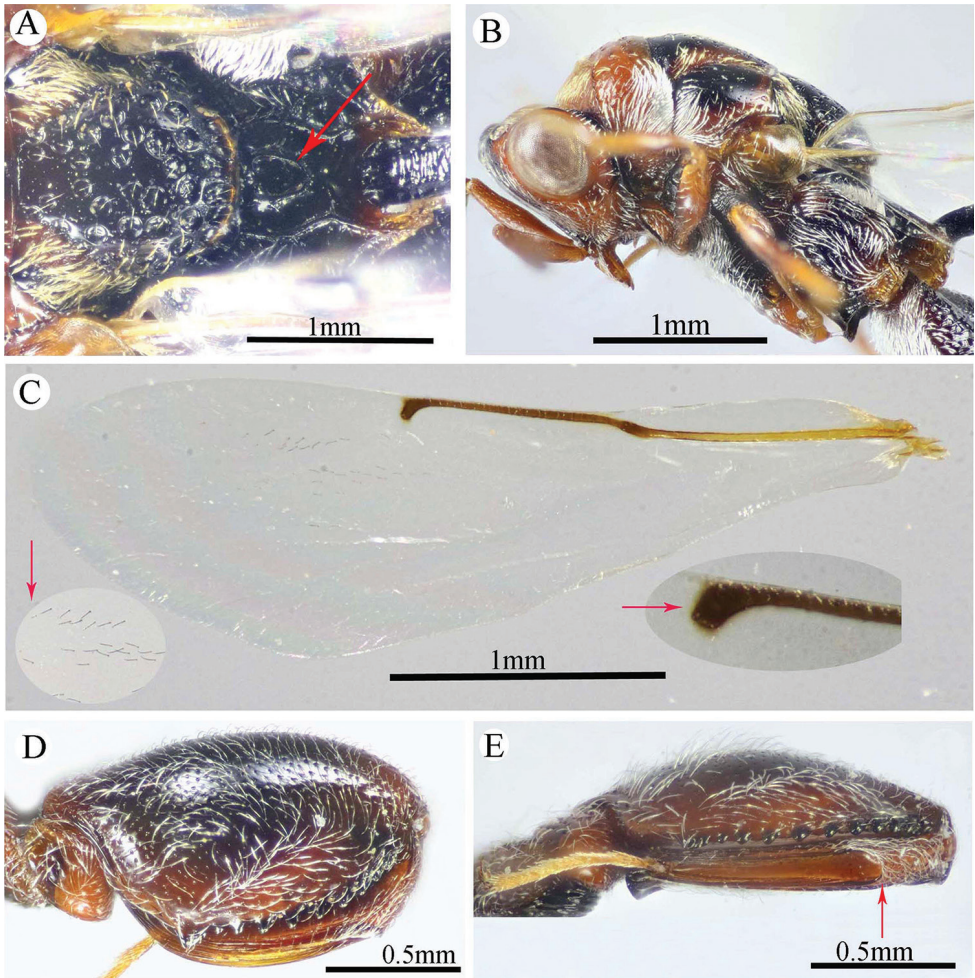


Figure 8. *Epitranus similis* Gadallah & Soliman, sp. nov. (holotype male) **A** mesoscutellum, metanotum & propodeum (dorsal view) **B** head & mesosoma (lateral view) **C** fore wing (parts of wing membrane and MV and STV magnified) **D, E** hind leg, excluding coxa (outer and ventral views respectively).

anteriorly, followed by deep and sparse setiferous punctures bearing fine setae; scapula nearly smooth, with few scattered punctures, antero-laterally clothed with dense lanceolate whitish setae; notauli deep, foveolate; axilla with dense, upwardly directed whitish setae, integument smooth beneath; tegula large, depressed near posterior margin, smooth anteriorly, finely alutaceous posteriorly and laterally, with broad angulate posterior margin that distinctly overlap base of hind wing. Mesoscutellum convex, hardly longer than wide ($1.1\times$), irregularly deeply foveate, the foveae large, widely separated medially and closer laterally, posterior margin broadly rounded, strigose. Propodeum deeply areolate; median areola $1.37\times$ as long as wide, with lateral ridges converging posteriorly and meeting slightly before adpetiolar areola; lateral areola transversely carinate; prestigmatic areola densely setose, setae oriented inwards. Adscrobal area of

mesopleuron densely clothed with long, suberect and whitish setae, femoral scrobe finely transversely strigose, ventral shelf of mesepisternum sparsely punctate, with adpressed long setae, interspaces between punctures smooth; epicnemial carina lamellate. Metepimeron closely foveolate throughout (bottom of foveae smooth), with dense, long adpressed and whitish setae; metepisternum densely reticulate, with two median carinae diverging posteriorly followed by two large and sharp submedian teeth; subcoxal teeth small; adpetiolar area concave, longitudinally striated, with a median longitudinal carina ends posteriorly with a strong subpentagonal subpetiolar areola.

Wings (Fig. 8C). Fore wing $3.2\times$ as long as wide, bare on upper side, sparsely setose subapically on underside; MV ca. $0.72\times$ as long as costal cell; STV rudimentary ($1.25\times$ as long as wide), strongly diverging from anterior margin of wing at an angle of ca. 80° . Hind wing hyaline and asetose, with three hamuli.

Hind leg (Figs 6C, 8D, E). Metacoxa widened basally, $2.45\times$ as long as wide, $0.9\times$ as long as metafemur, densely setose on ventral side, punctured but with transverse ridges near apex on outer dorsal side. Metafemur $1.9\times$ as long as wide, with dense setiferous punctures on outer face, its ventral margin with a triangular sub-basal tooth followed by nine teeth that are equally separated, progressively smaller towards apex. Tarsal scrobe of metatibia fully occupying the completely delimited, smooth and deep metatibial process, reaching sub-basal prominence anteriorly (Fig. 12E), the edge of the later with four denticles concealed by pubescence (could be seen when examined from dorsal view).

Metasoma (Figs 6A, 9A, B). Petiole quite long, $7.12\times$ as long as broad, $1.58\times$ as long as length of Gt_1 in dorsal view, and $1.2\times$ as long as length of gaster in dorsal view, dorsally with two, lateral and sublateral, longitudinal ridges that is vague along the apical two-thirds, the area between sublateral ridges transversely wrinkled. Gaster ovoid in dorsal view, $1.25\times$ as long as its height in lateral view. Gt_1 long ($0.75\times$ as long as gaster in dorsal view), deeply concave posteriorly, sparsely finely setiferous punctate (setae fine and short, punctures dense postero-laterally); remaining tergites short, sparsely finely punctate and finely setose.

Color (Figs 6A–C, 8C). Body black, except the following parts, bright reddish brown: frontal lobe, malar area, a relatively broad strip around eye, gena, pronotum, a lateral longitudinal strip on middle lobe of mesoscutum, lateral and posterior borders and postero-inner corner of scapula, inner part of axilla, area around epicnemial carina on mesopleuron, upper part of metepimeron, and posterior part of adpetiolar area on metepisternum. Gaster reddish brown with black tint dorsally. Antennal scape and pedicel reddish brown, flagellum brown. Legs reddish brown, with black tint on mesofemur, ventral face of metacoxa and outer face of metafemur. Tegula glassy golden yellow. Wings hyaline with brown veins that are paler on hind wing. Genitalia pale yellow.

Female. Unknown.

Variation. The paratype specimens differ from the holotype specimen in the predominance of red brown color on: head (except post-orbital and occipital carinae in one of the paratype specimens or a band along occipital carina, post-orbital carina and



Figure 9. *Epitranus similis* Gadallah & Soliman, sp. nov. (holotype male) **A, B** metasoma (dorsal and ventral views respectively).

a narrow longitudinal median strip on the frons in the other paratype specimen); middle lobe of mesoscutum (except a triangular area on disc); lateral lobe of mesoscutum (except an oval area on disc); the whole axilla, mesoscutellum (except longitudinal median strip); the whole metapleuron; metacoxa and metafemur (except black tint on the former).

Remarks. The new species is morphologically similar to *E. nitidus* (Schmitz) (Democratic Republic of Congo) especially the identical frontal projection; the absence of interantennal projection; similar flagellum; the presence of outstanding setae on mesosoma; similar STV, and similar petiole. But differs from it by the partly reddish head and mesosoma (entirely black in *E. nitidus*); the presence of distinctive setation on different parts of mesosoma as reported above (mesosoma with regular setation in *E. nitidus*); propodeum with petiolate median areola (complete in *E. nitidus*); shorter and relatively stouter metacoxa (quite slender in *E. nitidus*).

Etymology. The word *similis* is an adjective in Latin and means similar or resembling, referring to the similarity of this species to *E. nitidus*.

Hosts. Unknown.

Distribution. Saudi Arabia (Asir region).

***Epitranus subinops* Soliman & Gadallah, sp. nov.**

<http://zoobank.org/EDF024B1-4346-44E6-A08E-DAC73BC1CCB8>

Figures 10–13

Type material. *Holotype* ♀: **Kingdom of Saudi Arabia**, Asir, Regal Alma, Wadi Kasan (2 km North of El-Hebeal) [18°6'59.89"N, 42°13'54.92"E, Alt. 487 m], sweeping net, 12.IV.2019, leg. Ahmed M. Soliman [KSMA].

Diagnosis. Frontal lobe relatively long, its free margin trilobate (Fig. 11B); OOL ca. 1.5× as long as OD, and as long as AOL (Fig. 11C); POL 2.4× as long as OOL (Fig. 11C); interantennal projection well developed (lamellate) (Fig. 11B); scape ends a long distance from median ocellus (Fig. 11A); F1 relatively long, 1.75× as long as wide, following flagellomeres shorter, subequal (Fig. 11D); clava bi-segmented, relatively long ca. 2.7× as long as wide, tapering apically (Fig. 11D); frons with supra antennal surface delimited by step-like margin; frons sparsely punctured, with fine setae directed upwards, integument smooth behind (Fig. 11A); post-orbital carina joining genal carina at a level distinctly above the ventral edge of the eye (Fig. 12B); pronotal humeral angle rather sharp (Fig. 11C); mesoscutum with short setae and very sparse small punctures on anterior third of middle lobe (Fig. 11E); bottom of punctures on mesonotum and metepimeron smooth (Figs 11E, 12B); propodeum densely areolate, median areola complete (Fig. 12A); metafemur serrulate ventrally following a stout tooth at base (Fig. 13A, B); metatibia with oblique carina inside metatibial process (Fig. 13B); tarsal scrobe almost reaching sub-basal prominence (Fig. 13B); fore wing densely setose along apical two thirds (Fig. 12C); STV present but reduced, 2.0× as long as wide (Fig. 12C).

Description. *Female* (holotype). Body length 3.4–3.9 mm. Fore wing length 2.1–2.5 mm.

Head (Figs 11A–C, 12B). Transverse (1.16× as wide as high in frontal view), slightly wider than mesoscutum in dorsal view (1.1×), and ca. 2.45× as wide as its length in profile. Frontovertex 1.25× as wide as eye height. Vertex almost smooth, sparsely punctate between median ocellus and eyes, with AOL as long as OOL; OOL 1.5× OD; POL 2.4× OOL; orbital surface superficially transversely alutaceous, laterally with fine sparse setae directed upwards; malar area superficially wrinkled; malar space 0.57× as long as eye height in lateral view; malar carina faint and polished; gena coarsely foveolate, nearly bare; post-orbital carina well developed, joined genal carina at a level distinctly above the ventral edge of the eye, distinctly converging to the higher edge of the eye; preorbital and suborbital carinae developed. Occipital area densely reticulate; interantennal distance distinctly short, 0.4× as long as torulus diameter, interantennal projection well developed (lamellate); frontal lobe relatively long (subantennal distance 3.3× as long as interantennal distance), free margin with three lobes.

Antenna (Fig. 11D). 13-segmented, clava bi-segmented, with few scattered short setae; scape moderately long, longer than eye height (1.33×), ending a distance before median ocellus, densely punctured throughout; pedicel relatively short, conical shape, approximately as long as its width; anellus transverse, ca. 0.6× as long as wide;

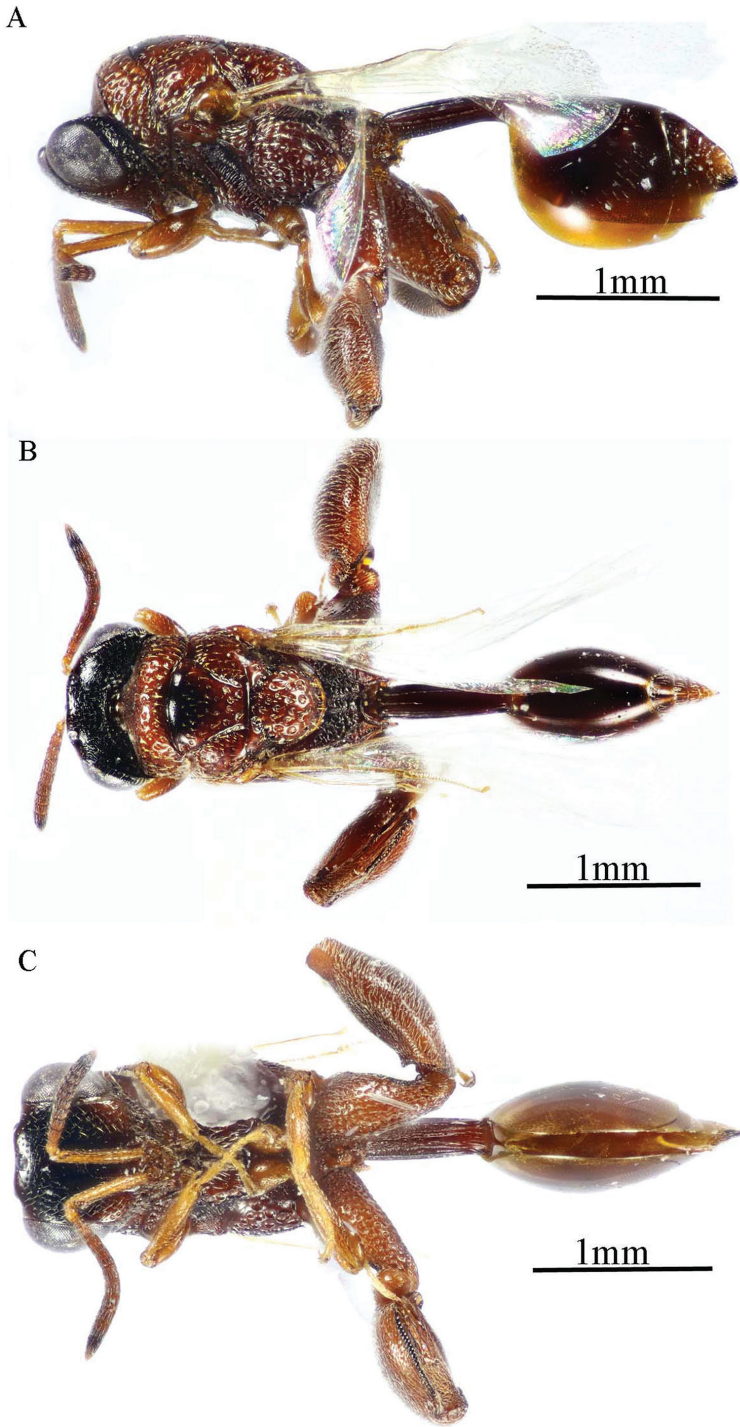


Figure 10. *Epitranus subinops* Soliman & Gadallah, sp. nov. (holotype female) **A, B, C** habitus (lateral, dorsal and ventral views respectively).

F1 relatively long, 1.75× as long as wide, following funiculars distinctly shorter, subequal; clava ca. 2.7× as long as wide, tapered apically.

Mesosoma (Figs 11E, 12A, B). 1.8× as long as mesoscutum width, with relatively short setae, that are somewhat thickened on pronotum and mesoscutellum. Pronotal collar 3.0× as wide as long, sparsely setiferous foveolate, that are denser laterally, with sides slightly convex; humeral angle sharp, nearly 90°; lateral carina not extended dorsally on collar. Mesoscutum 2.9× as long as pronotal collar median length, sparsely finely punctulate on anterior half of middle lobe, its anterior margin finely alutaceous; posterior half of middle lobe with large irregular foveolae, lateral lobes with dense setiferous punctures. Notauli very distinct and deep, linear (not crenulate). Tegula broadly rounded posteriorly, smooth. Mesoscutellum slightly longer than wide (1.1×), setiferous foveolate, foveolae smooth on bottom, with posterior margin broadly rounded. Propodeum strongly areolate, median areola slightly widened posteriorly, 2.6× as long as wide, weakly transversely striated on bottom, its lateral carinae slightly diverging posteriorly and reaching transverse carina of adpetiolar areola; submedian and basolateral areolae fused. Mesopleuron with adscrobal area coarsely foveolate, foveolae finely punctate inside; femoral scrobe coarsely transversely ridged, ventral shelf of mesepisternum finely punctate, with adpressed setae. Metepimeron densely, closely foveolate throughout, with fine, adpressed setae; metepisternum largely areolate throughout (bottom of areolae densely reticulate), with two median carinae slightly diverging posteriorly followed by two large and sharp submedian teeth; adpetiolar area concave, nearly smooth, with a median longitudinal carina ends posteriorly with a strong subpentagonal areola.

Wings (Fig. 12C). Fore wing ca. 3.0× as long as wide, rather densely setose on the underside of apical two-thirds, setae distinctly long; MV 0.6× as long as costal cell; STV somewhat reduced (0.1× as long as MV), 2.0× as long as wide, forming with anterior margin an angle of ca. 45°. Hind wing sparsely setose apically, with three hamuli.

Hind leg (Figs 10C, 13A, B). Metacoxa 2.2× as long as wide, widened basally, slightly shorter than metafemur (0.9×), finely transversely alutaceous on outer dorsal face, rest densely setiferous punctulate, interspaces between punctures smooth. Metafemur 1.75× as long as wide, with dense setiferous punctures throughout, outer ventral margin with broad triangular tooth basally, followed by a serrulation of minute teeth. Metatibia with an oblique carina inside metatibial process; tarsal scrobe almost reaching sub-basal prominence; sub-basal prominence is formed from three small blunt teeth partly hidden by dense pubescence.

Metasoma (Figs 10A, B, 12A, 13C). Petiole relatively short, 3.5× as long as wide, 0.92× as long as dorsal length of Gt_1 , and ca. 0.6× as long as gaster, with an incomplete median carina (0.45× as long as petiole length), two incomplete submedian carinae (0.73× as long as petiole length), and two complete lateral ridge, area between sublateral ridges nearly smooth and shiny. Gaster fusiform in dorsal view, 1.55× as long as its height in profile. Gt_1 0.6× as long as the whole length of gaster in dorsal view, deeply concave posteriorly, almost entirely smooth; remaining tergites short, densely finely punctate at base, finely setose. Gt_2 slightly concave posteriorly. Ovipositor slightly extended behind gaster.

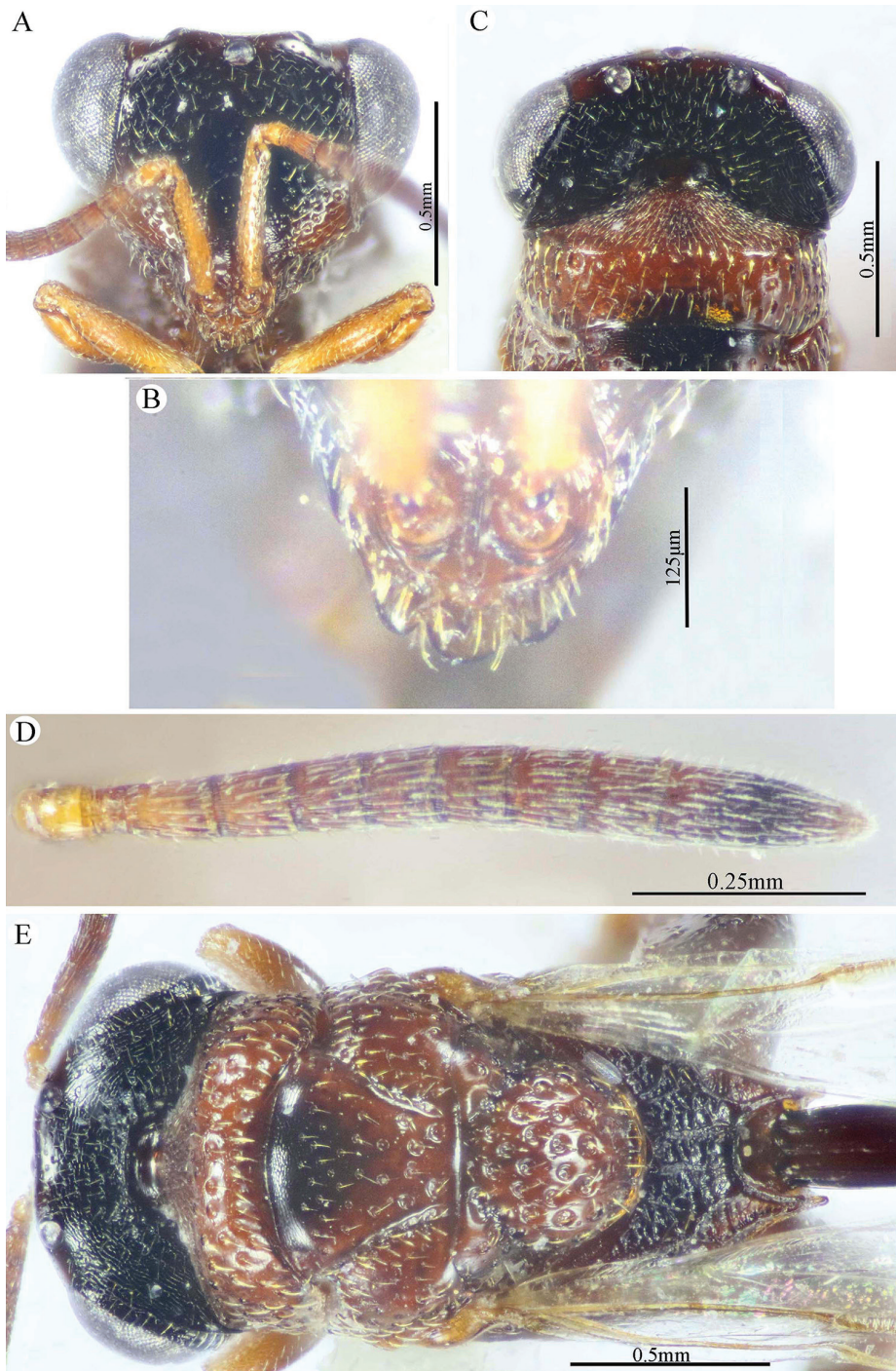


Figure 11. *Epitranus subinops* Soliman & Gadallah, sp. nov. (holotype female) **A** head (frontal view) **B** lower part of face showing frontal lobe (frontal view) **C** head and pronotum (dorsal view) **D** antennal pedicel and flagellum **E** head and mesosoma (dorsal view).

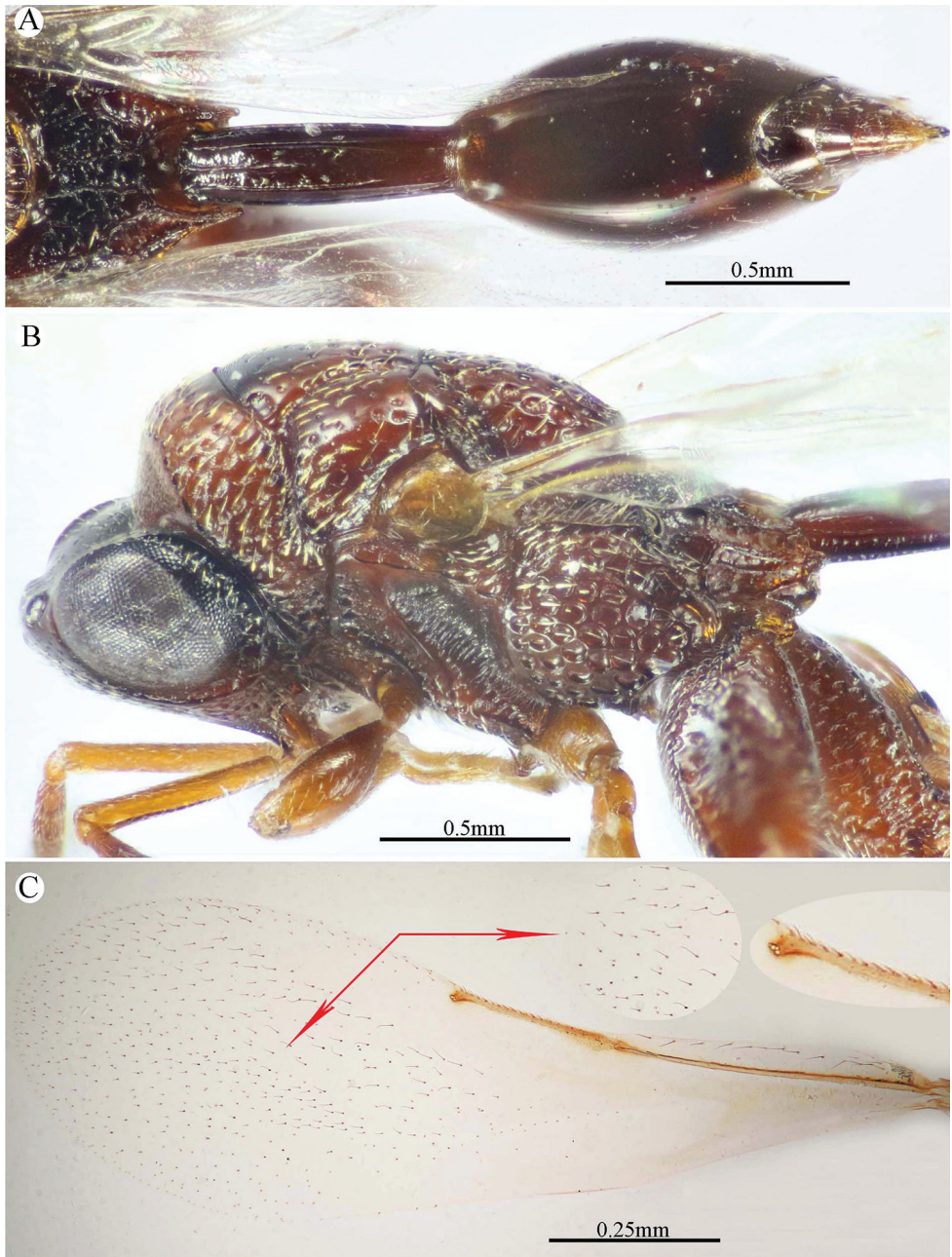


Figure 12. *Epitranus subinops* Soliman & Gadallah, sp. nov. (holotype female) **A** propodeum and metasoma (dorsal view) **B** head including antennal scape and mesosoma (lateral view) **D** fore wing (parts of wing membrane and MV and STV magnified).

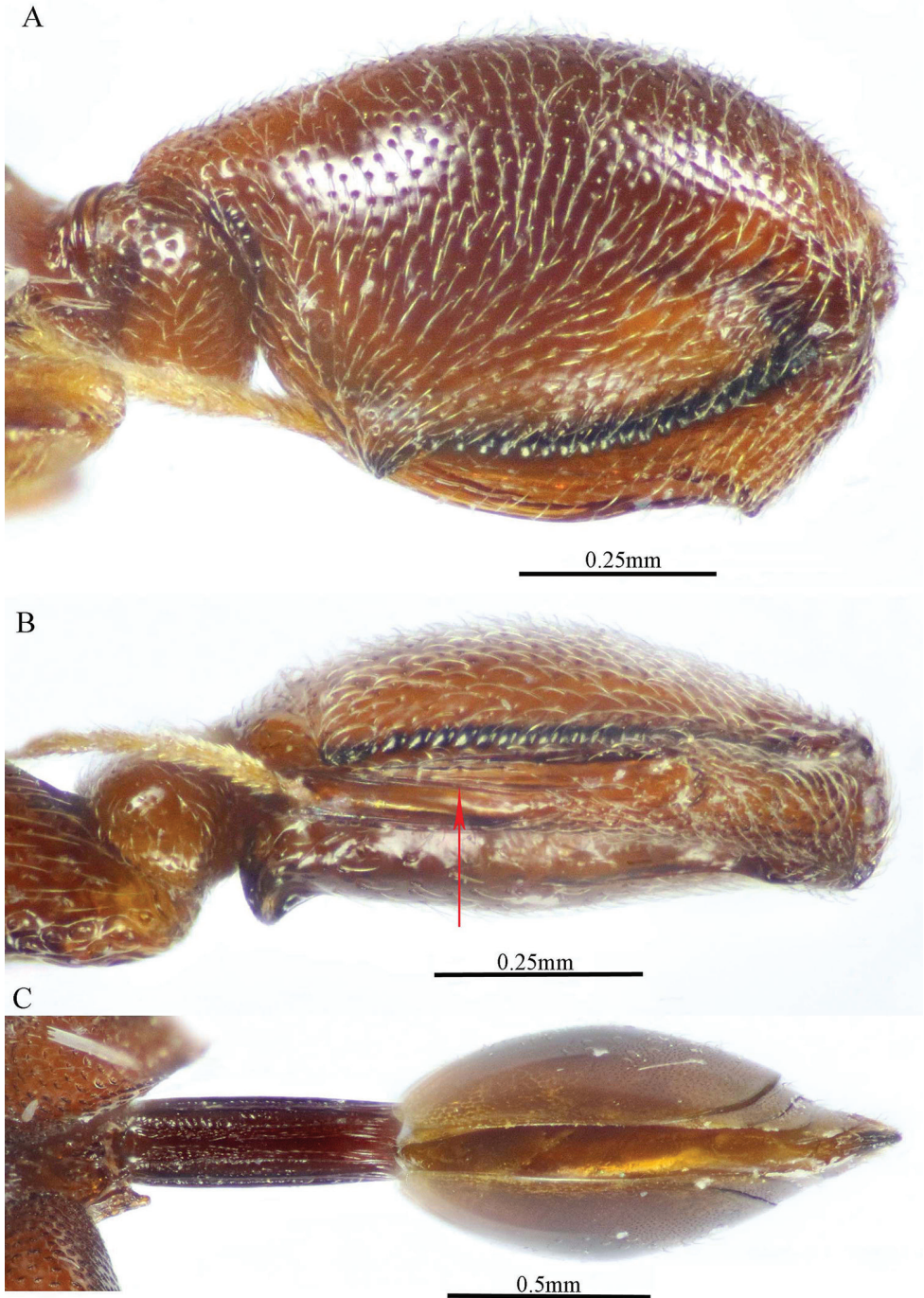


Figure 13. *Epitranus subinops* Soliman & Gadallah, sp. nov. (holotype female) **A, B** hind leg, excluding coxa (outer and ventral views respectively) **C** metasoma (ventral view).

Color (Figs 10A–C, 12C). Body generally reddish to reddish brown, with the following parts black: head (except lateral sides just below lower edge of eyes, and frontal lobe), anterior margin of mesoscutum middle lobe, propodeum (except postero-lateral margins). Metasoma dark reddish brown; antenna with scape and pedicel bright red, rest reddish brown; tegula testaceous. Wings hyaline with yellowish brown veins that are paler on hind wing.

Remarks. The new species closely similar to *E. inops*, but differs in the following: metatibia with oblique carina inside metatibial process (Fig. 13B) (metatibia without such carina in *E. inops* (Fig. 27C)); tarsal scrobe almost reaching sub-basal prominence (Fig. 13B) (tarsal scrobe short, far from reaching sub-basal prominence in *E. inops* (Fig. 27C)); frons with supra antennal surface completely delimited by a step-like margin (Fig. 11A) (supra antennal surface delimited only laterally by faint step-like ridge in *E. inops* (Fig. 26A)); mesoscutum with short, very small and sparse punctures on anterior part of middle lobe, while posterior area with coarse irregular foveolation (Fig. 11E) (setae on mesoscutum longer, denser and coarser on the whole middle lobe in *E. inops* (Fig. 25B)); mesoscutellum convex when seen in profile (Fig. 10A) (flat in *E. inops* (Fig. 25A)).

Male. Unknown.

Etymology. The new species name *subinops* refers to the similarity of this species to *E. inops*.

Hosts. Unknown.

Distribution. Saudi Arabia (Asir region).

List of new records

Epitranus clavatus (Fabricius, 1804)

Figures 14–16

Chalcis clavata Fabricius, 1804: 162; Bouček, 1982: 594: lectotype designation.

Epitranus fulvescens Walker, 1834: 26–27; Bouček, 1982: 594: synonymy.

Epitranus lacteipennis Cameron, 1883: 187–188; Bouček, 1982: 594: synonymy.

Anacryptus insidiosus Masi, 1917: 129–130; Bouček, 1982: 594: synonymy.

Anacryptus anpingius Masi, 1933: 14–15; Bouček, 1982: 594: synonymy.

Anacryptus cawnporensis Mani & Dubey in Mani, Dubey, Kaul & Saraswat, 1973: 30–31; Bouček, 1982: 594: synonymy.

Epitranus clavatus (Fabricius): Bouček, 1982: 594.

Re-description. Female (Figs 14–16). Body length ca. 3.75 mm. Fore wing length ca. 2.5 mm. Head and mesosoma mostly reddish, the later variously maculated with black (Fig. 14A, B), tegula brownish testaceous (Fig. 14B). This species is recognized by the following combination of characters: frontal lobe relatively long, its ventral margin with two submedian indentations (Fig. 15B); subantennal distance ca. 1.7× as long as interantennal distance, without median longitudinal carina; subtorular carina present; interantennal projection as small lamina (Fig. 15B); post-orbital groove granulate;

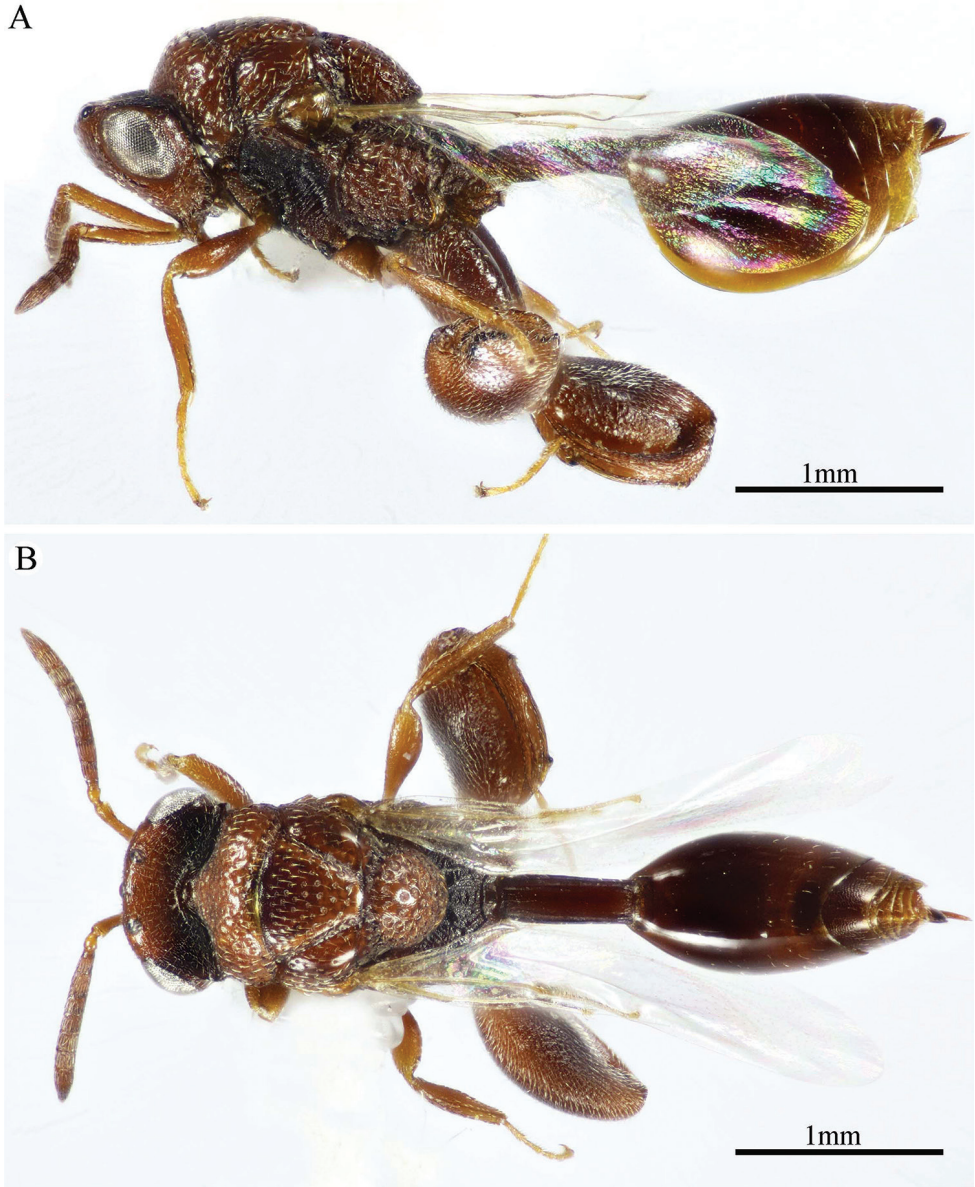


Figure 14. *Epitranus clavatus* (Fabricius) (female) **A, B** habitus (lateral and dorsal views respectively).

post-orbital carina joining genal carina at a level with ventral edge of eye (Fig. 14A); outline of frons slightly and regularly convex in dorsal view; supra antennal surface hardly delimited laterally by very faint step-like ridge; discal area very faintly strigulate, separated from inner orbit and median ocellus by four or five rows of setiferous points (Fig. 15A); flagellum somewhat slender (Fig. 15C), $0.82\times$ as long as head width; funiculars all somewhat longer than wide; mesosoma convex, its dorsal outline evidently

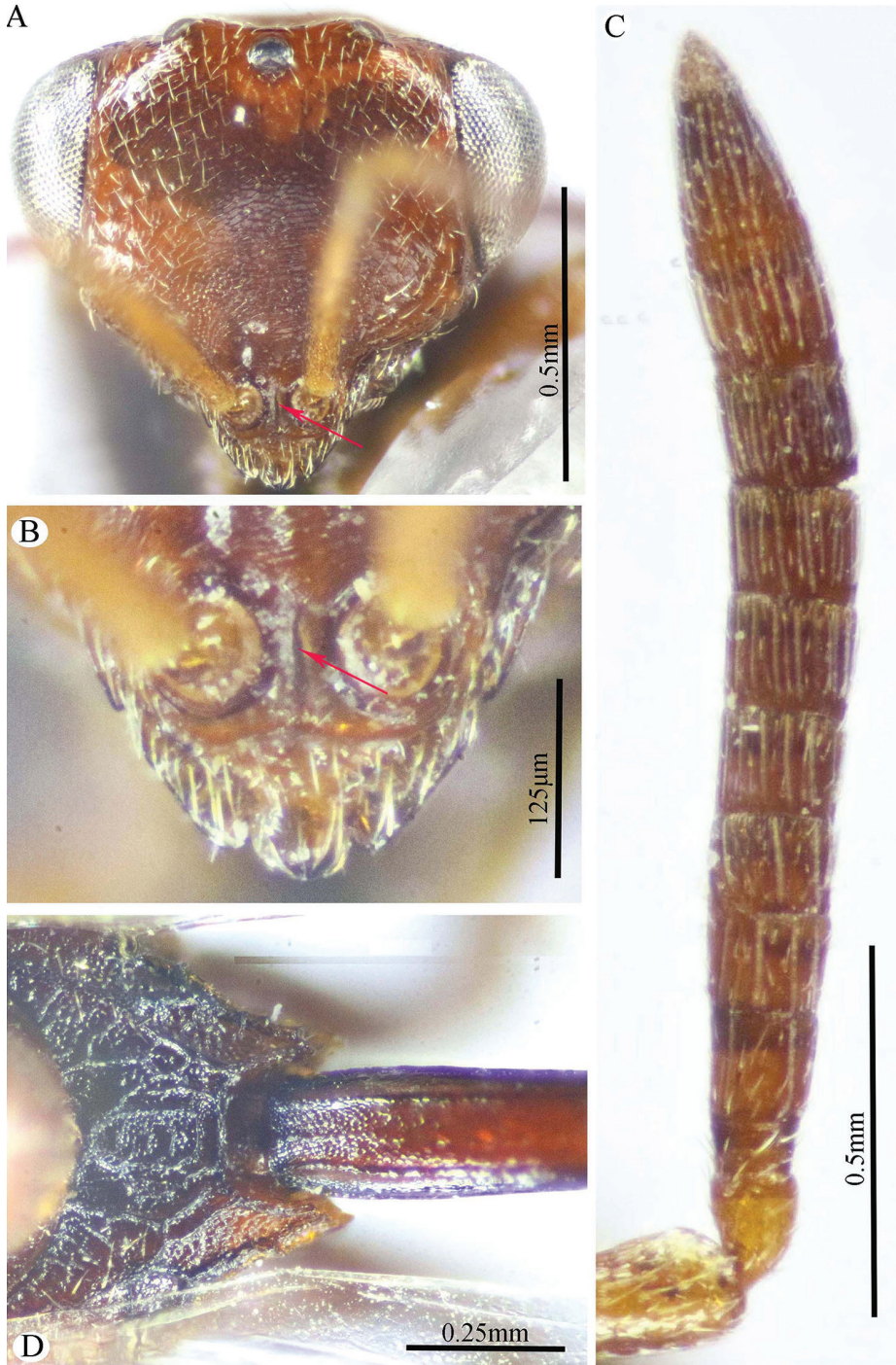


Figure 15. *Epitranus clavatus* (Fabricius) (female) **A** head (frontal view) **B** lower part of face showing frontal lobe (frontal view) **C** antennal pedicel and flagellum **D** propodeum and part of metasomal petiole (dorsal view).

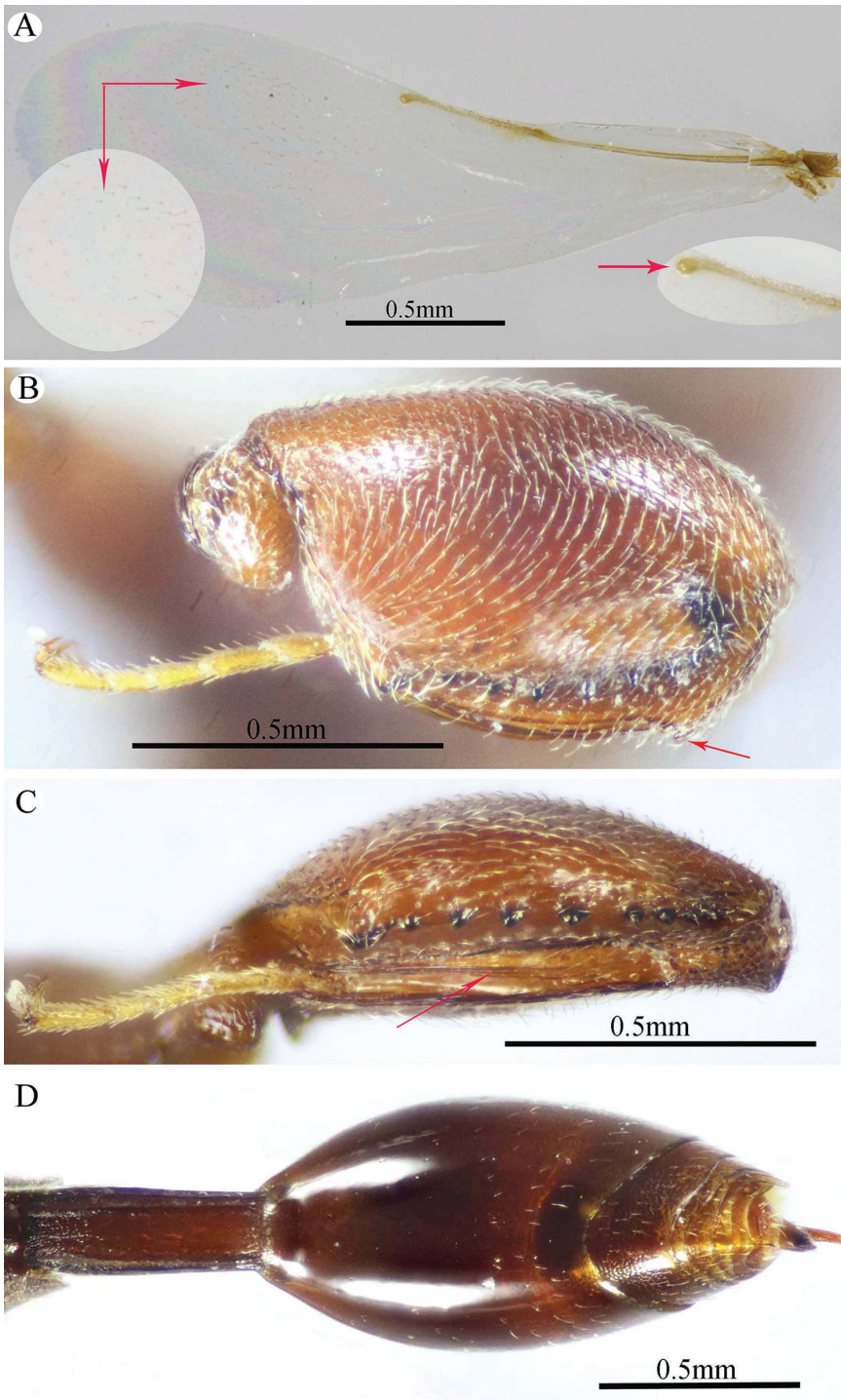


Figure 16. *Epitranus clavatus* (Fabricius) (female) **A** fore wing (parts of wing membrane and MV and STV magnified) **B, C** hind leg, excluding coxa (outer and ventral views respectively) **D** metasoma (dorsal view).

so (Fig. 15C); pronotal collar rounded anteriorly on dorsum (Fig. 14A); interspaces on mesonotum very faintly alutaceous; interspaces on mesepisternum and metepimeron coriaceous, dull (Fig. 14A); surface of propodeum densely reticulate, median areola complete but delimited by very faint submedian carina, sublateral carinae well raised on joining lateral carinae of adpetiolar areola, the latter nearly truncate anteriorly (Fig. 15D); pronotum, scapula (Fig. 14A, B) and ventral face of metacoxa sparsely setose, setae distinctly fine and short especially on pronotal collum; occiput (Fig. 14B) and propodeal prestigmatic areola (Fig. 15D) nearly bare, with scattered short and fine setae, the former finely alutaceous beneath. Fore wing (Fig. 16A) with sparse setae and microtrichiae on apical half of underside; STV distinctly oblique forming with the anterior margin of the wing an angle of ca. 35°. Metafemur with a stout basal tooth basoventrally, followed by eight small, widely spaced teeth (Fig. 16B); metatibial process with oblique carina inside, isolating the tarsal scrobe on inner side of tibia, the scrobe nearly reaching the sub-basal prominence anteriorly (Fig. 16C); prominence with three or four denticles concealed by the pubescence (when examined from behind). Metasomal petiole short, 2.7× as long as wide, 0.7× as long as dorsal length of Gt_1 , 0.5× as long as gaster (Fig. 16D), slightly swollen sub-basally, with two (sublateral and lateral) ridges extending along its whole length, area between sublateral ridges flat and faintly finely punctate. Gaster relatively elongate (1.5× as long as high).

Male. Similar to female but differs in having: body with extensive black tint on different parts; flagellum longer and slenderer (1.13× as long as head width); metasomal petiole longer (4.1× as long as wide, ca. 0.66× as long as dorsal length of gaster), with sides parallel and dorsum with weak median carina.

Hosts. Small Lepidoptera such as fungus moths (Tineidae): *Tinea antricola* Meyrick, and *Crypsithyris* sp. (Bouček 1982, Noyes 2019).

Material examined. 1♀ & 1♂, Kingdom of Saudi Arabia, Asir, Abha, Garf Raydah Natural Reserve [18°11'40.98"N, 42°23'45.66"E, Alt. 1861 m], sweeping net, 12.IV.2019, leg. Ahmed M. Soliman [KSMA]; 1♂, Kingdom of Saudi Arabia, Asir, Abha, Wadi Marabah [18°10'09.59"N, 42°22'15.12"E, 1205 m], sweeping net, 13.IV.2019, leg. Ahmed M. Soliman [KSMA].

Distribution. This species probably originates from SE Asia and was repeatedly introduced following trading (Bouček 1982), Iran (Moravvej et al. 2018), Saudi Arabia (Asir region) (new record).

Epitranus hamoni complex

Figures 17–24

Spilochalcis hamoni Risbec, 1957: 240.

Diagnosis. Female (Figs 17–20). Body length ca. 3.15 mm; fore wing length ca. 2.0 mm. Body blackish brown, with the following parts are red to reddish brown (Figs 17A, B, 18A): head (except a black, broad lower band on occiput), pronotum, scapula, propo-

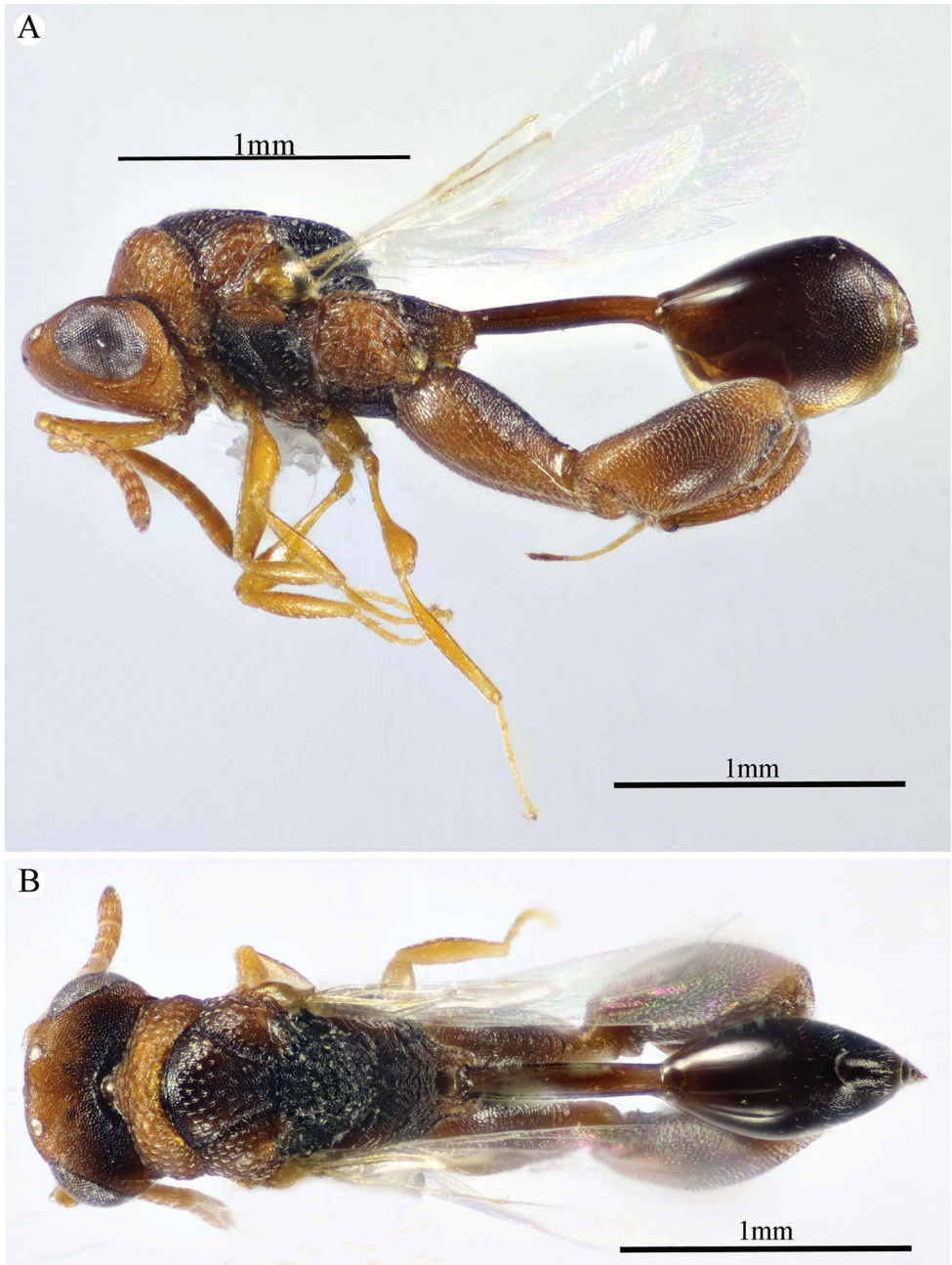


Figure 17. *Epitranus hamoni* complex (female, dark form) **A, B** habitus (lateral and dorsal views respectively).

deum postero-laterally, metepimeron, gastral petiole, antenna and legs (dorsal face of metacoxa and outer face of metafemur with black tint). This species is diagnosed by the following combination of characters: Occiput densely reticulate, nearly bare (Fig. 18D);

frontal lobe reduced to a faint transverse carina, thus exposing clypeus (Fig. 18B); interantennal projection represented by a low, but sharp lamina; flagellum somewhat clavate (Fig. 18C), ca. $0.93\times$ as long as head width; anellus transverse, ca. $0.3\times$ as long as wide; F1 as long as its width, ca. $0.9\times$ as long as F2; F3 as long as wide; clava ca. $2.45\times$ as long as wide. Interspaces between foveolae as well as their bottoms on mesosomal dorsum and pleura are densely reticulate (Fig. 18D); propodeum fairly dull, with areolae vague and finely punctate on their bottoms; median areola opened posteriorly, with lateral ridges short (not extending to meet transverse carina of adpetiolar areola) (Fig. 18D). Fore wing (Fig. 19A) with distinctly reduced pilosity, with scattered setae and microtrichiae on apical half of underside; STV reduced, gently sloping, forming with the anterior margin an angle of ca. 35° . Metafemur with a broad triangular tooth basoventrally followed by eight spaced teeth (Fig. 19B); tarsal scrobe on metatibia $0.6\times$ as long as metatibial length, polished and reaching sub-basal extremely low hump that represents the sub-basal prominence (Fig. 19C). Metasomal petiole relatively long ($5.7\times$ as long as wide, $1.1\times$ as long as dorsal length of Gt_1 , and $0.8\times$ as long as gaster), dorsally with two longitudinal (sublateral and lateral) ridges, of which sublateral one ends slightly before apex of petiole, area between them flat and finely punctate (Fig. 19D); Gaster relatively short, $1.43\times$ as long as high in profile (Fig. 17A).

Male (Figs 21–24). Similar to female except for: head and mesosoma generally dark brown to black, with inner margins of eye, lower half of face and pronotal lateral panel red, rest of the pronotum reddish brown (Figs 21A, B, 22A); interantennal projection absent (Fig. 22A); OOD short, ca. $1.43\times$ as long as OD (Fig. 22B); scape of antenna with deep excavation nearly along its dorsal mesal third (Fig. 22B); flagellomeres slenderer than in female (Fig. 22C); foveolae on mesosomal dorsum sparser; propodeal median areola narrow, $4.0\times$ as long as wide, reaching transverse carina of adpetiolar areola (Fig. 22D); petiole longer, ca. $8.0\times$ as long as wide (Fig. 23C, 24B).

Remarks. This species shows variation in color, some body sculpturing, and measurements among females and males as well. One of the three examined females, the body (including antennae and legs) is generally bright red, only darkened along the anterior and lateral sides of mesoscutellum, inner surface of metafemur, and gaster (Fig. 20A, B); in the other female specimens, body blackish brown, with the following parts are red to reddish brown (Figs 17A, B, 18A): head (except a black, broad lower band on occiput), pronotum, scapula, propodeum postero-laterally, metepimeron, gastral petiole, antenna and legs (dorsal face of metacoxa and outer face of metafemur with black tint). In the reddish specimen, the middle lobe of mesoscutum with denser and smaller setiferous punctures (Fig. 20B), mesoscutellum foveolate, with spaces less than a foveola diameter (ca. $0.5\times$ diameter apart), bottom of foveolae smooth (Fig. 20B) (in the dark specimens, punctures on mesoscutum sparser and a little larger (Fig. 18D); mesoscutellum densely and deeply foveolate, without considerable interspaces between foveolae (Fig. 17B)); in the red specimen, petiole $6.3\times$ as long as wide, $0.9\times$ as long as gaster in dorsal view (Fig. 20B) (in the dark specimens, petiole ca. $5.7\times$ as long as wide, $0.77\times$ as long as gaster in dorsal view (Fig. 17B)); in the reddish specimen, posterior margin of Gt_1 straight (Fig. 20B) (in the dark ones, posterior margin of Gt_1 deeply concave (Fig. 17B)); in the red-

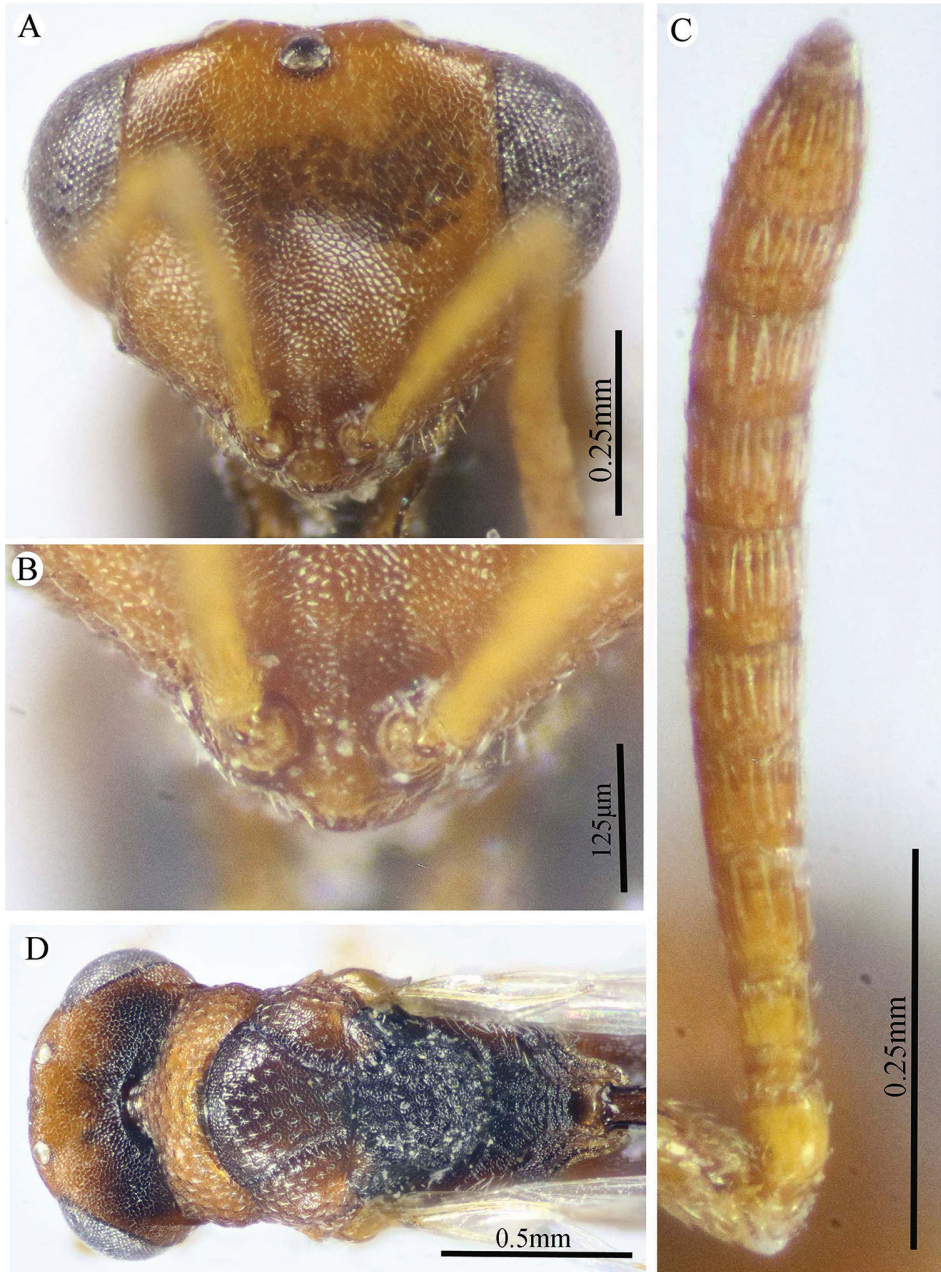


Figure 18. *Epitranus hamoni* complex (female, dark form) **A** head (frontal view) **B** lower part of face (frontal view) **C** antennal pedicel and flagellum **D** head and mesosoma (dorsal view).

dish specimen, F1 ca. 2.15 \times as long as wide, and distinctly longer than F7 (1.2 \times) (ca. 1.27 \times as long as wide, and slight shorter to as long as F7 in the dark specimens); STV obviously separated from anterior margin of the wing, making an angle of 45° in the

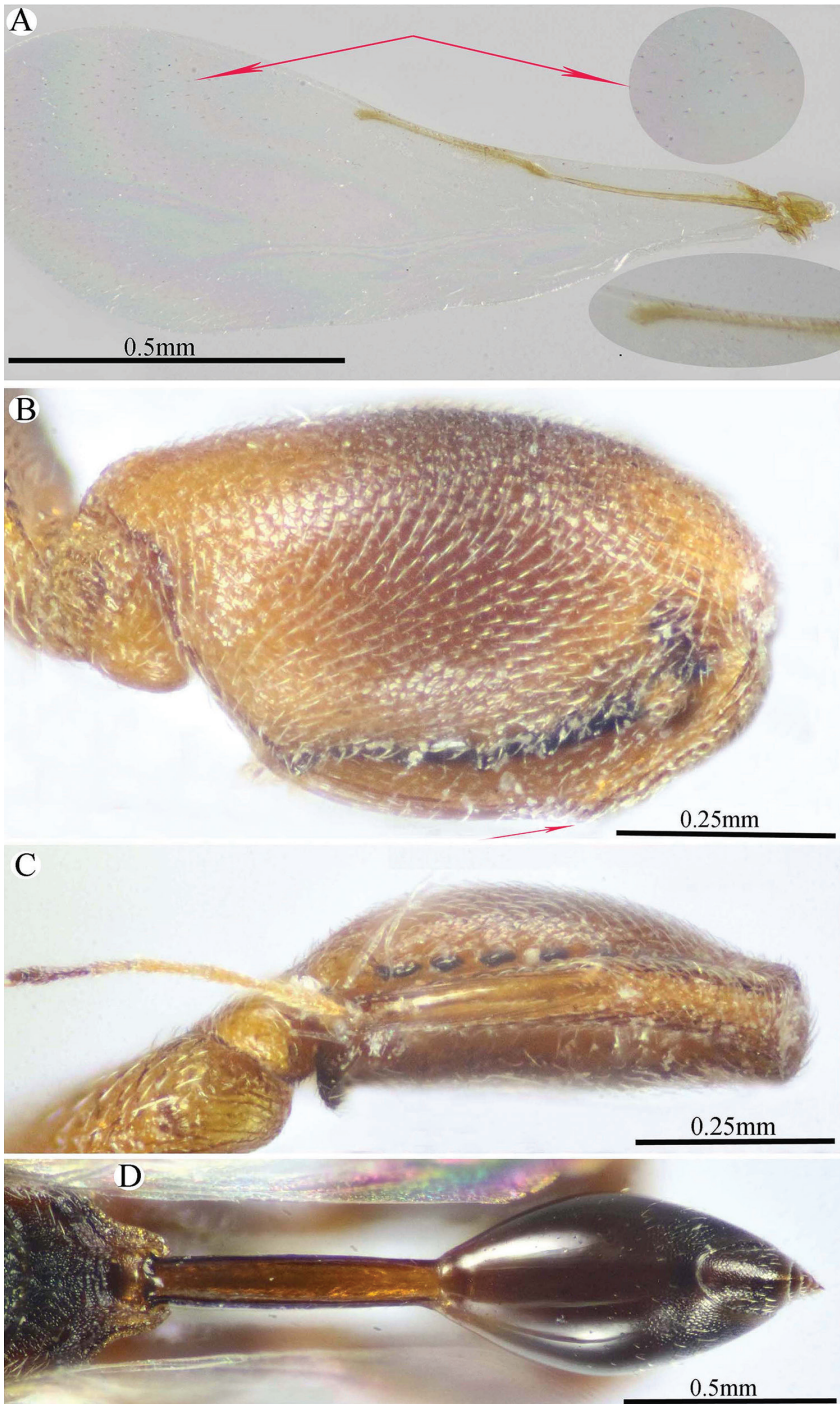


Figure 19. *Epitranus hamoni* complex (female, dark form) **A** fore wing (parts of wing membrane and MV and STV magnified) **B, C** hind leg, excluding coxa (outer and ventral views respectively) **D** propodeum and metasoma (dorsal view).

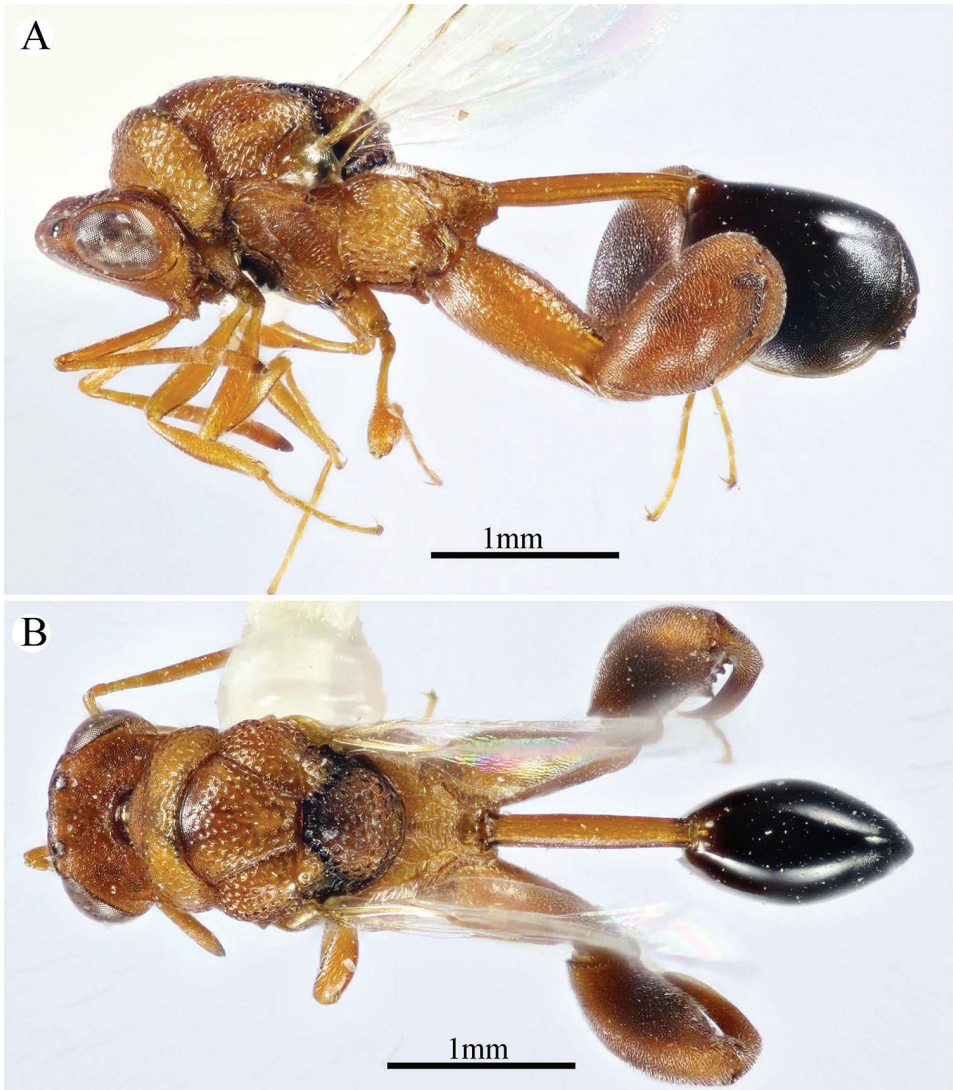


Figure 20. *Epitranus hamoni* complex (female, light form) **A, B** habitus (lateral and dorsal views respectively).

light specimen (while in the darker specimens STV adheres to anterior margin of the wing making an angle of ca. 35°).

In the two examined males, one with the red color predominates, being seen in the head (except dark occiput) including antennae, pronotal collar, propodeum, legs (hind legs darker), and petiole (Fig. 24A, B); the other male specimen is nearly entirely dark brown to black, with inner margins of eye, lower half of face and pronotal lateral panel red (Fig. 21A, B). In the reddish specimen, mesoscutum sparsely setiferous punctate anteriorly, and sparsely foveolate posteriorly (Fig. 24B) (in the dark specimen superficially, sparsely foveolate throughout (Fig. 21B); in the reddish specimen, head asetose postero-

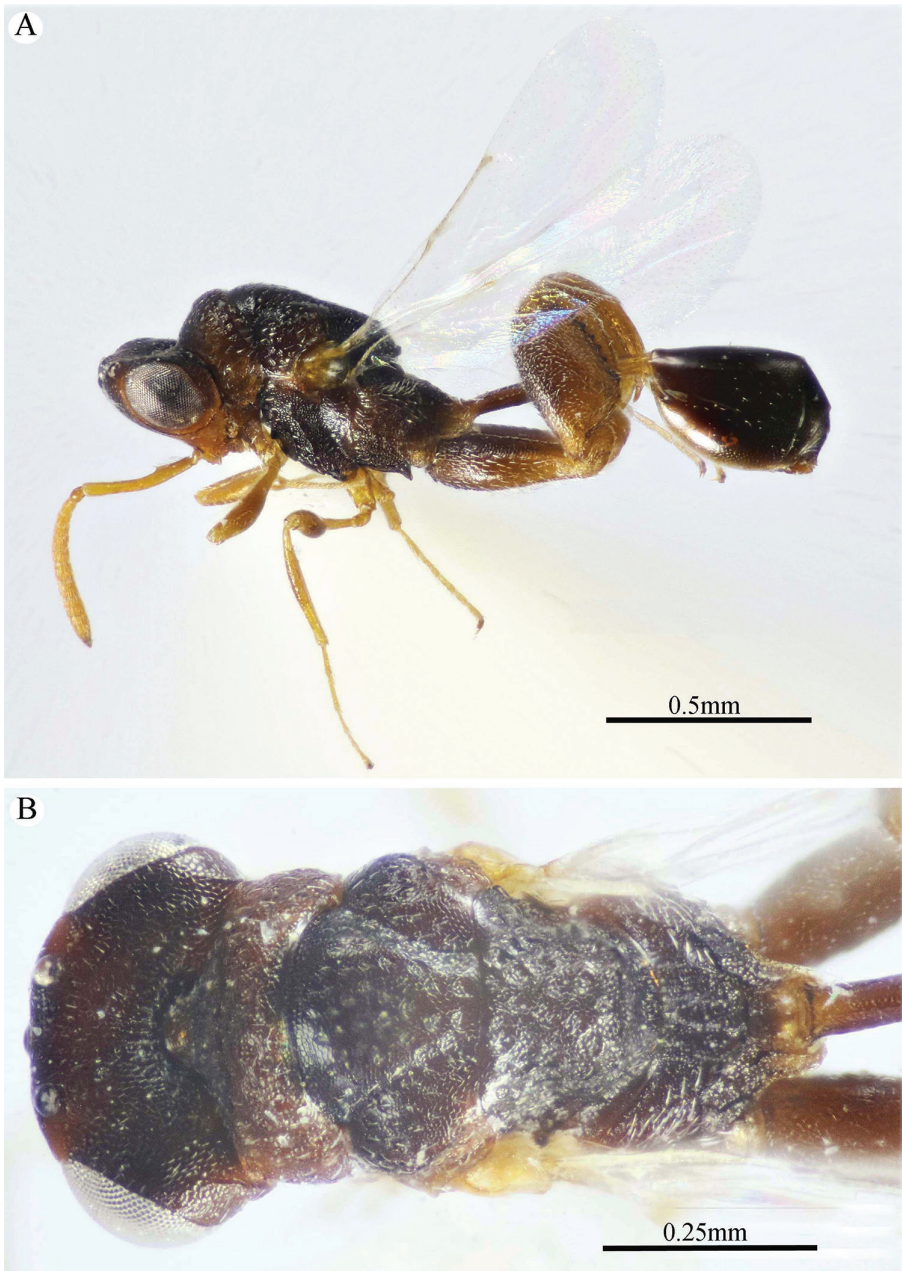


Figure 21. *Epitranus hamoni* complex (male, dark form) **A** habitus (lateral view) **B** head and mesosoma (dorsal view).

laterally (Fig. 24B) (in the dark one, head densely setose postero-laterally (Fig. 21B)); in the reddish specimen metacoxa 2.6× as long as wide (Fig. 24B) (in the dark specimen, metacoxa 2.77× as long as wide (Fig. 21A)); in the reddish specimen, petiole 9.3× as long

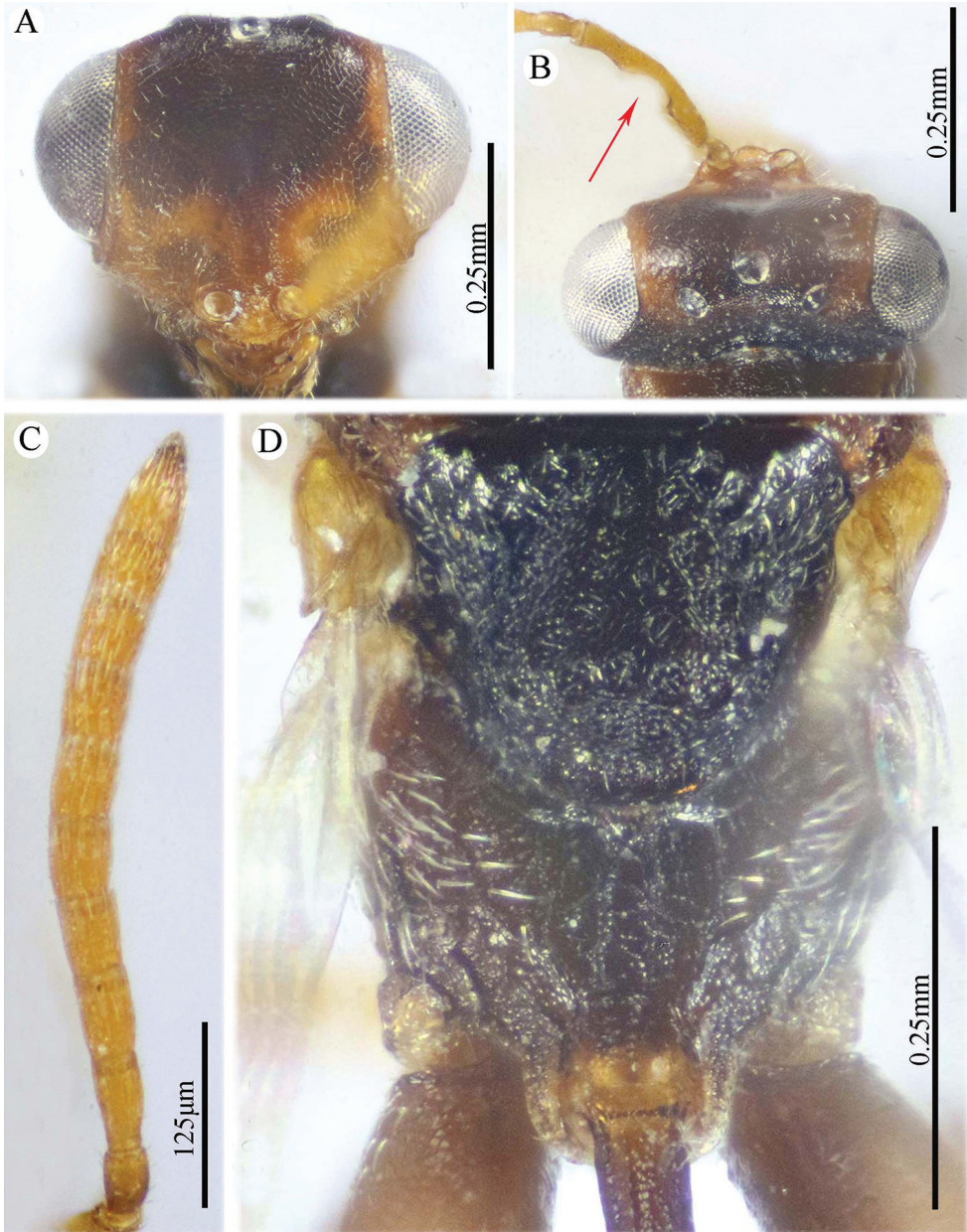


Figure 22. *Epitranus hamoni* complex (male, dark form) **A** head (frontal view) **B** head and antennal scape (dorsal view) **C** antennal pedicel and flagellum **D** mesoscutellum, metanotum & propodeum (dorsal view).

as wide, and approximately as long as gaster middle length in dorsal view (Fig. 24B), 1.6× as long as gaster height in lateral view (Fig. 24A) (in the dark specimen, petiole 8.0× as long as wide, 1.12× as long as gaster in dorsal view (Fig. 23C), 2.4× as long as gaster height in lateral view (Fig. 21A)); in the reddish specimen, posterior margin of

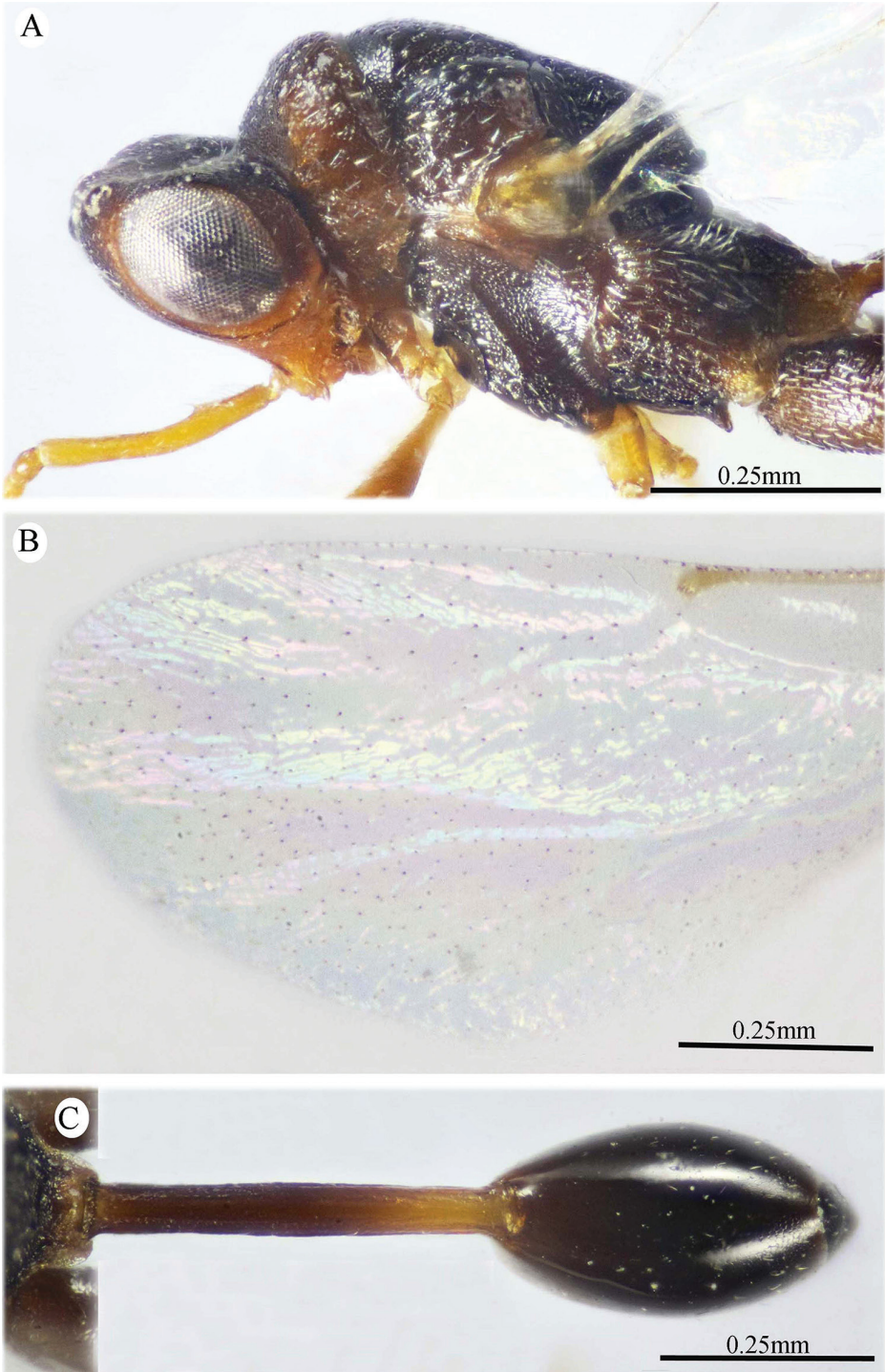


Figure 23. *Epitranus bamoni* complex (male, dark form) **A** head and mesonotum (lateral view) **B** apical part of fore wing **C** metasoma (dorsal view).

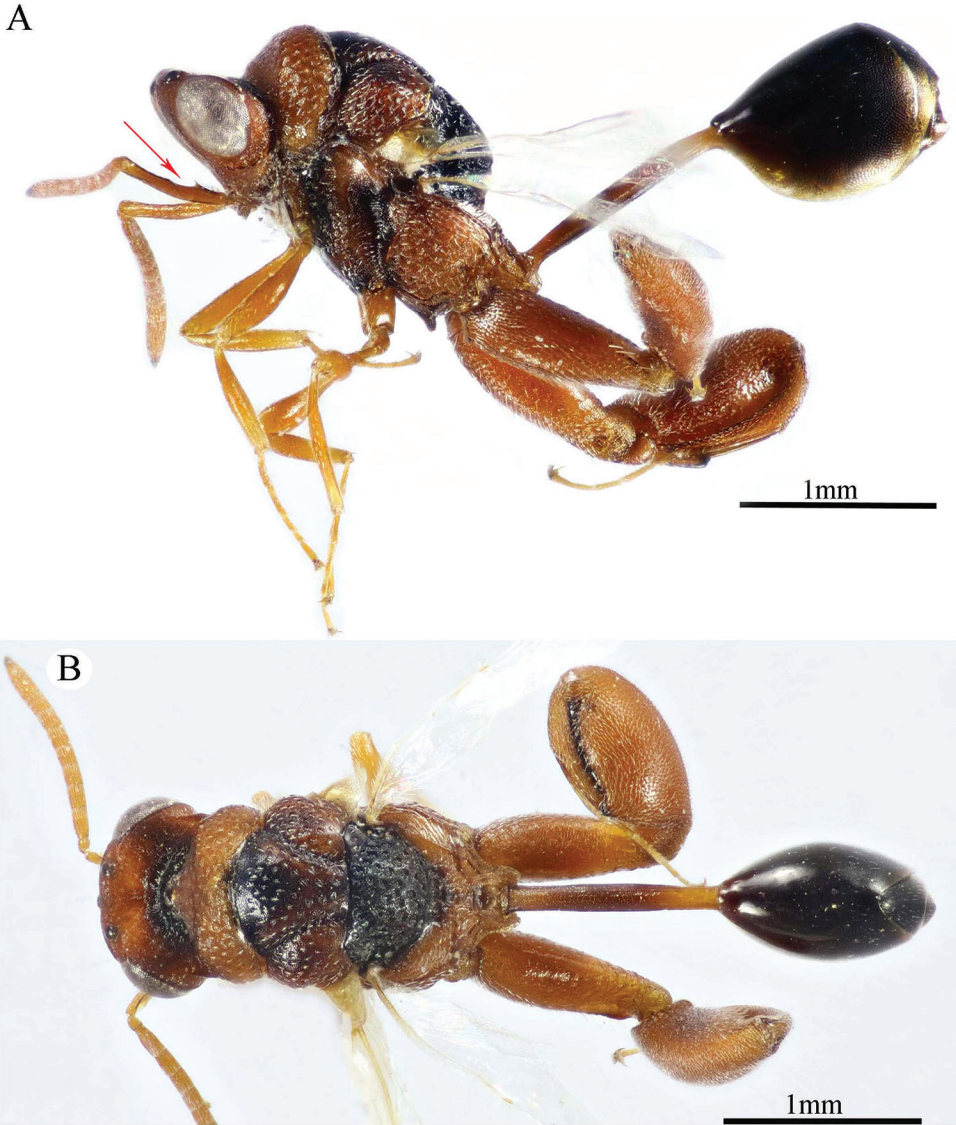


Figure 24. *Epitranus hamoni* complex (male, light form) **A, B** habitus (lateral and dorsal views respectively).

Gt₁ deeply concave (Fig. 24B) (in the dark specimen, posterior margin of Gt₁ straight (Fig. 23C)).

Hosts. Unknown.

Material examined. 1♂, Kingdom of Saudi Arabia, Al-Baha, Al Mikhwa, Shada Al-Ala Natural Reserve [19°50'34.48"N, 41°18'39.44"E, Alt. 1681 m], sweeping net, 27.VII.2015, leg. Ahmed M. Soliman [KSMA]; 1♀, Kingdom of Saudi Arabia, Asir, Abha, Garf Raydah Natural Reserve [18°11'36.93"N, 42°23'25.17"E, Alt. 1772 m], sweeping net, 16.IV.2016, leg. Ahmed M. Soliman [KSMA]; 1♂, Kingdom of

Saudi Arabia, Al-Baha, Al Mikhwa, Shada Al-Ala Natural Reserve [19°50'34.95"N, 41°18'40.04"E, Alt. 1679 m], sweeping net, 7.IV.2019, leg. Ahmed M. Soliman [KSMA]; 1♀, Kingdom of Saudi Arabia, Al-Baha, Al Mikhwa, Shada Al-Ala Natural Reserve [19°50'34.89"N, 41°18'39.43"E, Alt. 1689 m], sweeping net, 9.IV.2019, leg. Ahmed M. Soliman [KSMA]; 1♀, Kingdom of Saudi Arabia, Riyadh, Dirab Station of Research, [24°25'22.91"N, 46°39'15.02"E, Alt. 1689 m], Malaise trap, 19.VII–9.VIII.2020, leg. Ahmed M. Soliman [KSMA].

Distribution. Burkina Faso (Risbec 1957; Noyes 2019), UAE (Delvare 2017), Saudi Arabia (Al-Baha and Riyadh regions) (new record).

Epitranus inops Steffan, 1957

Figures 25–27

Epitranus inops Steffan, 1957: 75, 86–88. Original description. ♀, ♂. Democratic Republic of Congo.

Epitranus inops Steffan, 1957: Sauphanor et al. 1987: Ivory Coast: host.

Re-description. Female (Figs 25–27). Body length 3.4–3.9 mm. Fore wing length 2.1–2.5 mm. Head, except frontal lobe and antennal toruli, black (Fig. 26A); mesosoma reddish brown, with various extent of brownish, more or less dark, areas on mesoscutum, axilla, propodeum, mesopleuron, metepisternum anteriorly (Fig. 25B); tegula testaceous (Fig. 25A, B). This species is recognized by the following combination of characters: interantennal lamina present (Fig. 26A); frontal lobe moderately long (Fig. 26B); subantennal distance ca. 2.5× as long as interantennal distance, with two submedian indentations on ventral edge (Fig. 26B); supra antennal surface delimited laterally by faint step-like ridge; discal area faintly alutaceous, the network following curved lines, separated from inner orbit and median ocellus by four or five rows of moderately large punctures, interspaces between punctures smooth (Fig. 26A); preorbital groove vestigial dorsally, progressively thickened towards the suborbital groove; outline of frons slightly and regularly convex in dorsal view; funiculars, from F2, somewhat transverse (Fig. 26C); clava bi-segmented (Fig. 26C). Mesosoma hardly convex, with flattened mesoscutellum (Fig. 25A, B); setae on mesonotum thin, adpressed and longer than puncture diameter (Fig. 25B); propodeum dull, with numerous irregular rugae, median areola complete, with subparallel sides (Fig. 26D); adpetiolar areola with curved anterior carina (Fig. 26D). Fore wing (Fig. 27A) rather densely setose on apical half on underside; STV forming with anterior margin an angle of ca. 45°; metacoxal 2× as long as wide, with flattened outer dorsal side; metafemur serrulate behind the basal tooth (Fig. 27B); metatibial process only delimited posteriorly on inner side along tarsal scrobe, visible anteriorly through the presence of a wrinkle, tarsal scrobe far from reaching sub-basal prominence, the latter with four denticles on edge, visible solely from behind for being concealed by the pubescence (Fig. 27C); metasomal petiole 3.4–3.7× as long as wide, as long as or slightly shorter than dorsal length of



Figure 25. *Epitranus inops* Steffan (female) **A, B** habitus (lateral and dorsal views respectively).

Gt₁ (0.95×), and 0.50–0.65× as long as gaster length, its sides hardly convex, with a weak median carina evanescent on apical third, sublateral and lateral ridges complete, the area between sublateral ridges smooth and shiny (Fig. 27D); gaster 1.55–1.70× as long as high (Fig. 25A).

Male. Similar to female except flagellum 1.2× head width; anellus ca. 0.3× as long as wide; F1 twice as long as wide; F7 subquadrate; gastral petiole slightly longer, 4.5× as long as wide (Steffan 1957).

Hosts. The species was reared from stored yam together with *Euzopherodes vapidella* Man (Pyralidae), and other small moths (Sauphanor et al. 1987).

Material examined. 1♀: Kingdom of Saudi Arabia, Al-Baha, Al Mikhwa, Shada Al-Ala Natural Reserve [19°50'34.87"N, 41°18'40.04"E, 1686 m], sweeping net, 5.V.2015, leg. Ahmed M. Soliman [KSMA]; 1♀, Kingdom of Saudi Arabia, Al-Baha, Al Mikhwa, Shada Al-Ala Natural Reserve [19°50'34.89"N, 41°18'39.43"E, 1689 m], sweeping net, 9.IV.2019, leg. Ahmed M. Soliman [KSMA]; 1♀, Kingdom

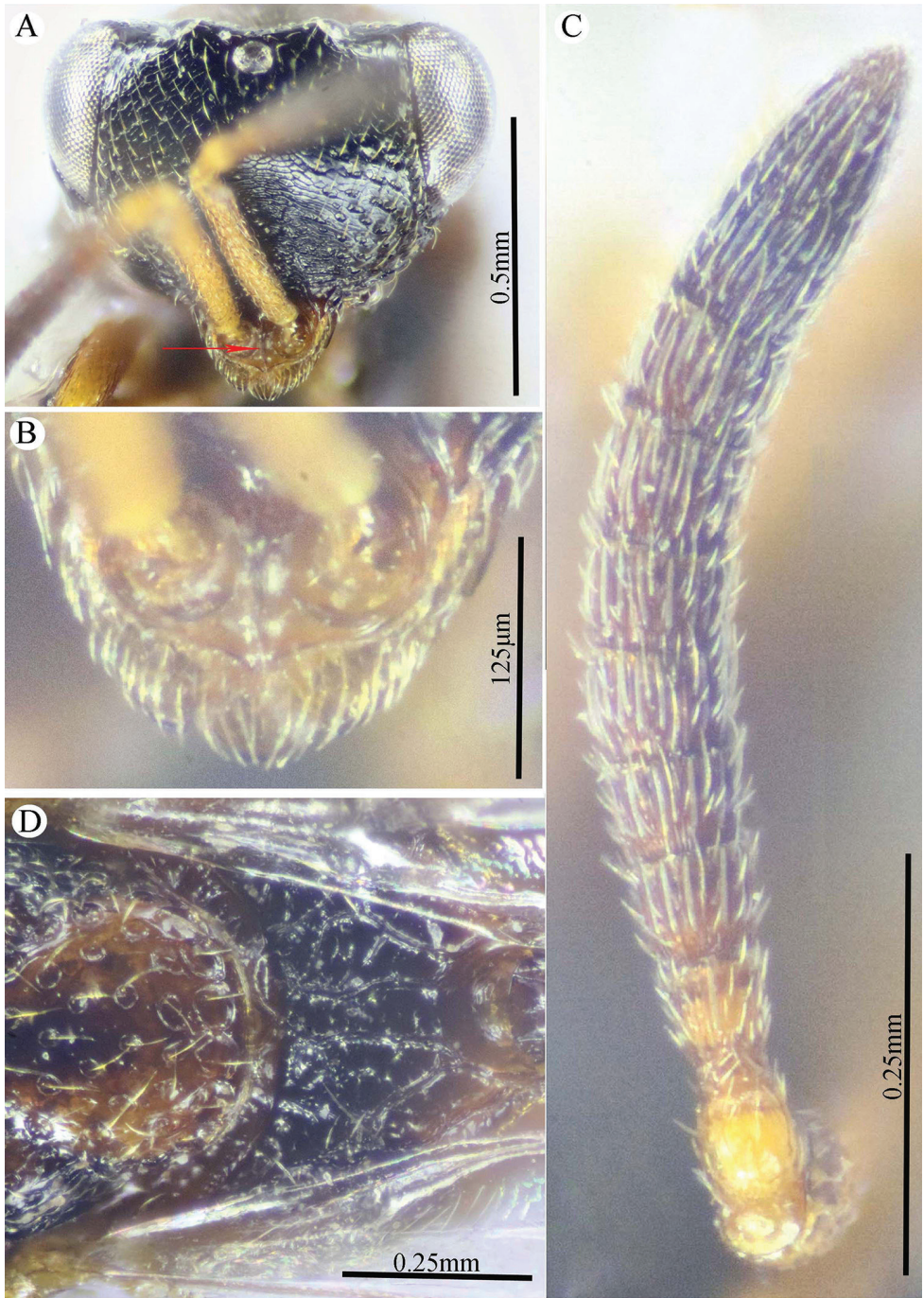


Figure 26. *Epitranus inops* Steffan (female) **A** head (frontal view) **B** lower part of face showing frontal lobe (frontal view) **C** antennal pedicel and flagellum **D** mesoscutellum and propodeum (dorsal view).

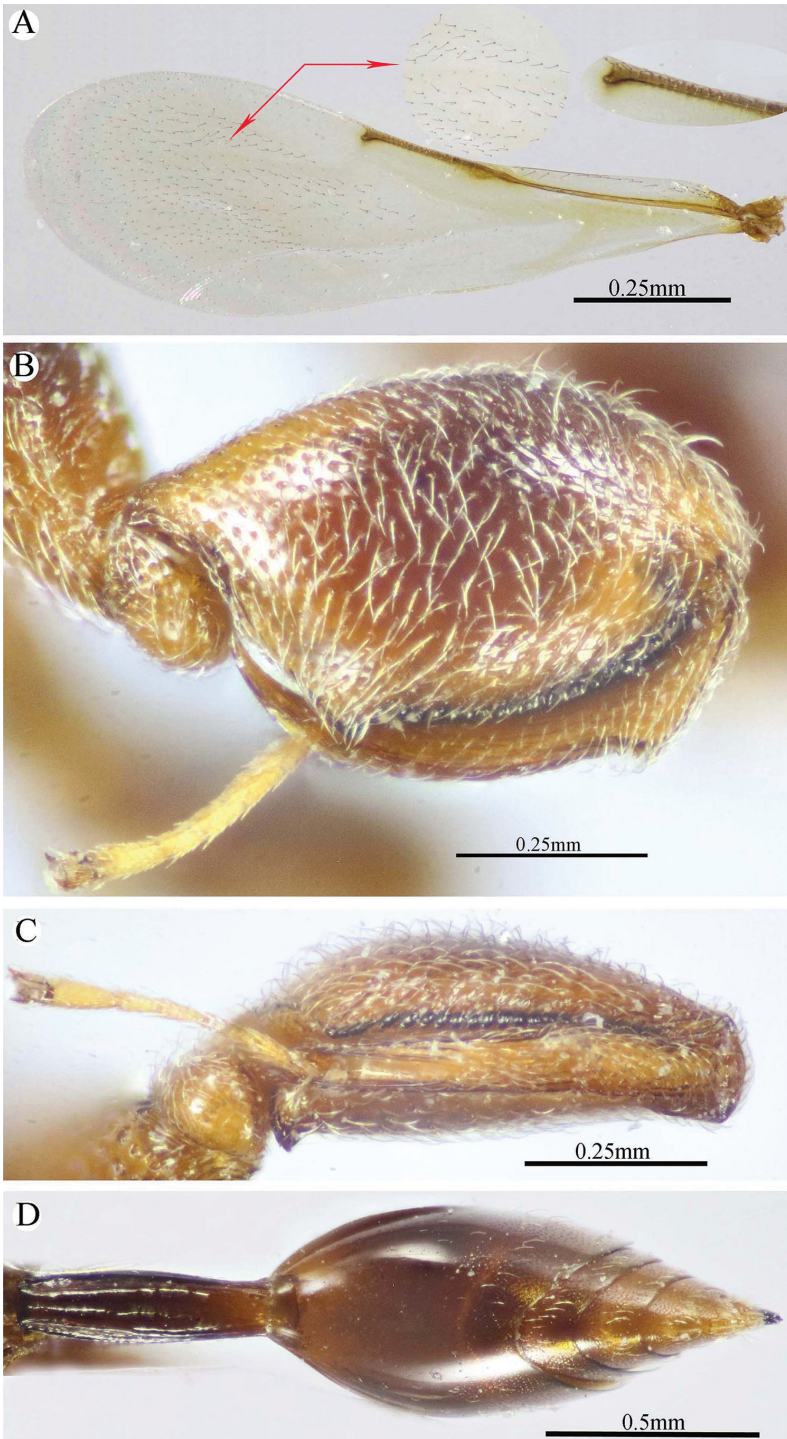


Figure 27. *Epitranus inops* Steffan (female) **A** fore wing (parts of wing membrane and MV and STV magnified) **B, C** hind leg, excluding coxa (outer and ventral views respectively) **D** metasoma (dorsal view).

of Saudi Arabia, Asir, Abha, Garf Raydah Natural Reserve [18°11'40.98"N, 42°23'45.66"E, 1861 m], sweeping net, 12.IV.2019, leg. Ahmed M. Soliman [KSMA].

Distribution. Democratic Republic of Congo (Zaire) (Steffan 1957), Ivory Coast (Sauphanor et al. 1987), Saudi Arabia (Al-Baha and Asir regions) (new record).

Epitranus torymoides (Risbec, 1953)

Figures 28–30

Chalcitella torymoïdes Risbec, 1953: 591. Original description ♂. Ivory Coast.

Epitranus torymoides Risbec, 1953: Delvare, 2017: 244.

Re-description. Female (Figs 28–30). Body length 2.65–3.20 mm. Fore wing length 1.85–2.00 mm. Head, except reddish frontal lobe, and mesosoma black (Figs 28A, B, 29A); metasoma dark brown with slight reddish tint laterally on tergites and on sternites (Fig. 28A, B); fore and mid legs, metatrochanter, metatarsus, scape and tegula testaceous (Fig. 28A); pedicel, flagellum and metafemur dark brown (Fig. 28A, B). This species is recognized by the following combination of characters: frons laterally and dorsally, and dorsum of mesosoma, with moderately long, suberect and thin setae (Figs 28B, 29A); interantennal projection absent (Fig. 29A); frontal lobe moderately protruding, with subantennal distance ca. 1.3× as long as interantennal distance, ventral edge of projection broadly rounded, entire (Fig. 29A); supra antennal surface smooth, completely delimited by step-like margin, 1.7× as high as wide; discal area reduced to a smooth crescentic surface above the supra antennal one; rest of the frons with moderately large setiferous punctures (Fig. 29A); gena areolate (Fig. 28A); preorbital, suborbital and postorbital grooves well impressed, the first one smooth, while the others areolate; postorbital carina joining genal carina at a level slightly below ventral edge of eye; outline of frons hardly and regularly convex in dorsal view; flagellum strongly clavate, 0.96× as long as head width (Fig. 29B); the two basal flagellomeres subquadrate, lacking MPS; clava bi-segmented (Fig. 29B); pronotum and mesonotum densely and regularly punctured (Fig. 28B); pronotal collar rounded on dorsum (Fig. 28B); propodeal surface with numerous secondary rugae, with fusiform median areola not quite reaching the truncate adpetiolar areola (Fig. 28B). Fore wing (Fig. 29C) with strongly reduced venation, only base of SMV present; apical half of wing membrane with scattered setae on underside; metacoxa with nearly smooth and flattened outer dorsal side; metafemur with seven or eight widely spaced teeth following the stout basal one on ventral margin (Fig. 30B); metatibial process only delimited on inner side along the short tarsal groove, the latter approximately one third, the rest of the process is visible as being sparsely and finely setose, the setation not concealing the integument surface there (Fig. 30A); sub-basal prominence vestigial, hardly visible, with a single denticle (Fig. 30A); metasomal petiole 2.8–3.0× as long as wide, 0.6× as long as dorsal length of Gt_1 , and 0.40–0.45× as long as gaster (Fig. 28B); the area



Figure 28. *Epitranus torymoides* (Risbec) (female) **A, B** habitus (lateral and dorsal views respectively).

between sublateral ridges on petiole flat and rough, with hardly indicated longitudinal median carina at base and apex, absent medially (Fig. 28A, B); Gaster 1.8× as long as high (Fig. 28A).

Male. Differs from female in the following: flagellum and metasomal petiole darker, dark brown to black, the latter reddish brown posteriorly; metasoma with black tint dorsally; anellus transverse; flagellum slender, F1 ca. 2× as long as wide, 1.28–1.30× as long as each of F2 and F7; petiole with a complete median carina.

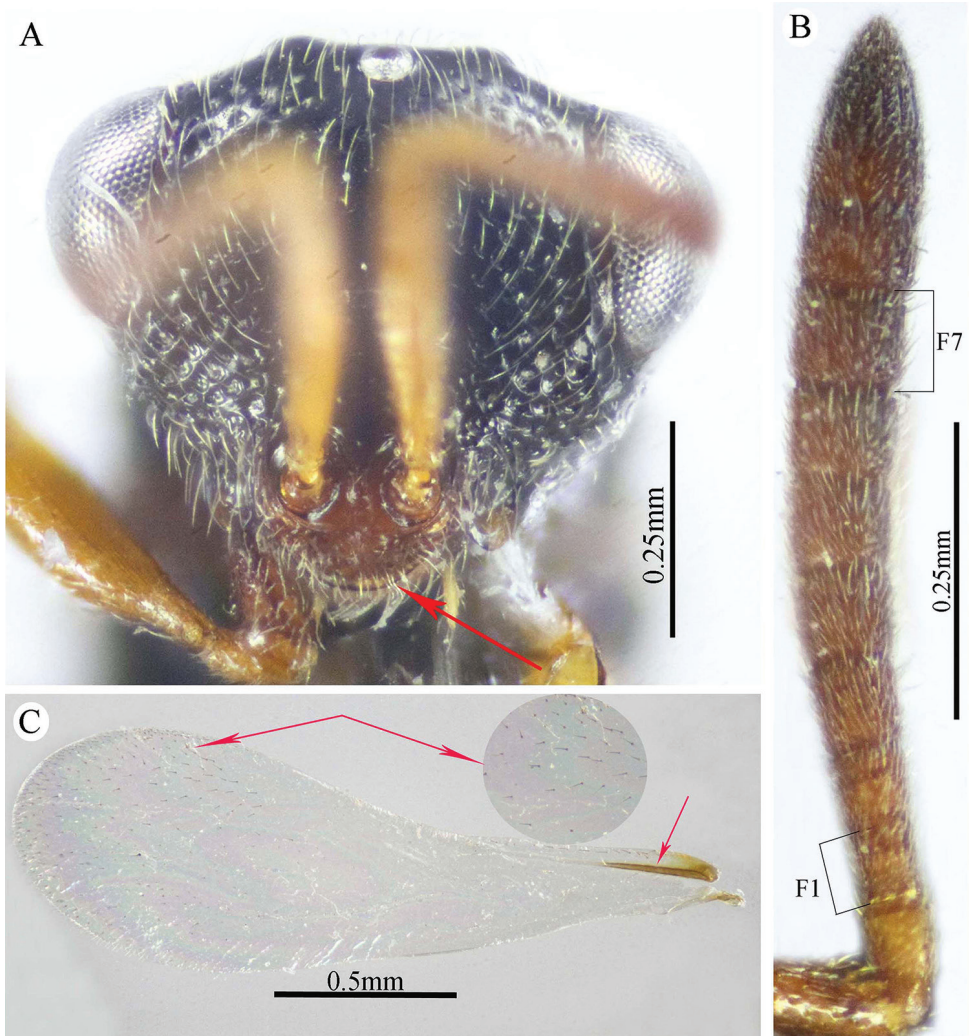


Figure 29. *Epitranus torymoides* (Risbec) (female) **A** head (frontal view) **B** antennal pedicel and flagellum **C** fore wing (part of wing membrane magnified).

Hosts. Unknown.

Material examined. 1♀: Kingdom of Saudi Arabia, Al-Baha, Al Mikhwa, Shada Al-Ala Natural Reserve [19°50'34.87"N, 41°18'40.04"E, 1686 m], sweeping net, 5.V.2015, leg. Ahmed M. Soliman [EFC]; 1♂: Kingdom of Saudi Arabia, Asir, Muhayil, Wadi Sabean [18°17'53"N, 42°07'39"E, 775 m], Sucking device, 10.II.2016, leg. A. Al-Ansi [KSMA]; 7♀ & 1♂: Kingdom of Saudi Arabia, Asir, Muhayil, Wadi Heli [18°30'10.66"N, 42°01'56.07"E, 450 m], sweeping net, 23.X.2016, leg. Ahmed M. Soliman [KSMA]; 1♂: Kingdom of Saudi Arabia, Jazan, Damad, Al Shuqayri [17°07'39.50"N, 42°48'44.88"E,



Figure 30. *Epitranus torymoides* (Risbec) (female) **A, B** hind leg, excluding coxa (outer and ventral views respectively).

90 m], Sucking device, 12.V.2018, leg. Ahmed M. Soliman [KSMA]; 1♀: Saudi Arabia, Asir, Abha, Garf Raydah Natural Reserve [18°11'40.98"N, 42°23'45.66"E, 1861 m], sweeping net, 12.IV.2019, leg. Ahmed M. Soliman [KSMA].

Distribution. Côte d'Ivoire (Risbec 1953), Saudi Arabia (Al-Baha, Asir, and Jazan regions) (new record).

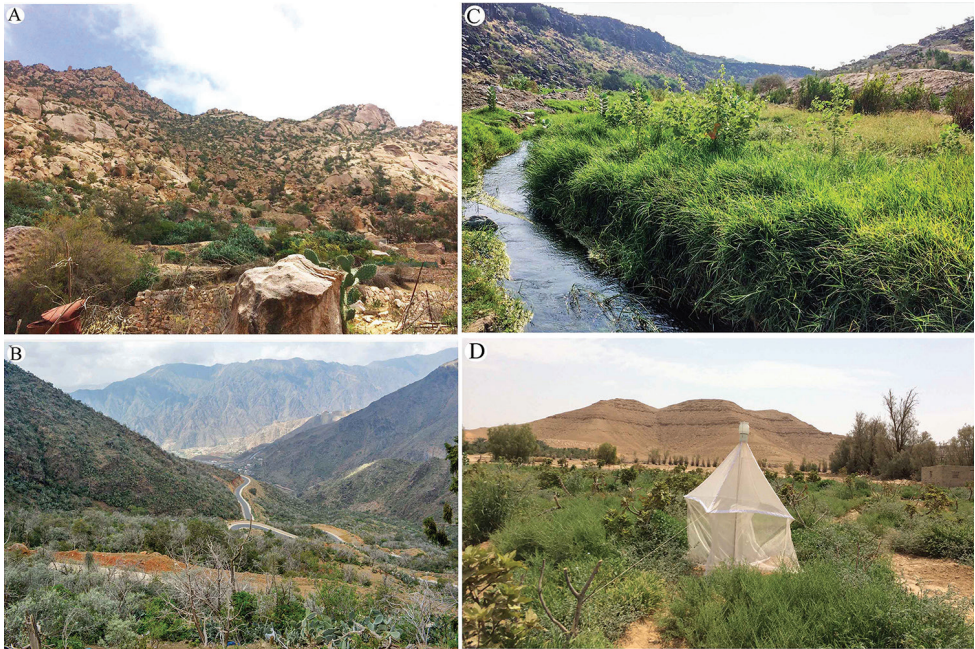


Figure 31. Examples of the habitat where the *Epitranus* species were collected **A** Shada Al-Ala Natural Reserve (Al-Baha) **B** Garf Raydah Natural Reserve (Asir) **C** Wadi Heli (Asir) **D** Dirab Station of Research (Riyadh).

Discussion

Epitraninae are native from the Old World were probably accidentally introduced in the New World before cautionary measures were made. Their presence in some parts of the New World countries as Caribbean islands and Brazil, pre-1900, strongly suggests their introduction via maritime ports.

The Afrotropical species of the genus *Epitranus* Walker were revised by Schmitz (1946, under *Anacryptus*) and Steffan (1957), who provided keys and described many new species. In addition, some sporadic studies who included descriptions of *Epitranus* species among other chalcidids (Westwood 1835; Walker 1862; Ruschka 1924; Masi 1940, 1943; Risbec 1953, 1957). Approximately 38% of the total number of species of the world possess Afrotropical affinities (see Noyes 2019). Since Steffan (1957), no further revisions covered the Afrotropical *Epitranus*.

In the Arabian Peninsula, *Epitranus* was recorded by one study (Delvare 2017), which reported two species, *E. hamoni* and *E. torymoides*, both in the United Arab Emirates.

The present study supplies new information in the Arabian Peninsula, and the first for Saudi Arabia. Here we reported four new records, *E. clavatus*, *E. hamoni* complex, *E. inops*, and *E. torymoides*, all of them with Afrotropical distribution. Three new species are also described and illustrated, *E. delvarei*, *E. similis*, and *E. subinops*, thus raising the total number in the whole Arabian Peninsula to seven species.

Little is known about the biology of the Afrotropical species of the genus *Epitranus*, from what is known from a single species, *E. inops*. It was reared from stored yam together with the pyralid moth, *Euzopherodes vapidella*, and other small moths (Sauphanor et al. 1987).

All species under study were collected from Al-Baha, Asir, Jazan, and Riyadh provinces (southwestern and central regions of Saudi Arabia). Consequently, the area under study (southwestern Saudi Arabia) should be included in the Afrotropical realm (see Gadallah and Brothers 2020), and this is closely correlated with the floristic composition of this area, thus supporting many of other previous works (El-Hawagry et al. 2013, 2015; Sharaf et al. 2014; Gadallah et al. 2018; Gadallah and Brothers 2020).

However, more species are expected to occur because of the biodiversity richness of the country, as it occupies the major part of the Arabian Peninsula (Aldhebiani and Howladar 2015). For this reason, more collection trips and studies are necessary to clarify the distributions as well as the host records of this interesting genus in other parts of Saudi Arabia.

Acknowledgements

Sincere gratitude to Gérard Delvare (CIRAD, France) for his great help in the identification of some species and for his valuable suggestions and critical review of the manuscript which led to its improvement. We also thank João Paulo Maires Hoppe for his valuable suggestions to improve the manuscript.

Sincere appreciation extended to the Deanship of Scientific Research at King Saud University for funding this research group number RGP-1437-009.

References

- Aldhebiani AY, Howladar SM (2015) Floristic diversity and environmental relations in two valleys, south west Saudi Arabia. *International Journal of Science and Research* 4(2): 1916–1925. https://www.ijsr.net/get_abstract.php?paper_id=SUB151587
- Ashmead WH (1904) Classification of the chalcid flies of the superfamily Chalcidoidea, with descriptions of new species in the Carnegie Museum, collected in South America by Herbert H. Smith. *Memoirs of the Carnegie Museum* 1(4): 225–551. <https://www.biodiversitylibrary.org/page/10924545>
- Bouček Z (1982) Oriental chalcid wasps of the genus *Epitranus*. *Journal of Natural History* 16: 577–822. <https://doi.org/10.1080/00222938200770451>
- Bouček Z (1988) Australasian Chalcidoidea (Hymenoptera). A Biosystematic Revision of Genera of Fourteen Families, with a Reclassification of Species. CAB International Wallingford, Oxon, Cambrian News Ltd; Aberystwyth, Wales, 832 pp. <https://www.cabdirect.org/cabdirect/abstract/19881109893>

- Burks BD (1936) The Nearctic Dirhinini and Epitranini (Hymenoptera: Chalcididae). Proceedings of the National Academy of Sciences of the United States of America, Washington 22: 283–287. <https://doi.org/10.1073/pnas.22.5.283>
- Cameron P (1883) Descriptions of new genera and species of Hymenoptera. Transactions of the Entomological Society of London 1883: 187–197. <https://doi.org/10.1111/j.1365-2311.1883.tb02945.x>
- Cruaud A, Delvare G, Nidelet S, Sauné L, Ratnasingham S, Chartois M, Blaimer BB, Gates M, Brady SG, Faure S, Noort S van, Rossi J-P, Rasplus J-Y (2020) Ultra-Conserved Elements and morphology reciprocally illuminate conflicting phylogenetic hypotheses in Chalcididae (Hymenoptera, Chalcidoidea). Cladistics 0: 1–35. <https://doi.org/10.1101/761874>
- Delvare G (2017) Order Hymenoptera, family Chalcididae. Arthropod fauna of the UAE 6: 225–274 <https://agritrop.cirad.fr/586551/1/Delvare%202017%20Fauna%20UAE%20%20Chalcididae.pdf>
- El-Hawagry MS, Khalil MW, Sharaf MR, Fadel HH, Aldawood AS (2013) A preliminary study on the insect fauna of Al-Baha Province, Saudi Arabia, with descriptions of two new species. ZooKeys 274: 1–88. <https://doi.org/10.3897/zookeys.274.4529>
- El-Hawagry MS, Sharaf MR, Al-Dhafer MH, Fadel HH, Aldawood AS (2015) Addenda to the insect fauna of Al-Baha Province, Kingdom of Saudi Arabia with zoogeographical notes. Journal of Natural History 50(19–20): 1209–1236. <https://doi.org/10.1080/00222933.2015.1103913>
- Fabricius JC (1804) Systema Piezatorum 2: 1–440. A.C. Reichard, Brunsvigae [Richards: Transactions of the Royal Entomological Society of London 83: 144. <https://www.biodiversitylibrary.org/page/11001084> [publ. 1804 (1805 latest): Hedicke, Mitteilungen der Entomologischen Gesellschaft 10: 82–83, text publ. 1804]
- Gadallah NS, Brothers DJ (2020) Biodiversity of aculeate wasps (Hymenoptera: Aculeata) of the Arabian Peninsula: Overview. Zootaxa 4754(1): 8–16. <https://doi.org/10.11646/zootaxa.4754.1.4>
- Gadallah NS, Soliman AM, Abu El-Ghiet UM, Elsheikh TY, Al Dhafer HM (2018) The family Leucospidae (Hymenoptera: Chalcidoidea) from the South of Saudi Arabia, with the first report of the genus *Micrapion* and description of *Leucospis arabica* sp. nov. Journal of Natural History 52(31–32): 2071–2096. <https://doi.org/10.1080/00222933.2018.1510557>
- Girault AA (1913) Some chalcidoid Hymenoptera from North Queensland. Archiv für Naturgeschichte (A) 79(6): 70–90. <https://doi.org/10.4039/Ent4742-2>
- Girault AA (1914) A new chalcid genus and species of Hymenoptera from Australia. Entomological News 25: 30. <https://www.biodiversitylibrary.org/page/2628628>
- Girault AA (1915) Australian Hymenoptera Chalcidoidea-XIV. The family Chalcididae with description of new genera and new species. Memoirs of the Queensland Museum 4: 314–365. <https://www.biodiversitylibrary.org/page/13217352>
- Habu A (1960) A revision of the Chalcididae (Hymenoptera) of Japan with description of sixteen new species. Bulletin of National Institute of Agricultural Sciences, Tokyo (c) 11: 131–363.
- Harris RA (1979) A glossary of the surface sculpturing. Occasional Papers of Entomology, California Department of Food and Agriculture 28: 1–31. <https://zenodo.org/record/26215#.X4DTUdAzbIU>

- Heraty JM, Burks RA, Cruaud A, Gibson GA, Liljebblad J, Munro J, Rasplus JY, Delvare G, Janšta P, Gumovsky A, Huber J, et al. (2013) A phylogenetic analysis of the megadiverse Chalcidoidea (Hymenoptera). *Cladistics* 29(5): 466–542. <https://doi.org/10.1111/cla.12006>
- Husain T, Agarwal MM (1982) Taxonomic studies on Indian Epitraninae (Hymenoptera: Chalcididae). *Oriental Insects* 15(4): 413–432. <https://doi.org/10.1080/00305316.1981.10434340>
- Mani MS, Dubey OP, Kaul BK, Saraswat GG (1973) On some Chalcidoidea from India. *Memoirs of the School of Entomology, St. John's College, Agra, No. 2*: 30–31.
- Masi L (1917) Chalcididae of Seychelles islands. (With an appendix by J.J. Kieffer), *Novitates Zoologicae* 24: 121–230. <https://doi.org/10.5962/bhl.part.23148>
- Masi L (1933) H. Sauters Formosa-Ausbeute. Chalcididae (Hym.). II Teil. *Konowia* 12: 1–18. https://www.nhm.ac.uk/resources/research-curation/projects/chalcidoids/pdf_X/Masi933b.pdf
- Masi L (1940) Descrizioni di Calcididi raccolti in Somalia dal Prof. G. Russo con note sulle species congeneri. *Bollettino del R. Laboratorio di Entomologia Agraria di Portici* 3: 247–324. https://www.nhm.ac.uk/resources/research-curation/projects/chalcidoids/pdf_X/Masi940c.pdf
- Masi L (1943) Nuove specie di imenotteri calcididi Diagnosti preventive. Missione biologica Sagan-Omo diretta dal Prof. E. Zavattari. *Bollettino della Società Entomologica Italiana* 75: 65–68. https://www.nhm.ac.uk/resources/research-curation/projects/chalcidoids/pdf_X/Masi943.pdf
- Moravvej SA, Lotfalizadeh H, Shishehbor P (2018) On the presence of the subfamily Epitraninae (Hymenoptera: Chalcidoidea, Chalcididae) in Iran. *North-Western Journal of Zoology* 14(2): 267–268
- Narendran TC (1989) Oriental Chalcididae (Hymenoptera: Chalcidoidea). *Zoological Monograph*. Department of Zoology, University of Calicut Kerala, India, 1–441. <https://archive.org/details/OrientalChalcididae>
- Narendran TC, van Achterberg C (2016) Revision of the family Chalcididae (Hymenoptera, Chalcidoidea) from Vietnam, with the description of 13 new species. *ZooKeys* 576: 1–202. <https://doi.org/10.3897/zookeys.576.8177>
- Noyes J (2019) Universal Chalcidoidea Database. World Wide Web electronic publication. <http://www.nhm.ac.uk/chalcidoids>
- Rasplus J-Y (1993) L'entomofaune de termitière morte de *Macrotermes*. Description d'une nouvelle espèce de *Spalangia* et note sur une espèce rare d'*Epitranus* (Hymenoptera, Pteromalidae, Chalcididae). *Revue Française d'Entomologie (Nouvelle Série)* 15(2): 81–84.
- Risbec J (1953) Chalcidoïdes et proctotrupoides de l'Afrique occidentale Française (2^e supplément). *Bulletin de l'Institut Français d'Afrique Noire* 15: 549–809.
- Risbec J (1957) Chalcidoïdes et proctotrupoides de l'Afrique occidentale Française (5^e supplément). *Bulletin de l'Institut Français d'Afrique Noire (A)* 19: 228–267.
- Ruschka F (1924) Wissenschaftliche ergebnisse der Unterstützung de Akademie der Wissenschaften in Wien aus der Erbschaft treitl von F. Werner Unternommenen Zoologischen expedition nach dem Anglo-Ägyptischen Sudan (Kordofan) 1914. XIII. Hymenoptera (Chalcididae). *Denkschriften der Akademie der Wissenschaften Wien. Mathematisch-Naturwissenschaften Klasse* 99: 99–100. https://www.nhm.ac.uk/resources/research-curation/projects/chalcidoids/pdf_X/Ruschk924c.pdf

- Sauphanor B, Bordat D, Delvare G, Ratnadass A (1987) Insects of stored yams in the Ivory Coast. Faunistic inventory and biological data. *L'Agronomie Tropicale*, Nogent-sur-Mame 42(4): 305–312.
- Schmitz G (1946) Chalcididae (Hymenoptera Chalcidoidea). Exploration du Parc National Albert. Mission G.F. de Witte (1933-1935) 48: 1–191. https://www.nhm.ac.uk/resources/research-curation/projects/chalcidoids/pdf_X/Schmit946.pdf
- Sharaf MR, Fischer BL, Aldawood AS (2014) First record of the Myrmicine ant genus *Meranoplus* Smith, 1853 (Hymenoptera: Formicidae) from the Arabian Peninsula with description of a new species and notes on the zoogeography of the southwestern Kingdom of Saudi Arabia. *PLOS One*: e111298. <https://doi.org/10.1371/journal.pone.0111298>
- Steffan J-R (1957) Epitraninae (Hym. Chalcididae) du Musée Royal du Congo Belge. *Revue de Zoologie et de Botanique Africaines* 56(1/2): 71–91.
- Walker F (1834) Monographia Chalciditum. (Continued). *Entomological Magazine* 2(1): 13–39. <https://www.biodiversitylibrary.org/page/25333985>
- Walker F (1862) Notes on the chalcidites, and characters of undescribed species. *Transactions of the Entomological Society of London* 3(1): 345–397. <https://www.biodiversitylibrary.org/page/32121299>
- Westwood JO (1835) Various hymenopterous insects from the collection of the Rev. F.W. Hope. *Proceedings of the Zoological Society of London* 3: 68–72. <https://antcat.org/references/129806>

Monomorium sahlbergi Emery, 1898 (Formicidae, Hymenoptera): a cryptic globally introduced species

Peter Boer¹, Ana Carolina Loss^{2,3}, Frederique Bakker¹,
Kevin Beentjes¹, Brian L. Fisher²

1 Department of Terrestrial Zoology, Naturalis Biodiversity Center, PO Box 9517, 2300 RA Leiden, The Netherlands **2** Entomology, California Academy of Sciences, 55 Music Concourse Drive, San Francisco, CA 94118, USA **3** National Institute of the Atlantic Forest (INMA), Santa Teresa, ES, Brazil

Corresponding author: Peter Boer (p.boer@quicknet.nl)

Academic editor: M. Borowiec | Received 11 June 2020 | Accepted 24 July 2020 | Published 27 October 2020

<http://zoobank.org/C92AD02C-71A4-4B18-BE19-255A4B58579B>

Citation: Boer P, Loss AC, Bakker F, Beentjes K, Fisher BL (2020) *Monomorium sahlbergi* Emery, 1898 (Formicidae, Hymenoptera): a cryptic globally introduced species. ZooKeys 979: 87–97. <https://doi.org/10.3897/zookeys.979.55342>

Abstract

The discovery in the Netherlands in a shipping container of the ant *Monomorium sahlbergi* Emery, 1898, a species similar to the invasive pharaoh ant *M. pharaonis* (Linnaeus, 1758), led to a quest to better define the distribution of this species, which was initially obscure due to uncertain specimen identifications. Here it is shown that *M. sahlbergi*, like *M. pharaonis*, is found worldwide, almost certainly as a result of introductions. Including quarantine interceptions, this species is recorded from seven global biogeographic regions, but its established outdoor distribution is currently limited to the tropics and subtropics. *Monomorium dichroum* Forel, 1902 is here presented as a junior synonym of *M. sahlbergi* **syn. nov.** based on morphometric and CO1 analyses.

Keywords

CO1, invasive species, *Monomorium dichroum*, *Monomorium pharaonis*

Introduction

Broadening transport networks and rising demand for commodities have led to increases in alien species worldwide (Hulme 2009), including ants (Suarez et al. 2001; Bertelsmeier et al. 2017). In the Netherlands, for example, a relatively large number

of non-native ant species are being recorded owing in part to the shipments of plant material imported into the country (Boer and Vierbergen 2008).

A concerted effort is underway to identify ant species introduced into the Netherlands, whether they are established or found during import inspections. Thus far 120 species have been identified (Boer et al. 2018). Many of these introduced species are poor colonisers and have not been able to establish and/or spread after arriving (Boer and Vierbergen 2008). The actual number of introduced species is almost certainly greater; some specimens are impossible to identify due to a lack of suitable identification keys and uncertainty about the origin of the ants. Limited identification tools and training increase the chances that species names are ascribed incorrectly, especially in the case of closely related species. In this work we describe an example of one invasive species remaining hidden in the guise of another, more common species. The case concerns two closely related species of the genus *Monomorium*, of which one, *M. pharaonis* (Linnaeus, 1758), is considered the most notorious pest ant species in the world (Wetterer 2010). In the Netherlands, *M. pharaonis* is the first recorded tramp ant species; the oldest specimen is dated 1877 (Boer and Vierbergen 2008).

On 2 June 2014, the pest controller A.J.A. Heetman intercepted ants found in a shipping container at a distribution company in the Netherlands and sent them to the first author. The shipping container, filled with glycine for the food industry, came from a chemical plant in Wuyi, Hengshui, Hebei, China. The intercepted ants appeared similar to the well-known and globally common tramp species *M. pharaonis*, but differed in their black gaster. While trying to identify the specimens, we came across images of identical specimens on AntWeb (<http://www.antweb.org>), where they were recorded under the provisional name *M. pharaonis_nr* (CASENT0173275, CASENT0246074) and *M. bicolor* complex (CASENT0178876).

Further comparison of our specimens with the images from AntWeb convinced us that the ants discovered in the Hebei shipping container were a previously described species, *M. dichroum* Forel, 1902 (Figs 1–3). *Monomorium dichroum* was reported as only known from India (type locality) (Imai et al. 1984, Bharti 2015) and China (Guénard and Dunn 2012).

Further exploration of similar species on AntWeb, however, suggested our specimens, and *M. dichroum* for that matter, were identical to *M. sahlbergi* Emery, 1898, a little-known species described from Israel. We set out to ascertain the true identity of our specimens and determine whether *dichroum* and *sahlbergi* are two distinct species.

Materials and methods

Available descriptions of all *Monomorium* species occurring in the area between Saudi Arabia in the west and China in the east were consulted. Syntype material of *M. dichroum* and *M. sahlbergi* were requested and investigated. *Monomorium pharaonis*, *M. cf. pharaonis*, *M. nr. pharaonis*, and *M. bicolor*-complex ants identified from the

collection of CASC and RMNH were investigated. In total, we examined hundreds of specimens from the Netherlands, France, Germany, Israel, Saudi Arabia, United Arab Emirates, Oman, Yemen, Seychelles, Papua, Nepal, New Zealand, Western Australia, Myanmar, Taiwan, China, Ivory Coast, Cameroon, Madagascar, Indonesia, Panama, Mexico, Trinidad, Netherlands Antilles, and the United States of America.

For morphometrical comparisons, 16 workers of *M. pharaonis* were examined (all in the collection of Naturalis Biodiversity Center, RMNH). The size and shape characters of these workers were quantified (Table 1) and reported as lengths or indices. All measurements are in millimetres. The numeric characters and abbreviations are defined below.

CI	Cephalic Index (CW/CL) $\times 100$.
CL	Maximum cephalic length in median line.
CW	Maximum cephalic width, across eyes.
EYI	Eye Index (maximum eye length / CW) $\times 100$.
Omm	Number of ommatidia across the widest diameter of the eye.
PI	Petiole Index (Maximum width of petiole / maximum width postpetiole) $\times 100$.
PrI	Promesonotal Index (Promesonotal width / CW) $\times 100$.
SI	Scape Index (Maximum straight line scape length excluding articular condyle / CW) $\times 100$.

The examined specimens in this study are deposited in the following institutions:

CASC	California Academy of Sciences, USA
MHNG	Museum d'Histoire Naturelle, Geneva, Switzerland
MSNG	Museo Civico di Storia Naturale 'Giacomo Doria', Genova, Italy
RMNH	Naturalis Biodiversity Center, Leiden, the Netherlands (the former Rijksmuseum van Natuurlijke Historie)
TAMU	Texas A & M University, Texas, USA
UCDC	R.M. Bohart Museum of Entomology, University of California, Davis, USA
NZAC	New Zealand Arthropod Collection, D.S.I.R., Auckland, New Zealand

DNA sampling

We sequenced 654 base pairs (bp) of mitochondrial cytochrome oxidase I (COI) gene from 39 *Monomorium* specimens previously identified as *M. pharaonis*, *M. dichroum*, or *M. sablbergi*. DNA extraction and COI sequencing were performed at University of Guelph (Ontario, Canada) and Naturalis Biodiversity Center (Leiden, the Netherlands), following the protocol described in Fisher and Smith (2008). All sequences are available at GenBank and Appendix 1. Phylogenetic analyses also included 20 *Monomorium* sequences from GenBank and two sequences as outgroup (*Huberia striata* and *Podomyrma* sp.), see Appendix 1 for sequence details.

Table 1. Morphometric data of workers of *Monomorium dichroum*, *M. sahlbergi*, and *M. pharaonis*. Arithmetic mean in parentheses.

	<i>M. dichroum</i> (n = 48)	<i>M. sahlbergi</i> (n = 32)	<i>M. pharaonis</i> (n = 16)	<i>M. pharaonis</i> (n = 50) from Bolton, 1987
CW	0.41–0.54 (0.44)	0.40–0.44 (0.42)	0.41–0.48 (0.44)	0.40–0.48
CL	0.49–0.66 (0.54)	0.49–0.54 (0.51)	0.52–0.59 (0.56)	0.52–0.60
CI	79–85 (82)	79–85 (81)	75–84 (80)	73–80
EYI	19–24 (21)	19–26 (22)	18–20 (19)	18–21
Omm	7–10 (9)	7–11 (9)	7–9 (8)	5–7
PI	67–86 (74)	64–73 (69)	71–82 (78)	–
SI	102–110 (103)	103–110 (106)	105–117 (109)	105–117

Molecular phylogenetic inference. Sequences were aligned using Geneious 11.1.5 (Biomatters Ltd.). The phylogenetic tree was inferred in MEGA7 using maximum likelihood and 100 bootstrap replicates. Nucleotide substitution model selection and genetic p-distance calculation were also performed using MEGA7 (Kumar and Tamura, 2016). The best fit model selected under the corrected Akaike Information Criteria (AICc) was GTR+G+I.

Results

COI

The phylogenetic tree recovered sequences of *M. dichroum* and *M. sahlbergi* in the same clade (Fig. 5), showing low within-clade genetic distance (1.0%). Genetic distance among sequences previously identified as *M. dichroum* and *M. sahlbergi* was also low (1.3%). All *M. pharaonis* sequences clustered together, showing 0.3% within genetic distance and 16.5% genetic distance between this and the *M. dichroum* + *M. sahlbergi* clade.

Morphological comparisons

Monomorium dichroum and *M. sahlbergi* show similar colouration, especially with regard to the infusate genae and the light spot on the posterior side of the gaster. Morphometrically, these ants are identical. None of the regression analyses of various morphometrical data, such as cephalic width versus cephalic length, scape length, maximum width of postpetiole, width of postpetiole versus width of petioles, comparisons between the cephalic index versus eye index, versus petiole index, versus scape index, and versus promesonotal index, showed any difference. The number of ommatidia across the widest diameter of the eye was the same. Nor could we find any differences in pilosity and pubescence. The surface sculpturing of the head, mesosoma, nodes, and gaster were the same.



Figure 1. *Monomorium sablbergi* from Sacramento, USA, imported from Thailand. Worker, CASENT0005783 **A** frontal view **B** lateral view **C** dorsal habitus.



Figure 2. *Monomorium dichroum*, syntype from Mumbai, India. Worker, CASENT0908718 **A** frontal view **B** lateral view **C** dorsal habitus.



Figure 3. *Monomorium sablbergi*, syntype from Jericho, Palestine. Worker, CASENT0904576 **A** frontal view **B** lateral view **C** dorsal habitus.



Figure 4. *Monomorium pharaonis* from Nampar Macing, Indonesia. Worker, CASENT0171086 **A** frontal view **B** lateral view **C** dorsal habitus.

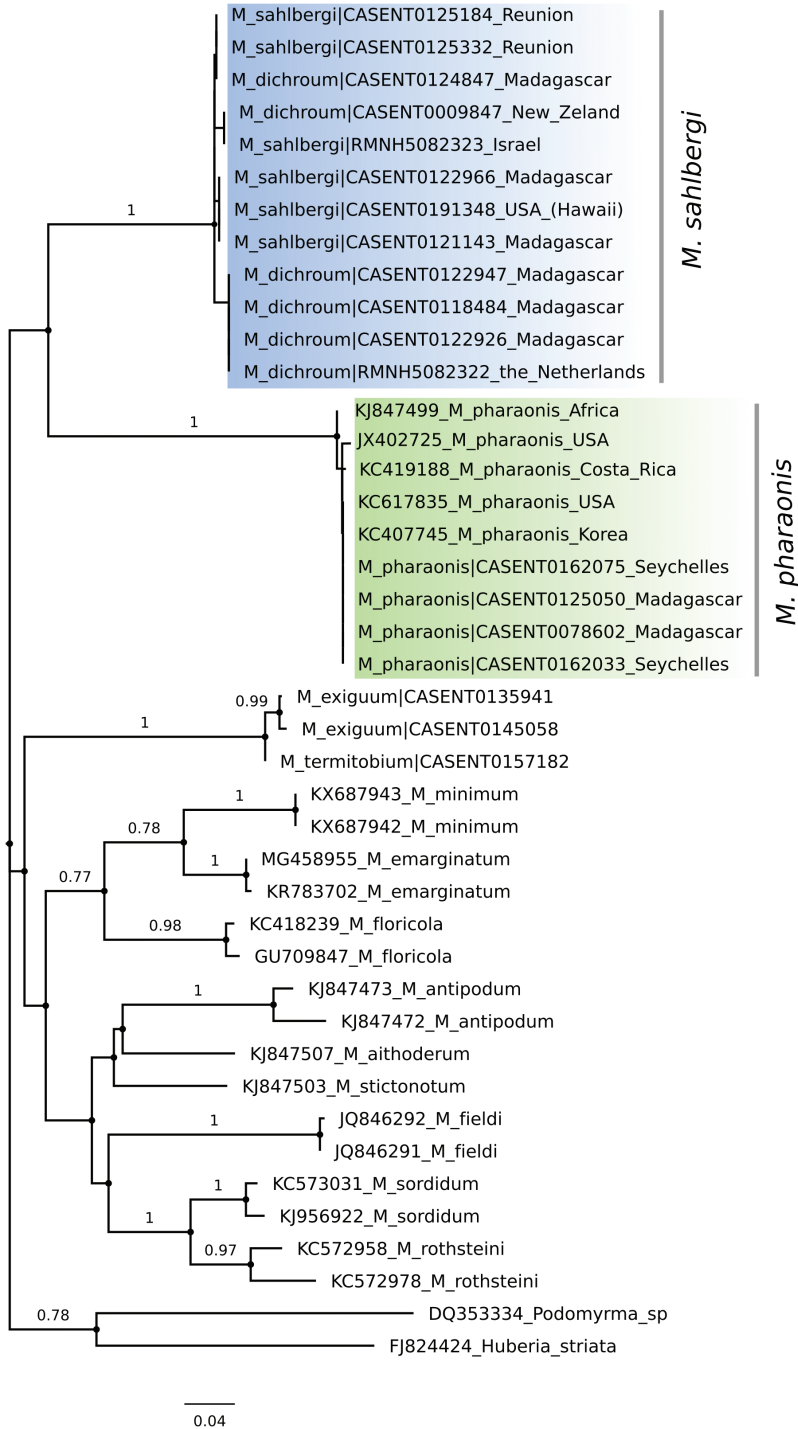


Figure 5. Maximum likelihood phylogeny of *Monomorium* COI sequences. Blue clade corresponds to *M. sahlbergi* and green clade to *M. pharaonis*. Values associated to nodes correspond to bootstrap values.

Both *Monomorium sahlbergi* and *M. pharaonis* belong to the *salomonis* group, as defined by Bolton (1987). For a detailed description of *M. pharaonis* see Heterick (2006). Morphometrically *M. sahlbergi* is similar to *M. pharaonis* (Table 1). Compared to the workers of *M. pharaonis*, 1/4 instead of 2/3 of the first gastral tergite (abdominal segment 4) is light-coloured; the structure of the frontal side of the head is strigulate rather than reticulate; the mesonotal groove is shallower; the pronotum and metanotum are higher than the propodeum in *M. pharaonis* as opposed to equally high in *M. sahlbergi* and promesonotal setae are missing on the mesosoma, in *M. pharaonis* two to six (Figs 1–4). Note that in *Monomorium* specimens the setae are quite stiff and break easily, thus reducing utility of this character in some specimens.

Taxonomic implications

Monomorium sahlbergi Emery

Monomorium sahlbergi Emery, 1898: 131. Syntype worker, ergatoid queen: [Jerico] Jericho, Palestine (J. Sahlberg) (MSNG; worker, unique specimen code CASENT0904576; ergatoid queen, CASENT0904577) [examined].

Monomorium dichroum Forel, 1902: 212. Syntype workers: Poona, India (Wroughton) (BMNH, CASENT0902222) [examined]; Bombay, India (Wroughton) (MHNG, CASENT0908718) [examined] **syn. nov.**

Distribution. All records of *M. sahlbergi* originate from desert-like, urban, industrial, and military areas ranging from sea level to an elevation of 1800 m. It is not clear from our research what the original geographic region of *M. sahlbergi* was. Based on the distribution of other species in the *salomonis* group, the native distribution would include specimens from the Indomalaya region (Nepal, India, Thailand). Our data came from the following main geographic regions: Palearctic (China, Israel, Netherlands (interception)), Australian (New Zealand, from likely interceptions), Nearctic (USA, in part interceptions), Neotropical (Panama, Galapagos), Afrotropical (Reunion, Madagascar) and Oceania (Hawaii) (Fig. 6).

Discussion

The global distribution of *Monomorium sahlbergi* suggests a history of introductions. Although the native distribution requires further evaluation, specimen records from disturbed habitats suggest that, like the introduction in the Netherlands, this species has already been introduced to other regions. Some distribution records suggest that *M. sahlbergi* could indeed be a successful invasive species, and is already successfully established in areas such as disturbed areas on the islands of the Galapagos (Ecuador) and urban areas in Texas, USA, Panama-City, Hawaii, Madagascar, and Reunion.

It is easy to confuse *M. sahlbergi* with the well-known pharaoh ant *M. pharaonis*, because the former also lives near or in human settlements and looks very similar to

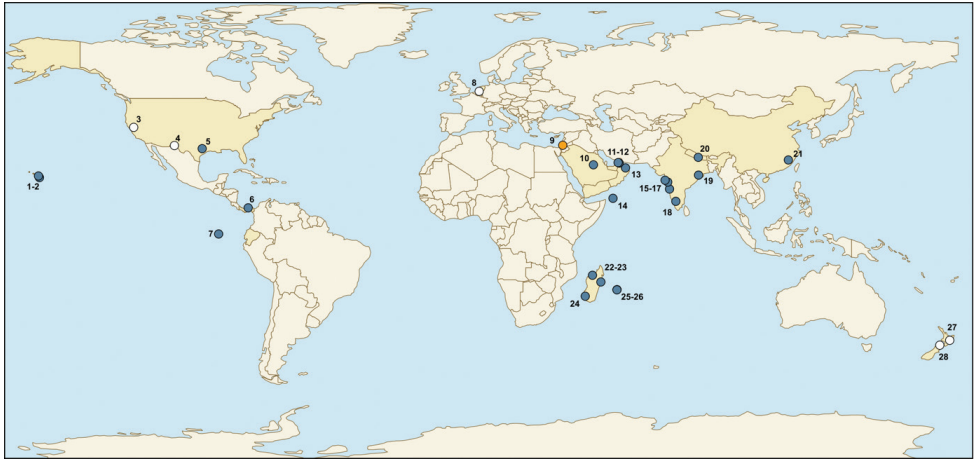


Figure 6. Distribution of *Monomorium sahlbergi*. White circles represent interceptions; orange circle represents type locality. Details of map locations are given in Appendix 2.

M. pharaonis. Therefore, we suspect that *M. sahlbergi* has more than once been misidentified as *M. pharaonis*, a view supported by the misidentifications encountered in this study. These findings suggest that *M. sahlbergi* is likely more common than we realise.

Acknowledgements

Without the rich photographic archive and specimen data of AntWeb, this study would not have been possible. We would like to thank all collectors and curators for their assistance, especially A.J.A. Heetman, for initiating this research by providing the specimens from the Netherlands. We thank G. Kapp (The Steinhardt Museum of Natural History, Tel Aviv) for providing us with a sample of *M. sahlbergi* from Israel, and Alex Wild for his information about *M. sahlbergi* from Panama. This work was partly supported by US National Science Foundation grant DEB-1655076. ACL was supported by Conselho Nacional Científico e Tecnológico (CNPq, Brazil; grant numbers 306772/2019-1 and 300737/2020-3).

References

- Bertelsmeier C, Ollier S, Liebhold A, Keller L (2017) Recent human history governs global ant invasion dynamics. *Nature Ecology & Evolution* 1: 0184. <https://doi.org/10.1038/s41559-017-0184>
- Bharti H (2018) Ants of India. <https://doi.org/10.4324/9780429320118-5>
- Boer P, Vierbergen B (2008) Exotic ants in The Netherlands (Hymenoptera: Formicidae). *Entomologische Berichten* 68: 121–129.

- Boer P, Noordijk J, Loon AJ van (2018) Ecologische atlas van Nederlandse mieren (Hymenoptera: Formicidae). EIS Kenniscentrum Insecten en andere ongewervelden, Leiden, 125 pp.
- Bolton B (1987) A review of the *Solenopsis* genus-group and revision of Afrotropical *Monomorium* Mayr (Hymenoptera: Formicidae). Bulletin of the British Museum of Natural History (Entomology) 54: 263–452.
- Emery C (1898) Beiträge zur Kenntniss der palaearktischen Ameisen. Öfversigt af Finska Vetenskaps-Societetens Förhandlingar 20: 124–151.
- Fisher BL, Smith MA (2008) A revision of Malagasy species of *Anochetus* Mayr and *Odontomachus* Latreille (Hymenoptera: Formicidae). PLoS ONE 3(5): e1787.
- Forel A (1902) Myrmicinae nouveaux de l'Inde et de Ceylan. Revue Suisse de Zoologie 10: 165–249. <https://doi.org/10.5962/bhl.part.13792>
- Guénard B, Dunn RR (2012) A checklist of the ants of China. Zootaxa 3558: 1–77. <https://doi.org/10.11646/zootaxa.3558.1.1>
- Heterick B (2006) A revision of the Malagasy Ants Belonging to Genus *Monomorium* Mayr, 1855 (Hymenoptera: Formicidae). Proceedings of the California Academy of Sciences 4th series 57: 69–202.
- Hulme PE (2009) Trade, transport and trouble: managing invasive species pathways in an era of globalization. Journal of Applied Ecology 46: 10–18. <https://doi.org/10.1111/j.1365-2664.2008.01600.x>
- Imai HT, Baroni Urbani C, Kubota M, Sharma GP, Narasimhanna MH, Das BC (1984) Karyological survey of Indian ants. Japanese Journal of Genetics 59: 1–32. <https://doi.org/10.1266/jjg.59.1>
- Kumar S, Stecher G, Tamura K (2016) MEGA7: Molecular Evolutionary Genetics Analysis version 7.0 for bigger datasets. Molecular Biology and Evolution 33: 1870–1874. <https://doi.org/10.1093/molbev/msw054>
- Linnaeus C (1758) Systema naturae per regna tria naturae, secundum classes, ordines, genera, species, cum characteribus, differentiis, synonymis, locis. Tomus I. Editio decima, reformata. Holmiae [= Stockholm]: L. Salvii, 824 pp. <https://doi.org/10.5962/bhl.title.542>
- Suarez AV, Holway DA, Case TJ (2001) Patterns of spread in biological invasions dominated by long-distance jump dispersal: insights from Argentine ants. Proceedings of the National Academy of Sciences USA 98: 1095–1100. <https://doi.org/10.1073/pnas.98.3.1095>
- Wetterer JK (2010) Worldwide spread of the pharaoh ant, *Monomorium pharaonis* (Hymenoptera: Formicidae). Myrmecological News 13: 115–129.

Appendix I

Monomorium and outgroups COI sequences information. Asterisks (*) in the final column indicate duplicated haplotypes not included in the phylogeny.

Species	Specimen ID number	Geographical region	GenBank accession number	BOLD process ID number		
<i>Monomorium aithoderum</i>		Australia	KJ847507			
		Australia	KJ847472			
		Australia	KJ847473			
<i>Monomorium emarginatum</i>		USA	KR783702			
		USA	MG458955			
<i>Monomorium exiguum</i>	CASENT0135941-D01	Madagascar	MT887664	ASNAU286-09		
	CASENT0145058-D01	Madagascar	MT887665	ASNAU751-09		
	CASENT0147596-D01	Madagascar	MT887669	ASNAU850-09	*	
<i>Monomorium fieldi</i>		Australia	JQ846291			
		Australia	JQ846292			
<i>Monomorium floricola</i>	CASENT0136664-D01	Comoros	GU709847	ASANO792-09		
		Costa Rica	KC418239	ACGAJ207-11		
<i>Monomorium minimum</i>		USA	KX687942			
		USA	KX687943			
<i>Monomorium pharaonis</i>		Africa	KJ847499			
		Costa Rica	KC419188	ACGAJ043-11		
		Korea	KC407745			
	CASENT0078602-D01	Madagascar	GU710435	ASANP639-09		
	CASENT0120402-D01	Madagascar	GU710434	ASANP651-09	*	
	CASENT0120437-D01	Madagascar	GU710437	ASANP653-09	*	
	CASENT0120835-D01	Madagascar	GU710436	ASANP657-09	*	
	CASENT0122487-D01	Madagascar	GU710439	ASANP666-09	*	
	CASENT0122499-D01	Madagascar	GU710438	ASANP667-09	*	
	CASENT0123480-D01	Madagascar	GU710441	ASANP675-09	*	
	CASENT0125050-D01	Madagascar	GU710440	ASANP679-09		
	CASENT0159459-D01	Seychelles	HQ546947	ASAND352-10	*	
	CASENT0159472-D01	Seychelles	HQ546950	ASAND355-10	*	
	CASENT0160217-D01	Seychelles	HQ546997	ASAND421-10	*	
	CASENT0160424-D01	Seychelles	HQ547018	ASAND445-10	*	
	CASENT0161400-D01	Seychelles	HQ547092	ASAND546-10	*	
	CASENT0162033-D01	Seychelles	HQ547099	ASAND557-10		
	CASENT0162075-D01	Seychelles	HQ547102	ASAND560-10		
		USA	JX402725			
		USA	KC617835	DIRTT037-11		
	<i>Monomorium rothsteini</i>		Australia	KC572958		
			Australia	KC572978		
<i>Monomorium sablbergi</i>	RMNH.5082323	Israel	MT943758	MONOM001-20		
	CASENT0118484-D01	Madagascar	MT887671	ASAMY032-07		
	CASENT0121143-D01	Madagascar	GU709866	ASANO669-09		
	CASENT0122926-D01	Madagascar	GU709869	ASANO683-09		
	CASENT0122935-D01	Madagascar	GU709868	ASANO684-09	*	
	CASENT0122940-D01	Madagascar	GU709871	ASANO685-09	*	
	CASENT0122947-D01	Madagascar	GU709870	ASANO686-09		
	CASENT0122966-D01	Madagascar	GU709873	ASANO687-09		
	CASENT0122991-D01	Madagascar	GU709872	ASANO688-09	*	
	CASENT0124847-D01	Madagascar	GU709875	ASANO692-09		
	CASENT0009847-D01	New Zealand	MT887667	ASAMI149-07		
	CASENT0125184-D01	Reunion	MT887663	ASAMY578-07		

Species	Specimen ID number	Geographical region	GenBank accession number	BOLD process ID number	
<i>Monomorium sahlbergi</i>	CASENT0125194-D01	Reunion	MT887660	ASAMY580-07	*
	CASENT0125332-D01	Reunion	MT887666	ASAMY588-07	
	CASENT0125334-D01	Reunion	MT887662	ASAMY590-07	*
	CASENT0125339-D01	Reunion	MT887661	ASAMY591-07	*
	RMNH.5082322	Netherlands	MT943757	MONOM002-20	
	CASENT0191347-D01	USA (Hawaii)	MT887670	ASANE610-10	
CASENT0191348-D01	USA (Hawaii)	MT887668	ASANE611-10	*	
<i>Monomorium sordidum</i>		Australia	KC573031		
		Australia	KJ956922		
<i>Monomorium stictonotum</i>		Australia	KJ847503		
<i>Monomorium termitobium</i>	CASENT0157182-D01	Madagascar	JN283174	ASANH122-10	
<i>Huberia striata</i>		New Zealand	FJ824424		
<i>Podomyrma</i> sp.		Australia	DQ353334		

Appendix 2

Distribution details of the mapped specimens of *Monomorium sahlbergi*.

Map ID number	Locality	Country	Latitude	Longitude
1	Maui	USA	20.63	-156.1
2	Kawaihae	USA	20.04	-155.8
3	Elk Grove	USA	38.41	-121.3
4	El Paso	USA	31.76	-106.4
5	College Station	USA	30.63	-96.33
6	Panama City	Panama	8.98	-79.52
7	Galapagos	Ecuador	-0.59	-90.32
8	Rijen	Netherlands	51.59	4.92
9	Jericho	Israel	31.86	35.46
10	Riyadh	Saudi Arabia	24.71	46.68
11	Um-al-Quwain	UAE	25.52	55.71
12	Wadi Madaq	UAE	25.35	56.09
13	Muscat	Oman	23.59	58.41
14	Socotra	Yemen	12.46	53.82
15	Mumbai	India	19.08	72.88
16	Pune	India	18.4	73.85
17	Belgaum	India	15.85	74.5
18	Coonoor	India	11.35	76.8
19	Odisha	India	20.95	85.1
20	Hetauda	Nepal	27.44	85
21	Fujian	China	26.48	117.92
22	Mahajanga	Madagascar	-15.69	46.33
23	Toamasina	Madagascar	-18.14	49.4
24	Toliara	Madagascar	-23.35	43.69
25	Grotte des Premiers Français	Reunion	-21.02	55.26
26	Le Port	Reunion	-20.94	55.3
27	Napier Port	New Zealand	-39.48	176.91
28	Port Nelson	New Zealand	-41.26	173.28

Taxonomy and phylogeny of the genus *Gastrocentrum* Gorham (Coleoptera, Cleridae, Tillinae), with the description of five new species

Ganyan Yang¹, Xingke Yang², Hongliang Shi¹

1 College of Forestry, Beijing Forestry University, Beijing 100083, China **2** Key Laboratory of Zoological Systematics and Evolution, Institute of Zoology, Chinese Academy of Sciences, Beijing, 100101, China

Corresponding author: Hongliang Shi (shihl@bjfu.edu.cn)

Academic editor: R. Gerstmeier | Received 29 April 2020 | Accepted 14 August 2020 | Published 27 October 2020

<http://zoobank.org/BC56F2AE-D8F9-411E-9C92-81945738E264>

Citation: Yang G, Yang X, Shi H (2020) Taxonomy and phylogeny of the genus *Gastrocentrum* Gorham (Coleoptera, Cleridae, Tillinae), with the description of five new species. ZooKeys 979: 99–132. <https://doi.org/10.3897/zookeys.979.53765>

Abstract

The genus *Gastrocentrum* Gorham, 1876 is revised to include nine species. Five new species are described in this genus: *G. magnum* **sp. nov.** (NE India), *G. regulare* **sp. nov.** (Cameron Highlands, Malaysia), *G. xiaodongi* **sp. nov.** (Gyirong, Xizang, China), *G. zayuense* **sp. nov.** (Zayü, Xizang, China), and *G. gaoligongense* **sp. nov.** (Fugong, Yunnan, China). *Gastrocentrum nitidum* Schenkling, 1916 is transferred to the genus *Tillus* as a new combination. All the species in this genus are described (except *G. brevicolle*), and a key is provided for their identification. Illustrations of male genitalia, female reproductive organs, and other important structures are provided. An interspecific phylogeny-estimate of *Gastrocentrum* is presented based on morphological data, with two main clades recognized: a clade containing *G. unicolor* and *G. laterimaculatum*, and a clade containing the remaining six species (the latter a polytomy consisting of *G. magnum* **sp. nov.**, *G. dux*, and *G. regulare* **sp. nov.**, and a well-supported sub-clade representing the remaining species). Additionally, the taxonomic and phylogenetic importance of female reproductive organs is discussed.

Keywords

Australian region, female, morphology, Oriental region, systematics

Introduction

Gastrocentrum Gorham, a genus of checkered beetles distributed throughout the Oriental and Australian regions, was established by Gorham (1876) who erected it for *G. pauper* Gorham, from Luzon, Philippines. Later, Gahan (1910) transferred *Notoxus unicolor* White, 1849 (type locality: India), and *Tillus dux* Westwood, 1852 (type locality: Australia) to *Gastrocentrum*, synonymizing *G. pauper* with the former species. The description of three more species (viz., *G. nitidum* Schenkling, 1916 from Taiwan, *G. brevicolle* Pic, 1940 from Sri Lanka, and *G. laterimaculatum* Gerstmeier, 2005 from Malaysia) brought the total number of valid *Gastrocentrum* species to five.

Mawdsley (1999) briefly reviewed this genus, but apart from the type specimens, he had only examined specimens from India and Sri Lanka, and male genitalia were not compared. In our research, specimens from a wide range of Oriental and Australian regions were examined, and both male genitalia and female reproductive organs are dissected and compared. Thus, this paper aims to re-evaluate the species components of genus *Gastrocentrum*, describe five new species, and analyses infra-generic phylogenetic relationships; besides, discuss the significance of female reproductive organs in taxonomy.

Materials and methods

Taxonomic study

The materials used in this work are from the following collections:

FBFU	College of Forestry, Beijing Forestry University, Beijing, China
IZAS	Institute of Zoology, Chinese Academy of Sciences, Beijing, China
MNHN	Muséum national d'Histoire naturelle, Paris, France
NHMB	Naturhistorisches Museum, Basel, Switzerland
NKME	Naturkundemuseum Erfurt, Germany
NMPC	Národní Muzeum Přírodovědecké Muzeum, Prague, Czech Republic
RGCM	Roland Gerstmeier Collection, Munich (deposited in Zoologische Staatssammlung München), Germany
SDEI	Senckenberg Deutsches Entomologisches Institut, Müncheberg, Germany
ZMAN	Zoological Museum Amsterdam, Naturalis Biodiversity Center, Leiden, Netherlands
CCCC	Collection of Chen Changchin, Taiwan, China
CBWX	Collection of BI Wenxuan, Shanghai, China

Male genitalia and female reproductive organs of specimens were extensively dissected. The dissected process follows Yang et al. (2013), and female membranous parts

of reproductive organs were dyed with Chlorazol Black. Habitus images were captured using a Nikon D7000 digital camera with a Tamron SP 90mm lens. Terminalia images were captured by a Canon 450D digital camera fitted to a Nikon SMZ-1500 stereoscopic dissecting microscope.

Morphological terminology follows the works of Ekis (1977) and Opitz (2010) in general. For the convenience of taxonomic description and phylogenetic analysis, elytral asetiferous punctations are classified into primary asetiferous punctation (**PAP**) and accessory asetiferous punctation (**AAP**). PAP refers to the major ten rows of punctations which are also present in many other genera of Tillinae, such as *Tillus*, *Cladiscus*, *Diplopherusa*, and *Diplocladus* (Fig. 10B, C). AAP is the additional punctation that presents on interspaces among PAP rows and, in *Gastrocentrum* specifically, AAP presents on interspaces between 1st–2nd, 3rd–4th, and 5th–6th PAP rows (Fig. 10B, a). In some species such as *G. zayuense*, PAP decreases in quantity and PAP rows are less than ten rows.

The term microtrichia on the inner surface of elytra was adopted from Gorb (2001). A new term interphallic plate was introduced to depict a plate that inserted at the membranous part of phallus where situated between the two phallic plates (Fig. 11C, H, ipp).

Phylogenetic analysis

Phylogenetic analysis was made using PAUP 4.0a (build 167) (Swofford 2002). Twenty-two morphological characters for eight ingroup and two outgroup taxa were compiled and analyzed. *Gastrocentrum brevicolle* was not included. Both the two species of *Isocymatodera* (*I. kolbei* and *I. atricolor*) were selected as outgroups. Exheuristic maximum parsimony analyses were performed. Characters were unordered and of equal weight. Branch support was determined for parsimony analyses using bootstrap with 1000 replicates in PAUP*. A bootstrap consensus tree and a list of character changes were obtained by PAUP*, and unambiguous character were mapped onto the tree by Illustrator 21.0.0.

Morphological characters used in the phylogenetic analysis are listed below. All the characters were coded as binary. Unknown or not applicable data coded as "?". The data matrix is given in Table 1.

1. 4th antennomeres serrate, extended laterally: (0) no; (1) yes.
2. Male 7th antennomeres broadly extended laterally: (0) no (Fig. 11I); (1) yes (Fig. 15I).
3. Female 7th antennomeres broadly extended laterally: (0) no; (1) yes.
4. Elytral inner surface with wedge-shaped protuberance: (0) no; (1) yes (Fig. 20A, B).
5. Elytral interspace between 1st–2nd PAP rows possesses AAP: (0) no (Fig. 10C–H); (1) yes (Fig. 10A, B).
6. Elytral interspace between 3rd–4th and 5th–6th PAP rows possesses AAP: (0) no (Fig. 10C–H); (1) yes (Fig. 10A, B).

Table 1. Morphological character matrix used in estimation of phylogeny.

	1	2	3	4	5	6	7	8	9	10	11	12	13	14	15	16	17	18	19	20	21	22
<i>I. kolbei</i>	1	1	1	0	1	0	0	0	1	1	1	0	1	0	0	0	1	0	1	1	1	1
<i>I. atricolor</i>	1	1	1	0	1	0	0	0	1	1	1	0	1	0	0	0	1	0	1	1	1	0
<i>G. unicolor</i>	0	0	0	1	1	1	1	1	1	1	0	1	1	1	1	0	0	1	1	1	1	0
<i>G. laterimaculatum</i>	0	0	?	1	1	1	1	0	1	1	0	1	1	1	1	0	?	?	?	?	?	?
<i>G. magnum</i>	0	1	1	1	1	1	0	1	1	0	0	1	1	1	1	1	0	1	1	1	0	1
<i>G. dux</i>	0	?	1	1	1	1	0	1	1	0	0	1	0	?	?	?	0	1	0	1	0	0
<i>G. regulare</i>	0	1	1	1	0	0	0	1	1	0	0	1	1	1	1	0	0	1	1	0	0	0
<i>G. xiaodongi</i>	0	?	0	0	0	0	0	1	1	0	0	1	0	?	?	?	0	1	1	0	0	0
<i>G. zayuense</i>	0	0	1	0	0	0	0	1	0	0	0	1	0	1	0	1	0	1	1	0	0	0
<i>G. gaoligongense</i>	0	0	1	1	0	0	0	1	0	0	0	1	0	1	0	1	0	0	1	0	0	0

7. Elytral AAP distinctly arranged in two rows: (0) no; (1) yes.

8. Distance between 2nd-3rd PAP rows greater than diameter of PAP: (0) no; (1) yes (Fig. 10A–H).

9. Elytral punctations reach lateral margins: (0) no (Fig. 10E–H); (1) yes (Fig. 10A–D).

10. Protibial outer-apical tooth present: (0) absent; (1) present (Gerstmeier 1993: fig. 2).

11. Mesotibial outer-apical tooth present: (0) absent; (1) present (Gerstmeier 1993: fig. 2).

12. Abdomen with lateral ridge on 1st-5th segments: (0) no; (1) yes (Fig. 20C, D, ridge).

13. Intercoxal process of first abdominal ventrite grooved longitudinally: (0) no (Fig. 20C, ip); (1) yes (Fig. 20E, ip).

14. The micro-hooked connecting membrane of male aedeagus extended to ventral surface: (0) no (Fig. 17G); (1) yes (Fig. 15D, E).

15. Male 6th ventrite with membranous region extending to posterior margin: (0) no; (1) yes (Fig. 11F, G)

16. Male tegmen apices hooked: (0) no (Figs 11h, 15b); (1) yes (Figs 13A, 17A, 19B).

17. Female vagina with sclerites: (0) no (Figs 12F, 16A); (1) yes (Fig. 22A, C, D, E).

18. Female bursa copulatrix clearly defined: (0) no (Fig. 22A, C, E); (1) yes (Figs 12F, 16A, 18A, 21).

19. Female spermathecal gland with a top tail: (0) no (Fig. 14D); (1) yes (Figs 12E, 14C, 16A, F, 18A, 22A, 22C).

20. Female spermathecal gland with one or more lateral tails: (0) no (Figs 16A, F, 18A, 22E); (1) yes (Figs 12E, 14C, D, 22A, C).

21. Female spermathecal gland with two lateral tails: (0) no (Figs 14C, D, 16A, F, 18A, 22E); (1) yes (Figs 12E, 22B, C).

22. Female spermathecal gland with any of the tail extremely long, much longer than ovipositor: (0) no (Fig. 16A, F); (1) yes (Figs 14C, 22C).

Results

Taxonomic accounts

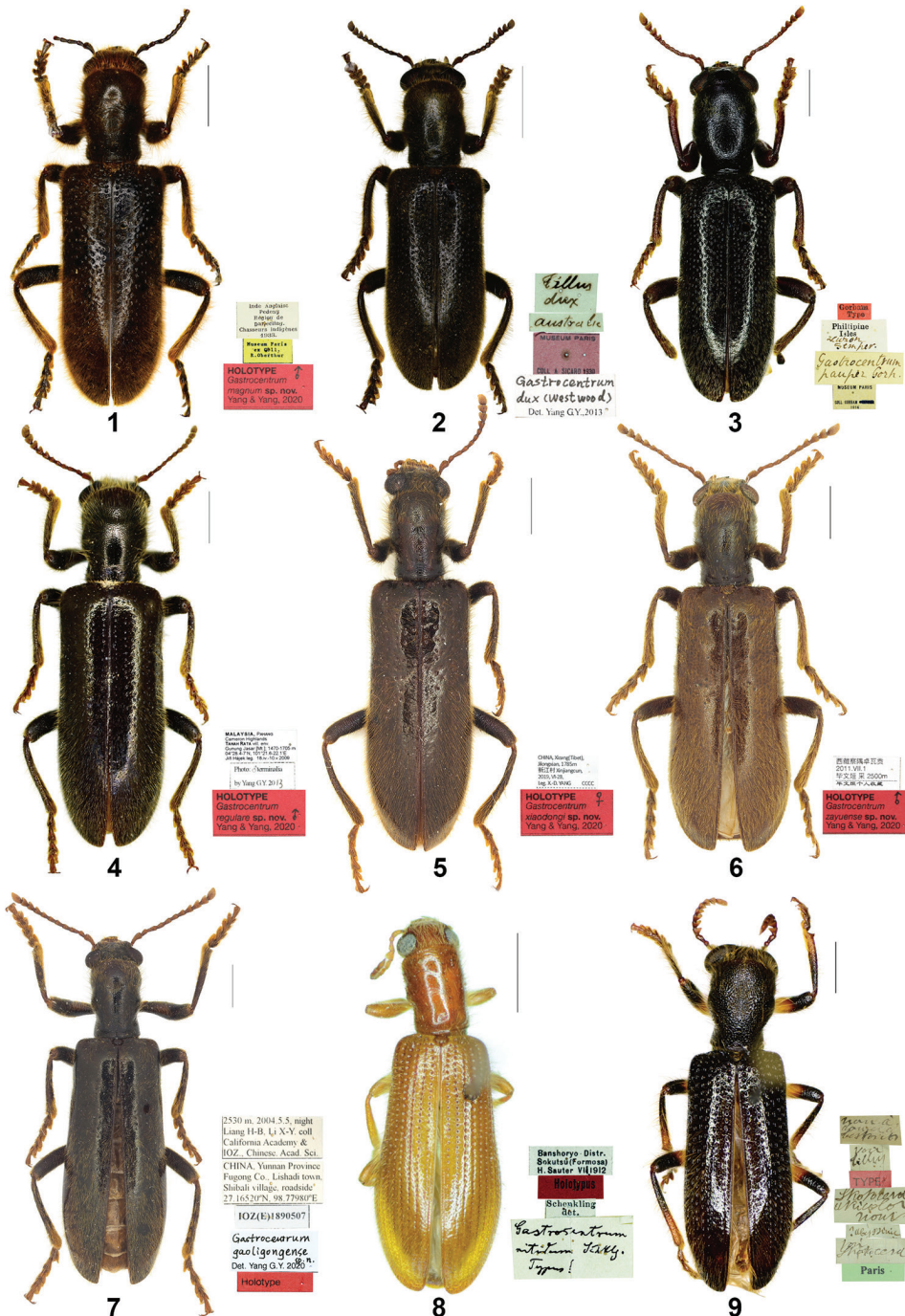
Genus *Gastrocentrum* Gorham, 1876

Gastrocentrum Gorham, 1876: 63 (Type species: *Gastrocentrum pauper* Gorham, 1876; by original designation); Chapin, 1924: 166, 179 (redescription).

Exocentrum Pic, 1940: 3 (printer error).

Diagnosis. The genus *Gastrocentrum* was included in the *Philocalus* genus group close to the genus *Isocymatodera* (Gerstmeier 2005; Gerstmeier and Weiss 2009). Both genera have the claw with one inner denticle, which is similar to and only very slightly smaller than the apical portion of the claw (Fig. 20F). The genus *Gastrocentrum* can be differentiated from *Isocymatodera* by antennae broadly expanded laterally from 7th or 8th antennomeres onwards, the connecting membrane of male aedeagus specialized in both dorsal and ventral surface, the female vagina devoid of sclerites. While in *Isocymatodera*, the antennae are expanded laterally from 3rd or 4th antennomeres onwards, the connecting membrane of male aedeagus is only specialized in dorsal surface, and the female vagina possesses sclerites.

Redescription. General appearance: body length 9–29 mm; oblong, somewhat robust; all the species except *G. laterimaculatum* uniformly dark brown (Figs 1–9); vested with long, yellow setae all over the body. **Head:** hypognathous, moderately large, including eyes slightly broader than pronotum; eyes sizable, emarginate, coarsely faceted, ocular notch small, distance of eyes as long as or only slightly greater than transverse diameter of eyes; gula broad, gular sutures parallel or slightly converging in anterior; antenna comprised of eleven antennomeres, broadly expanded laterally from 7th or 8th–11th, the expanded antennomeres triangular except the last one cultriform, all the expanded antennomeres clothed with fine and dense pubescence; labrum emarginate, mandibles stout with inner dens, terminal segment of maxillary palpi digitiform, that of labial palpi broadly securiform. **Thorax:** pronotum long campaniform, constricted posteriorly, anterior transverse depression feeble, surface punctate, faintly wrinkled, clothed with long, yellow hairs; pro-intercoxal process thin. **Elytra:** oblong, sides parallel, anterior ridge present from humerus to scutellum; inner surface with a wedge-shaped protuberance at lateral middle of each elytron (Fig. 20A, B), leaning to the lateral side of first ventrite of abdomen in resting position (except for two species: *G. xiaodongi* and *G. zayuense*), and with a microtrichia field on antero-lateral area (Fig. 20A, mt; similar to the structure found in Tenebrionidae, Gorb, 2001: 125, fig. 8.1, EAL); elytra have two types of punctations: asetiferous and setiferous punctations, the former comprised of primary asetiferous punctation (PAP) and accessory asetiferous punctation (AAP); each elytron possesses ten rows of PAP in general, the fifth row situate just before the humerus (Fig. 10C, D), sometimes PAP vanish in lat-



Figures 1–9. Habitus. **1** *Gastrocentrum magnum* sp. nov. Holotype **2** *G. dux* from Australia **3** *G. unicolor* (Lectotype of *G. pauper*) **4** *G. regulare* sp. nov. Holotype **5** *G. xiaodongi* sp. nov. Holotype **6** *G. zayuense* sp. nov. Holotype **7** *G. gaoligongense* sp. nov. Holotype **8** *Tillus nitidus* comb. nov. Holotype **9** *Isocymatodera atricolor* Syntype. Scale bars: 5mm (1, 2) 2mm (3–9).

eral elytron (in *G. zayuense* and *G. gaoligongense*, Fig. 10E–H); AAP may present on the interspaces between 1st–2nd, 3rd–4th, and 5th–6th PAP rows and similar with PAP in size, making these two types of punctations more or less indistinguishable (Fig. 10A, B); setiferous punctations minute, bearing setae, densely dispersed over the whole elytral surface, not in rows. **Legs:** tibia without longitudinal ridge, tibial spur formula 1–2–2 (but in *G. laterimaculatum* 0–2–2), protibia without tooth at outer apex (except in *G. unicolor* and *G. laterimaculatum* where protibia possess a blunt tooth at outer apex); tarsi formula 5–5–5, first to fourth tarsomeres of all legs more or less bilobed and bearing evident pulvilli; claw with one inner denticle, which similar to and only very slightly smaller than apical portion of claw (Fig. 20F). **Abdomen:** abdomen longer than broad, parallel in front and tapering in rear; first to fifth abdominal ventrites each with a pair of short longitudinal ridges (Fig. 20D) and a pair of less pigmented circles (Fig. 20C) in lateral; sixth ventrite partly or totally slid under the fifth, so in parts of specimens only five ventrites visible; intercoxal process of the first ventrite keel-like, with or without longitudinal groove; first ventrite strongly ridged behind metacoxae. **Male genitalia:** pygidium subquadrate; sixth ventrite subtriangular to semicircle, posterior margin somewhat rounded, secondary sexual modifications slight (Figs 11F, G, 13G, 15H, 17G, 19G); central parts of sixth ventrite membranous, shape of membranous region different among species; spicular fork well developed, plates slender, apodemes not fused centrally, longitudinal intraspicular plate present (Figs 11D, 13E, 15F, 17E, 19E); tegmen tubiform, sclerotized from dorsal midline to lateral sides, barely sclerotized and unpigmented in ventral middle, tegmen lobed distally, parameres bent to ventral direction, tip simple or hooked, phallobasic apodeme present (Fig. 15B, C); phallus comprised of two thin phallic plates devoid of dentations, an interphallic plate present on the membrane between the two phallic plates (Fig. 11C, H, ipp), phallus apex simple, knot-like, phallic struts long and slender; connecting membrane between tegmen and phallus well sclerotized and thickened except the dorsal midline and ventral midline, forming a nearly whole sheath covering the phallus, which surface densely equipped with microhooks (Fig. 11A–C). **Female reproductive organs:** pygidium subquadrate; sixth ventrite sub-triangular, disc membranous (Figs 12H, 14B, 16C, E, 18C), spiculum ventrale present; ovipositor as long as abdomen, moderately sclerotized, light yellow, semi-transparent (Figs 12F, 14C, D, 16A, F, 18A, ovp), with proctigeral bacculi in dorsal surface (Fig. 16F, pgb) and ventral and oblique bacculi in ventral surface (Fig. 14C, vtb, olb); vagina and alimentary canal partially enclosed in ovipositor, unenclosed part of vagina as long as or slightly longer than ovipositor, tubular or saccular; bursa copulatrix clearly defined and positioned distally (Figs 12F, 16A, 18A, bc) with the exception of the species *G. gaoligongense*, where bursa copulatrix is a mere swollen continuation of the vagina (Fig. 22E); spermatheca attached to the base of bursa copulatrix, boundary between spermathecal duct and spermathecal capsule somewhat obscure (Figs 16G, 21), spermathecal duct slender (Fig. 16A) or sometimes inflated in distal and continuous with spermatheca (Figs 16G, 18A), spermathecal capsule moderately to minimally sclerotized, both spermathecal duct and spermathecal capsule with spiral micro-texture, distal part of spermathecal capsule strongly bent,

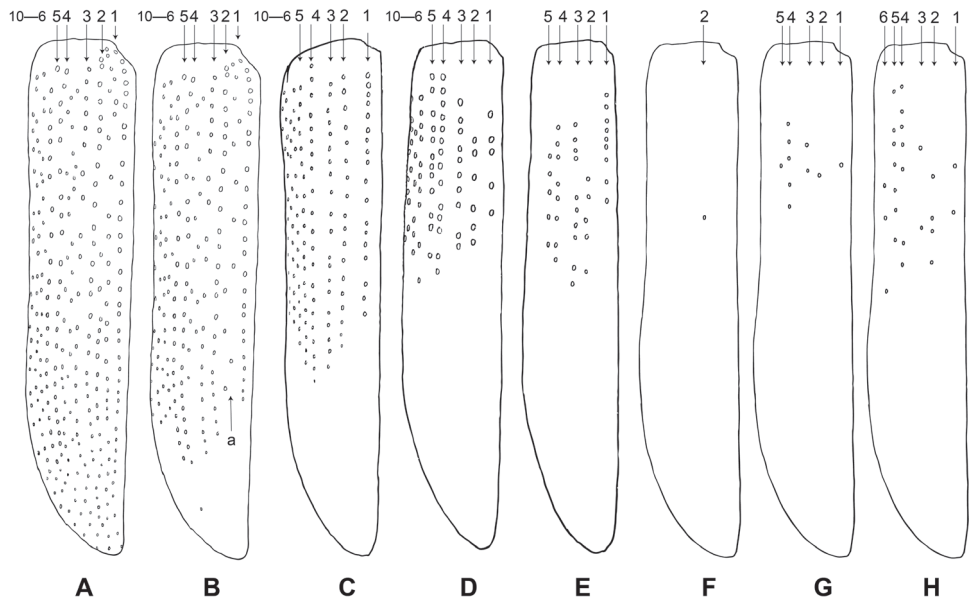


Figure 10. Drawing of elytral asetiferous punctations. **A** *Gastrocentrum magnum* sp. nov. **B** *G. dux* **C** *G. regulare* sp. nov. **D** *G. xiaodongi* sp. nov. **E** *G. gaoligongense* sp. nov. **F–H** *G. zayuense* sp. nov. The numbers 1–10 annotate the serial rows of primary asetiferous punctations (PAP). Abbreviations: **a** accessory asetiferous punctations.

angled no more than 90° (Fig. 16A, G), spermathecal gland duct inserted at the outer edge of the angle (Fig. 21, spgd); in ground-plan, spermathecal gland have three tail-like endings: one located distally, opposite to its opening to spermatheca (top tail, Figs 12E, 14C, spgtd), the other two situated laterally (lateral tail, Figs 12E, 14C, spglt), any of which may be missing in different species and sometimes can be extremely long (Fig. 14C, spglt).

Distribution. Indian subcontinent to Indochinese Peninsula and south through Malay Archipelago to Australia, including the following countries: India, Sri Lanka, Philippines, China, Vietnam, Laos, Malaysia, Indonesia, Australia (Fig. 25).

Key to species of *Gastrocentrum* Gorham (not including *G. brevicolle*)

- 1 Antennae expanded laterally from 3rd or 4th antennomere onwards *Isocymatodera*
- Antennae expanded laterally from 7th (Fig. 15I) or 8th (Fig. 11I) antennomere onwards **2**
- 2 AAP present on elytral interspaces between 1st–2nd, 3rd–4th, and 5th–6th PAP rows, total punctations arranging in more than ten rows (Fig. 10A, B) **3**
- AAP absent on elytral interspaces between 1st–2nd, 3rd–4th, and 5th–6th PAP rows, total punctations arranging in ten or less rows (Fig. 10C–H) **6**

- 3 Elytra uniformly brown; punctations smaller, with diameter smaller than interspace between 2nd and 3rd PAP rows 4
- Elytra yellow-brown; each elytron with a nearly semicircular large dark spot in lateral middle, elytral punctations larger, with diameter greater than interspace between 2nd–3rd rows..... ***G. laterimaculatum***
- 4 Antennae broadly expanded laterally from 7th antennomere onwards (Fig. 15I) 5
- Antennae broadly expanded laterally from 8th antennomere onwards (Fig. 11I) ***G. unicolor***
- 5 Elytral asetiferous punctations continuing to the tip (Fig. 10A), intercoxal process of first abdominal ventrite grooved longitudinally (Fig. 20E); female pygidium with a small triangular notch in anterior margin (Fig. 14A); top tail of spermathecal gland present (Fig. 14C, spggt), lateral tail ca. 2× the length of ovipositor (Fig. 14C, spglt) ***G. magnum sp. nov.***
- Elytral asetiferous punctations stop by apical fifth, not continuing to the tip (Fig. 10B), intercoxal process of first abdominal ventrite not grooved longitudinally (Fig. 20C, ip); female pygidium with a large semi-circle notch in anterior margin; top tail of spermathecal gland absent, lateral tail much shorter than ovipositor (Fig. 14D, spglt) ***G. dux***
- 6 Elytral punctations reach lateral margin of elytra, arranging in ten rows (Fig. 10C, D) 7
- Elytral punctations vanished at lateral sides of elytra, arranging in six rows at most (Fig. 10E–H) 8
- 7 7th antennomere conspicuously expanded laterally (Fig. 15I); elytra asetiferous punctations stop by apical third (Fig. 10C); elytral inner surface with wedge-shaped protuberance (Fig. 20A, B); intercoxal process of first abdominal ventrite grooved longitudinally (Fig. 20F, ip); spermathecal capsule slender, tapering to the tip, length/width ratio = 3.6 (Fig. 16A, sp)..... ***G. regulare sp. nov.***
- 7th antennomeres barrel-shaped, not expanded laterally; elytra asetiferous punctations stop by middle (Fig. 10D); elytral inner surface without wedge-shaped protuberance; intercoxal process of first abdominal ventrite not grooved longitudinally (Fig. 20C, ip); spermathecal capsule thicker, rounded in apex, length/width ratio = 2.0 (Fig. 16F, sp). ***G. xiaodongi sp. nov.***
- 8 Elytral inner surface without wedge-shaped protuberance; male tegmen apices with ventral surface streamlined (Fig. 17a); female bursa copulatrix clearly defined, much narrower than vagina, distal part of spermathecal capsule short, more or less inflated, length/width ratio < 2.5 (Fig. 18A) ***G. zayuense sp. nov.***
- Elytral inner surface with wedged-shaped protuberance (Fig. 20A, B); male tegmen apices with ventral surface bulged (Fig. 19b); female bursa copulatrix not differentiated, merely a swollen continuation of the vagina, distal part of spermathecal capsule long and slender, length/width ratio > 5 (Fig. 22E)..... ***G. gaoligongense sp. nov.***

***Gastrocentrum unicolor* (White, 1849)**

Figures 3, 11, 12, 25

Notoxus unicolor White, 1849: 56 (type locality: “India”); Gahan, 1910: 61 (*Gastrocentrum*); Schenkling, 1912: 323 (Taiwan); Chapin, 1924: 179, pl. 1, f. 4 (Philippines); Corporaal, 1950: 55 (catalogue); Mawdsley, 1999: 270 (Sri Lanka).

Gastrocentrum pauper Gorham, 1876: 63 (type locality: “Luzon, Philippines”); Schenkling, 1903 (Dindigul, S. India); Gahan, 1910: 61 (synonymized with *G. unicolor* White).

Type specimens examined. Lectotype of *G. pauper* designated herein (Fig. 3): “Gorham Type / Phillipine Isles, Luzon, Semper / *Gastrocentrum pauper* Gorh. [hw. by Gorham] / Museum Paris, Coll. Gorham, 1914” (MNHN, male, dissected); **Paralectotype of *G. pauper***: “Gorham Type / Camiguin de Luzon / *Gastrocentrum* genus novum, *G. pauper* Gorh. [hw. by Gorham] / Museum Paris, Coll. Gorham, 1914” (MNHN, 1 female, dissected).

Other specimens examined. China: Taiwan: 1994-VII-30, Taiwan, Taoyuan County, Fuxing Township, Shang Baling, 1200 m (CCCC, 1 male, dissected); 2005-IX-4, Taiwan, Taidung County, Beinan Township, Lijia Forest Trail, 1300 m, W-I. Chou leg. (CCCC, 1 male, dissected); 11-IX-1996, Taiwan, Pingtung County, Kenting National Park, W. I. Chou leg. (CCCC, 1 male, dissected); Taiwan, Formosa, IV, *Gastrocentrum unicolor* White (*pauper* Gorh.), Museum Paris Coll. M. Pic (MNHN, 1 female); **Hainan:** Hainan, Wuzhi Mountain, 2011.IX.20, BI Wenxuan (CBWX, 1 female, dissected); Hainan Prov., Baisha, Nankai Town, on vegetation or ground, 18.9741°N, 109.2956°E, 790 m, 2010.4.13 D, Lin Meiying coll. (IZAS, 1 female, dissected). **Vietnam:** “Museum Paris, Tonkin N., Env. d’Ha-giang, Lieut. Col. Bonifacy 1913” (MNNH, 1 female, dissected). **Laos:** “Laos-NE, Houa Phan prov., 20°13'09–19°N 103°59'54"–104°00'03"E, 1480–1550 m, PHOU PANE Mt., 1.-16.vi.2009, Zdeněk Kraus leg./NHMB Basel, NMPC Prague, Laos 2009 Expedition: M. Brancucci, M. Geiser, Z. Kraus, D. Hauck, V. Kuban” (NHMB, 1 female, dissected). **Thailand:** N. Thailand, Meo Village, near Chiang Mai, V.1998 (RGCM, 1 ex.); Thailand, Corat, 26.III.1988 (RGCM, 1 ex.); Thailand, Chiangmai, Doi Pui, 12.VI.1985 (RGCM, 1 ex.). **Malaysia: Peninsular Malaysia:** Bukit Kutu, Selangor, April 1915, 3457 / ex. Coll. Zoologisch Museum Amsterdam (MNHN, 1 male, dissected); Malaysia, Pahang, Cameron Highlands, Tanah Rata vill. env., Gunung Jasar [Mt]; 1470–1705m, 04°28.4–7'N, 101°21.6–22.1'E, Jiří Hájek leg., 18.iv–10.v.2009 (NMPC, 1 female, dissected); **East Malaysia:** Elopura, N.-E. Borneo, W. B. Pryer. / Museum Paris ex Coll. R. Oberthur (MNHN, 2 males 1 female, dissected); Borneo, Sabah, Keningau district, Jungle Girl Camp. 5.4430°N, 116.4512°E; 1182 m; Shi H. L. & Liu Y. lgt. light trap, night, 2016.IV.25 (2 ex.), 2016.IV.29 (3 ex.), 2016.IV.30 (1 ex.), 2016.V.1 (1 ex.), 2016.V.2 (3 ex.) (FBFU). **Indonesia:** W. Celebes, G. Rangkoenau, J. P. Ch. Kalis, 900 '. 1937 (MNHN, 5 males, 4 females in total, of which 3 males, 4 females dissected); W. Celebes, Loda, Paloe, J.P. Ch. Kalis, 4000 '. 1937 (MNHN, 1 male, dissected); W. Celebes, Sjaon-

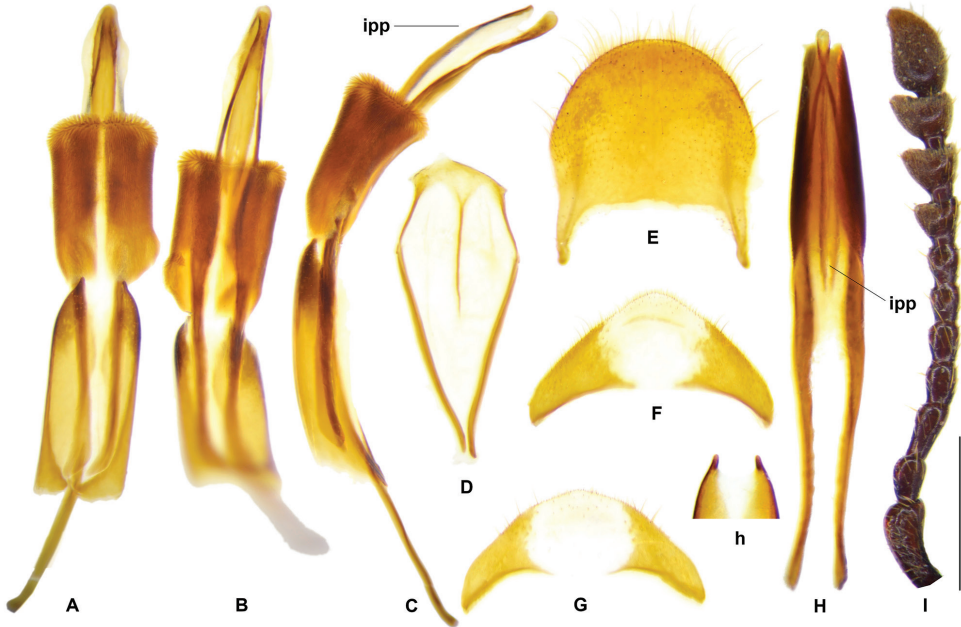


Figure 11. *Gastrocentrum unicolor*. **A–F** Lectotype of *G. pauper*. **A** aedeagus in dorsal view **B** aedeagus in ventral view **C** aedeagus in lateral view **D** spicular fork **E** pygidium **F** sixth ventrite. **G, H** specimen from Sulawesi. **G** sixth ventrite **H** phallus enveloped by connecting membrane, ventral view **h** apex of tegmen, ventral view **I** antenna. Abbreviations: **ipp** interphallic plate. Scale bar: 1 mm.

ta Paloe, J. P. Ch. Kalis, 4500'. 1937 (MNHN, 1 male, dissected); Bonthain, Celebes 8. '38 (MNHN, 1 male, dissected).

Diagnosis. This species has the broadest distribution range in this genus. It is different from *G. magnum* sp. nov., *G. dux* sp. nov. and *G. regulare* sp. nov. in antennae broadly extended laterally from 8th antennomere onwards (Fig. 11I); different from *G. xiaodongi* sp. nov., *G. zayuense* sp. nov., and *G. gaoligongense* sp. nov. in having AAP on interspaces between elytral 1st–2nd, 3rd–4th, and 5th–6th PAP rows.

Redescription (based on type specimens of *G. pauper* and other specimens from SE Asia only). **General appearance:** length 9–16 mm, oblong, robust, uniformly dark brown. **Head:** including eyes feebly broader than pronotum; eyes moderately large, distance between eyes faintly larger than the transverse diameter of eye; gular suture parallel; antennae expanded laterally from 8th antennomere onwards (Fig. 11I); vertex and frons densely punctate, postgenae rugose. **Pronotum:** oblong, length/width ratio ca. 1.4, constricted posteriorly; surface densely punctate, faintly rugose, clothed with long, yellow hairs. **Elytra:** oblong, sides subparallel, length/width ratio ca. 2.3, vested with dense light yellow or off-white setae; wedge-shaped protuberance present on inner surface (Fig. 20A, B); asetiferous punctations arranged in more than ten rows, PAP in ten rows, AAP on interspaces between 1st–2nd, 3rd–4th, and 5th–6th PAP rows, AAP setting in two rows on each interspace; AAP almost same size as PAP; interspace between 2nd–

3rd PAP rows much wider than punctuation diameter; both PAP and AAP beginning to decrease in size postmedially to apical third, and completely vanished at apical fourth to fifth. **Legs:** outer apex of protibia extending outwards and forming a blunt tooth. **Abdomen:** intercoxal process of the first ventrite conspicuously grooved longitudinally. **Male genitalia:** pygidium subquadrate, posterior margin rounded (Fig. 11E); sixth ventrite sub-triangular, ca. 2 × as broad as long, posterior margin more or less angulate, central membranous region pentagonal or subquadrate, extending from anterior margin to posterior margin (Fig. 11F, G); tegmen with phallobasic apodeme 0.6 time as long as phallobase (Fig. 11A–C); paramere apices simple, petty, unhooked (Fig. 11A, h); interphallic plate slightly shorter than half length of phallus (Fig. 11C, H, ipp); phallus apex usually knot-like, 2–3 × as long as wide (Fig. 11H). **Female reproductive organs:** pygidium slightly broader than long, posterior margin rounded (Fig. 12G); sixth ventrite 2.7 × broader than long, central membranous region elliptical, apical accessory membranous region petty (Fig. 12H); vagina swollen in well-preserved specimens, bursa copulatrix clearly defined (Fig. 12F), spermathecal gland with a top tail of medium length and two lateral tails that almost reduced (Fig. 12A–E); spermatheca boot-shaped in general (Fig. 12A, C–E).

Variation. The tegmen apices of *G. unicolor* are simple, unhooked, unspecialized (Fig. 11A). However, specimens from Sulawesi with tegmen apices slightly more prominent than those from other regions. Phallus apex is normally knot-like with the two phallic plates convergent at a point before the tip (Fig. 11H), but in the holotype of *G. pauper*, edges of the two phallic plates are almost parallel to the tip (Fig. 11B). The apical tip of phallus is longer than broad, with length/width ratio varied in a range of 2.0–3.0; usually teardrop-shaped with length/width ratio 2.0–2.5, but oblong in specimens from Sulawesi with length/width ratio approximate to 3.0 (Fig. 11H).

Both of the two female specimens examined from Hainan has spermatheca tubiform (Fig. 12B), which is different from those from other localities with spermatheca inflated distally (Fig. 12A, C, D). However, given its same external structure and lacking male specimens, we consider the specimens from Hainan as the same species with *G. unicolor*.

Distribution. This species is widespread, from Indian subcontinent to Indochinese Peninsula, south to Malay Archipelago, including the countries and regions: India, Sri Lanka, Philippines, China (Taiwan, Hainan), Vietnam, Laos, Thailand, Malaysia (Peninsular Malaysia, Sabah), Indonesia (Sulawesi).

Discussion. Gahan (1910) proposed that *G. pauper* was a junior synonym of *G. unicolor* without explanation, which treatment was afterward followed by Schenkling (1912), Chapin (1924), Corporaal (1950), and temporarily by Mawdsley (1999) and the present paper. In our research, we have only examined specimens from SE Asia and determined they are identical with *G. pauper*. However, additional materials from India or Sri Lanka need to be compared with those from SE Asia thoroughly, which will lead to the confident assignment of the synonymy.

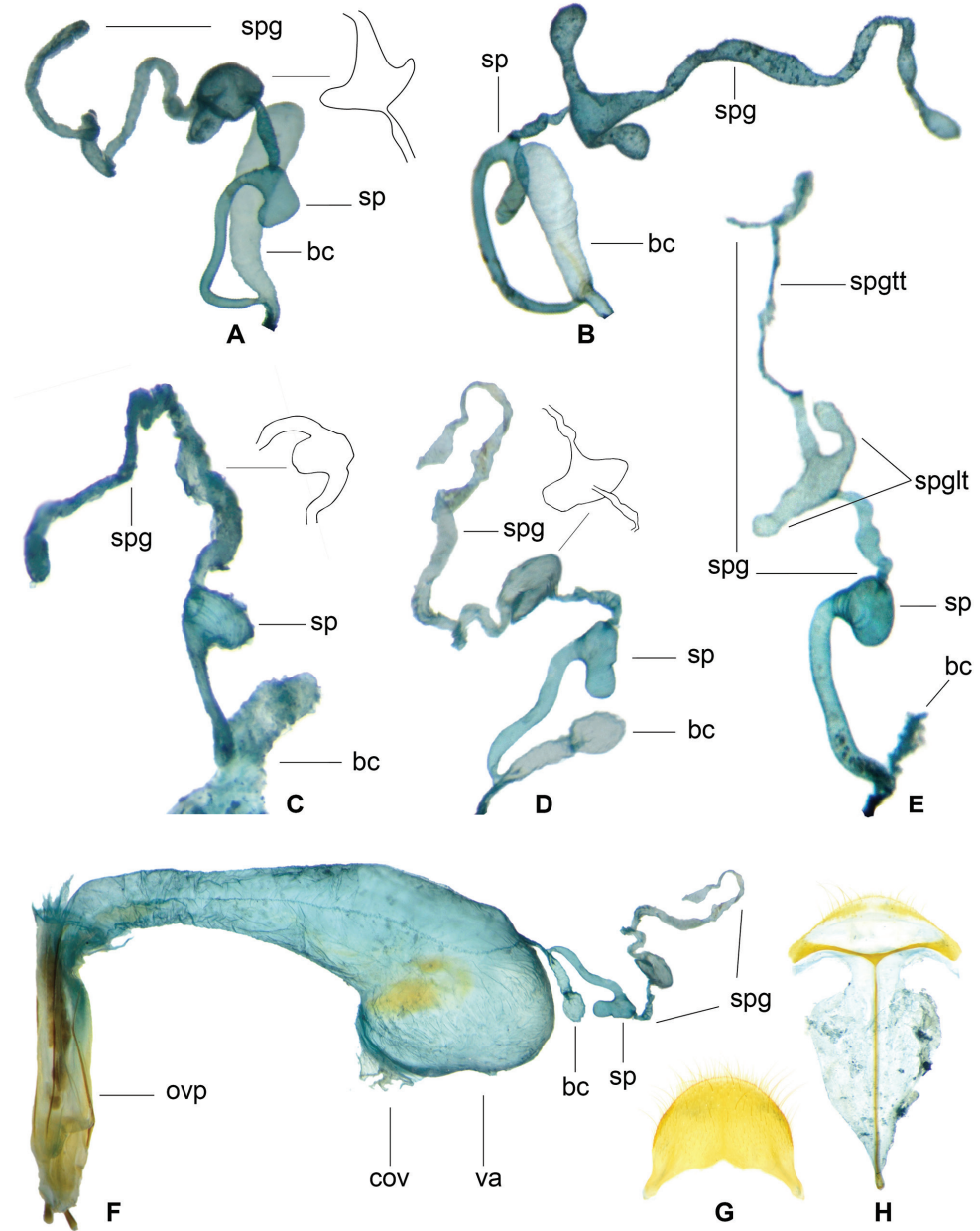


Figure 12. *Gastrocentrum unicolor* female reproductive organs specimens from different localities. **A** from Laos **B** from Hainan **C** from Philippines, Lectotype of *G. pauper* **D** from Borneo **E** from Sulawesi **F** from Borneo **G** pygidium **H** sixth ventrite. Abbreviations: **bc** bursa copulatrix **cov** common oviduct i.e. median oviduct **ovp** ovipositor **sp** spermatheca **spg** spermathecal gland **spglt** lateral tail of spermathecal gland **spgltt** top tail of spermathecal gland **va** vagina.

***Gastrocentrum laterimaculatum* Gerstmeier, 2005**

Figure 25

Gastrocentrum laterimaculatum Gerstmeier, 2005: 56 (type locality: Malaysia, Cameron Highlands).

Specimens examined. Malaysia: H. C. Siebers, M. O. Borneo Exp. Long Hoet, 3.VIII.1925 (ZMAN, 1 ex.); Borneo, Sabah, Keningau district, Jungle Girl Camp., 5.4430°N, 116.4512°E, 1182m, Shi H. L. & Liu Y. lgt. light trap, 2016. V. 1. N (FBFU, 1 male); Malaysia, N. Borneo, Sabah, Keningau distr., Trus Madi Mt., h = 1160 m, leg. J. Chew, 20.VI.2011 (RGCM, 1 ex.).

Diagnosis. This species is the only one in this genus that has elytral pattern and can be separated from other species without difficulty. Its elytra is yellow-brown, with a pair of large semicircular dark spots in lateral sides which is extended to the lower sides of humeri; elytral asetiferous punctations larger than other species, with punctuation diameter greater than interspace between 2nd–3rd PAP rows; antennae broadly extended laterally from 8th antennomere onwards.

Supplementary description. Elytral wedge-shaped protuberance present on inner surface; elytral asetiferous punctations somewhat irregular, arranged in more than ten rows, PAP in ten rows, AAP on interspaces between 1st–2nd, 3rd–4th, and 5th–6th PAP rows, AAP setting in two rows on each interspace; AAP almost same size as PAP, which is more sizable than punctations in other species, with punctuation diameter greater than interspace between 2nd–3rd PAP rows; both PAP and AAP beginning to decrease in size postmedially to apical third, and completely vanished at apical fifth; elytral inner surface with a wedge-shaped protuberance at lateral middle; tibiae spur formula 0–2–2 (other species in this genus 1–2–2); protibia with a blunt tooth at outer apex; 1st–2nd abdominal ventrites dark brown, 3rd–5th yellow, 6th light yellow to transparent; first abdominal ventrite strongly ridged behind coxae, intercoxal process raised, triangular, slightly longer than broad, grooved longitudinally.

Distribution. Malaysia (Peninsular Malaysia, Sabah).

***Gastrocentrum magnum* sp. nov.**

<http://zoobank.org/111FBA09-A72D-401D-8178-8163A7F41C0F>

Figures 1, 10A, 13, 14, 25

Holotype. India: “Inde Anglaise, Pedong, Région de Darjeeling. Chasseurs indigènes, 1933 /Museum Paris, 1952, Coll. R. Oberthür / *Gastrocentrum magnum* sp. nov. males, Det. Yang G. Y. 2019 / Holotype: *Gastrocentrum magnum* sp. nov. Yang & Yang, 2020” (MNHN, male) (Fig. 1). **Paratypes. India:** “Assam / Museum Paris ex Coll. R. Oberthür” (MNHN, 1 male); “Assam, [...] / *Gastrocentrum dux* Westw. / Museum Paris ex Coll. R. Oberthür / Ex-Musaeo H. W. Bates, 1892 / Museum Paris / females” (MNHN, 1 female); “Sikkim, Guntok, Été 1894, Chasseurs Breteandeu



Figure 13. *Gastrocentrum magnum* sp. nov. Holotype. **A** tegmen in lateral view **a** apex of tegmen in lateral view **B** tegmen in ventral view **C** phallus in lateral view **D** phallus in ventral view **E** spicular fork **F** pygidium **G** sixth ventrite **H** right antenna lacking last three segments. Scale bar: 1 mm.

/ *Gastrocentrum dux* Westw. c.f. Gahan / Museum Paris ex Coll. R. Oberthur” (MNHN, 1 female). **China:** China, Xizang, Mêdog, Nyingchi, Baibung, 876 m, 2016.VIII.09, light trap, LU Yanquan leg. (CCCC, 1 female); Yunnan, Longchuan, 1770 m, 2016.VI.3, light trap, YANG Xiaodong leg. 16Y (CCCC, 1 female); “Hainan, Jianfengling, Tianchi, 2010.IV.15-20/Wenxin Lin, 950 m, Collection of CHEN Changchin” (CCCC, 1 female); China, Yunnan, Honghe, Lvshuihe, 640 m, 23°1'41"N, 103°24'19"E, 07.V.2019, leg. L.Z. Meng (NKME, 3 ex., RGCM, 1 ex.); China, Yunnan, Honghe, Gulinqin, 585 m, 22°43'51"N, 103°59'35"E, 07.V.2019, leg. L.Z. Meng (RGCM, 2 ex.); China, S-Yunnan, Xishuangbanna, 20 km NW Jinghong, Man Dian NNNR-office, 22°07.80N, 100°40.05E, 740 m, LFF, 24.V.2008, leg. A. Weigel (RGCM, 1 ex.). **Vietnam:** C-Vietnam, ThuaThien – Hue Pr., Phu Loc, Bach Ma NP, Top area, 1250–1400 m, 16°11'39"N, 107°51'12"E, 5–9.V.2019, leg. A. Weigel LFF (RGCM, 1 ex.). **Thailand:** 18.–23.4.1991, Dol Suthep Pui, 1300–1500 m, leg. P. Pacholatko (RGCM, 1 male).

Diagnosis. Earlier researchers identified one of the paratypes of this new species as *G. dux*. The new species can be separated from *G. dux* by: asetiferous punctations on elytra continuing to the tip (Fig. 10A); intercoxal process of first abdominal ventrite grooved longitudinally (Fig. 20F); female pygidium with anterior margin notched in a shallow triangular shape (Fig. 14A), and lateral tails of spermathecal gland extremely long, ca. 2 × the length of ovipositor (Fig. 14C, spglt). *Gastrocentrum unicolor* is sym-

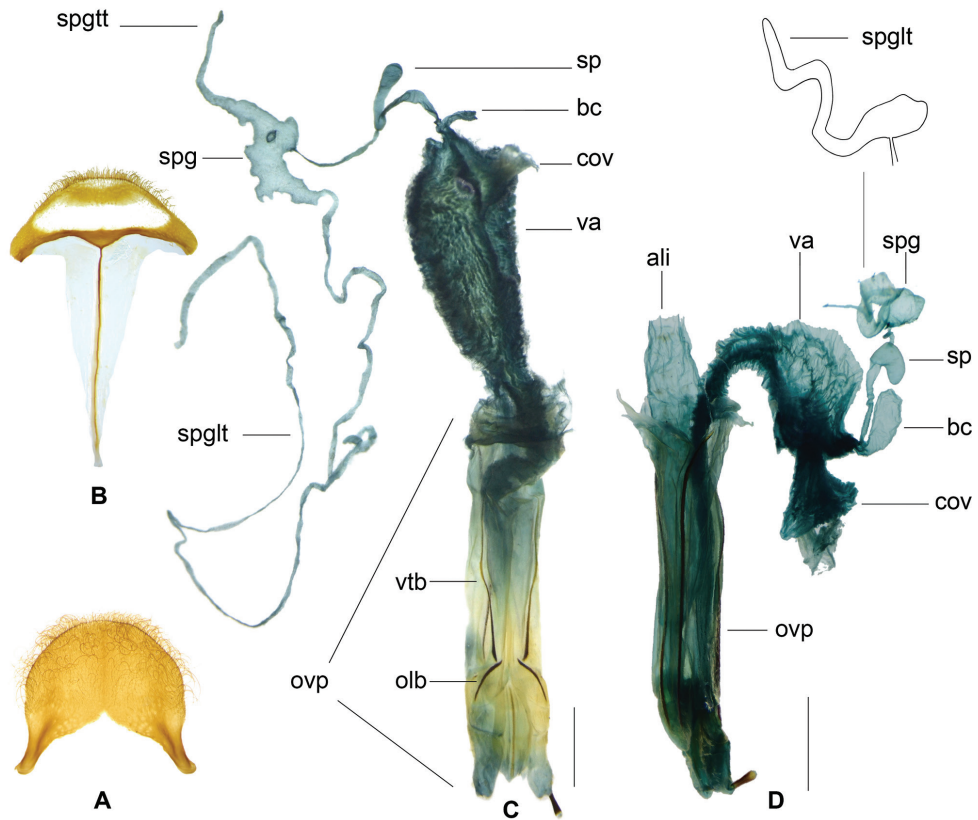


Figure 14. **A–C** *Gastrocentrum magnum* sp. nov. female, paratype from Assam **A** pygidium **B** sixth ventrite **C** female reproductive organ **D** *Gastrocentrum dux* from Australia, female reproductive organ. Abbreviations: **ali** alimentary canal **bc** bursa copulatrix **cov** common oviduct **olb** oblique bacculi **ovp** ovipositor **sp** spermatheca **spg** spermathecal gland **spglt** top tail of spermathecal gland **spglt** lateral tail of spermathecal gland **va** vagina **vtb** ventral bacculi. Scale bar: 1 mm.

patric with the new species in India, but *G. magnum* can be separated from it by much larger body size and five expanded terminal antennomeres (Fig. 13H).

Description. **General appearance:** length 22–25 mm, robust, dark brown. **Head:** including eyes feebly broader than pronotum; eyes moderately large, distance between eyes slightly greater than the transverse diameter of eye; gular suture convergent in anterior; antennae expanded laterally from 7th antennomere onwards (Fig. 13H); vertex and frons with dense punctations, with a very faint ridge along the midline, postgenae rugose. **Pronotum:** oblong, length/width ratio ca. 1.5, constricted posteriorly; surface finely and densely punctate, faintly rugose, clothed with long, yellow hairs. **Elytra:** oblong, sides subparallel, length/width ratio ca. 2.4, vested with dense golden setae; wedge-shaped protuberance present on inner surface; asetiferous punctations rows somewhat irregular, PAP in ten rows, AAP on interspaces between 1st–2nd, 3rd–4th, and 5th–6th PAP rows; AAP present in two incomplete rows, with lon-

gitudinal spacing between neighboring punctations uneven; AAP faintly smaller than or as big as PAP, interspace between 2nd–3rd PAP rows larger than punctation diameter (Fig. 10A); both PAP and AAP beginning to decrease in size postmedially and continuing to the tip, which are quite irregular near apical 1/5 of elytra (Fig. 10A). **Legs:** outer apex of protibia not extending outwards. **Abdomen:** intercoxal process of the first ventrite grooved longitudinally. **Male genitalia:** pygidium subquadrate, posterior margin rounded (Fig. 13F); sixth ventrite arciform, 3 × wider than length, posterior margin well rounded, central membranous region inverted trapezoidal, extending from anterior margin to posterior margin (Fig. 13G); tegmen tubiform, length ratio of phallobasic apodeme to phallobase ca. 1: 3.7 (Fig. 13A, B); parameres hooked (Fig. 13A, a); interphallic plate shorter than half length of phallus (Fig. 13D); phallus apex knot-like, faintly longer than broad (Fig. 13C, D). **Female reproductive organs:** pygidium slightly wider than length, posterior margin rounded (Fig. 14A); sixth ventrite trapezoidal, 3 × wider than long, posterior margin truncated, central membranous region broad, apical accessory membranous region petty (Fig. 14B); bursa copulatrix clearly defined; spermathecal gland with a short top tail (Fig. 14C, spggt) and an extremely long lateral tail, which longer than twice length of ovipositor (Fig. 14C, spglt); spermatheca curved tubiform (Fig. 14C, sp).

Variation. The female paratype collected from Hainan has the spermatheca faintly bifurcated distally. This individual variation was also observed in specimens of *G. zayuense* collected from the same locality (Fig. 18D–J).

Distribution. India (Assam, Sikkim), China (Xizang, Yunnan, Hainan), Vietnam, Thailand.

Etymology. This new species, together with *G. dux*, have the largest body size in this genus. The specific epithet comes from the Latin adjective *magnum* (=large).

Gastrocentrum dux (Westwood, 1852)

Figures 2, 10B, 14D, 25

Tillus dux Westwood, 1852: 46, pl. 24, f. 11 (type locality: “Nova Hollandia apud Fluvium Cygnorum”, = Australia, Swan River); Blackburn, 1900: 119 (*Tillus*); Gahan, 1910: 61 (*Gastrocentrum*); Corporaal, 1950: 55 (catalogue; “Ceylon, India, Laos, Java?, Australia??”); Mawdsley, 1999: 270 (Sri Lanka).

Specimens examined. Australia: “*Tillus dux* / australie / Museum Paris, Coll. A. Sicard 1930 / *Gastrocentrum dux* (Westwood, 1852), Det. Yang G. Y. 2013” (MNHN, 1 female, dissected; Fig. 2).

Diagnosis. The specimen examined can be separated with *G. magnum* by elytral asetiferous punctations stop by apical fifth, not continuing to the tip (Fig. 10B), intercoxal process of first abdominal ventrite not grooved, female pygidium with a semi-circle membranous region proximally, reaching half length of pygidium, lateral tail of spermathecal gland much shorter, only slightly longer than spermatheca (Fig. 14D, spglt).

Description. *General appearance:* length 23–29 mm, robust, dark brown. *Head:* including eyes feebly broader than pronotum; eyes moderately large, distance between eyes nearly as long as the transverse diameter of eye; gular suture slightly convergent in anterior; antennae expanded laterally from 7th antennomere onwards; vertex and frons densely punctate, with a very faint ridge along midline, postgenae rugose. *Pronotum:* oblong, length/width ratio ca. 1.4, constricted posteriorly; surface finely and densely punctate, clothed with light yellow hairs. *Elytra:* oblong, sides subparallel, length/width ratio ca. 2.31, vested with light yellow setae; wedge-shaped protuberance present on inner surface; PAP in ten rows, AAP on interspaces between 1st–2nd, 3rd–4th, and 5th–6th PAP rows; AAP present in two very incomplete rows, number of AAP less than that in *G. magnum*; AAP faintly smaller than PAP; interspace between 2nd–3rd PAP rows greater than punctation diameter; elytral punctations decreasing in size postmedially, and completely vanished at apical fifth (Fig. 10B). *Legs:* outer apex of protibia very faintly extending outwards, not forming a distinct tooth. *Abdomen:* intercoxal process of the first ventrite flat, not grooved. *Male genitalia:* not studied. *Female reproductive organs:* pygidium slightly wider than long, posterior margin rounded, a semi-circle membranous region present proximally, reaching to half length of the pygidium; sixth ventrite trapezoidal, wider than long; bursa copulatrix clearly defined; spermathecal gland only with one lateral tail, which slightly longer than spermatheca in fully stretched condition (Fig. 14D, spgl); spermatheca boot-shaped (Fig. 14D, sp).

Note on type specimen. Mawdsley (1999) claimed that the type specimen of *G. dux* was deposited in the Hope Department of Entomology, University Museum, Oxford, United Kingdom, but it was not located during a visit to that museum in 2011 by the first author. Westwood (1852) indicated that the type specimen was from “Mus. Melly”, but efforts to locate it in Melly’s collection in the Natural History Museum, Geneva, yielded no results either. The whereabouts of the type specimen remains unknown.

Discussion. The Australian type locality of this species is doubted by the Australian entomologist and clerid worker Justin Bartlett who, after viewing the Cleridae holdings of all major museum, and several agricultural and private collections from all Australian states, is yet to find a single *Gastrocentrum* specimen, and therefore does not believe *G. dux* to be an Australian species. He also doubts that the locality label of the specimen examined in this manuscript represents an actual collecting event, but rather was labelled after it was identified as *G. dux*, with the associated type locality of ‘Australie’ (pers. comm. J Bartlett). He also pointed out that another apparently Australian specimen from Melly’s collection, a longicorn *Hephaestion acraetus* Newman, is in fact a Chilean species (see Saunders 1850), providing a precedent for erroneously labelled specimens from Melly’s collection. Despite this, no more practical specimen-based evidence for or against this argument has been found. Hence, we can only describe this species based on the specimen mentioned above at the moment, as we can only take the label at face value and assume it to represent an actual collecting label.

We found a Tenebrionidae beetle with the same Swan River type locality also originating from Melly’s collection and described by Westwood: *Prophanes aculeatus* Westwood, 1849. It is presently treated as a valid species, with an eastern, not western,

Australian distribution (Westwood 1849; Carter 1913; Matthews 1992). *Gastrocentrum dux* may have a similar historical story and its correct occurrence could be in other areas of Australia or in other regions of the world, but this hypothesis needs to be proved by further specimens.

***Gastrocentrum regulare* sp. nov.**

<http://zoobank.org/8463F3C7-F2A3-439E-AACD-0E238902A57A>

Figures 4, 10C, 15, 16, 25

Holotype. Malaysia: “Malaysia, Pahang, Cameron Highlands, Tanah Rata vill. env., Gunung Jasar [Mt.]; 1470-1705m, 04°28.4–7'N, 101°21.6–22.1'E, Jiří Hájek leg. 18.iv–10.v.2009 / Holotype: *Gastrocentrum regulare* sp. nov. Yang & Yang, 2020” (NMPC, male, Fig. 4); **Paratype.** Same data as holotype (NMPC, 1 female).

Diagnosis. This species is distinct in the genus in having ten regular rows of asetiferous punctations exceeding half of elytra, without AAP between the PAP rows. It can be differentiated from *G. xiaodongi* by: antennae expanded laterally from 7th antennomere onwards (Fig. 15I); elytra punctations rows stop by apical third (Fig. 10C); inner surface of elytron with a wedge-shaped protuberance; intercoxal process of first abdominal ventrite grooved longitudinally; spermathecal capsule slenderer, tapering to the tip (Fig. 16A, sp).

Description. General appearance: length 12–14 mm, robust, dark brown. **Head:** including eyes feebly broader than pronotum; eyes moderately large, distance between eyes almost as long as the transverse diameter of eye; gular suture almost straight-up; antennae expanded laterally from 7th antennomere onwards (Fig. 15I); vertex and frons roughly punctate, postgenae rugose. **Pronotum:** oblong, length-width ratio ca. 1.5, constricted posteriorly; surface finely and densely punctate, clothed with long, yellow hairs. **Elytra:** oblong, sides subparallel, length/width ratio ca. 2.6, vested with grayish white setae; wedge-shaped protuberance present on inner surface; PAP arranged in ten rows, AAP absent; interspace between 2nd–3rd PAP rows ca. 2 × as wide as the punctation diameter; asetiferous punctations decreasing in size postmedially, and completely vanished at apical third (Fig. 10C). **Legs:** outer apex of protibial apex slightly extending obliquely, not forming a distinct tooth. **Abdomen:** intercoxal process of the first ventrite grooved longitudinally; metacoxal abdominal depressions weakly ridged in anterior margin, perpendicular carinae absent. **Male genitalia:** pygidium subquadrate, posterior margin rounded (Fig. 15G); sixth ventrite arciform, 3 × wider than length, posterior margin rounded, central membranous region oval, extending from anterior margin to posterior margin (Fig. 15H); tegmen tubiform, length ratio of phallobasic apodeme to phallobase ca. 1: 2.1 (Fig. 15A–C); parameres expanded, unhooked (Fig. 15B, b); interphallic plate shorter than half length of phallus (Fig. 15E); phallus apex knot-like, rounded (Fig. 15D, E). **Female reproductive organs:** pygidium slightly wider than long, posterior margin rounded (Fig. 16B); sixth ventrite trapezoidal, 3 × wider than long, central membranous region broad, apical accessory membranous



Figure 15. *Gastrocentrum regulare* sp. nov. male Holotype. **A** aedeagus in ventral view **B** tegmen in lateral view **b** apex of tegmen in lateral view **C** tegmen in ventral view **D** phallus with connecting membrane inverted, lateral view **E** phallus with connecting membrane inverted, ventral view **F** spicular fork **G** pygidium **H** sixth ventrite **I** antenna. Scale bar: 1 mm.

region absent (Fig. 16C); bursa copulatrix clearly defined; spermathecal gland with a top tail of medium length (Fig. 16A, spg); spermathecal duct slender; spermathecal capsule slender, tapering to the tip, length/width ratio = 3.6 (Fig. 16A, sp).

Distribution. Malaysia (Peninsular Malaysia).

Etymology. Refer to the highly regular elytral asetiferous punctations of this species.

***Gastrocentrum xiaodongi* sp. nov.**

<http://zoobank.org/B249CD1A-1BBC-4698-AA3C-961FF427B647>

Figures 5, 10D, 16D–H, 25

Holotype. China: “Xizang (Tibet), Jilongxian [Gyirong county], 1785m, Xinjiangcun, 2019.VI.28, leg. X-D. YANG / Holotype: *Gastrocentrum xiaodongi* sp. nov. Yang & Yang, 2020” (CCCC, female, Fig. 5). **Paratypes. Nepal:** Manaslu Mts., E slope of Ngadi Khola valley, 2000–2300 m, 14–16.V.2005, leg. J. Schmidt, 28°22'N, 84°29'E (RGCM, 1 male); W-Nepal, Modi Khola, Bhakta B.; Banthanti – 2500 – Landrung – 1600 m, 2.VI.1984 (NHMB, 1 female).

Diagnosis. This new species is different from *G. regulare* sp. nov. by: antennae expanded laterally from 8th antennomere onwards; elytral asetiferous punctations stop by middle (Fig. 10D); elytral inner surface without wedge-shaped protuberance; intercoxal process of first abdominal ventrite not grooved (Fig. 20C, ip); spermathecal

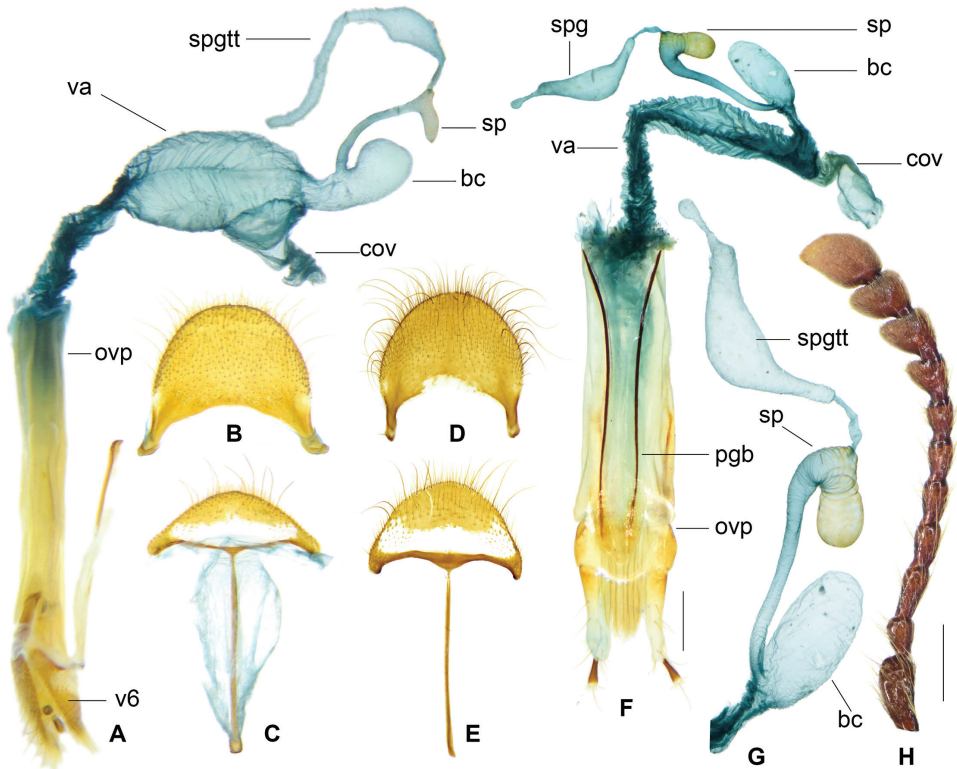


Figure 16. **A–C** *Gastrocentrum regularare* sp. nov. female paratype **A** female reproductive organ **B** pygidium **C** sixth ventrite **D–H** *Gastrocentrum xiaodongi* sp. nov. female holotype **D** pygidium **E** sixth ventrite **F, G** female reproductive organ **H** antenna. Abbreviations: **bc** bursa copulatrix **cov** common oviduct **ovp** ovipositor **pgb** proctigeral bacculi **sp** spermatheca **spg** spermathecal gland **spggt** top tail of spermathecal gland **va** vagina **v6** sixth ventrite. Scale bars: 0.5mm (**A–F, H**).

capsule thicker, rounded distally (Fig. 16F, sp). The new species also looks similar to *G. zayuense* sp. nov. and *G. gaoligongense* sp. nov. at first glance, but it differs from the latter two species by: elytral asetiferous punctations somewhat larger and reaching lateral margins (Fig. 10D), female antennae expanded laterally from 8th antennomere onwards (Fig. 16H). It also differs from *G. gaoligongense* sp. nov. by elytral inner surface without a wedge-shaped protuberance.

Description. General appearance: length 14 mm, brown, a little slenderer than previous species. **Head:** including eyes slightly broader than pronotum; eyes moderately large, distance between eyes slightly greater than the transverse diameter of eye; female antennae expanded laterally from 8th antennomere onwards (Fig. 16H); vertex and frons rugose, densely punctate, postgenae rugose. **Pronotum:** oblong, length/width ratio ca. 1.6, constricted posteriorly; surface finely and densely punctate, clothed with long, yellow hairs. **Elytra:** oblong, sides subparallel in basal half and weakly widened in apical half, length/width ratio ca. 2.4, vested with yellow setae; wedge-shaped

protuberance absent on inner surface; PAP only present on basal half in ten rows, AAP absent, PAP a little larger than those in *G. regulare*, *G. zayuense*, and *G. gaoligongense*; interspace between 2nd-3rd PAP rows greater than punctation diameter (Fig. 10D). **Legs:** outer apex of protibia not extending outwards. **Abdomen:** intercoxal process of the first ventrite not grooved longitudinally; metacoxal abdominal depressions weakly ridged in anterior margin, perpendicular carinae absent. **Male genitalia:** not studied. **Female reproductive organs:** pygidium slightly broader than long, posterior margin rounded (Fig. 16D); sixth ventrite semi-circle, central membranous region broad, apical accessory membranous region absent (Fig. 16E); both dorsal and ventral lamina have three incisions; bursa copulatrix clearly defined; spermathecal gland with a short top tail; spermathecal duct slightly inflated distally; spermathecal capsule rounded in apex, length/width ratio = 2.0. (Fig. 16F, G).

Distribution. China (Xizang, Gyirong), Nepal.

Etymology. We are pleased to dedicate this species to its collector and our friend, Mr Yang Xiaodong.

***Gastrocentrum zayuense* sp. nov.**

<http://zoobank.org/BF8965BA-6A05-4D76-B545-2A844A5453FA>

Figures 6, 10F–H, 17, 18, 21, 24, 25

Holotype. China: Xizang Autonomous Region, Nyingchi prefecture, Zayü County, Zhougoin, 2011.VII.1, BI Wenxuan leg, 2500 m / **Holotype:** *Gastrocentrum zayuense* sp. nov. Yang & Yang, 2020 (CBWX, male, Fig. 6); **Paratypes.** same as holotype (CBWX, 15 ex.); same as holotype but collected by LIU Ye on 2011.VII.3 (IZAS, 9 ex.); same but collected by Yang Xiaodong on 2011.VII.3 (CCCC, 1 ex.).

Diagnosis. This species differs from *G. gaoligongense* sp. nov. by elytral inner surface without wedge-shaped protuberance; tegmen apices with ventral surface streamlined in lateral view (Fig. 17a), female bursa copulatrix clearly defined, much narrower than vagina, distal part of spermathecal capsule short, length/width ratio < 2.5 (Fig. 18A).

Description. General appearance: length 13–18 mm, somewhat slenderer than *G. regulare*, light brown. **Head:** including eyes feebly broader than pronotum; eyes moderately large, distance between eyes slightly greater than the transverse diameter of eye; gular suture slightly convergent in anterior; female antennae broadly expanded laterally from 7th antennomere onwards, while male 7th antennomere less expanded (Fig. 17H); vertex and frons finely punctate, postgenae rugose. **Pronotum:** oblong, length/width ratio ca. 1.5, constricted posteriorly; surface finely and densely punctate, clothed with long, yellow hairs. **Elytra:** oblong, sides subparallel in basal half and a little widened in apical half, length/width ratio ca. 2.5, vested with light yellow setae; wedge-shaped protuberance absent on inner surface; elytron smooth without asetiferous punctations or with very few asetiferous punctations, number of PAP ranged from 0–27 (n = 26), present on elytral basal disc in six rows in maximum, AAP absent (Fig. 10F–H). **Legs:** outer apex of protibia not extending outwards.

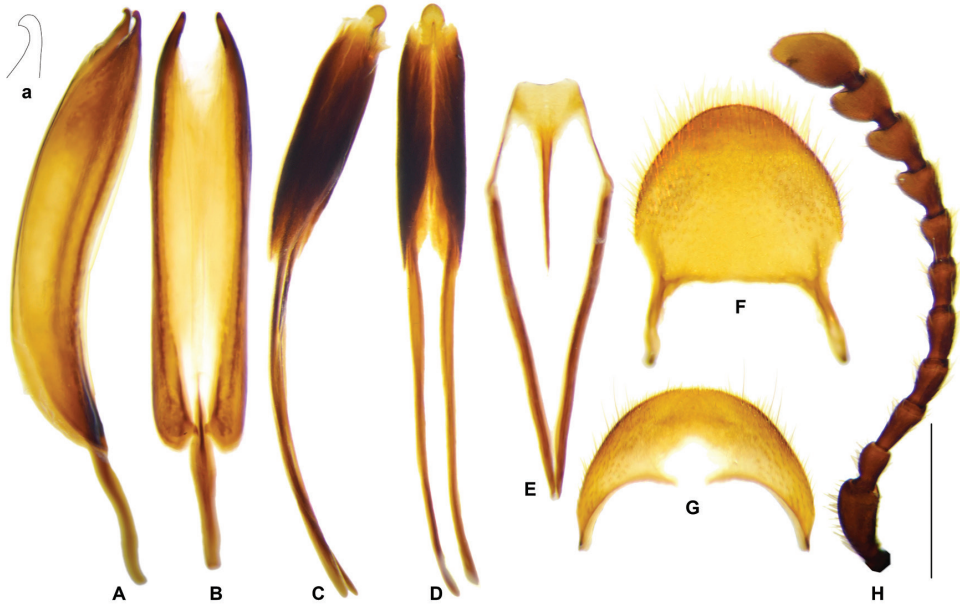


Figure 17. *Gastrocentrum zayuense* sp. nov. Holotype male. **A** tegmen in lateral view **a** apex of tegmen in lateral view **B** tegmen in ventral view **C** phallus in lateral view **D** phallus in ventral view **E** spicular fork **F** pygidium **G** sixth ventrite **H** antenna. Scale bar: 1mm.

Abdomen: intercoxal process of the first ventrite not grooved longitudinally (Fig. 20C); metacoxal abdominal depressions weakly ridged in anterior margin, perpendicular carinae absent. **Male genitalia:** pygidium with posterior margin rounded (Fig. 17F); sixth ventrite arciform, width twice length, posterior margin rounded, central membranous region small, rhombic, extending from anterior margin to half-length of the ventrite (Fig. 17G); tegmen tubiform, length ratio of phallobasic apodeme to phallobase ca. 1: 3.2 (Fig. 17A, B); parameres hooked, ventral surface of the hook streamlined in lateral view (Fig. 17a); interphallic plate shorter than half length of phallus (Fig. 17D); phallus apex knot-like, approximately as long as wide (Fig. 17C, D). **Female reproductive organs:** pygidium subquadrate, posterior margin rounded (Fig. 18B); sixth ventrite trapezoidal, twice as broad as long, rounded posteriorly, central membranous region broad and extending posteriorly at sides, apical accessory membranous region absent (Fig. 18C); bursa copulatrix clearly defined; spermathecal gland with a top tail of medium length; spermathecal duct inflated distally where continuous with spermathecal capsule; spermathecal capsule simple or feebly bifurcate (Fig. 18D–J), distal part of spermathecal capsule short, length/width ratio < 2.5 (Fig. 18A, E–J).

Variation. All examined specimens are from exactly same locality, they vary individually in the number of punctations on one elytron from zero to 27, and spermatheca apex being simple or feebly bifurcate distally.

Distribution. China (Xizang, Zayü).

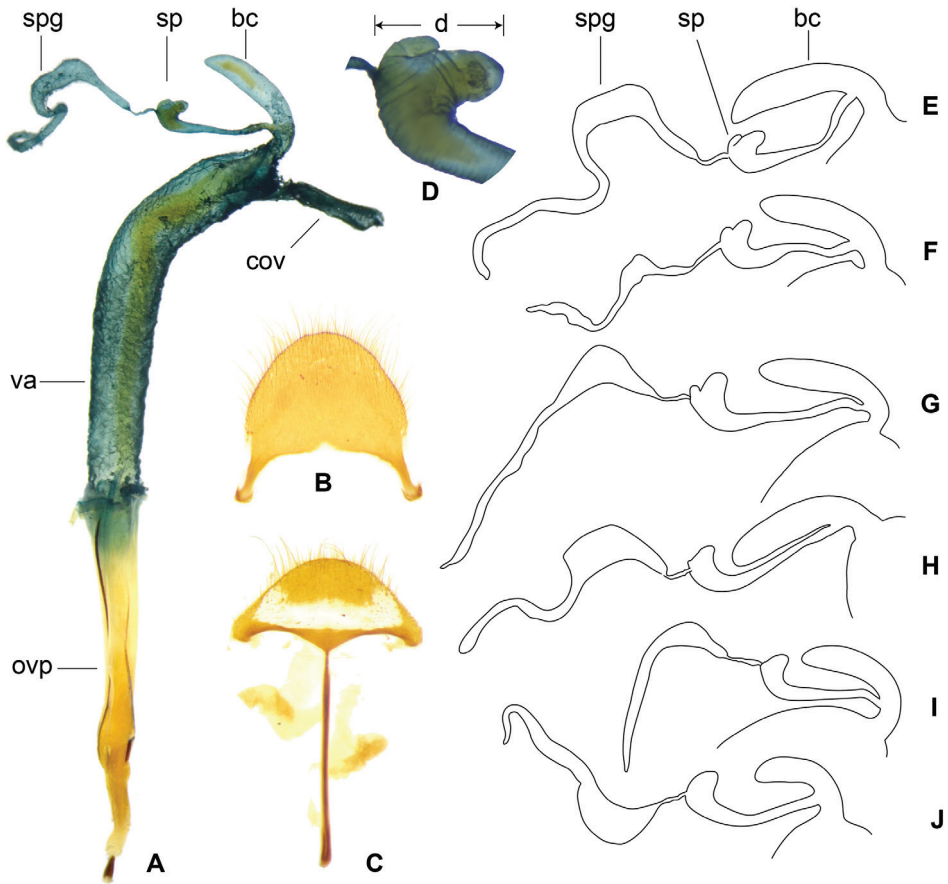


Figure 18. *Gastrocentrum zayuense* sp. nov. paratypes, female reproductive organs of different specimens showing morphological variations. **A** female reproductive organ **B** pygidium **C** sixth ventrite **D** spermatheca **E–J** drawings of bursa copulatrix, spermatheca and spermathecal gland of six females. Abbreviations: **bc** bursa copulatrix **cov** common oviduct **d** distal part of spermathecal capsule **ovp** ovipositor **sp** spermatheca **spg** spermathecal gland **spgtt** top tail of spermathecal gland **spglt** lateral tail of spermathecal gland **va** vagina.

Ecology. Habitat is shown in Fig. 24. The specimens were collected on the tree trunk at night.

Etymology. The new species is named after its type locality.

***Gastrocentrum gaoligongense* sp. nov.**

<http://zoobank.org/A1EC3952-6CAA-4F94-9222-3D5324686AA2>

Figures 7, 10E, 19, 22E, 25

Holotype. China: “CHINA, Yunnan Province, Fugong Co., Lishadi town, Shibali village, roadside, 27.16520°N, 98.77980°E / 2530 m, 2004.5.5, night, Liang H-B,

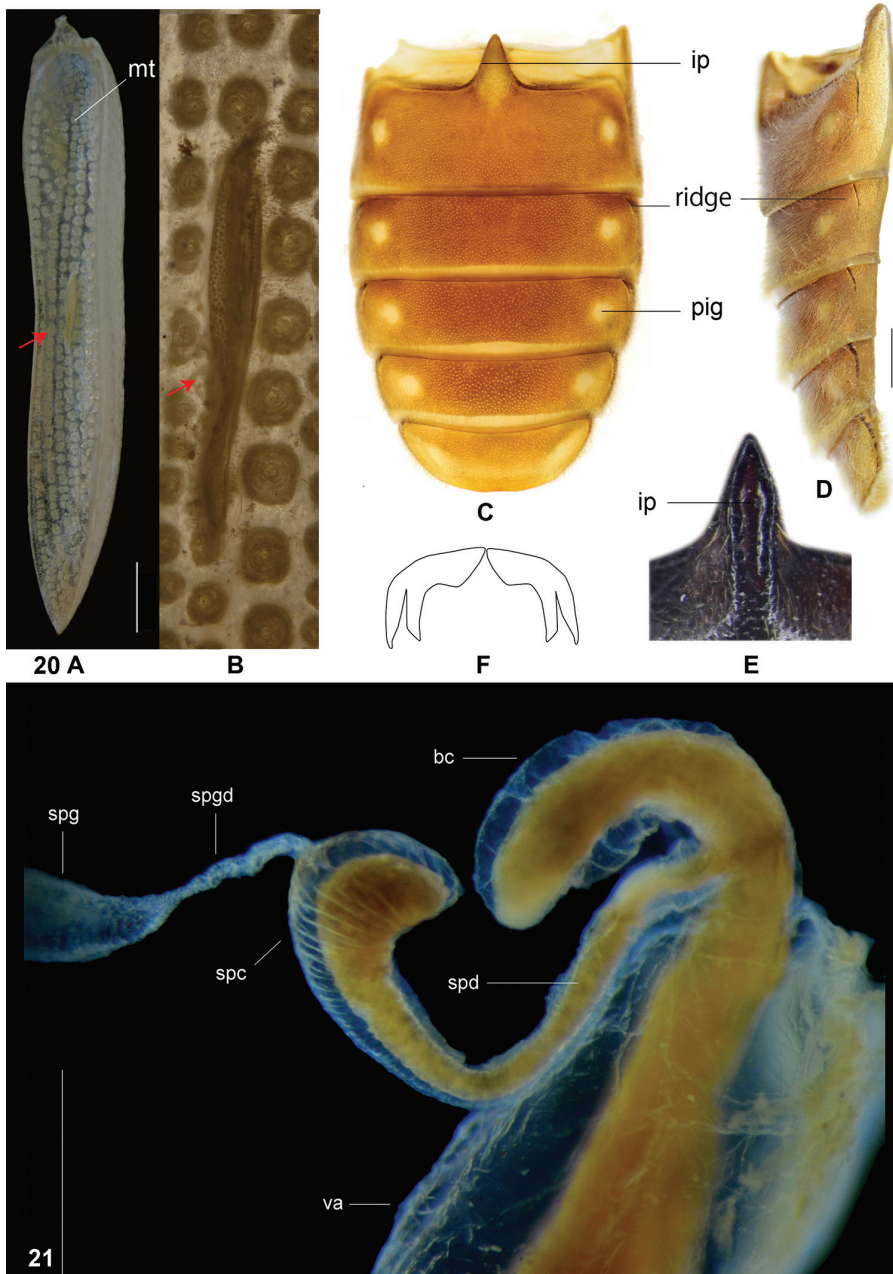


Figure 19. *Gastrocentrum gaoligongense* sp. nov. Holotype male. **A** aedeagus in ventral view **B**, tegmen in lateral view **b** apex of tegmen in lateral view **C** tegmen in ventral view **D** phallus in ventral view **d** apex of phallus **E** spicular fork **F** pygidium **G** sixth ventrite **H** antenna. Scale bars: 1mm.

Li X-Y, coll., California Academy & IOZ., Chinese Acad Sci / IOZ(E) 1890507 / Holotype / *Gastrocentrum gaoligongense* sp. nov. Det. Yang G.Y. 2020” (IZAS, male) (Fig. 7). **Paratypes.** CHINA: Yunnan, Gongshan, Menggaguo, 2800 m, Light, 2016. VII.8, Yu-Tang Wang leg. (CCCC, 1 male, 1 female); same but 2016.VI.30 (CCCC, 1 male); same but 2016.VI.24 (CCCC, 1 female).

Diagnosis. The new species differs from *G. zayuense* sp. nov. by: elytra with a pair of wedge-shaped protuberance on inner surface; tegmen apices bulged on ventral surface (Fig. 19b); female bursa copulatrix not differentiated, merely a swollen continuation of the vagina, distal part of spermathecal capsule, long and slender, length/width ratio > 5 (Fig. 22E).

Description. General appearance: length 13–19 mm, slenderer than all the other species, dark brown. **Head:** including eyes slightly broader than pronotum; eyes moderately large, distance between eyes slightly longer than the transverse diameter of eye; gular suture slightly convergent in anterior; female antennae broadly expanded laterally from 7th antennomere onwards, while male 7th antennomere less expanded (Fig. 19H); vertex and frons with dense and somewhat coarse punctations, postgenae rugose. **Pronotum:** oblong, length/width ratio ca. 1.6, constricted posteriorly, faintly constricted anteriorly; surface finely and densely punctate, clothed with long, yellow hairs. **Elytra:** oblong, sides subparallel in basal half and weekly widened in apical half, length/width ratio ca. 2.6, vested with light yellow setae; wedge-shaped protuberance present on inner surface; elytra with very few



Figures 20–21. 20A, B wedge-shaped protuberance on inner surface of elytron with *G. unicolor* as an example C, D abdomen of *G. zayuense* in ventral and lateral view showing 1st–5th ventrites with short lateral ridges on each segments E intercoxal process of first ventrite of *G. unicolor* showing the longitudinal groove F claws of *Isocymatodera atricolor*. 21 Female reproductive organs of *G. zayuense* sp. nov. not stained and with the dark background, revealing the internal tissues. Abbreviations: bc bursa copulatrix ip intercoxal process mt microtrichia field pig less pigmented circles on abdominal segments ridge short ridges on abdominal segments spc spermathecal capsule spd spermathecal duct spg spermathecal gland spgd spermathecal gland duct va vagina. Scale bars: 0.5 mm (20A–D) 1 mm (21).

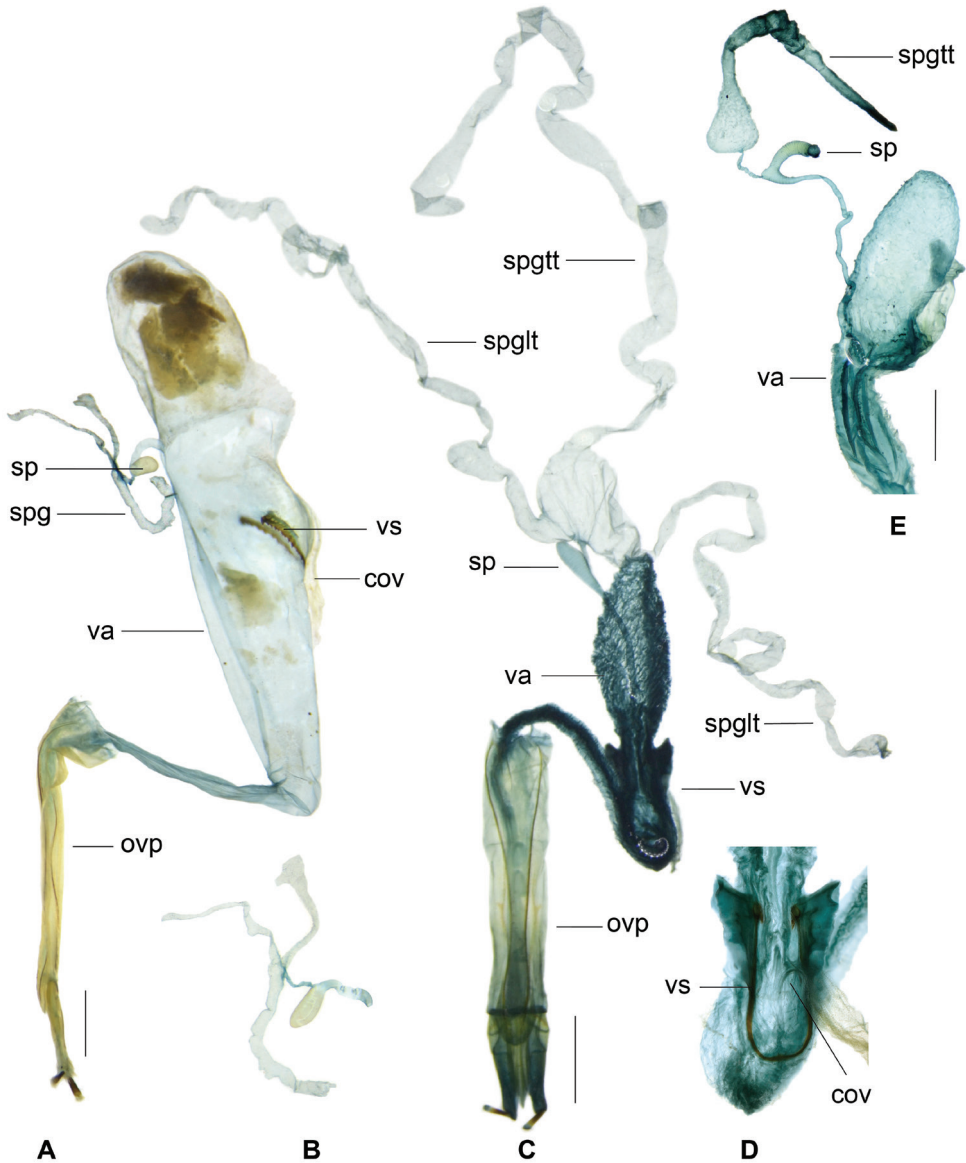


Figure 22. **A, B** *Isocymatodera atricolor*. **C, D** *I. kolbei*. **E** *Gastrocentrum gaoligongense*. Abbreviations: **cov** common oviduct **ovp** ovipositor **sp** spermatheca **spg** spermathecal gland **spglt** top tail of spermathecal gland **spglt** lateral tail of spermathecal gland **va** vagina **vs** vaginal sclerite. Scale bar: 1 mm.

asetiferous punctations, number of PAP on each elytron ranged from 2-39 (n = 5), present on elytral basal disc in five rows in maximum, AAP absent (Fig. 10E). **Legs:** outer apex of protibia not extending outwards. **Abdomen:** intercoxal process of the first ventrite not grooved longitudinally; metacoxal abdominal depressions weakly ridged in anterior margin. **Male genitalia:** pygidium with posterior margin rounded (Fig. 19F); sixth ventrite arciform, width twice length, posterior

margin rounded, central membranous region small, extending from the anterior margin, not reaching half-length of ventrite (Fig. 19G); tegmen tubiform, length ratio of phallobasic apodeme to phallobase ca. 1: 3.2 (Fig. 19A–C); parameres hooked, ventral surface of the hook bulged in lateral view (Fig. 19b); interphallic plate shorter than half length of phallus (Fig. 19D); phallus apex knot-like, slightly longer than wide (Fig. 19D, d). **Female reproductive organs:** pygidium slightly broader than long, posterior margin rounded; sixth ventrite widely trapezoidal, 2.5 × broader than long, rounded posteriorly, central membranous region broad, apical accessory membranous region absent; bursa copulatrix unclearly defined, merely swollen continuation of vagina; spermathecal gland with a top tail of medium length; spermathecal duct long and slender; spermathecal capsule feebly bifurcate in sub-apex; distal part of spermathecal capsule long and slender, length/width ratio > 5 (Fig. 22E).

Distribution. China (Yunnan).

Etymology. The holotype and paratypes of this new species were collected from two sites of the Gaoligong Mountains in Yunnan Province, China. The specific name is an adjective that refers to this mountain.

***Gastrocentrum brevicolle* (Pic, 1940)**

Exocentrum brevicolle Pic, 1940: 3 (type locality: “Ceylan”); Corporaal, 1950: 55 (*Gastrocentrum*); Mawdsley, 1999: 271 (Sri Lanka); Gerstmeier, 2005: 56.

Note. This species was not studied because specimens were unavailable. Gerstmeier (2005) stated that the position of this species in the genus *Gastrocentrum* is doubtful because its pronotum was not elongated, but rather spherical.

***Tillus nitidus* (Schenkling, 1916), comb. nov.**

Figure 8

Gastrocentrum nitidum Schenkling, 1916: 117 (type locality: “Banshoryo-Distrikt, Sokutsu”, Taiwan); Corporaal, 1950: 55 (catalogue).

Type specimen examined. Holotype. “Banshoryo Distr. Sokutsu (Formosa), H. Sauter VII. 1912 / Holotypus / Schenkling det. / *Gastrocentrum nitidum* Schklg. Typus!” (SDEI, female; Fig. 8).

Notes. This species is transferred to the genus *Tillus* for its claw with two inner denticles (basal denticle trigonal). This type of claw was imaged in Burke (2017: 179, fig. B) of the species *Cymatodera balteata*.

***Isocymatodera atricolor* (Pic, 1935)**

Figures 9, 20F, 22A, 22B

Strotocera atricolor Pic, 1935: 6 (type locality: “Indochine”); Gerstmeier, 2009: 5 (*Isocymatodera*).

Type specimens examined. Syntypes. “[...] / voi Tillus / Type [printed] *Strotocera atricolor* nouv. [hw. by Pic] / ?abyssinie / voi *Strotocera* / type [hw. by Pic] / Paris” (MNHN, 1 female; Fig. 9); “Baria / Baria (Cochinchina) / acq. 1930 coll. Ch. Madon (Le Moul) / Cotype: *Strotocera atricolor* Pic, 1934 / *Strotocera atricolor* Pic, 1935, ZMAN type 1939.1” (ZMAN, 1 female).

Other specimens. China. Hainan, Changjiang County, Bawangling Forest Nature Reserve (IZAS, 6 ex.); Ledong County, Jianfengling Tropical Rainforest National Park (IZAS, 4 ex.); Baisha County (IZAS, 1 ex.). **Vietnam.** “Baria [...] / Baria (Cochinchina) / acq. 1930 coll. Ch. Madon (Le Moul) / Homotype: (Corporaal comp.): *Strotocera atricolor* Pic” (ZMAN, 1 ex.).

Note. This species is recorded from China for the first time, and hence we provide a short note here.

Phylogenetic relationships

A phylogenetic analysis resulted in eight most parsimonious trees in PAUP* (L = 36, CI = 0.611, RI = 0.659, RC = 0.402) (Fig. 23). The eight species comprise two clades, the first clade including *G. unicolor* and *G. laterimaculatum* (bootstrap value 73), and the second clade including the other six species (bootstrap value 62). The monophyly of the first clade is supported by the 7th antennomere not extended laterally (character 2: 0; CI = 0.500) and AAP distinctly arranging in two rows (character 7: 1; CI = 1.000). The second clade is supported by inclusive synapomorphies: protibial outer-apical tooth absent (character 10: 0; CI = 1.000) and female spermathecal gland not having two lateral tails (character 21: 0; CI = 1.000).

The second clade forms a polytomy consisting of *G. magnum* sp. nov., *G. dux*, *G. regulare* sp. nov., and a moderately supported sub-clade representing the remaining ingroup species. The monophyly of this sub-clade (bootstrap value 69) is supported by elytral interspace between 1st-2nd PAP rows without AAP (character 5: 0; CI = 0.500), intercoxal process of first abdominal ventrite not grooved (character 13: 0; CI = 0.500) and female spermathecal gland without any lateral tail (character 20: 0; CI = 0.500). Within this sub-clade, *G. xiaodongi* sp. nov. is the sister group of *G. zayuense* sp. nov. + *G. gaoligongense* sp. nov.; the monophyly of the latter is supported by elytral punctations not reaching lateral margins (character 9: 0; CI = 1.000).

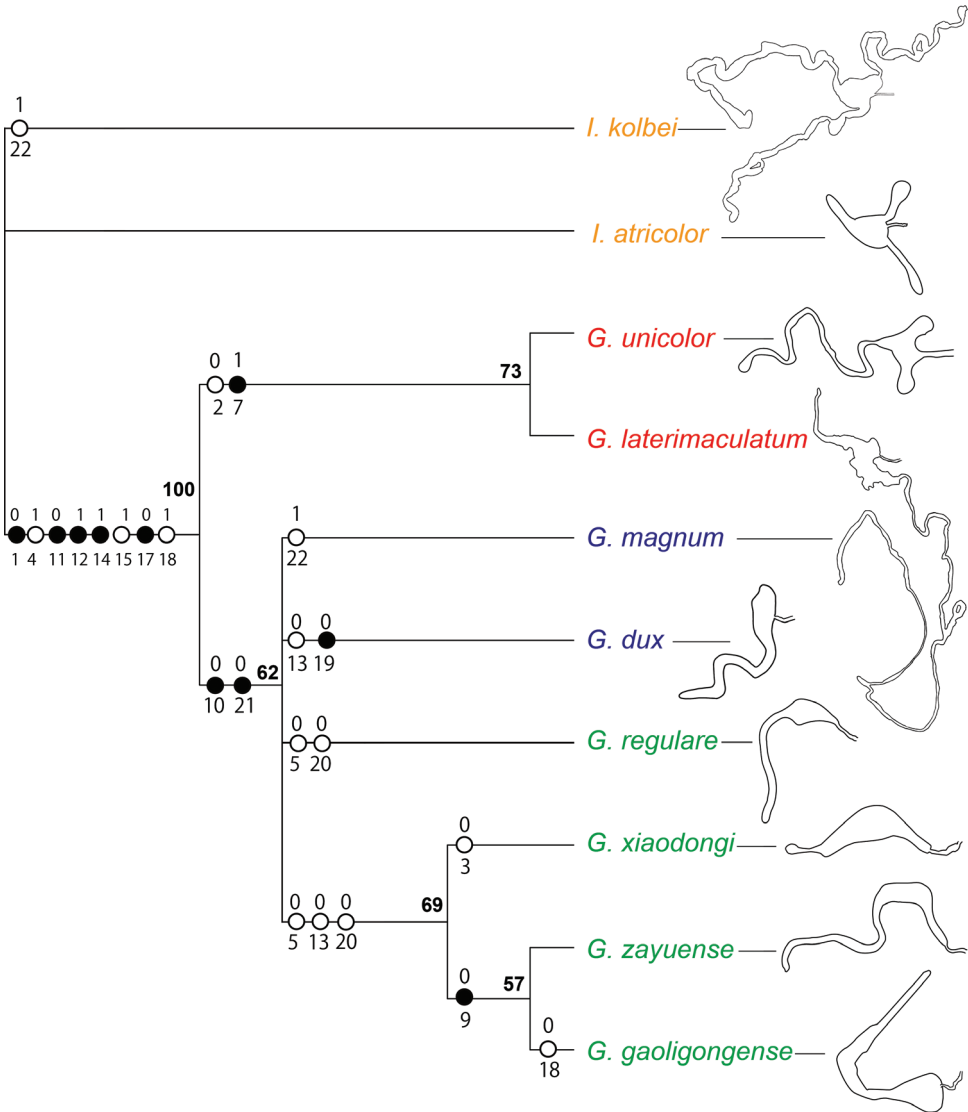


Figure 23. A preliminary phylogenetic analysis of *Gastrocentrum*, showing 50% majority-rule consensus MP tree. Only unambiguous characters are shown. Black circles represent characters having a CI of 1.000 while each state is derived only once, whereas white circles represent characters having a CI less than 1.000 while each state is derived more than once. Bootstrap support values are given at nodes. Female spermathecal glands are illustrated with top tail orientated to left side, but it is not known in *G. laterimaculatum*.

Significance of female reproductive organs

Female reproductive organs are inferred to have taxonomic and phylogenetic importance in genus *Gastrocentrum*.

In certain Oriental genera of Tillinae, the vagina is equipped with a pair of sclerites or a joint sclerite, such as in *Tillus* (Kolibáč 1989: 17, figs 46, 47), *Isocymatodera* (Fig. 22A, C, D) and *Cladiscus* (unpublished data), but this sclerite is absent in all the species of *Gastrocentrum*.

In the present study, we find that almost all the species in *Gastrocentrum* have a clearly defined bursa copulatrix (Figs 12, 14, 16, 18), the only exception being *G. gaoligongense* (Fig. 22E). This disproves the idea of Opitz (2010: 51) that the presence or absence of a bursa copulatrix is consistent within stable genera.

The morphology of the spermathecal gland was rarely extensively studied previously in Cleridae. In *Gastrocentrum*, we find that this structure was phylogenetically significant at the infra-generic level (Fig. 23). The three-tailed spermathecal gland occurring in *G. unicolor* and the outgroup *Isocymatodera* was supposed to be plesiomorphic in *Gastrocentrum* (Fig. 23). In *G. magnum* and *G. dux* one lateral tail was lost, while in *G. regulare*, *G. zayuense*, *G. xiaodongi*, and *G. gaoligongense*, two lateral tails were lost. The absence of the top tail was autapomorphic for *G. dux*.

The shape of the spermathecal capsule was believed by Opitz (2010: 51) to be consistent within stable genera, however, we found that this structure was different among several *Gastrocentrum* species and thus was of some value for species-level identification, for example, the spermathecal capsules were tapered in *G. regulare* (Fig. 16A), barrel-shaped in *G. xiaodongi* (Fig. 16G), short in *G. zayuense* (Fig. 18A), and long and slender in *G. gaoligongense* (Fig. 22E).



Figure 24. Habitat of *G. zayuense* sp. nov. Photograph by BI Wenxuan.

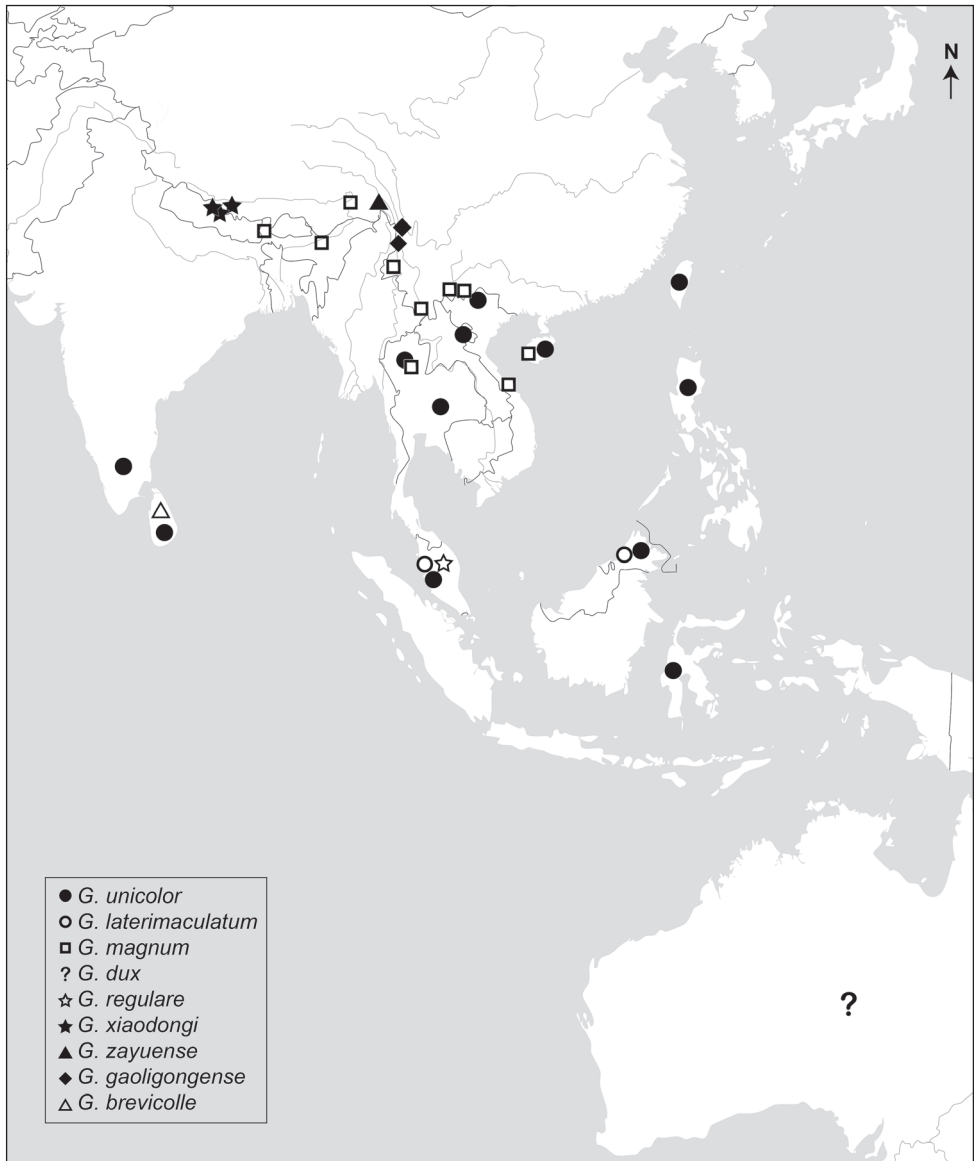


Figure 25. Geographical distribution map of the genus *Gastrocentrum*.

Acknowledgments

We are indebted to the following curators or persons for their kind help accessing the valuable materials: Dr Stephan Blank (SDEI, Müncheberg), Dr Oliver Montreuil and Antoine Mantilleri (MNHN, Paris), Dr Michel Brancucci and Michael Geiser (NHMB, Basel), Dr Jiří Hájek (NMPC, Prague), Dr Roland Gerstmeier (RGCM, Munich), Mr CHEN Changchin (CCCC, Taiwan), Mr BI Wenxuan (CBWX, Shanghai).

We thank Dr LIANG Hongbin, Mr YANG Xiaodong, Mr LIU Ye, and Mr WANG Yutang for collecting the new species and thank Mrs Emily Lee for checking the English language. We are grateful to Dr Roland Gerstmeier, Dr Justin Bartlett, and Dr Jiří Kolibáč for critically reviewing the manuscript and providing helpful comments, and to Ivan Löbl for help in locating the type of *G. dux*. This research was supported by the Beijing Key Laboratory for Forest Pest Control, Beijing Forestry University, and the National Natural Science Foundations of China (grant number: 31770687).

References

- Burke, AF, Zolnerowich G (2017) A taxonomic revision of the subfamily Tillinae Leach sensu lato (Coleoptera, Cleridae) in the New World. *ZooKeys* 179: 75–157. <https://doi.org/10.3897/zookeys.179.21253.figure1>
- Blackburn BA (1900) Further notes on Australian Coleoptera, with descriptions of new genera and species. *Transactions of the Royal Society of South Australia* 24 (2): 113–169.
- Chapin EA (1924) Classification of the Philippine components of the Coleopterous Family Cleridae. *The Philippine Journal of Science* 25: 159–286.
- Corporaal JB (1950) Cleridae In: Hinks WD (Ed.) *Coleopterorum catalogus supplementa*, Pars 23 (2nd ed). W. Junk, Gravenhagen, 373 pp.
- Ekis G (1977) Classification, phylogeny, and zoogeography of the genus *Perilypus* (Coleoptera: Cleridae). *Smithsonian Contributions to Zoology*. Number 227. Smithsonian Institution Press, Washington, 138 pp. <https://doi.org/10.5479/si.00810282.227>
- Gahan CJ (1910) Notes on Cleridae and descriptions of some new genera and species of this Family of Coleoptera. *The Annals and Magazine of Natural History: including Zoology, Botany and Geology Ser. 8, 5*: 55–76. <https://doi.org/10.1080/00222931008692725>
- Carter HJ (1913) Revision of Australian species of the subfamilies Cyphaleinae and Cnodaloninae. *Proceedings of the Linnean Society of New South Wales* 38: 61–105. <https://doi.org/10.5962/bhl.part.13554>
- Gerstmeier R (1993) Short communications on systematics of Cleridae. 3. The Genus *Isocymatodera* Hintz, 1902 (Coleoptera, Cleridae, Tillinae). *Mitteilungen der Münchner Entomologischen Gesellschaft* 83(31): 43–45.
- Gerstmeier R (2005) A new species of *Gastrocentrum* Gorham, 1876, from Malaysia (Coleoptera: Cleridae, Tillinae). *Entomologische Zeitschrift* 115(2): 55–56.
- Gerstmeier R, Weiss I (2009) Revision of the Genera *Diplocladus* Fairmaire and *Strotocera* Schenkling (Coleoptera: Cleridae, Tillinae). *Zootaxa* 2242: 1–54. <https://doi.org/10.11646/zootaxa.2242.1.1>
- Gorb S (2001) *Attachment devices of Insect cuticle*. Kluwer Academic Publishers, Dordrecht, The Netherlands, 305 pp.
- Gorham HS (1876) Notes on the Coleopterous family Cleridae, with description of new genera and species. *Cistula Entomologica* II: 57–106.
- Kolibáč J (1989) Further observations on morphology of some Cleridae (Coleoptera) (1). *Acta scientiarum naturalium Academiae Scientiarum Bohemicae, Brno* 23(1): 1–50.

- Matthews EG (1992) Classification, relationships and distribution of the genera of Cyphaeini (Coleoptera: Tenebrionidae). *Invertebrate Taxonomy* 6: 437–522. <https://doi.org/10.1071/IT9920437>
- Mawdsley JR (1999) Review of the Genus *Gastrocentrum* Gorham 1876 (Coleoptera Cleridae Tillinae), with biological notes on species from Sri Lanka. *Tropical Zoology* 12(2): 267–272. <https://doi.org/10.1080/03946975.1999.10539393>
- Opitz W (2010) Classification, natural history, phylogeny, and subfamily composition of the Cleridae and generic content of the subfamilies (Coleoptera: Cleridae). *Entomologica Basiliensia et Collectionis Frey* 32: 31–128.
- Pic M (1940) Diagnoses de Coléoptères exotiques. *L'Échange, Revue Linnéenne* 56(479): 2–4.
- Saunders WW (1850) On various Australian longicorn beetles. *The Transactions of the Entomological Society of London (new series)* 1: 76–85. <https://doi.org/10.1111/j.1365-2311.1850.tb02486.x>
- Schenkling S (1903) Coleoptera, Malacodermata. Fam. Cleridae. In: Wytzman (Ed.) *Genera Insectorum. Fascicle 13*. Wytzman, Bruxelles, 124 pp.
- Schenkling S (1912) H. Sauter's Formosa-Ausbeute. Cleridae (Col.). *Entomologische Mitteilungen* 1: 321–330. <https://doi.org/10.5962/bhl.part.25902>
- Schenkling S (1916) H. Sauter's Formosa-Ausbeute: Cleridae II (Col.). *Archiv für Naturgeschichte A* 82(5): 117–118. <https://doi.org/10.5962/bhl.part.25111>
- Swofford DL (2002) PAUP*. *Phylogenetic Analysis Using Parsimony (*and other methods)*. Version 4. Sinauer Associates, Sunderland, Massachusetts.
- Westwood JO (1852) Descriptions of new species of Cleridae, from Asia, Africa, and Australia. *Proceedings of the Zoological Society of London* 20: 34–55. [pls 24–27]
- Westwood JO (1849) Descriptions of some new exotic Coleoptera. *Transactions of the Entomological Society of London* 5: 202–214.
- White A (1849) *Nomenclature of Coleopterous Insects in the collection of the British Museum – Part IV: Cleridae*. London, 68 pp.
- Yang GY, Montreuil O, Yang XK (2013) Taxonomic revision of the genus *Callimerus* Gorham s. l. (Coleoptera, Cleridae). Part I. *latifrons* species-group. *ZooKeys* 294: 9–35. <https://doi.org/10.3897/zookeys.294.4669>

A new species of Rain Frog (Brevicipitidae, *Breviceps*) endemic to Angola

Stuart V. Nielsen^{1,2,3}, Werner Conradie^{4,5,6}, Luis M. P. Ceriaco^{7,8}, Aaron M. Bauer⁹,
Matthew P. Heinicke¹, Edward L. Stanley², David C. Blackburn²

1 University of Michigan-Dearborn, Dearborn, Michigan, USA **2** Florida Museum of Natural History, University of Florida, Gainesville, Florida, USA **3** Marquette University, Milwaukee, Wisconsin, USA **4** Port Elizabeth Museum (Bayworld), Humewood, Republic of South Africa **5** Nelson Mandela University, George, Republic of South Africa **6** National Geographic Okavango Wilderness Project, Wild Bird Trust, Republic of South Africa **7** Museu de História Natural e da Ciência da Universidade do Porto, Porto, Portugal **8** Museu Nacional de História Natural e da Ciência, Lisboa, Portugal **9** Villanova University, Villanova, Pennsylvania, USA

Corresponding author: Stuart V. Nielsen (snielsen@floridamuseum.ufl.edu)

Academic editor: A. Crottini | Received 31 July 2020 | Accepted 5 September 2020 | Published 27 October 2020

<http://zoobank.org/2043280A-1591-4D51-ACE3-F9015F170890>

Citation: Nielsen SV, Conradie W, Ceriaco LMP, Bauer AM, Heinicke MP, Stanley EL, Blackburn DC (2020) A new species of Rain Frog (Brevicipitidae, *Breviceps*) endemic to Angola. ZooKeys 979: 133–160. <https://doi.org/10.3897/zookeys.979.56863>

Abstract

Recent molecular phylogenetic work has found that *Breviceps* Merrem, 1820 comprises two major clades, one of which, the *B. mossambicus* group, is widely distributed across southern sub-Saharan Africa. This group is notable for harboring abundant cryptic diversity. Of the four most recently described *Breviceps* species, three are members of this group, and at least five additional lineages await formal description. Although *Breviceps* has long been known to occur in Angola, no contemporary material has been collected until recently. The three most widespread taxa, *B. adspersus*, *B. mossambicus*, and *B. poweri*, may all occur in Angola, but accurate species assignment remains challenging given the rampant morphological similarity between these taxa, and, until recently, the lack of genetic resources. Phylogenetic, morphological, and acoustic analyses of recently collected samples from disparate localities within Angola provide evidence for an undescribed species that is sister to *B. poweri*. The new species can be diagnosed from its sister taxon by lacking pale spots along the flanks, a pale patch above the vent, and a short, dark band below the nares (all present in *B. poweri*). Additionally, the male advertisement call differs from the three other *Breviceps* that might occur in Angola in having both a longer interval between consecutive calls and a higher average dominant frequency. We here describe this lineage as a distinct species, currently only known from Angola, and discuss the presence of other *Breviceps* taxa within Angola.

Resumo

Investigações moleculares recentes revelaram que o género *Breviceps* Merrem, 1820, é composto por duas linhagens principais, uma das quais, o grupo *B. mossambicus*, é amplamente distribuído na região sul da África subsaariana. Este grupo é notável por albergar uma abundante diversidade críptica. Das quatro espécies de *Breviceps* recentemente descritas, três pertencem a este grupo, e pelo menos outras cinco linhagens adicionais aguardam a sua descrição formal. Apesar de o género ser conhecido de Angola desde há muito tempo, só muito recentemente foram colhidos novos espécimes. Os três taxa mais amplamente distribuídos, *B. adspersus*, *B. mossambicus* e *B. poweri* podem todos, porventura, ocorrer em Angola, no entanto a correta identificação destas espécies têm sido problemática devido às semelhanças morfológicas extremas entre este taxa, e, até muito recente, a completa ausência de material genético. Análises filogenéticas, morfológicas e acústicas dos espécimes recentemente colhidos em diferentes locais de Angola apontam para a existência de uma espécie nova para a ciência, irmã de *B. poweri*. A nova espécie pode ser diferenciada do seu táxon irmão pela falta de marcas pálidas nos flancos, mancha pálida acima do ventre e pequena banda negra abaixo do nariz (presentes em *B. poweri*). Para além destas características, o chamamento dos machos difere das outras três espécies de *Breviceps* que podem ocorrer em Angola por ter um maior intervalo entre chamamentos consecutivos e uma maior frequência média dominante. Descrevemos aqui esta linhagem como uma espécie distinta, atualmente apenas conhecida de Angola, e discutimos a presença de outras espécies de *Breviceps* em Angola.

Keywords

Afrobatrachia, Anura, *Breviceps ombelanonga* sp. nov., cryptic species, multilocus, novel species, Sub-Saharan Africa

Palavras Chave

África Subsahariana, Afrobatrachia, Anura, *Breviceps ombelanonga* sp. nov., espécies crípticas, espécies novas, multilocus

Introduction

Breviceps Merrem, 1820 is a genus of fossorial frogs widely distributed across southern sub-Saharan Africa, from Angola in the northwest, through Zambia, the southern portions of the Democratic Republic of the Congo and Tanzania, and southward throughout virtually all of southern Africa (Minter 2004; Minter et al. 2017). It currently comprises 18 species, although a recent molecular phylogenetic study indicates that this is an underestimate (Nielsen et al. 2018). Six species have been described since 2003 (Minter 2003; Channing and Minter 2004; Channing 2012; Minter et al. 2017), largely representing cryptic taxa embedded within what were previously considered widespread species or species complexes, namely *B. mossambicus* Peters, 1854 and *B. adspersus* Peters, 1882 (Nielsen et al. 2018). The justification for recent descriptions has largely been variation in nuptial call characteristics, geography, and mitochondrial genetic distances, yet many additional distinct genetic lineages have been identified and await formal description. Large-scale taxonomic revision is required but this remains problematic due in large part to limited genetic sampling (Nielsen et al. 2018), especially in the northwestern extent of the genus in Angola.

The taxonomy of Angolan *Breviceps* has long been problematic. Bocage (1870, 1873) was the first to report *Breviceps* in Angola based on two specimens from “Biballa” (currently Bibala, Namibe Province) that he referred to *Breviceps gibbosus* (Linnaeus, 1758). After receiving more specimens from other localities in Huambo and Huíla provinces, Bocage (1895) provided a more detailed description of the Angolan material and assigned all of these records to *B. mossambicus*. He noted that compared with other *Breviceps* (which, at the time, included only three species), Angolan specimens lacked a heavily granular dorsum (vs. granular in *B. verrucosus*) and had a continuous dark gular patch (vs. paired patches in *B. adspersus*). Unfortunately, the majority of these specimens were lost in the 1978 fire that destroyed the Lisbon Museum (Almaça 2000; Marques et al. 2018). Subsequent workers provided additional records from western Angola (Bengo Province: Parker 1934; Huambo and Huíla provinces: Monard 1938; Benguela Province: Monard 1938, Helmich 1957) and northeastern Angola (Lunda-Sul and Moxico provinces: Laurent 1964; Ruas 1996), all of which were reported as *B. mossambicus*. In a second review of the same material, Ruas (2002) revised her previous conclusions and referred the specimens from Moxico Province to the “*Breviceps mossambicus-adspersus* complex” (sensu Poynton 1982; Poynton and Broadley 1985), noting genetic data were needed to resolve their taxonomy. This species complex has been suggested to have a broad hybridization zone across southern Africa (Poynton 1982), and Angolan *Breviceps* were noted to share aspects of coloration with both *B. mossambicus* and *B. adspersus*, yet were distinct from *B. poweri* Parker, 1934 from the Zambezi Basin (Poynton and Broadley 1985). More recent synopses of Angolan material have either referred historical material to *B. cf. adspersus* (Baptista et al. 2019) or simply as *B. sp.* in recognition of the taxonomic uncertainties for these populations (Marques et al. 2018; Ceríaco et al. 2020).

A recent phylogenetic study of *Breviceps* (Nielsen et al. 2018), while lacking Angolan material, confirmed the presence of *B. poweri* in northwestern Zambia, as well as nomintotypical *B. adspersus* within 3 km of the Angolan border in Namibia (Fig. 1A). This suggests that both might also occur in Angola (Marques et al. 2018), although the evidence for *B. poweri* is based mainly on tertiary references (see Channing and Rödel 2019). Based solely on external morphology, Ceríaco and Marques (2018) recently identified specimens from Moxico Province, in eastern Angola, as *B. poweri*; these are the same specimens previously identified by Ruas (1996, 2002) as *B. mossambicus* and *B. mossambicus-adspersus*, respectively. While *B. mossambicus* has been historically listed as part of the Angolan anuran fauna, recent genetic analyses have so far only confirmed populations from Mozambique as corresponding to this name (Nielsen et al. 2018). Due to substantial morphological similarity, scarcity of genetic sampling, and potential for hybridization among *B. mossambicus*, *B. poweri*, and *B. adspersus* (Poynton 1964, 1982; Poynton and Broadley 1985; Minter et al. 2017), taxonomic identification of any historical Angolan material should therefore be considered tentative at best.

Angola’s long civil war, which lasted from 1975 to 2002, effectively stifled biological exploration and discovery (for additional summary, see Marques et al. 2018). Recent surveys, many by authors of this manuscript, have produced the only contemporary records of Angola’s herpetofauna (e.g., Ceríaco et al. 2014, 2016, 2018; Conradie

et al. 2016; Heinicke et al. 2017; Marques et al. 2018; Baptista et al. 2019; Butler et al. 2019; Ernst et al. 2020), including the only recent records of *Breviceps* in Angola. The nearest samples with confident identifications and associated genetic data are at least 600 km away (i.e., *B. adspersus* in Namibia and *B. poweri* in Zambia; Nielsen et al. 2018). Here we analyze these recently collected Angolan *Breviceps* in a phylogenetic framework and assess their taxonomic status, resulting in the description of a new species so far known only from Angola.

Materials and methods

Species concept

We consider species as units of separately evolving metapopulation lineages, following the conceptual framework developed by Simpson (1951, 1961), Wiley (1978), and de Queiroz (2007).

Sampling

Between 2016 and 2019, specimens referable to the genus *Breviceps* were collected from three main localities within Angola (Fig. 1A; Table 1). Animals were euthanized via immersion in or injection of MS-222 (tricaine methanesulfonate) soon after capture (Conroy et al. 2009). Tissue samples (liver) were removed postmortem and preserved in 95% ethanol for genetic analysis. Specimens were formalin-fixed for 48 hours and then transferred to 70% ethanol for long-term storage in the herpetological collections of the Florida Museum of Natural History (FLMNH), the Museu de História Natural e da Ciência da Universidade do Porto, Portugal (MHNCUP), South African Institute for Aquatic Biodiversity (SAIAB), and the Port Elizabeth Museum, South Africa (PEM). Besides the newly collected material, historical specimens housed in the collections of the Museum of Comparative Zoology at Harvard University, USA (MCZ), Musée d'Histoire Naturelle de La Chaux-de-Fonds (MHNC), the Natural History Museum of London, United Kingdom (NHMUK) the Zoologische Staatssammlung München, Germany (ZSM), the Instituto de Investigação Científica Tropical, Portugal (IICT), and the Museu Regional do Dundo, Angola (MD) were also consulted (see Appendix I).

We amplified partial sequences of two mitochondrial (12S and 16S ribosomal rRNA genes) and two nuclear loci (recombination activating protein 1, RAG1; brain derived neurotrophic factor, *BDNF*) using the PCR primers and cycling conditions outlined in Nielsen et al. (2018). PCR success was evaluated via 1.5% agarose gel electrophoresis, then amplicons were sent to GeneWiz or the University of Michigan sequencing core for Sanger sequencing. We then assembled and quality trimmed raw sequences using Geneious v.8 (Biomatters; <http://www.geneious.com>). Sequences were submitted to GenBank (Table 1). Uncorrected mean pairwise sequence divergence (p) values were calculated for both 12S and 16S (Table 2) using MEGA v.6.0 (Tamura et al. 2013).

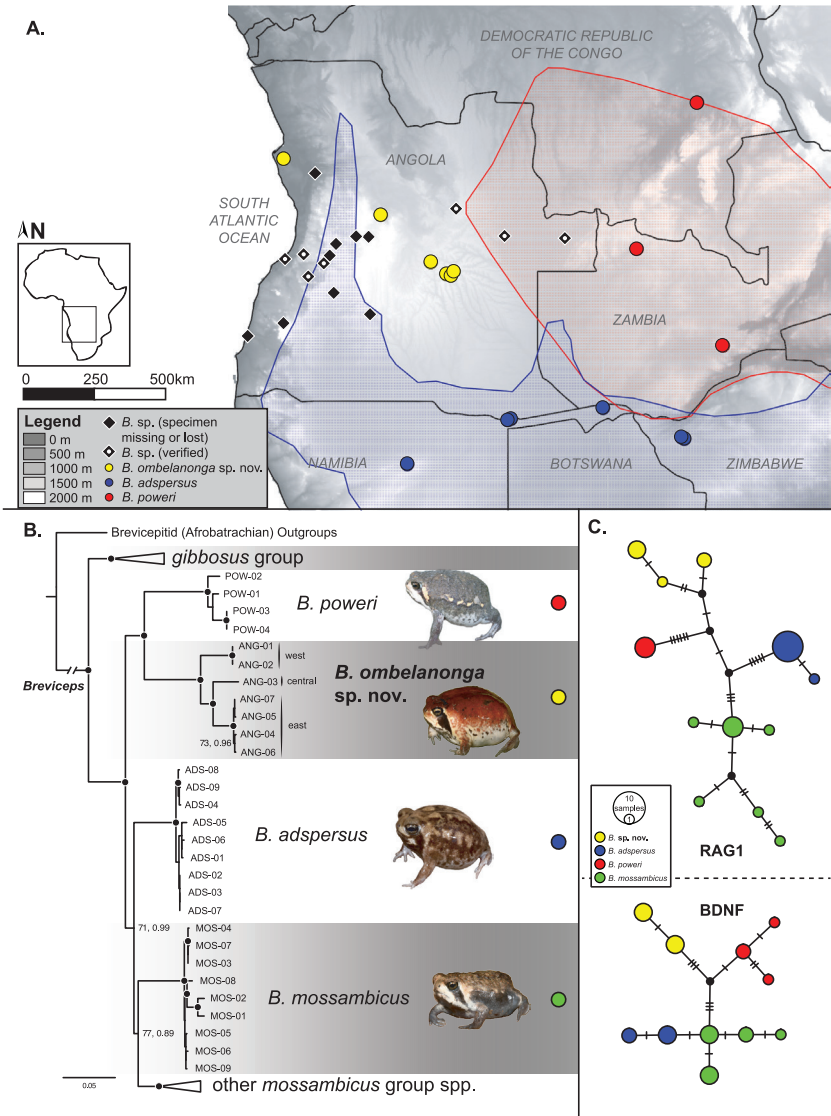


Figure 1. Geographic distribution and phylogenetic relationships of *Breviceps* spp. included in this study. **A** Map of Angola and surrounding countries with all known *Breviceps* spp. sampling localities indicated on legend. The proposed distributions of *B. adspersus* and *B. poweri* (blue and red polygons, respectively) are from IUCN (2013a, b), but should be considered tentative and worthy of reevaluation in light of recent studies. Furthermore, *B. mossambicus* is not mapped as no samples of certain identification occur west of Malawi (see Nielsen et al. 2018). **B** Multi-locus phylogeny of *Breviceps*, with select clades collapsed that are not relevant directly to the *B. mossambicus* group. The backbone is from the likelihood analysis, although Bayesian analyses produced a nearly identical topology (with any topological differences subtended by poor support). A black dot at each node indicates high support (e.g., Bayesian posterior probability > 0.95, Maximum Likelihood bootstrap > 90), while values below that cutoff are indicated for deep nodes only. Tapered bars to the right of voucher IDs indicate from which Angolan locality they were collected. **C** Median-joining networks for the two nuclear loci indicating a lack of shared haplotypes between candidate and recognized species. Hash marks indicate unique sequence differences between lineages, and black circles are hypothetical intermediate haplotypes.

Table 1. Sampling information including specimens/field IDs (Museum Abbreviations: MCZ, Museum of Comparative Zoology, Harvard University, USA; MH-NCUP, Natural History and Science Museum of the University of Porto, Portugal; MVZ, Museum of Vertebrate Zoology, University of California, Berkeley, USA; PEM, Port Elizabeth Museum, South Africa; SAIAB, South African Institute for Aquatic Biodiversity, South Africa), GPS coordinates, and GenBank accession details for the samples included in our analyses.

species	Tree ID	Specimen ID	Field ID	Latitude and Longitude	Country	Locality	RAG1	BDNF	12S	16S
<i>Breviceps ombelamanga</i> sp. nov.	ANG-01	UF Hep 187172	MCZ A-36476	-9.183833, 13.371472	ANG	Kawa Camp (1 km S of the Kwanza R.), Kissama NP, Luanda Prov.	MT944215	MT944224	MT944230	MT944241
	ANG-02	UF Hep 187173	MCZ A-36495	-9.183833, 13.371472	ANG	Kawa Camp (1 km S of the Kwanza R.), Kissama NP, Luanda Prov.	MT944216	MT944225	MT944231	MT944242
	ANG-03	MHNCUP_ANF 0320	AMB11736	-11.083845, 16.667410	ANG	Embala Seque (14 km N of Casumbi village), Bie Province	MT944217	MT944226	MT944232	MT944243
	ANG-04	PEM A12587	WC-3924	-12.689351, 18.360115	ANG	Cuito River source lake, Mexico Province	MT944218	MT944227	MT944233	MT944244
	ANG-05	PEM A12800	WC-4591	-13.089343, 18.894850	ANG	Cuanavale River source lake, Mexico Province	MT944219	MT944228	MT944234	MT944245
	ANG-06	PEM A12787	WC-4756	-13.135440, 19.043970	ANG	Queumbo River source lake, Mexico Province	MT944220	MT944229	MT944235	MT944246
	ANG-07	PEM A12770	WC-4827	-13.003340, 19.135640	ANG	Cuando River source, Mexico Province	–	–	MT944236	MT944247
<i>B. adpersus</i>	ADS-01	MCZ A-137796	AMB8318	-22.708056, 29.528333	RSA	Farm Celine, Limpopo	MT944221	–	MT944237	MT944248
	ADS-02	MCZ Hep A-148603	MCZ-FS-A27931	-18.670972, 26.953472	ZIM	Hwange	MT944222	–	MT944238	MT944249
	ADS-03	MCZ Hep A-148653	MCZ-FS-A28024	18.628793, 26.872087	ZIM	Miombo Safari Camp	MT944223	–	MT944239	MT944250
	ADS-04	MCZ Hep A-149504	MCZ-FS-A28774	-19.528500, 17.564167	NAM	Farm Ochange, Otjozondjupa	–	–	MT944240	MT944251
<i>B. mossambicus</i>	ADS-05	–	SVN 766	-23.731926, 27.579803	RSA	Ellisras	MH340062	MH340138	MH340291	MH340369
	ADS-06	–	SVN 768	-23.731926, 27.579803	RSA	Ellisras	MH340063	MH340139	MH340292	MH340370
	ADS-07	MCZ Hep A-148557	AMB7963	-17.623556, 24.199583	NAM	Katima Mulilo	MH340064	MH340140	MH340293	MH340371
	ADS-08	–	AMB7972	-18.000000, 21.070000	NAM	Caprivi	MH340065	MH340141	MH340294	MH340372
	ADS-09	MCZ Hep A-148563	AMB7980	-18.035500, 20.971528	NAM	Caprivi	MH340066	MH340142	MH340295	MH340373
	MOS-01	MVZ:Herp:265910	DMP 344	-15.463942, 36.977847	MOZ	Gurue	MH340075	MH340151	MH340304	MH340382
	MOS-02	MCZ Hep A-137055	MCZ-FS-A34284	-15.933333, 35.516667	MW	Mulanje	MH340076	MH340152	MH340305	MH340383
	MOS-03	SAIAB 88161.1	RB09-159	-15.030944, 40.740944	MOZ	Ila de Mozambique	MH340077	MH340153	MH340306	MH340384
	MOS-04	SAIAB 88161.2	RB09-179	-15.030944, 40.740944	MOZ	Ila de Mozambique	MH340078	MH340154	MH340307	MH340385
	MOS-05	SAIAB 88176.1	RB09-030	-12.963611, 40.529444	MOZ	Pemba	MH340079	MH340155	MH340308	MH340386
	MOS-06	SAIAB 88176.2	RB09-046	-12.963611, 40.529444	MOZ	Pemba	MH340080	MH340156	MH340309	MH340387
	MOS-07	SAIAB 88586	RB10-A097	-15.030722, 40.741222	MOZ	Nampula	MH340081	MH340157	MH340310	MH340388
	MOS-08	PEM A14008	NIMB 112	-13.308060, 35.244114	MOZ	Lichinga	MH340082	MH340158	MH340311	MH340389
	MOS-09	PEM A11021	Syran 12	-13.288667, 38.681528	MOZ	Balama	MH340083	MH340159	MH340312	MH340390
	POW-01	–	ELI 325	-7.277700, 27.389800	DRC	Manono	MH340084	MH340160	MH340313	MH340391
	POW-02	SAIAB 98182	JWH10-A114	-12.237778, 25.341944	ZAM	Katumbila	MH340085	MH340161	MH340314	MH340392
POW-03	SAIAB 98788.1	RB10-F003	-15.510278, 28.260528	ZAM	Lusaka	MH340086	MH340162	MH340315	MH340393	
POW-04	SAIAB 98788.1	RB10-F012	-15.510278, 28.260528	ZAM	Lusaka	MH340087	MH340163	MH340316	MH340394	

Phylogenetics

Datasets (concatenated and partitioned by locus/codon) of all samples were analyzed using maximum likelihood (RAxML v.8.2; Stamatakis 2014) and Bayesian (MrBayes v.3.2; Ronquist et al. 2012) methods via the CIPRES Science Gateway 3.1 for online phylogenetic analysis (Miller et al. 2010; <http://www.phylo.org/index.php/portal/>). Maximum likelihood analyses were performed using the default settings for RAxML using the GTRGAMMA model of sequence evolution (Stamatakis 2006) and ceasing bootstrapping when extended majority rule bootstrapping criteria had been reached. An appropriate partitioning strategy and molecular models for Bayesian analyses were chosen using PartitionFinder 2 (Lanfear et al. 2017), which assessed all possible candidate positions (e.g., each codon in the nuclear DNA) using the Bayesian information criterion. The resulting partition scheme is as follows: subset 1 (RAG1pos2, RAG1pos1) K80+G; subset 2 (RAG1pos3, BDNFpos3) K80+G; subset 3 (BDNFpos1, BDNFpos2) JC; and subset 4 (12S, 16S) GTR+I+G. Final Bayesian analyses ran for 100 million generations with four independent chains, and were sampled every 100,000 generations. We checked for stationarity using Tracer v.1.6 (Rambaut et al. 2018), after which a 25% burn-in was removed, leaving 750 trees for posterior analysis. For comparison with tree-based methods and in order to view gene tree (haplotype) relationships among the ingroup, median joining networks (MJN; Bandelt et al. 1999) for each nuDNA locus were constructed using PopART (<http://popart.otago.ac.nz>).

Morphology

Specimens were measured to the nearest 0.1 mm using digital calipers under a dissecting stereomicroscope for the following 24 morphological characters as defined by Watters et al. (2016): snout-vent length (SVL, from the tip of the snout to the vent), snout-urostyle length (SUL, from the tip of the snout to the posterior end of the urostyle), head length (HL, from the posterior of the jaws to the tip of the snout), snout length (ES, from the tip of the snout to the anterior corner of the eye), nostril-ocular distance (NOD, from anterior corner of the eye to the posterior margin of the nostril), eye diameter (ED, horizontally from the anterior to posterior corner of the eye), nostril-upper lip distance (NLD, medial margin of nostril to ventral margin of upper lip), eye-upper lip distance (ELD, lower margin of eye to margin of upper lip), internarial distance (IND, between the inner margins of the nostrils), mouth width (MW, between the corners of the mouth), head width (HW, at the widest point; i.e. angle at the jaws), forearm length (EF3, elbow to base of digit 3), length of manual digit I (F1L, from distal end of digit to proximal base of most proximal subarticular tubercle), length of manual digit II (F2L, to proximal subarticular tubercle), length of manual digit III (F3L, to proximal subarticular tubercle), length of manual digit IV (F4L, to proximal subarticular tubercle), thigh length (THL, from vent to knee), crus length (CL, distance from the outer surface of the flexed knee to the heel/tibio-tarsal inflection), length of pedal digit I (T1L, to distal margin of metatarsal tubercle),

length of pedal digit III (T3L, to proximal subarticular tubercle), length of pedal digit IV (T4L, to proximal subarticular tubercle), foot length (FL, from the base of the inner metatarsal tubercle to the tip of pedal digit IV), length of pedal digit V (T5L, to distal margin of metatarsal tubercle), outer metatarsal tubercle length (OMTL), and inner metatarsal tubercle length (IMTL) when separate from OMTL. All measurements were taken on the right side of the body for consistency. A subset of ten measurements (HL, HW, ED, ES, IOD, IND, THL, CL, FL, and F3L) was taken from specimens of *B. adspersus* (n = 24), *B. mossambicus* (n = 9), *B. poweri* (n = 8), and the putative new Angolan species (n = 6) and checked for normality using a Shapiro-Wilks test (see Appendix 1, Suppl. material 1: Table S1). In order to avoid potential species misidentifications, specimens used in the comparative morphological analyses were derived from localities within the core geographic range of each species, as supported by the phylogenetic results of Nielsen et al. 2018. All were examined to confirm the presence of traits diagnostic for *B. adspersus*, *B. mossambicus*, or *B. poweri*, respectively. All measurements were corrected for body size via a generalized least squares linear regression on SVL using the *gls* function in R {nlme}. The residuals were then analyzed using the *prcom* (Principal Components Analysis; PCA) function in R {stats}. The components accounting for 75% of the cumulative variance were retrieved from the analysis. The relationship in morphospace between the putative new species and closely related *Breviceps* species was evaluated by plotting principal component (PC) scores.

Advertisement calls

Advertisement calls were recorded in the field using an Samsung Galaxy Note 3 cell-phone at a sampling rate of 44100 kHz, and analyzed using Sound Ruler Acoustic Analysis v.0.9.6.0 using default settings (Gridi-Papp 2007) and graphical presentations of calls were produced with the R package *seewave* (Sueur et al. 2008). Only a single male call was recorded from the Cuanavale River source lake (PEM A12800) on 24 October 2016. The call was compared to that of *B. mossambicus* and *B. poweri* from Ribaué, Mozambique, and to other published call data (Minter 1997, 2003). We further compared our call to that of *B. adspersus* provided by Du Preez and Carruthers (2017). The small number of calls did not allow for statistical analysis but the following standard measurements were taken: call duration, call interval, number of pulses per call, and dominant frequency in kilohertz (kHz).

Nomenclatural acts

The electronic edition of this article conforms to the requirements of the amended International Code of Zoological Nomenclature (ICZN), and hence the new names contained herein are available under that Code from the electronic edition of this article. This published work and the nomenclatural acts it contains have been registered in ZooBank, the online registration system for the ICZN. The ZooBank LSIDs (Life Science Identifiers) can be resolved and the associated information viewed through any standard web browser by appending the LSID to the prefix “<http://zoobank.org/>”.

Table 2. Uncorrected mean pairwise 12S and 16S mitochondrial sequence differences between ingroup *Breviceps* sequence pairs (above/below the diagonal, respectively) and within species (along the diagonal) conducted in MEGA.

16S/12S		12S			
	<i>B. ombelanonga</i> sp. nov.	<i>B. adspersus</i>	<i>B. poweri</i>	<i>B. mossambicus</i>	
	<i>B. ombelanonga</i> sp. nov.	0.04/0.03	0.09	0.09	0.11
16S	<i>B. adspersus</i>	0.11	0.01/0.01	0.09	0.08
	<i>B. poweri</i>	0.12	0.11	0.02/0.02	0.09
	<i>B. mossambicus</i>	0.12	0.08	0.10	0.01/0.01

The LSID for this publication is: <http://zoobank.org/References/2043280A-1591-4D51-ACE3-F9015F170890>. The electronic edition of this work was published in a journal with an ISSN, and has been archived and is available from the following digital repositories: PubMed Central, LOCKSS.

Results

Phylogenetics

Our concatenated, multi-locus dataset was 1,852 bp long, of which 390 characters were parsimony informative. Phylogenetic analyses resulted in a well-supported species-level phylogeny and high support that *Breviceps* is monophyletic (bootstrap [bs] 100, posterior probability [pp] 1.0; Fig. 1B). All Angolan samples were recovered as monophyletic with high support (bs 100, pp 1.0), sister to *B. poweri* (bs 86, pp 1.0), and thus embedded within the *B. mossambicus* group (bs 99, pp 1.0). We also failed to recover any nuclear haplotype sharing among taxa (Fig. 1C). We recovered high genetic divergence (≥ 9 –11% 12S/16S uncorrected *p*-distances; Table 2) between the Angolan material and the three most closely related (and potentially sympatric and/or morphologically similar) taxa, *B. adspersus*, *B. mossambicus*, and *B. poweri*, as well as substantial intraspecific diversity (3–4% 12S+16S uncorrected *p*-distances). The values are comparable with, or exceed other species level differences within recognized species of *Breviceps* (see Nielsen et al. 2018).

Morphology

Mensural and meristic data are presented in Table 3. The first four principal components account for 78.9% of the variation in the data (Table 4). The first principal component loads strongly on the measurements of head shape and limb length, including strong negative loadings on head length and snout length, and positive loadings for crus length, but does not differentiate the putative new species from Angola from its close relatives (Fig. 2). The second principal component axis loads strongly and positively on measurements of head width, thigh length, the lengths of the third manual digit and foot, and distinguishes the new species from other species due to its more narrow head, shorter thigh, and shorter third manual digit and foot. The third

Table 3. Measurements (mm) of type series.

	UF Herp 187172	UF Herp 187173	MHNCUP_ ANF 0320	PEM A12800	PEM A12537	PEM A12787	PEM A12770	SAIAB 204537	Average	SD
SVL	30.5	27.5	24.6	25.4	18.3	26.6	30.1	26.5	26.2	3.80
SUL	26.3	24.9	–	23	17.6	23.2	29	25.2	24.2	3.53
HL	7.2	7.3	7.3	10.8	6.4	9.6	12.7	9.3	8.8	2.17
ES	3.2	2.8	2.9	3.1	2.2	2.7	3.3	2.5	2.8	0.37
NOD	2.0	1.7	1.6	2.1	2.5	1.7	2.2	2.1	2.0	0.30
ED	2.7	2.8	3.2	3.4	1.3	3.1	3.6	2.8	2.9	0.70
NLD	1.7	1.7	1.3	1.4	1	1.2	1.8	1.3	1.4	0.28
ELD	1.7	1.3	1.7	1.8	1.4	2.1	2.3	1.9	1.8	0.33
IND	1.9	1.9	2	1.6	1.4	1.8	2.2	2	1.9	0.25
MW	7.2	6.8	5.1	6.9	4.7	6.3	7.9	7	6.5	1.08
EAD	9.1	9.3	4.1	4.5	3.6	4.3	5.3	–	5.7	2.42
F1L	1.7	1.5	1.5	2.7	1.7	2.7	2.5	2.8	2.1	0.59
F2L	1.9	1.9	1.7	3.6	1.8	3.2	2.6	2.7	2.4	0.71
F3L	2.9	3.0	2.2	3.9	2.6	3.9	3.6	3.7	3.2	0.64
F4L	1.2	1.3	1.2	1.8	0.9	2	1.5	1.4	1.4	0.35
T1L	1.0	1.1	1	1.4	0.6	1.5	1.6	1.2	1.2	0.32
T3L	1.8	1.9	2.9	2.4	2	2.7	1.5	2.7	2.2	0.51
T4L	4.4	4.2	4.6	4.1	3.2	5	4.9	4.6	4.4	0.57
FT	10.9	10.4	8	8.9	6	10.3	10.5	9.7	9.3	1.65
T5L	4.0	5.0	0.8	4	3.2	4.9	5.3	4.7	4.0	1.46
MTL	1.0	1.0	1.2	2.3	1.7	2.3	–	–	1.6	0.61
IMTL	3.0	2.9	3	3.2	2.3	3.4	3.6	3.7	3.1	0.45
TIB	8.5	8.3	–	6.4	4.8	7.4	8.8	8.1	7.5	1.43

Table 4. Principal components analysis (PCA) loadings based on 10 size corrected morphological characters (head length, HL; head width, HW; eye diameter, ED; snout length, ES; interorbital distance, IOD; internarial distance, IND; thigh length, THL; crus length, CL; foot length, FL; and length of manual digit III, F3L).

	PC1	PC2	PC3	PC4	SShapiro-Wilks test
Proportion of Variance	29.92	26.57	13.70	8.67	
Cumulative Proportion	29.92	56.49	70.19	78.86	
Loadings					
Head Length (HL)	-0.3025245	0.35446298	-0.3789378	0.02808779	W = 0.943, p = 0.083
Head Width (HW)	0.33281314	0.38971121	0.08705045	0.33211061	W = 0.956, p = 0.205
Eye diameter (ED)	-0.2210569	0.22060777	-0.6170786	-0.1165699	W = 0.963, p = 0.312
Snout length (ES)	-0.4530121	-0.0316756	0.28394189	-0.1665634	W = 0.973, p = 0.567
Interorbital distance (IOD)	-0.3043034	0.24152256	0.52046607	0.21274977	W = 0.959, p = 0.240
Internarial distance (IND)	-0.4018886	0.1543163	0.09759718	0.52889612	W = 0.965, p = 0.360
Thigh length (THL)	0.2280386	0.3347664	0.24257868	-0.4343642	W = 0.965, p = 0.360
Crus length (CL)	0.45829394	0.12745601	0.05499745	0.20448849	W = 0.975, p = 0.636
Pes length (FT)	-0.1152479	0.43230304	0.17838021	-0.5130485	W = 0.900, p = 0.005
Manual digit III length (F3L)	0.11914774	0.52484652	-0.115415	0.16994577	W = 0.989, p = 0.978

principal component has a strong negative loading on the diameter of the eye and a strong positive loading on distance between orbits, but the new species is not distinguished from other species on this axis.

Advertisement calls

The advertisement call of the eastern population is pulsed, has a call duration of 0.175 ± 0.083 s, with relatively long intervals between consecutive calls (0.996 ± 0.133 s), a high number of pulses per call (28–34; Table 4, Fig. 3), and a dominant call frequency of 2156 Hz. It most resembles the whistle-like call of *B. adspersus* (call

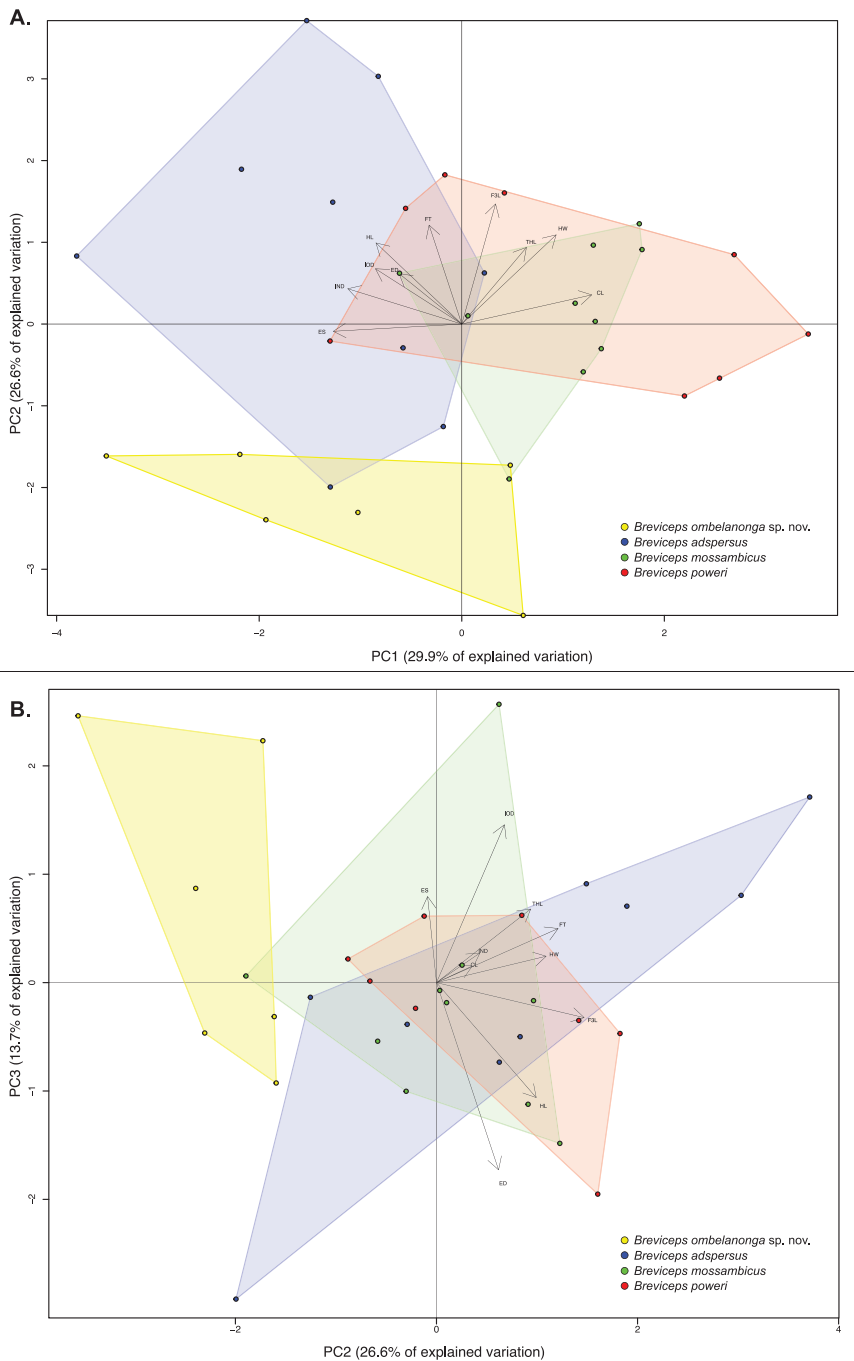


Figure 2. PCA plots of ten size-corrected morphological characters from specimens of *B. adspersus* ($n = 24$), *B. mossambicus* ($n = 9$), *B. poweri* ($n = 8$), and the putative new Angolan species ($n = 6$) (Suppl. material 1: Table S1), illustrating the PC1 and PC2 (**A**) and PC2 and PC3 (**B**) axes of variation, which combined represent ~ 70% of the total variation (Table 4).

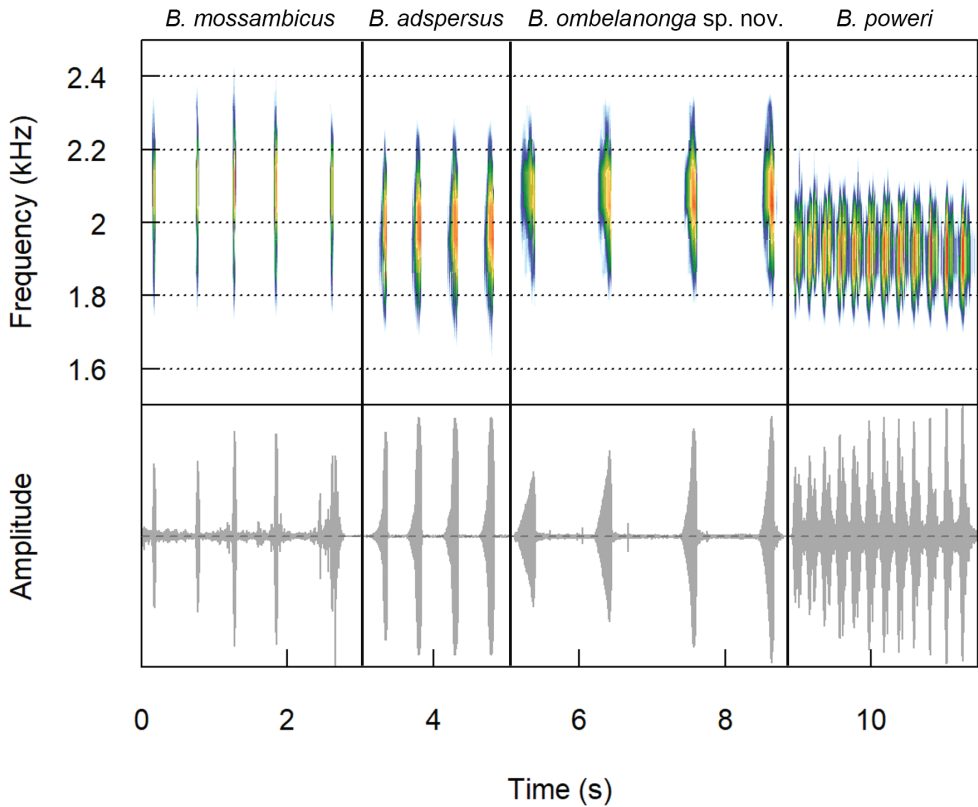


Figure 3. Spectrograms and oscillograms showing a series of notes of the putatively novel Angolan *Breviceps* taxon compared to three closely related congeners.

duration: 0.196 ± 0.047 s; interval between consecutive calls: 0.745 ± 0.636 s; pulses per call: 14–31), yet differs from the ‘chirp’-like call of *B. mossambicus* (call duration: 0.500 ± 0.070 s; interval between consecutive calls: 0.710 ± 0.168 s; pulses per call: 7–31) and the tonal, rapid call of *B. poweri* (pulses per call: 7–31; dominant call frequency: 1557–1903 Hz). Because ambient temperature was not documented when the call was recorded, these results carry some uncertainty.

Systematics

Our phylogenetic analyses indicate that sampled individuals from Angola form a clade that is genealogically exclusive from other described species of *Breviceps* (Fig. 1). These populations are morphologically diagnosable from other closely related taxa, specifically possessing distinct coloration and pattern that differ from the sister taxon, *B. poweri*. A PCA of mensural and meristic data indicates that the Angolan individuals fall within a unique region of morphospace, with a relatively narrower head, shorter thigh, and shorter manual digit III in comparison to closely related species. Lastly, there are

distinct acoustic differences associated with the male nuptial call. Thus, we here describe these populations as a new species.

***Breviceps ombelanonga* sp. nov.**

<http://zoobank.org/E3815018-4176-4073-92B8-E65274D354FB>

Figs 4–7

Suggested common names: Angolan Rain Frog (English), Sapinho das Chuvas de Angola (Português).

Chresonymy.¹

Breviceps gibbosus: Bocage (1870: 68).

Breviceps gibbosus: Bocage (1873: 227).

Breviceps mossambicus: Bocage (1895: 182); Parker (1934: 194); Monard (1937: 29, 1938: 56); Laurent (1964: 156); Cei (1977: 17, 18); Ruas (1996: 23).

Rana mossambicus: Hellmich (1957: 30).

Breviceps “*mossambicus-adspersus*” complex: Poynton (1982: 67); Ruas (2002: 142).

Breviceps adspersus [part]: Poynton and Broadley (1985: 52).

Breviceps sp.: Marques et al. (2018: 81); Ceriáco et al. (2020: 63).

Breviceps cf. *adspersus*: Baptista et al. (2019: 270).

Material examined. Holotype. UF Herp 187172 (field number MCZ A-36476), an adult male, Kawa Camp Headquarters, 1 km south of the Kwanza River, Kissama National Park (-9.183068, 13.369314, WGS-84, elevation 151 m above sea level), Luanda Province, Angola, collected by LMPC, Mariana P. Marques, Philip Pastor, and John Cavagnaro on 2 June 2016 at approx. 22:00. **Paratypes** (5 males, 1 female, 1 sex unknown) UF Herp 187173 (field number MCZ A-36495), an adult male, Kawa Camp Headquarters, 1 km south of the Kwanza River, Kissama National Park (-9.183068, 13.369314, WGS-84, elevation 151 m above sea level), Luanda Province, Angola, collected by LMPC, Mariana P. Marques, Philip Pastor, and John Cavagnaro on 8 June 2016; MHNCUP/ANF 320 (field number AMB 11736), sub-adult (sex unknown), Embala Seque, 14 km N of Cassumbi village (-11.083845, 16.66741), Bié Province, Angola, collected by LMPC, Mariana P. Marques, and Adam Ferguson on 16 June 2019; PEM A12800 (field number WC-4591), adult male, Cuanavale River source lake (-13.089343, 18.89485, 1396 m above sea level), Moxico Province, Angola, collected by Werner Conradie and Luke Verburgt on 24 October 2016; PEM A12537 (field number WC-3924), juvenile male, Cuito River source lake (-12.68935, 18.36012, 1435 m above sea level), Moxico Province, Angola, collected by Werner Conradie and Ninda Baptista on 18 February 2016 October; PEM A12787 (field

¹ We here provide only the usages that have been applied to Angolan populations, albeit with some inherent uncertainty given the pervasive morphological similarity among members of the *B. mossambicus* group.



Figure 4. *Breviceps ombelanonga* sp. nov. holotype male (UF Herp 187172): **A** in life photo **B** dorsal and ventral aspects **C** additional views of the holotype, including the left pes, frontal, right lateral, and left manus and mental. Scale bar: 10 mm. Photographs by J. Cavagnaro (**A**) and SVN (**B, C**).

number WC-4756), adult male, Quembo River source lake (-13.13544, 19.04397, 1375 m above sea level), Moxico Province, Angola collected by Werner Conradie on 11 November 2016; PEM A12770 (field number WC-4827), adult female, Cuando River source (-13.00334, 19.13564, 1364 m above sea level), Moxico Province, Angola, collected by Werner Conradie and James Harvey on 22 November 2016; SAIAB 204537 (field number Ang16-RB12), adult male, Quembo River source lake (-13.13583, 19.04528), Moxico Province, Angola, collected by Roger Bills on 9 November 2016.

Diagnosis. A species referable to *Breviceps* due to the following characteristics (Poynton 1964; Minter et al. 2017): snout extremely abbreviated; mouth narrow and downturned near jaw joint; short limbs which, at rest in life, are held close to the body, not projecting beyond the body outline; digits I and V short or rudimentary; inner metatarsal tubercle well developed and notably longer than pedal digit III, narrowly separated from a prominent conical outer metatarsal tubercle. Additionally, the results of the molecular phylogenetic analyses support this species as embedded within the diversity of *Breviceps*, specifically within the *B. mossambicus* group (Fig. 1B). *Breviceps ombelanonga* can be diagnosed from other species of *Breviceps* and especially those in the *B. mossambicus* group by the combination of lacking a visible tympanum, males having a single, uniformly dark gular patch that is continuous with the mask extending from the eye, having generally smooth dorsal skin, lacking many small tubercles on the palmar surfaces (as in, e.g., *B. branchi* and *B. sylvestris*; FitzSimons 1930; Channing 2012), lacking pale spots along flanks and a pale patch above the vent (both present in *B. poweri*; Parker 1934; du Preez and Carruthers 2017), lacking short dark band below nares (as in *B. poweri*; du Preez and Carruthers 2017), lacking confluent inner and outer metatarsal tubercles, having a relatively narrower head, shorter thigh, and shorter manual digit III (Fig. 2; Table 4), and having an advertisement call with both a longer interval between consecutive calls and a higher average dominant frequency (Fig. 3).

The new species can be distinguished from other species of *Breviceps* occurring in the region by the following: pale paravertebral and dorsolateral patches are lacking, although a fine dorsolateral band may be present (versus no pale paravertebral or dorsolateral spots or patches in *B. mossambicus*; series of both paravertebral and dorsolateral pale spots and patches present in *B. adspersus*, a series of pale dorsolateral spots or patches present in *B. poweri*); no conspicuous light patch above vent (present in *B. poweri*); manual digit IV reaching approximately midway between the proximal and distal subarticular tubercles of manual digit III (versus nearly reaching distal subarticular tubercle of manual digit III in *B. mossambicus*; not reaching or barely passing the proximal subarticular tubercle of the manual digit III in *B. poweri*; similar to *B. adspersus* in usually not reaching the distal subarticular of manual digit III); gular region with a single uniformly dark patch (versus a pair of marbled to freckled patches in *B. adspersus*).

The advertisement call of the new species (Table 5, Fig. 3) can be differentiated from other potential Angolan congeners by its duration (0.175 ± 0.083 s; shorter than in *B. adspersus* 0.196 ± 0.047 s and *B. mossambicus*, 0.500 ± 0.070 s, and longer than in *B. poweri*, 0.140 ± 0.012 s), longer interval between consecutive calls (0.996 ± 0.133 s; *B. adspersus*, 0.745 ± 0.636 s; *B. mossambicus*, 0.710 ± 0.168 s; *B. poweri*, 0.743 ± 0.166 s), and a higher dominant frequency (2156 Hz; *B. adspersus*,

Table 5. Comparison of the main variables for the advertisement calls of *Breviceps ombelanonga* sp. nov., *Breviceps mossambicus*, *Breviceps adpersus* and *Breviceps poweri*. Comparative data taken from Minter (1997, 2003).

	<i>B. ombelanonga</i> sp. nov.		<i>B. adpersus</i>		<i>B. mossambicus</i>		<i>B. poweri</i>	
	avg \pm sd	range	avg \pm sd	range	avg \pm sd	range	avg \pm sd	range
Call duration (s)	0.175 \pm 0.083	0.064–0.342	0.196 \pm 0.047	0.077–0.293	0.500 \pm 0.070	0.036–0.079	0.140 \pm 0.012	0.111–0.160
Call interval (s)	0.996 \pm 0.133	0.742–1.190	0.745 \pm 0.636	0.363–0.745*	0.710 \pm 0.168	0.396–1.17	0.743 \pm 0.166	0.500–1.100
No. of pulses/call	30 \pm 2.6	28–34	23 \pm 3.3	14–31	9 \pm 1.2	7–13	30 \pm 16.3	10–74
Dominant frequency (Hz)	2156	na	1742 \pm 100	1482–2179	1835 \pm 107	1600–2193	1728 \pm 83	1557–1903

1742 \pm 100 Hz; *B. mossambicus*, 1835 \pm 107 Hz; *B. poweri*, 1728 \pm 83 Hz). The number of pulses per call (28–34) are similar to *B. adpersus* (14–31), *B. mossambicus* (7–31), and *B. poweri* (10–74).

Description of the holotype. Adult male (SUL 30.5 mm), with globular body and well-developed short limbs with medialmost and lateralmost digits reduced (Fig. 4; Table 3); snout abbreviated, protruding and angular in lateral profile, blunt and rectangular in dorsal view; eyes projecting beyond profile of head in both dorsal and ventral views; pupils horizontally elliptical; nares small oval slits, directed horizontally and visible in dorsal and lateral views; mouth narrow and directed ventrally near jaw joint; choana largely obscured by maxillae in ventral view; well-developed gland at midline of palate between choana; tongue ovoid and filling floor of mouth, and lacking median papilla; single medial bony point on lower jaw at symphysis; tympana not distinguishable; teeth absent on premaxilla, maxilla, and vomer.

Skin of dorsum and head smooth, and weakly glandular with irregular folds; skin of ventrum smooth; skin folds overlying vent creating triangular shape.

Limbs short with digits I and V short or rudimentary; webbing absent on manus and pes; nuptial pads absent and adhesive glands not discernable; relative manual digit lengths when addressed: III>II>I>IV; only tip of first pedal digit extending beyond fleshy webbing and sole; fourth (outer) manual digit reaches midway between the large tubercle at metacarpophalangeal joint and subarticular tubercle at most proximal interphalangeal joint; finger tips conical, not expanded; several small globular palmar tubercles; single subarticular tubercles present on pedal digits II, III, and IV; pedal digit V very short, falling short of most proximal subarticular tubercle of pedal digit IV; well-developed (though not keratinized) inner metatarsal tubercle visibly longer than pedal digit III, separated from conical outer metatarsal tubercle by deep cleft.

Coloration. In life, dorsum of body mottled dark brown on pale tan base, transitioning to golden yellow on the lateral aspects, before stark transition to solid dark brown flanks with a dark boundary becoming paler ventrally (Fig. 4); limbs dark grayish brown dorsally; plantar and palmar surfaces pale grayish brown; subarticular, palmar, and inner and outer metatarsal tubercles pale gray; posterior dorsum dark gray-brown with scattered pale gray spots; bold facial mask composed of broad dark brown stripe running obliquely downwards, from margin of lower eyelid towards base of arm (but not attaining it) and joining dorsolateral aspect of gular patch, giving appearance

of a large dark bib; region below nares generally same coloration as dorsal and lateral rostrum, and not more darkly pigmented; lower eyelid with white opaque patch at anterior margin; margins of mouth and lateral angle of mouth off-white to cream; gular patch uniformly dark anteriorly, becoming mottled posteriorly and merging with ventral coloration; pectoral region and ventrum creamy pale gray with scattered punctate gray dots sometimes coalescing into larger spots in the gular region and laterally; iris bright orange, scattered with dark brown flecks (dark brown in preservative), with black pupil (pale gray in preservative; no mid-vertebral line; faint pale line extending across posterior hindlimbs extending between heels.

In preservative, coloration is largely similar but more muted and overall darker (Fig. 4).

Measurements. Measurements of the type series are shown in Table 3.

Variations. All specimens resemble the holotype in the absence of a visible tympanum, and skin that is densely granular dorsally and laterally and smooth ventrally (Figs 5–6). The distal tip of manual digit IV reaches well past the proximal subarticular tubercle of manual digit III in all specimens. PEM A12770 have both manual digit II and III proximal subarticular tubercles divided. Inner and outer metatarsal tubercles not separated by a deep cleft in paratypes PEM A12800, PEM A12537, PEM A12787, PEM A12770 and SAIAB 204537.

Color and pattern in UF Herp 187173 is very similar to the holotype. Dorsum gray with scattered black spots (MHNCUP/ANF 320); red with scattered black blotches in two specimens (PEM A12537 and PEM A12770), dark brown to black with red spots and markings (PEM A12787 and PEM A12800), light brown with red spots and darker black blotches (SAIAB 204537). Interocular bar visible in all paratypes, except PEM A12537, PEM A12770 and SAIAB 204537. Light dorsolateral patches present in PEM A12878, absent in PEM A12770, dark black band present in PEM A12537. Mid-vertebral line present in most paratypes, but very faint in PEM A12537 and PEM A12770, and absent in SAIAB 204537 and MHNCUP/ANF 320. Heel-to-heel line present in all specimens, but faint in UF Herp 187173, PEM A12537, and PEM A12770. A broad, black stripe runs obliquely downwards from margin of lower eyelid towards base of arm, not reaching the shoulder in all specimens. Dark orbital band partly reaching the gular patch in all specimens, falling short in PEM A12770 (female). Anterior to the orbital bar, a broad white stripe runs down to angle of mouth and onto upper and lower lips in all individuals. Gular patch uniform dark brown to black in all paratypes, except PEM A12537 in which it is dark brown with scattered darker blotches. Pectoral region white, with scattered spots in all specimens. Ventrums white with scattered darker spots in all paratypes.

Advertisement call. The following call description is based on a recording of a paratype male (PEM A12800) from the source lake of the Cuanavale River recorded on 24 October 2016 at 8:50 in the morning. Ambient temperature was not recorded. Frogs began calling during the daytime following heavy rains, and stopped after sunset. Call sites were among leaf litter in dense miombo woodland. The call can be described as a short whistle with a call duration of 0.064–0.342 seconds and call interval of

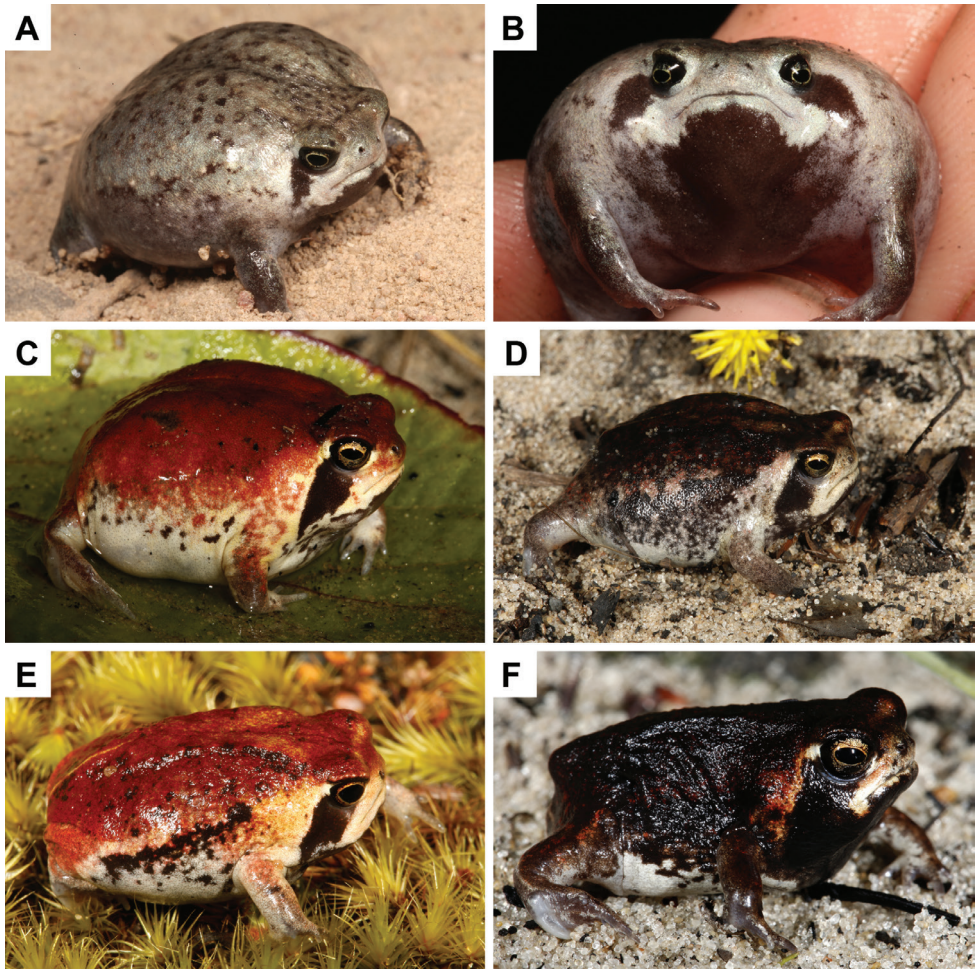


Figure 5. Variation in color and pattern within living paratypes of *B. ombelanonga* sp. nov.: **A, B** sub-adult (of unknown sex) from Embala Seque (14 km N of Cassumbi village), Bié Province (MHNCUP_ANF 0320) **C** juvenile male, Cuito River source lake, Moxico Province (PEM A12537) **D** adult female, Cuando River source, Moxico Province (PEM A12770) **E** adult male, Quembo River source lake, Moxico Province (PEM A12787) **F** adult male, Cuanavale River source lake, Moxico Province (PEM A12800). Photographs by LMPC (**A, B**) and WC (**C–F**).

0.742–1.190 seconds. Each call consists of about 28–34 pulses and a dominant frequency of 2156 Hz (Table 4, Fig. 2). The small number of calls from a geographically restricted sample does not allow for further statistical analysis.

Distribution. Based on our phylogenetic analysis, this species is currently confirmed from three widely separated localities and elevations ranging from near sea level to > 1400 m: i) Kissama National Park, on the outskirts of Angola’s capital city, Luanda, in coastal western Angola (Luanda Province); ii) central Angola (Bié Province); and iii) the source of the Cuanavale, Cuito, Cuando and Quembo rivers (Moxico Prov-

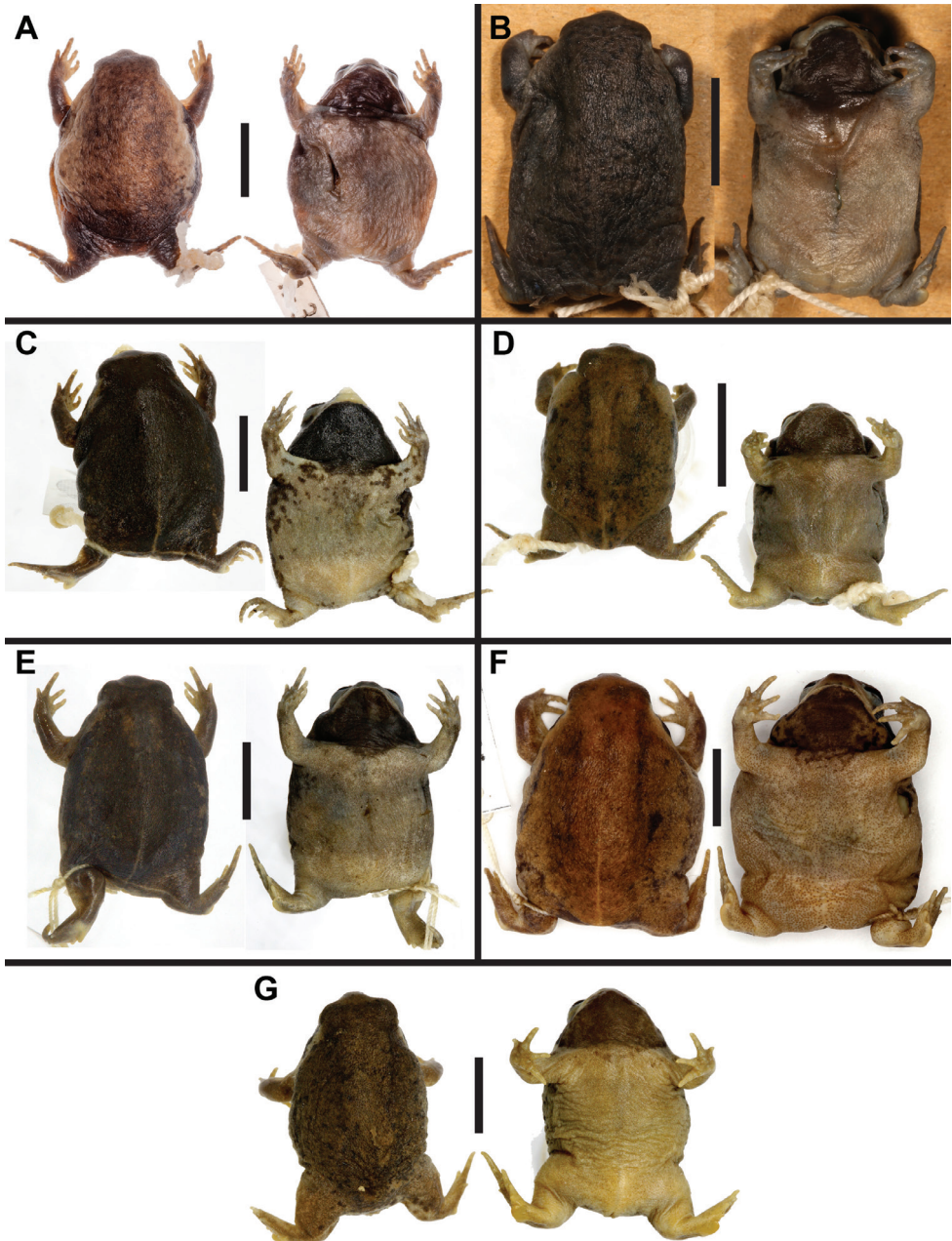


Figure 6. Variation in color and pattern within preserved paratypes of *B. ombelanonga* sp. nov.: **A** an adult male from Kawa Camp Headquarters, Luanda Province (UF Herp 187173) **B** sub-adult (of unknown sex) from Embala Seque, Bié Province (MHNCUPANF 320) **C** adult male from Cuanavale River source lake, Moxico Province (PEM A12800) **D** juvenile male from Cuito River source lake, Moxico Province (PEM A12537) **E** adult male from Quembo River source lake, Moxico Province (PEM A12787) **F** adult female from Cuando River source, Moxico Province (PEM A12770); and **G** adult male from Quembo River source lake, Moxico Province (SAIAB 204537). Photographs by SVN (**A**), LMPC (**B**), and WC (**C-G**).

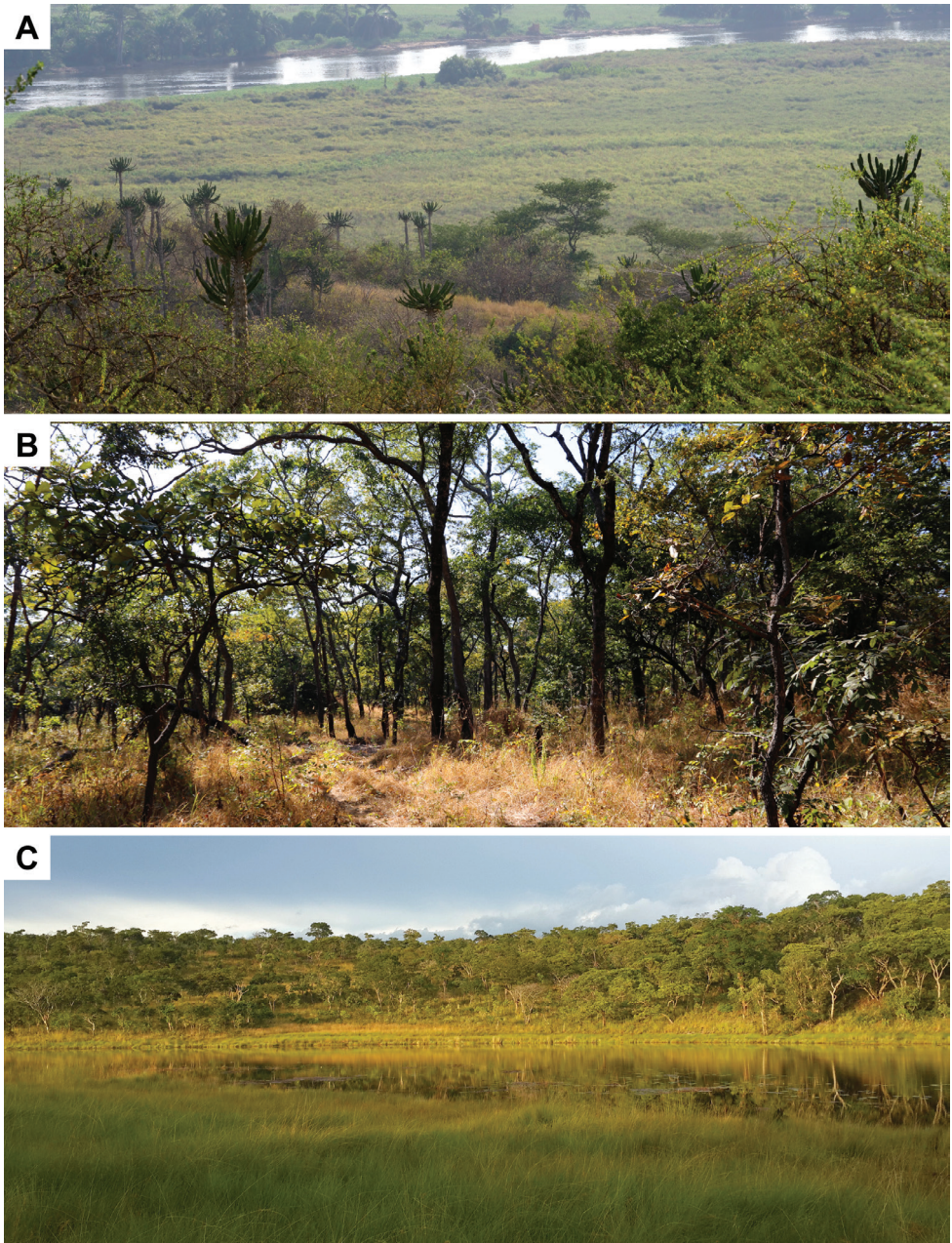


Figure 7. Photos of typical habitat of *B. ombelanonga* sp. nov.: **A** a view of the Kwanza River and bordering savannah, near the type locality, in Kissama National Park, Luanda Province **B** savannah near Embala Seque (14 km N of Cassumbi village), Bié Province **C** Cuanavale River source lake and associated miombo savannah woodland. Photographs by LMPC (**A, B**) and WC (**C**).

ince). The identity of other known Angolan localities for *Breviceps* (black diamonds) remain uncertain without additional sampling and genetic data (Fig. 1, Appendix 1; see Marques et al. 2018).

Genetic divergence. *Breviceps ombelanonga* differs from other species within the *B. mossambicus* group by net uncorrected mitochondrial *p*-distances of at least 9% (12S) and 11% (16S; Table 2), as well as unique nuclear haplotypes for both RAG1 and BDNF (Fig. 1B).

Habitat and natural history notes. The preferred habitat for *B. ombelanonga* ranges from typical western Angolan savannah, with sandy soils and vegetation dominated by *Adansonia digitata*, *Euphorbia conspicua*, *Acacia welwitschii* and *Combretum* sp., together with a good grass coverage (Grandvaux-Barbosa 1970), to dense Angolan wet miombo woodland in the east (Fig. 7). The type series was collected after gentle rains, either by hand or in traps. The holotype was first observed feeding on small, unidentified ants (family Formicidae). No information is available on egg deposit sites and clutch sizes. One of us (WC) has discovered remains of *B. ombelanonga* in the stomach contents of two snake species, *Kladiostratus acutus* (Psammophiidae; PEM R23450) and *Causus bilineatus* (Viperidae; PEM R23321) from the Cuando and Cuito River sources, respectively.

Etymology. The name *ombelanonga* is a derived combination of two words in Umbundu, a native Angolan language, for rain (*ombela*) and frog (*anonga*). The species epithet is used as an invariable noun in apposition to the generic name.

Conservation status. Given that it appears widely distributed, we suggest that *B. ombelanonga* be included in the IUCN category of Least Concern. The type locality lies within Kissama National Park, which grants some legal protection from major habitat degradation and loss, though the park has recently experienced significant wildfires. Additionally, the paratype localities in southeastern Angola (visited during field activities related to the National Geographic Okavango Wilderness Project 2017) are relatively pristine and ecologically intact miombo savannah that comprise an area recently proposed for formal protection.

Discussion

Breviceps ombelanonga sp. nov. represents a phylogenetically distinct evolutionary lineage that is an Angolan endemic apparently geographically isolated from its closest congeners (Fig. 1). It forms a clade with morphologically similar members of the *B. mossambicus* group but can be differentiated from its sister taxon, *B. poweri*, phylogenetically, morphologically, and acoustically (Figs 1–3). Unlike *B. poweri*, *B. ombelanonga* lacks pale spots along the flanks, a pale patch above the vent, and a short, dark band below the nares (Fig. 4). We also recovered high intraspecific genetic diversity among populations of *B. ombelanonga*, which for the most part exceeds the reported interspecific distances for some recently described *Breviceps* species (Minter 2003; Minter et al. 2017; see Nielsen et al. 2018). Given the limited morphological variation within the novel taxon (and the *B. mossambicus* group more broadly), we elected to conservatively consider these three disjunct populations as one taxon.

Further work is required to confirm the distributional range of *B. ombelanonga*, as well as whether it overlaps in distribution with either its sister taxon, *B. poweri*, or the

more distantly related *B. adspersus*. Both occur in neighboring countries, *B. poweri* to the east/northeast (Zambia, Democratic Republic of Congo) and the *B. adspersus* to the south/southeast (Namibia, Botswana), and both have been suggested to occur in Angola (Ruas 2002; Marques et al. 2018; Baptista et al. 2019; Channing and Rödel 2019; Fig. 1A). Due to the amount of morphological similarity found among most members of the *B. mossambicus* group, identifying museum specimens to species is difficult without having genetic data with which to assign populations. Therefore, we have elected to leave the historical specimens from Angola as unassigned (see Appendix 1). Revisiting historical collection localities, or in some cases attempting to acquire ‘historical’ DNA sequence data from museum specimens, carries high priority and should help to illuminate the composition and distribution of Angola’s resident *Breviceps* species.

We are not the first to recognize the lack of morphological variation within members of this anuran clade, which has led to historical taxonomic confusion and invoking hybridization for specimens that failed to conform to often scant descriptions of the type specimens (Poynton 1964, 1982; Poynton and Broadley 1985; Minter et al. 2017). The only comprehensive molecular phylogenetic study to date failed to find support for hybridization (Nielsen et al. 2018). Furthermore, many recent studies have shown that species discovery is still ongoing within this group (Minter et al. 2017), and that species thought to be widespread are often species-complexes composed of taxa with much narrower geographic ranges (Nielsen et al. 2018). Future, fine-scale fieldwork efforts targeting the many undersampled regions across the subcontinent where the *B. mossambicus* species group is likely to occur, combined with population genetic/phylogenomic methods, will be necessary to better investigate the presence of hybridization within *Breviceps*. We are optimistic that future studies scrutinizing morphological data (both morphometric and anatomical, i.e., via CT-scanning) of large numbers of genotyped *B. mossambicus* group samples will reveal diagnostic morphological differences between species and/or populations that are otherwise difficult to discern by individual specimens (Fig. 2).

As mentioned above, there is considerable genetic structure within *B. ombelanonga*, as well as among the four most closely related members of the *B. mossambicus* group (Fig. 1B, C). The Great Escarpment is a major topographical feature of southern Africa that separates the central plateau from coastal plains semi-continuously from Angola in the northwest, south through Namibia and South Africa, before petering out along the border of Zimbabwe and Mozambique in the northeast. This feature is coincident with changes in habitat and climate as one moves from the coast inland, and is consequently reflected in the distribution and diversification of various organisms (Clark et al. 2011; Nielsen et al. 2018). The western and central populations of *B. ombelanonga*, for example, are separated by the escarpment, although further study is needed to verify that the genetic structure we observed (between all three populations) is not just an effect of isolation by distance, compounded by limited sampling. Unfortunately, this is not unique to the *B. mossambicus* group. Many recent studies on other herpetofauna have stated that large sampling gaps across sub-Saharan Africa may cause misleading biogeographic conclusions (Medina et al. 2016; Jongsma et al. 2018). The central and eastern localities of *B. ombelanonga*, as well as the latter from either *B. adspersus* or *B. poweri*, may be

separated by drainage basins; however, with no contemporary sampling across regions spanning hundreds of kilometers, it is difficult to test these broad biogeographic hypotheses. Many recent initiatives have improved the current state of knowledge of Angola's herpetofauna, as well as to identify priority areas for future field survey work (Ceriaco et al. 2014, 2016, 2018; Conradie et al. 2016; Heinicke et al. 2017; Marques et al. 2018; Baptista et al. 2019; Butler et al. 2019; Ernst et al. 2020), yet these efforts have still only scratched the surface. Additional, comprehensive field surveys, particularly those with focused/specialized efforts to record hard-to-find, seasonal, and/or fossorial taxa (e.g., by deploying pitfall traps, drift fence arrays, artificial refuges, etc., for an extended period of time or repeatedly throughout the year), should be priorities in the near future.

Acknowledgements

We are grateful to Mariana P. Marques, Adam Ferguson, Ben Marks, John Cavagnaro, Philip Pastor, Suzana Bandeira, Ilola Jorge, Alvaro “Varito” Baptista, Ninda Baptista, Kerllen Costa, James Harvey, Roger Bills, Götz Neef, and Luke Verburgt for their invaluable field assistance, support, advice, and companionship. John Cavagnaro provided the life photo of the holotype. Mohamad Beidoun assisted with molecular work. This work was supported in part by the US National Science Foundation (DEB-1556255, 1556559 and DEB-1556585 to DCB, AMB, and MPH), the JRS Biodiversity Foundation (to DCB and AMB), and the National Geographic Society (Okavango Wilderness Project EC0715-15 to WC). The funders had no role in study design, data collection, and analysis, the decision to publish, or manuscript preparation. Field components of this work were facilitated by a Memorandum of Understanding between the University of Florida and The National Institute for Biodiversity and Protected Areas (INBAC) in Angola. Material used in this study was exported under the following permit numbers: 083/INBAC.MINAMB/2016 (to Villanova University) and 31/GGPCC/2016 (to the PEM). Some of the molecular work was completed at Marquette University and SVN would like to thank the good Dr. Gamble for his generosity. We would lastly thank the reviewers, Drs. Louis Du Preez and Alan Channing, for their kind words and edits that helped improve this manuscript, as well as our subject editor, Dr. Angelica Crottini.

References

- Almaça C (2000) Museu Bocage, Ensino e Exibição. Museu Bocage – Museu Nacional de História Natural, Lisboa.
- Bandelt H, Forster P, Röhl A (1999) Median-joining networks for inferring intraspecific phylogenies. *Molecular Biology and Evolution* 16(1): 37–48. <https://doi.org/10.1093/oxfordjournals.molbev.a026036>
- Baptista N, Conradie W, Vaz Pinto P, Branch WR (2019) The amphibians of Angola: Early studies and the current state of knowledge. In: Huntley BJ, Russo V, Lages F, Ferrand de Almeida N (Eds) *Biodiversity in Angola*. Science & Conservation: A Modern

- Synthesis: 243–281. Cham, Switzerland, Springer Open. XVIII, 549 pp. https://doi.org/10.1007/978-3-030-03083-4_12
- Bocage JVB (1870) Description de un “saurien” nouveau de l’Afrique occidentale. *Jornal de Ciencias Mathematicas, Physicas e Naturaes* 3: 66–68.
- Bocage JVB (1873) Mélanges erpétologiques. II. Sur quelques reptiles et batraciens nouveaux, rares ou peu connus d’Afrique occidentale. *Jornal de Ciencias Mathematicas, Physicas e Naturaes* 4: 209–227.
- Bocage JVB (1895) Herpétologie d’Angola et du Congo. Ministério da Marinha e das Colónias, Lisbonne, Portugal. 203 pp. [20 pls]
- Boulenger GA (1907) Description of a new engystomatid frog of the genus *Breviceps* from Namaqualand. *Annals & Magazine of Natural History Series* 7 20: 46–47. <https://doi.org/10.1080/00222930709487295>
- Butler BO, Ceriáco LM, Marques MP, Bandeira S, Júlio T, Heinicke MP, Bauer AM (2019) Herpetological survey of Huíla Province, Southwest Angola, including first records from Bicular National Park. *Herpetological Review* 50: 225–240.
- Cei JM (1977) Chaves para uma identificação preliminar dos batráquios anuros da R. P. de Angola. *Boletim da Sociedade Portuguesa de Ciências Naturais* 17: 5–26.
- Ceriáco LMP, Marques MP (2018) Angolan Herpetological Collection – ICT. Version 1.1. Instituto de Investigação Científica Tropical. [Occurrence dataset accessed via GBIF.org on 2020-06-26]
- Ceriáco LMP, Bauer AM, Blackburn DC, Lavres ACFC (2014) The herpetofauna of the Capanda Dam region, Malanje, Angola. *Herpetological Review* 45: 667–674.
- Ceriáco LMP, de Sá SDAC, Bandeira S, Valério H, Stanley EL, Kuhn AL, Marques MP, Vindum JV, Blackburn DC, Bauer AM (2016) Herpetological survey of Iona National Park and Namibe Regional Natural Park, with a synoptic list of the amphibians and reptiles of Namibe Province, southwestern Angola. *Proceedings of the California Academy of Sciences* 63: 15–61.
- Ceriáco LMP, Marques MP, Bandeira S, Blackburn DC, Bauer AM (2018) Herpetological survey of Cangandala National Park, with a synoptic list of the amphibians and reptiles of Malanje Province, Central Angola. *Herpetological Review* 49: 408–431.
- Ceriáco LMP, Agarwal I, Marques MP, Bauer AM (2020) A review of the genus *Hemidactylus* Goldfuss, 1820 (Squamata: Gekkonidae) from Angola, with the description of two new species. *Zootaxa* 4746: 1–71. <https://doi.org/10.11646/zootaxa.4746.1.1>
- Channing A (2012) A new species of Rain Frog from Namaqualand, South Africa (Anura: Brevicipitidae: *Breviceps*). *Zootaxa* 3381: 62–68. <https://doi.org/10.11646/zootaxa.3381.1.4>
- Channing A, Minter LR (2003) A new rain frog from Tanzania (Microhylidae: *Breviceps*). *African Journal of Herpetology* 53: 147–154. <https://doi.org/10.1080/21564574.2004.9635507>
- Channing A, Rödel MO (2019) Field Guide to the Frogs and Other Amphibians of Africa. Cape Town, South Africa: Struik Nature, 408 pp.
- Conradie W, Bills R, Branch WR (2016) The herpetofauna of the Cubango, Cuito, and lower Cuando river catchments of south-eastern Angola. *Amphibian & Reptile Conservation* 10(2): 6–36.

- Conroy CJ, Papenfuss T, Parker J, Hahn NE (2009) Use of tricaine methanesulfonate (MS222) for euthanasia of reptiles. *Journal of the American Association for Laboratory Animal Science* 48(1): 28–32.
- de Queiroz K (2007) Species concepts and species delimitation. *Systematic Biology* 56: 879–886. <https://doi.org/10.1080/10635150701701083>
- Du Preez L, Carruthers V (2017) *Frogs of Southern Africa. A Complete Guide*. Struik Nature, Cape Town, 519 pp.
- Ernst R, Lautenschläger T, Branquima MF, Hölting M (2020) At the edge of extinction: a first herpetological assessment of the proposed Serra do Pingano Rainforest National Park in Uíge Province, northern Angola. *Zoosystematics and Evolution* 96: 237–262. <https://doi.org/10.3897/zse.96.51997>
- Frétey T, Dewynter M, Blanc CP (2011) Amphibiens d’Afrique central et d’Angola. Clé de Détermination illustré des amphibiens du Gabon et du Mbini. Biotope, Mèze/Muséum national d’Histoire naturelle, Paris, France, 232 pp.
- Grandvaux-Barbosa LA (1970) Carta Fitogeografica de Angola. Instituto de Investigação Científica de Angola, Luanda, 323 pp.
- Gridi-Papp M (2007) SoundRuler: Acoustic analysis for research and teaching. <http://soundruler.sourceforge.net> [accessed 25 May 2019]
- Heinicke MP, Ceríaco LMP, Moore IM, Bauer AM, Blackburn DC (2017) *Tomopterna damarensis* (Anura: Pyxicephalidae) is broadly distributed in Namibia and Angola. *Salamandra* 53: 461–465.
- Helmich W (1957) Herpetologische Ergebnisse einer Forschungsreise in Angola. *Veröffentlichungen der Zoologischen Staatssammlung München* 5: 1–92.
- Hewitt J (1925) Descriptions of three new toads belonging to the genus *Breviceps* Merrem. *Annals of the Natal Museum* 5: 189–194.
- IUCN [SSC Amphibian Specialist Group] (2013a) *Breviceps adpersus*. The IUCN Red List of Threatened Species 2013: e.T57712A3061969. <https://doi.org/10.2305/IUCN.UK.2013-2.RLTS.T57712A3061969.en> [downloaded on 01 April 2020]
- IUCN [SSC Amphibian Specialist Group] (2013b) *Breviceps poweri*. The IUCN Red List of Threatened Species 2013: e.T57718A18362273. <https://doi.org/10.2305/IUCN.UK.2013-2.RLTS.T57718A18362273.en> [downloaded on 01 April 2020]
- Jongsma GF, Barej MF, Barratt CD, Burger M, Conradie W, Ernst R, Greenbaum E, Hirschfeld M, Leaché AD, Penner J, Portik DM, Zassi-Boulou A-G, Rödel M-O, Blackburn DC (2018) Diversity and biogeography of frogs in the genus *Amnirana* (Anura: Ranidae) across sub-Saharan Africa. *Molecular Phylogenetics and Evolution* 120: 274–285. <https://doi.org/10.1016/j.ympev.2017.12.006>
- Lanfear R, Frandsen PB, Wright AM, Senfeld T, Calcott B (2017) PartitionFinder 2: new methods for selecting partitioned models of evolution for molecular and morphological phylogenetic analyses. *Molecular Biology and Evolution* 34: 772–773. <https://doi.org/10.1093/molbev/msw260>
- Laurent RF (1964) Reptiles et amphibiens de l’Angola. (Troisième contribution). *Publicações Culturais da Companhia de Diamantes de Angola* 67: 1–165.

- Linnaeus C (1758) *Systema naturae per regna tria naturae, secundum classes, ordines, genera, species, cum characteribus, differentiis, synonymis, locis*. Vol. 1. 10th Edition. L. Salvii. Stockholm, 824 pp. <https://doi.org/10.5962/bhl.title.542>
- Marques MP, Ceriaco LMP, Blackburn DC, Bauer AM (2018) Diversity and distribution of the amphibians and terrestrial reptiles of Angola: Atlas of historical and bibliographic records (1840–2017). *Proceedings of the California Academy of Sciences Series 4 65, Supplement II*, 501 pp.
- Medina MF, Bauer AM, Branch WR, Schmitz A, Conradie W, Nagy ZT, Hibbitts TJ, Ernst R, Portik DM, Nielsen SV, Colston TJ, Kusamba C, Behangana M, Rödel MO, Greenbaum E (2016) Molecular phylogeny of *Panaspis* and *Afroablepharus* skinks (Squamata: Scincidae) in the savannas of sub-Saharan Africa. *Molecular Phylogenetics and Evolution* 100: 409–423. <https://doi.org/10.1016/j.ympev.2016.04.026>
- Merrem B (1820) *Tentamen Systematis Amphibiorum*. J.C. Krieger, Marburg, Hesse, 191 pp.
- Miller MA, Pfeiffer W, Schwartz T (2010) “Creating the CIPRES Science Gateway for inference of large phylogenetic trees” in *Proceedings of the Gateway Computing Environments Workshop (GCE)*, 14 Nov. 2010, New Orleans, LA., 1–8. <https://doi.org/10.1109/GCE.2010.5676129>
- Minter LR (1997) Advertisement call structure and morphology of *Breviceps mossambicus* Peters and *B. poweri* Parker (Anura: Microhylidae) from northern Mozambique. *Annals of the Natal Museum* 38: 5–19.
- Minter LR (2003) Two new cryptic species of *Breviceps* (Anura: Microhylidae) from southern Africa. *African Journal of Herpetology* 52(1): 9–21. <https://doi.org/10.1080/21564574.2003.9635473>
- Minter LR, Netherlands EC, Du Preez LH (2017) Uncovering a hidden diversity: two new species of *Breviceps* (Anura: Brevicipitidae) from northern KwaZulu-Natal, South Africa. *Zootaxa* 4300: 195–216. <https://doi.org/10.11646/zootaxa.4300.2.3>
- Monard A (1938) Contribution à la batrachologie d'Angola. *Arquivos do Museu Bocage* 9: 52–120.
- National Geographic Okavango Wilderness Project (2017) Initial Findings from Exploration of the Upper Catchments of the Cuito, Cuanavale, and Cuando Rivers, May 2015 to December 2016. Unpublished report.
- Nielsen SV, Daniels SR, Conradie W, Heinicke MP, Noonan BP (2018) Multilocus phylogenetics in a widespread African anuran lineage (Brevicipitidae: *Breviceps*) reveals patterns of diversity reflecting geoclimatic change. *Journal of Biogeography* 45(9): 2067–2079. <https://doi.org/10.1111/jbi.13394>
- Parker HW (1934) A monograph of the frogs of the family Microhylidae. Trustees of the British Museum, London, 208 pp.
- Parker WK (1868) A monograph on the structure and development of the shoulder girdle and sternum in the Vertebrata. No. 42 Ray Society Series. Robert Hardwicke, London, 237 pp. <https://doi.org/10.5962/bhl.title.31928>
- Peters WCH (1854) Diagnosen neuer Batrachier, welche zusammen mit der früher (24. Juli und 18. August) gegebenen Übersicht der Schlangen und Eidechsen mitgeteilt werden. Bericht über die zur Bekanntmachung geeigneten Verhandlungen der Königlich Preussischen Akademie der Wissenschaften zu Berlin, Berlin, 1854: 614–628.

- Peters WCH (1882) *Naturwissenschaftlich Reise nach Mossambique auf befehl Seiner Mäjestat des Königs Friedrich Wilhelm IV in den Jahren 1842 bis 1848 ausgeführt*. Zoologie 3 (Amphibien). G. Reimer, Berlin, 670 pp.
- Power JH (1926) A monographic revision of the genus *Breviceps*, with distribution records and descriptions of new species. *Annals of the South African Museum* 20: 451–471.
- Poynton JC (1963) Descriptions of southern African amphibians. *Annals of the Natal Museum* 15: 319–332.
- Poynton JC (1964) The Amphibia of Southern Africa: a faunal study. *Annals of the Natal Museum* 17: 1–334.
- Poynton JC (1982) On species pairs among Southern African amphibians. *African Journal of Zoology* 17: 67–74. <https://doi.org/10.1080/02541858.1982.11447782>
- Poynton JC, Broadley DG (1985) Amphibia Zambesiaca 1. Scolecomorphidae, Pipidae, Microhylidae, Hemisidae, Arthroleptidae. *Annals of the Natal Museum* 26: 503–553.
- Ronquist F, Teslenko M, van der Mark P, Ayres DL, Darling A, Höhna S, Larget B, Liu L, Suchard MA, Huelsenbeck JP (2012) MRBAYES 3.2: Efficient Bayesian phylogenetic inference and model selection across a large model space. *Systematic Biology* 61: 539–542. <https://doi.org/10.1093/sysbio/sys029>
- Ruas C (1996) Contribuição para o conhecimento da fauna de batráquios de Angola. Parte I: Famílias Pipidae, Bufonidae, Microhylidae, Ranidae, Hemisidae e Arthroleptidae. *Garcia de Orta, Séria de Zoologia* 21(1): 19–41.
- Ruas C (2002) Batráquios de Angola em colecção no Centro de Zoologia. *Garcia de Orta, Séria de Zoologia* 24(1–2): 139–146.
- Simpson GG (1951) The species concept. *Evolution* 5: 285–298. <https://doi.org/10.1111/j.1558-5646.1951.tb02788.x>
- Simpson GG (1961) *Principles of Animal Taxonomy*. Columbia University Press, New York, USA, [XIV +] 250 pp. <https://doi.org/10.7312/simp92414>
- Sueur J, Aubin T, Simonis C (2008) Equipment review: Seewave, a free modular tool for sound analysis and synthesis. *Bioacoustics* 18: 218–226. <https://doi.org/10.1080/09524622.2008.9753600>
- Stamatakis A (2014) RAxML version 8: a tool for phylogenetic analysis and post-analysis of large phylogenies. *Bioinformatics* 30(9): 1312–1313. <https://doi.org/10.1093/bioinformatics/btu033>
- Tamura K, Stecher G, Peterson D, Filipski A, Kumar S (2013) MEGA6: molecular evolutionary genetics analysis version 6.0. *Molecular Biology and Evolution* 30(12): 2725–2729. <https://doi.org/10.1093/molbev/mst197>
- Watters JL, Cummings ST, Flanagan RL, Siler CD (2016) Review of morphometric measurements used in anuran species descriptions and recommendations for a standardized approach. *Zootaxa* 4072(4): 477–495. <https://doi.org/10.11646/zootaxa.4072.4.6>
- Wiley EO (1978) The evolutionary species concept reconsidered. *Systematic Zoology* 27: 17–26. <https://doi.org/10.2307/2412809>

Appendix I

Additional *Breviceps* material examined

***Breviceps* sp.:** **Angola:** Lunda Sul Province: Alto Chicapa (MD 5426, 5865); Rives du lac Calundo (MD 5599); Moxico Province: Cazombo (MD 5770; MCZ A-35892–893); Luso: Calombe (IICT 339–1959, 404–1959, 453–6–1959); Benguela Province: Benguela (BMNH 1906.10.8.10–11); Ebanga (MHNC 90.008, 90.009); Chimbassi [= Chimbasse] (ZSM 173/1953); Quissange (BMNH 1887.3.23.5); Huambo Province: Bimbi (MCZ A-23721).

B. adspersus: **Botswana:** Serowe (PEM A4800); **Namibia:** Damaraland (ZMB 6294 [lectotype]), Okahandja (PEM A4723); **South Africa:** Limpopo Province: Waterpoort (PEM A14226); Mpumalanga Province: Botshabelo (ZMB 10087 [paralectotype]); Northern Cape Province: Rooipoort (PEM A8001–2, PEM A9431, PEM A9433–4), Tswalu (PEM A9444), Kuruman River Reserve (PEM A13883).

B. mossambicus: **Malawi:** Mount Mulanje (PEM A7861); **Mozambique:** Cabo Delgado Province: Balama (PEM A11021); Nampula Province: Insula Mossambique (ZMB 75399–400 [syntypes]), Mount Namuli (PEM A11310), Mount Ribaué (PEM A11362), Ribaué town (PEM A13952, PEM A13956), Nagonha Village (PEM A6717); Niassa Province: Lichinga (PEM A14008); Zambezi Province: Mount Lico (PEM A13725–6); **Tanzania** (ZMB 24793).

B. poweri: **Democratic Republic of the Congo:** Lualaba Province: Kalakundi (PEM A8453–6); Haut-Katanga Province: Sakania (UF Herp 27586); **Mozambique:** Nampula Province: Ribaué town (PEM A13957); **Zambia:** Northern Province: Mporokoso (PEM A2794); Northwestern Province: Solwezi (CAS 196527); **Zimbabwe:** Melsetter (PEM A4735).

Supplementary material I

Table S1. Morphological data used to perform PCAs

Authors: Stuart V. Nielsen, Werner Conradie, Luis M. P. Ceriaco, Aaron M. Bauer, Matthew P. Heinicke, Edward L. Stanley, David C. Blackburn

Data type: morphological data

Explanation note: Morphological data used to perform PCAs. See Table 1 and Appendix 1 for sample information. Specimens were derived from localities within the core geographic range of each species, as supported by the phylogenetic results of Nielsen et al. 2018. All were examined to confirm the presence of traits diagnostic for *B. adspersus*, *B. mossambicus*, or *B. poweri*, respectively.

Copyright notice: This dataset is made available under the Open Database License (<http://opendatacommons.org/licenses/odbl/1.0/>). The Open Database License (ODbL) is a license agreement intended to allow users to freely share, modify, and use this Dataset while maintaining this same freedom for others, provided that the original source and author(s) are credited.

Link: <https://doi.org/10.3897/zookeys.979.56863.suppl1>